Potentiating stem cell-derived hepatocyte function

Fouzeyyah Ali Alsaeedi
130574866

Thesis submitted in fulfilment of the requirements for the degree of
Doctor of Philosophy
Newcastle University
Faculty of Medical Sciences
Institute of Cellular Medicine
May 2019

Declaration

I hereby declare that this thesis has been composed by myself and has not been submitted in any previous application for a degree. All work was performed by myself unless otherwise stated. All sources of information have been acknowledged appropriately by means of a reference.

Fouzeyyah Alsaeedi

Abstract

The rat pancreatic AR42J-B13 (B-13) cell line differentiates into non-replicative hepatocyte-like (B-13/H) cells in response to glucocorticoid. As this response is dependent on the induction of serine/threonine protein kinase 1 (SGK1), this suggests a general essential role for SGK1 in hepatocyte maturation. To test this hypothesis, B-13 cells infected with AdV-SGK1F in the absence of glucocorticoid resulted in the expression of Flag-tagged SGK1F protein; increases in β-catenin phosphorylation; decreases in Tcf/Lef transcriptional activity; expression of hepatocyte marker genes and the conversion of B-13 cells to a cell phenotype near-similar to B-13/H cells. Given this demonstration of functionality, the effects of expressing adenoviral-encoded flag-tagged human SGK1F (AdV-SGK1F) in induced pluripotent human stem cells (iPSCs) was investigated. iPSCs directed to differentiate to hepatocyte-like cells using the standard protocol for chemical inhibitors and mixtures of growth factors, were infected with AdV-SGK1F at different stages of their differentiation to hepatocytes, either at an early point during differentiation to endoderm; during endoderm differentiation to anterior definitive endoderm and hepatoblasts and once converted to hepatocyte-like cells. SGK1F expression did not affect differentiation to endoderm, most possibly due to low levels of expression. However, expression of SGK1F in both iPSCs-derived endoderm and hepatocyte-like cells both resulted in the promotion of cells to an hepatoblast phenotype. These data demonstrate that the effect of expressing SGK1F in human iPSC-derived cells contrasts with its effects when expressed in B-13 cells. Given that SGK1 expression promotes an hepatoblast phenotype rather than maturation of human iPSC towards a mature hepatocyte phenotype, these data suggest a temporary role for Sgk1 in promoting a hepatoblast state in B-13 trans-differentiation to B-13/H cells.

Acknowledgements

In the name of Allah, the Most Gracious and the Most Merciful, Praise be to Allah who gave me the health, strength and patience to conduct this work.

I would like to express my gratitude to my supervisor Professor Matthew Wright for the patient guidance, encouragement and advice he has provided throughout my time as his student. His helpful instruction and expert guidance have been invaluable throughout each stage of the work, I greatly appreciate the support he offered when required and for his prompt responses to all to my questions. Also, I must acknowledge my second supervisor Professor Lyle Armstrong and the technicians in his lab who made this work possible and kindly provided me with the stem cells to carry out an essential part of this thesis. Many thanks also to the members of the Wright Group and the Institute of Cellular Medicine for their technical assistance.

This work would not have been possible without the financial support provided by Taif University and the Ministry of Education of the Kingdom of Saudi Arabia.

I dedicate this work to the memory of my late father (Mr Ali Alsaeedi). I miss him every day. He has gone, but I always remember his prayers for me which gave me the hope and patience to finish this thesis. Similarly, I want to dedicate this work with my warmest words of thanks to my mother (Mrs Mastorah Althubaity) who always believed in my ability to be successful; her believe, endless love and support have made this journey possible. I would also like to thank all my brothers and sisters. I cannot thank them enough for encouraging me throughout this experience.

A special thanks to my beloved husband (Mr Mohammad Althubaity), words cannot express how grateful I am to him for keeping things going and for always showing how proud he is of me. This thesis is also, dedicated to my beloved daughters Rose (5 years) and Al-Yasmin (1 year) who have been the light of my life and have given me the extra strength and motivation to get things completed.

Last but not least, I want to express my sincere gratitude to my great friend (Lotfia Shames Nawafa) who have always been a major source of support when things were very challenging, and I became discouraged.

Table of Contents

List of Figures

List of Tables

List of Abbreviations

11β-hydroxysteroid dehydrogenase **(HSD2)**
Adenomatosis polyposis Coli **(APC)**
Adenosine diphosphate **(ADP)**
Adenosine triphosphate **(ATP)**
Adenovirus **(Ad)**
Adenovirus encoding green fluorescent protein **(AdV-GFP)**
Adenovirus serotype 5 **(Ad5)**
Aldosterone **(ALD)**
Amyotrophic lateral sclerosis **(ALS)**
Anterior definitive endoderm **(ADE)**
AR42J-B13 cells **(B-13)**
Arginase 1 **(Arg1)**
Basic fibroblast growth factor **(bFGF)**
Biliary epithelial cells **(BECs)**
Bone morphogenetic protein **(BMP)**
Bovine serum albumin **(BSA)**
Carbamoyl phosphate synthase I**(CPS1)**
Casein kinase 1α **(CK1α)**
CCAAT/enhancer-binding protein alpha **(CEBPa)**
CCAAT/enhancer binding protein **(C/EBP**)
Central nervous system **(CNS)**
Chemically defined medium- Poly Vinyl Alcohol **(CDM-PVA)**
Complementary deoxyribonucleic acid **(cDNA)**
Coxsackie- and adenovirus receptor **(CAR)**
Cytochrome P450 2F 2 **(Cyp2f2)**
Cytomegalovirus **(CMV)**
Definitive endoderm **(DE)**
Dexamethasone **(DEX)**
Diamidino-2-phenylindole **(DAPI)**
Dickkopf-related protein 1 **(DKK)**
Dihydrolipoamide ***(Dlat)***
Dimethyl sulfoxide **(DMSO**)
Dishevelled **(Dsh)**
Dithiothreitol **(DTT)**
Double-stranded DNA **(dsDNA)**
Drug metabolising enzymes **(DMEs)**
Drug metabolism enzyme and transporter **(DMET)**
Dulbecco's Modified Eagle's Medium **(DMEM)**
Embryonic stem cells **(ESCs)**
Enhanced chemical luminescence reagents **(ECL)**
Epidermal growth factor **(EGF)**
Epithelial cell adhesion molecule **(EpCAM)**
Epithelial Na+ channel **(ENaC)**
Epithelial-mesenchymal transition **(EMT)**
Ethylenediaminetetraacetic acid **(EDTA)**
Extracellular matrix **(ECM)**
Fetal calf serum **(FCS)**
Fibroblast growth factor **(FGF)**
Fibroblast growth factor 4 **(FGF4)**

Fluorescein isothiocyanate **(FITC)**
Forkhead box protein **(Foxa2)**
Frizzled receptors **(Fzd)**
Fructose bisphosphatase **(FBPase)**
GATA-binding proteins **(Gata4–6)**
Glucocorticoid receptor antagonist **(Ru486)**
Glucocorticoid Receptors **(GR)**
Glutamine synthetase **(Gs)**
Glutathione S-transferase mu ***(Gstm)***
Glycogen synthase kinase 3 **(GSK3**)
Glycogen synthase kinase 3β **(GSK3β)**
Green fluorescent protein **(GFP)**
Hematopoietic stem cells **(HMSCs)**
Hepatic progenitor cells **(HPCs)**
Hepatic stellate cells **(HSCs)**
Hepatocellular carcinoma **(HCC)**
Hepatocyte Basal Medium **(HBM)**
Hepatocyte growth factor **(HGF)**
HMG domain DNA-binding factor **(Sox17)**
Horseradish peroxidase **(HRP)**
Human embryonic kidney 293 **(HEK293)**
Human embryonic stem cells **(hESCs)**
Human hepatocytes **(HH)**
Hypothalamus-pituitary-adrenal **(HPA)**
Induced pluripotent cell stem cells **(iPSCs)**
Inner cell mass **(ICM)**
Inverted terminal repeats **(ITRs)**
Iscove's Modified Dulbecco's Medium **(IMDM)**
Isocitrate dehydrogenase 3a **(Idh3a)**
Kinase-dead **(KD)**
Krüppel-like transcription factor 4 **(Klf4)**
Lipoprotein receptor-related protein **(LRP)**
Liver sinusoidal endothelial cells **(LSECs)**
Liver-enriched transcription factors **(LETFs)**
Low-density lipoprotein **(LDL)**
Luciferase assay reagent **(LAR II)**
Luria broth **(LB)**
Lymphatic enhancement factor **(LEF)**
Messenger ribonucleic acid **(mRNA)**
MicroRNA **(miRNA)**
Mineralcorticoid receptors **(MR)**
Minor-groove binding **(MGB**)
Multiplicity of infection **(MOI)**
Myelocytomatosis viral oncogene **(c-Myc)**
Non-Essential Amino Acids **(NEAA)**
Nuclear transfer **(NT)**
Octamer-binding transcription factor 4 **(Oct4)**
Oncostatin M **(OSM)**
Pancreatic and duodenal homeobox gene 1 **(PDX1)**
Phosphate buffered saline **(PBS)**
Phosphoenolpyruvate carboxykinase 1 **(pck1)**
Plaque forming unit **(PFU)**

Platelet-derived growth factor **(PDGF)**
Poly Vinyl Alcohol **(PVA)**
Polymerase chain reaction **(PCR)**
Pregnane x receptor **(PXR)**
Primitive streak **(PS)**
Progesterone receptor **(Pgr)**
Prospero homeobox protein 1 **(PROX1)**
Protein phosphatase 2A (PP2A)
Real-time reverse transcription PCR **(qRT-PCR)**
Receptor tyrosine kinase **(RTK)**
Replication-defective **(RD)**
Reverse transcription polymerase chain reaction **(RT-PCR)**
Ribonucleic acid **(RNA)**
Room temperature **(RT)**
Roswell Park Memorial Institute 1640 Medium **(RPMI)**
RPMI medium supplemented with B27 **(RPMI-B27)**
Secreted Frizzled-related protein **(sFRP)**
Serine/threonine protein kinase **(SGK1)**
Sex-determining region Y box-2 **(Sox2)**
Sgk1 kinase inhibitor 100nM **(GSK 650394)**
Sodium dodecyl sulphate **(SDS)**
Sodium ion **(Na+)**
Sodium-dodecyl sulphate polyacrylamide gel electrophoresis **(SDS- PAGE)**
Sonic hedgehog **(Shh)**
Sulfotransferase **(Sult5a1)**
T cell factor **(TCF)**
T-cell factor/lymphoid enhancing factor **(TCF/LEF)**
Terminal protein **(TP)**
Tetramethylethylenediamine **(TEMED)**
Three dimensional **(3D)**
Transforming growth factor-β **(TGFb)**
Triiodothyronine **(T3)**
Ubiquitin ligase **(Nedd4-2)**
α- fetoprotein **(Afp)**

Chapter 1. **Introduction**

1.1 Stem cells

A stem cell is a cell characterised by its ability for self-replication via cell division throughout the life of the organism. Stem cells can differentiate into diverse types of cells in the body of the organism. They are unspecialised cells which can be physiologically or experimentally induced to give rise to specialised cells. Embryonic stem cells (ESCs) and adult stem cells are the main types of stem cells in mammals. ESCs are isolated from the inner cell mass (ICM) of blastocysts and can differentiate all the specialised cells from the three germ layers (ectoderm, endoderm and mesoderm) [1,2]. Adult stem cells are located in different tissues such as blood, skin or intestinal tissues. In adult organisms, stem cells work as a repair system replenishing damaged adult tissues.

According to their differentiation potentiality into different sorts of cells, stem cells are categorised into totipotent, pluripotent, multipotent and unipotent stem cells. Totipotent stem cells are the stem cells that have the ability to differentiate into extraembryonic and embryonic cell types. Such cells can build a complete, viable organism. They are formed within the first few divisions of the egg being fertilised [3]. Pluripotent stem cells are totipotent derived cells which can differentiate between every cell in an organism except for extraembryonic tissue [4]. Multipotent stem cells are adult stem cells and only give rise to specific lineages of cells. Unipotent stem cells can differentiate into their cell type only; however, unipotent cells are able to self-renew, which distinguishes them from non-stem cells (e.g. progenitor cells, which cannot self-renew) [5] (Figure 1.1). Adult stem cells are frequently used for therapeutic purposes (e.g., bone marrow transplantation) [6]. Stem cells can now be expanded *in vitro* and directed to differentiate into specific cell types with features which are consistent with the cells of different tissues, for instance, muscles or nerves. ESC lines and induced pluripotent stem cells (iPSCs) are promising candidates for regenerative medicine, disease modelling and drug discovery. [7 8]

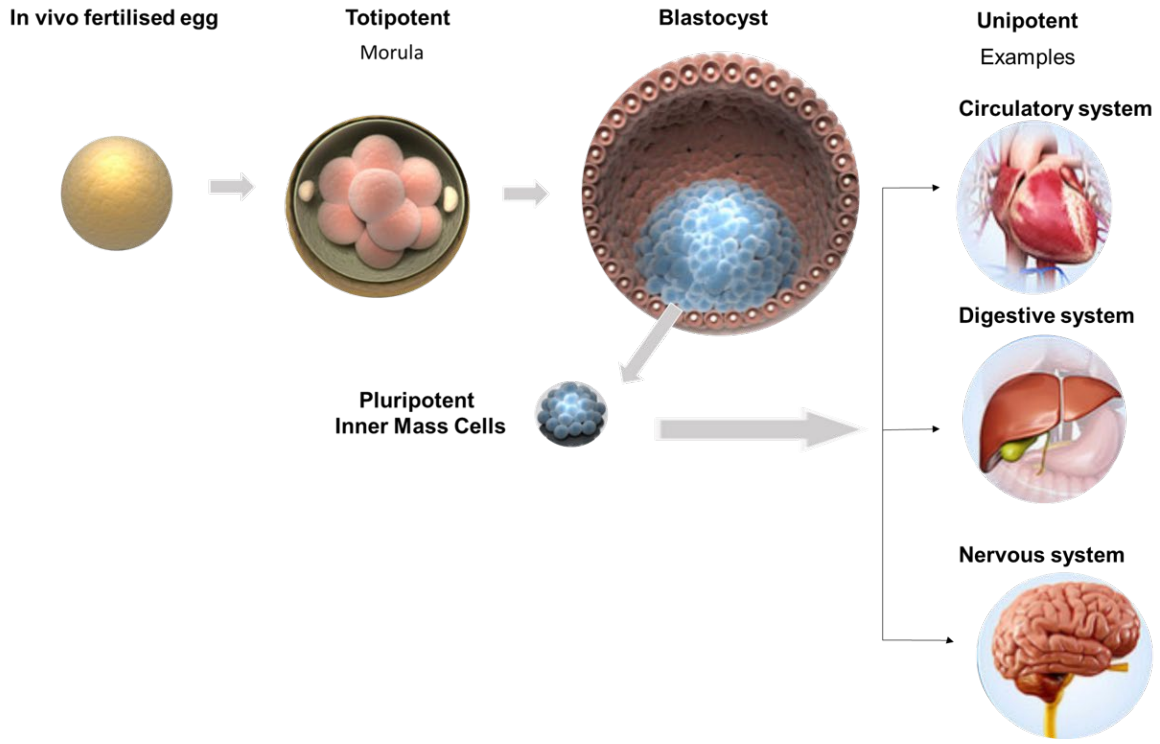

Figure 1.1 Stem cells potency. Totipotent cells or morula which are embryonic cells within the first couple of cell divisions after fertilisation, are the only cells that are totipotent and able to form all the cell types in a body in addition to the extraembryonic (placental) cells. ESCs are considered pluripotent and initiate within a blastocyst as ICM. These stem cells can differentiate all of the cell types that make up the body excluding the placenta. Unipotent cells can generate only their own type though they have the ability to self-renew. Figure adapted from https://vignette.wikia.nocookie.net/mmg-233-2014-genetics-genomics/images/f/f6/3D-Medical-Illustration-Pluripotent-Stem-Cells.jpg/revision/latest?cb=20141013062832[9].

1.1.1 Embryonic Stem Cells

ESCs are pluripotent stem cells originating from the ICM of mammalian blastocysts. These cells exhibit a remarkable ability to proliferate indefinitely and maintain their pluripotent potential to differentiate into all cell lineages in the body [1,2]. The discovery of mouse ESCs by Evans et al. (1981) and Martin et al. (1981) and the isolation of human embryonic stem cells (hESCs) in 1998 by Thomson et al., helped to realise the genuine potential of stem cells. Efficient differentiation of ESCs to any cells types suggests the ability to create new models of mammalian development and to establish additional supplies of cells for regenerative medicine. Embryological studies have offered valuable understandings into essential pathways controlling the differentiation of ESCs, which have resulted in improvements in gastrulation modelling *in vitro* and consequently, the effective induction of all germ layers; specifically, endoderm, mesoderm and ectoderm, in addition to arrays of their derivatives cells. Consequently, for culturing of particular types of specialised cells for example; blood, muscle, nerve or heart, the

researchers directed their efforts at controlling the differentiation of embryonic stem cells by amending the chemical composition of the culture medium, altering the surface of the culture dish or modifying the cultured cells by expressing certain genes. During years of investigations, these attempts have led to efficient protocols for the differentiation of a range of cell types from stem cells [10].

Gastrulation is a critical process in embryogenesis in which all germ layers: ectoderm, mesoderm and endoderm are generated (Figure 1.2A). In the mouse, it begins with primitive streak (PS) structure formation in the region of the epiblast. During this process, uncommitted epiblast cells mobilise via the PS and leave either as the definitive endoderm (DE) or mesoderm [11](Figure 1.2B). Lineage mapping and molecular analyses have described the zones of PS as posterior, mid and anterior, that vary in developmental potential and gene expression patterns. Numerous genes involving Mixl1 [12] and Brachyury (T) [13] are found all through the PS, while other genes are expressed favourably in the anterior zone, such as forkhead box protein (Foxa2) [14] or posterior zone (HoxB1, Evx1) [15,16].

Mapping has demonstrated that the distinct subpopulations of mesoderm and endoderm are specified by both temporal and spatial control. The extraembryonic mesoderm is derived from the first mobilised epiblast cells that cross the posterior PS [17]. When gastrulation continues, cells move through more parts of the anterior regions of the PS and produce cardiac and cranial mesoderm, then axial paraxial mesoderm. Epiblast cells passing most parts of the anterior zone of the PS give rise to DE. Unlike DE and mesoderm, ectoderm descends from the anterior region of the epiblast that does not cross the PS. The spatial and temporal separation of cell outcomes detected via gastrulation proposes that the various parts of the PS or the cell populations near the PS, comprise different signalling environments which control the initiation of certain lineages.

The results of gene-targeting studies have revealed that members of the WNT family [18], as well as members of the transforming growth factor-β (TGFb) family compromising Bone morphogenic protein (BMP4)[19] and Nodal are vital for the germ layer development [20] [21]. Furthermore, the altered expression levels of the agonists of these pathways, in addition to the region-specific expression of inhibitors, combine to form signalling domains that regulate germ layer induction and specification [22]. Therefore, germ layer formation is a dynamic process that is controlled, partly, by the organised activation and local inhibition of the signalling pathways: WNT, Nodal and BMP.

The differentiation of ESCs *in vitro* offers a powerful tool for developmental studies, drug screening and regenerative medicine. However, the ethical limitations regarding human embryo donation and destruction; immune system incompatibility and likelihood of cancer developing due to the challenges in determining the correct cues to direct differentiation in the specific desired cell types in vitro and in vivo and preventing teratoma formation [23] has resulted in the avoidance of ESC-based therapies.

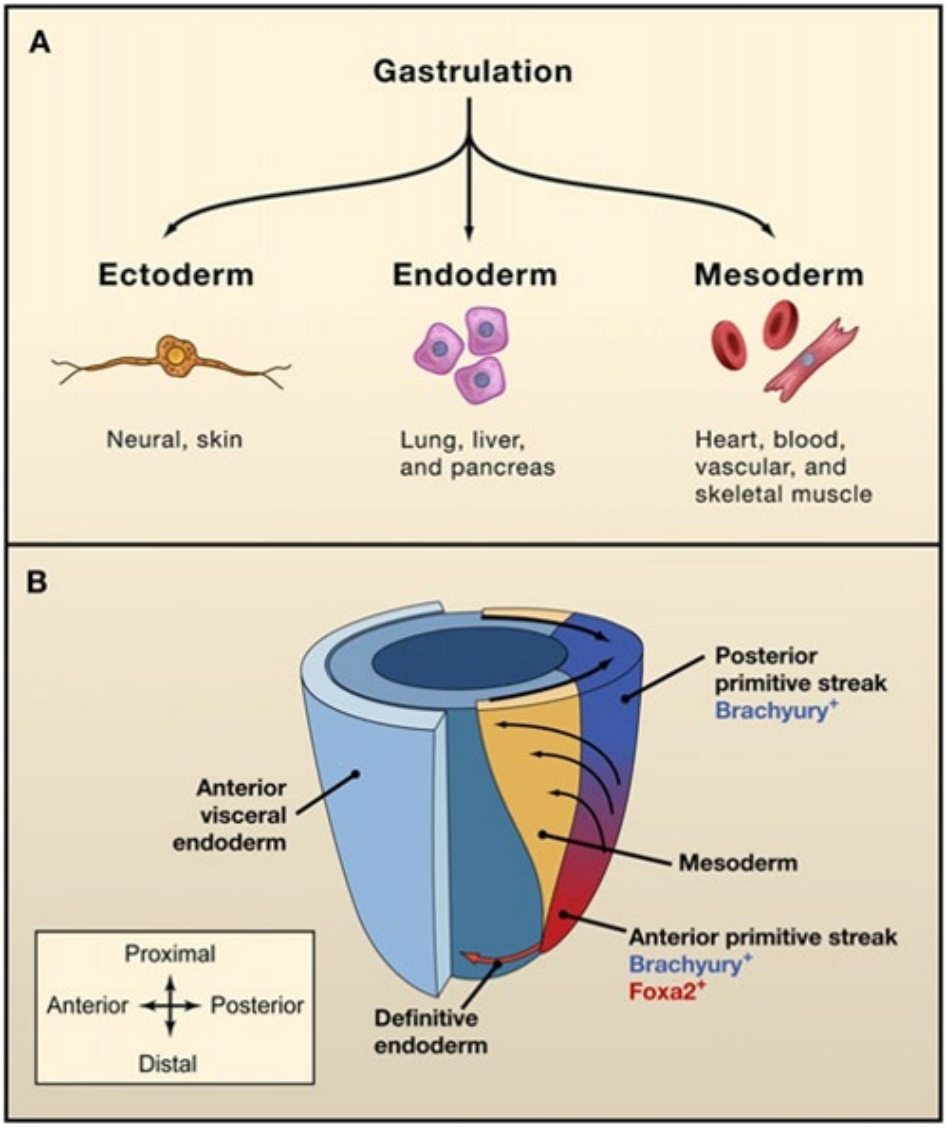

Figure 1.2 Germ layer formation during mouse gastrulation. A: three primary germ layers generated during gastrulation: ectoderm, mesoderm and endoderm. B: gastrulation in the mouse embryo. The blue indicates the posterior region of the primitive streak that expresses the marker Brachyury, whilst the red demonstrates the anterior region of the primitive streak which expresses both Foxa2 and Brachyury. The thick black arrows at the top of the embryo indicate the entry of epiblast cells into the primitive streak. The orange/yellow region shows the new formation of the mesoderm and the thin black arrows present the movement of these cells away

from the primitive streak. The red arrow at the bottom depicts the movement of the earliest DE cells [10].

1.1.2 Adult stem cells

Adult stem cells are undifferentiated cells which exist in the postnatal organism; they are either multipotent or unipotent [24]. They can make duplicate copies of themselves for extended periods and differentiate into some specialised cell types to preserve and repair the tissue in which they are found. Tissue homeostasis due to normal cell turnover and replacing cells that die because of injury or disease, are the primary functions of adult stem cells [25]. Adult stem cells are hypothesised to exist in a stem cell niche which contains a specific micro-environment for the stem cells [26]. Depending on their local environment, their development is restricted to the tissues or organs in which they reside, for example, in bone marrow; hematopoietic stem cells (HMSCs) differentiate into blood cells only [27].

Adult stem cells have been identified in several tissues, such as brain, bone marrow, peripheral blood, dental pulp, spinal cord, blood vessels, skeletal muscle, epithelia of the skin and digestive system, cornea, retina, liver and pancreas [28,29,30,31,32]. Adult stem cells show some advantages that overcome the drawbacks of working with ESCs. They are derived from adult tissue and therefore escape the ethical issues associated with ESCs. Additionally, they can also be patient-specific and thus avoid immuno-rejection concerns, and in contrast to ESCs, adult stem cells do not form tumours when transplanted *in vivo*. However, the limited capacity of adult stem cells to divide *in vitro*, their scarcity in each tissue makes their use challenging. An additional disadvantage of adult stem cells is that they can only be induced to differentiate into only a few specialized cell types

In several laboratories, researchers are attempting to discover reliable methods for adult stem cell expansion to large numbers followed by differentiation into specific cell types. Examples of potential treatments include bone regeneration using bone marrow stroma derived cells which has been reported to give rise to a variety of cell types: bone cells (osteoblasts and osteocytes), cartilage cells (chondrocytes), fat cells (adipocytes), and stromal cells that support blood formation. Generation of insulin-producing cells for type 1 diabetes; differentiation to insulin-producing cells can be achieved from adult stem cells, such as pancreatic stem cells can differentiate and be re-programmed to ensure the manifestation of a phenotype producing insulin. However, advanced strategies are needed to isolate and grow adult pancreatic stem cells, and to differentiate them into β cells. hepatic stem cells recent study demonstrated that small molecules could be used to differentiate rat hepatic stem-like cells into insulin-producing

cells that expressed distinct pancreatic-cell marker genes [33]. and using cardiac muscle cells to restore damaged heart muscle after a heart attack as the evidence suggests that the heart contains a small population of endogenous stem cells that most likely facilitate the minor repair and turnover-mediated cell replacement. The cells can be harvested in limited quantity from human endomyocardial biopsy specimens and can be injected into the site of infarction to promote cardiomyocyte formation and improvements in systolic function. [34,35]. *In vivo*, tissues can regenerate new cell populations upon damage or during normal tissue turnover by means of several mechanisms. A: transient de-differentiation of resident mature cells into precursor cells followed by re-differentiation to generate new cells [26]. This mechanism has been reported to occur in pancreatitis [36], B: resident adult stem/progenitor cells can be signalled to expand and differentiate upon damage and injury to the tissue. This method of tissue regeneration is established in high turnover tissues such as the blood system and intestine.

In recent years many studies have shown that adult stem cells can differentiate into cell types from different germ layers. For instance, mesoderm-derived stem cells in bone marrow can differentiate into endoderm-derived cells for instance liver or ectoderm-derived cells such as skin cells [37]. In the scientific literature, as of yet, there is no correct name for this phenomenon; however, it is described as stem cell plasticity or transdifferentiation. *In vivo*, it can be induced by transplanting stem cells into an organ of the body which differs from the tissue they were originally isolated from or by amending the growth medium when they are cultured *in vitro*.

The characteristics of stem cells that can regenerate the liver of adult mammals are uncertain. Typically, oval cells, initially derived from endoderm differentiate to either hepatocyte or the epithelium of the bile ducts. The well-known regenerative capacity of the liver is however, carried out by the hepatocyte mitoses themselves [38,39,40,41]. Recent studies in rodents illustrate that mesoderm-derived HMSCs may be able to move to the damaged liver and showed plasticity in converting into hepatocytes [42]. Adult stem cells identified in many tissues and organs show several advantages over working with ESCs, however, their limited capacity for renewal and the limited number of stem cells in each tissue make the generation of large quantities of stem cells difficult.

1.1.3 Induced Pluripotent Stem Cells (iPSCs)

Mouse ESCs were first generated in 1981 [1] with culture conditions that allow the longstanding maintenance of pluripotency subsequently established [43]. Advances in nuclear reprogramming resulted in the induction of differentiated somatic cells into the pluripotent state, the technique that subsequently produced the cloning of Dolly the sheep in 1997 [44]. The successful somatic

cloning demonstrated that differentiated cells have all the necessary genetic information required for the development of whole organisms and also confirmed that oocytes contain factors capable of somatic cell nuclei reprogramming. In 2001, Takashi Tada's group demonstrated that ESCs also have factors that can reprogramme somatic cells [45]. All these discoveries have produced the iPSCs technology established by Shinya Yamanaka and the reprogramming of mouse fibroblast in 2006 [46]. A year later, human somatic cells were reprogrammed into human iPSCs by the exogenous expression of 4 transcription factors; octamer-binding transcription factor 4 (Oct4), sex-determining region Y box-2 (Sox2), Krüppel-like transcription factor 4 (Klf4) and myelocytomatosis viral oncogene (c-Myc)[47,48]. As for ESCs, iPSCs are self-renewable and can differentiate into all cell types of the body, showing great hopes in the field of regenerative medicine (Figure 1.3).

These days, the most common source for iPSCs are fibroblasts which are easily obtainable with a skin biopsy [49]. Reprogrammed fibroblasts (iPSCs) have been converted to various somatic cells, for example, neural cells [50], hepatocytes [51,52], cardiac myocytes [53] and hematopoietic progenitor cells [54]. However, iPSCs can be reprogrammed from a wide range of cells, such as circulating T cells, which are derived from the mesoderm; hepatocytes which have an endoderm origin and keratinocytes which are derived from the ectoderm. Each of these cells type have been successfully reprogrammed into iPSCs with 0.1% efficiency for circulating T cells and hepatocytes [55].

Integrating vectors such as retroviruses and lentivirus have been used initially for reprogramming factor overexpression [46,47,56]. Tumorigenicity is significant risk arising from the use of oncogenes (c-Myc and Klf4)[57,58] in addition to the possible presence of undifferentiated cells [59]. Moreover, the integrating vectors (retroviruses and lentivirus) might also cause insertional mutagenesis [60,61]. The advances in iPSCs technology have led to the generation of iPSC in the absence of these factors either without c-Myc or both c-Myc and Klf4 [62] decreasing liability to tumour formation in its chimaeras. Similarly, there is substantial progress regarding exogenous material exclusion by means of different methods. These methods include the plasmid [63], adenovirus [64] and Sendai virus [65] which are now routinely used in many laboratories. Moreover, it has recently been revealed that it is possible to reprogramme cells using messenger ribonucleic acid (mRNA) [66], besides microRNA (miRNA) [67] at higher efficiencies.

Currently, the study of several human diseases is performed through the use of animal models and cell lines that approximate to specific cell types. However, robust disease models are difficult to achieve because animal models inescapably involve inter-species variabilities and

primary human cells are difficult to retain in culture for an extended period [68]. An advantage of human iPSCs is that they can provide more accurate human disease models.

As mentioned, iPSCs were differentiated to various somatic cells in addition to patient-specific iPSC lines. Consequently, disease modelling has been reported, such as motor neurons from an 82-year-old amyotrophic lateral sclerosis (ALS) patient [69], motor neurons from spinal muscular atrophy [70,71] and familial dysautonomia [72].

Applying iPSC technology to drug screening is something that is widely used. iPSC-derived models of disease deliver both a practical and functional assessment of how an individual will respond to a specific therapeutic agent [73]. The utilisation of iPSC-derived disease modelling tools in high-throughput screening assays could permit better prognosis of drug-induced toxicity, for instance, hepatotoxicity and cardiotoxicity [72]

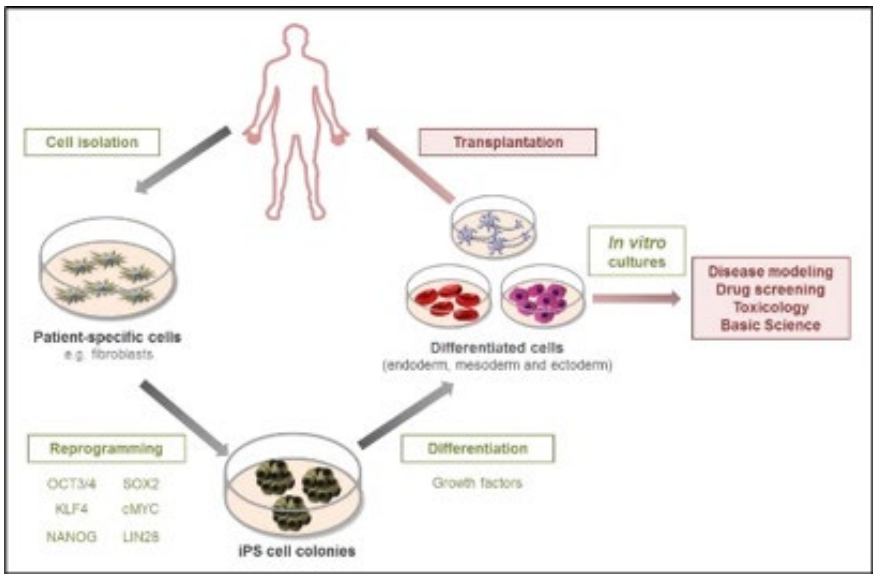

Figure 1.3 A schematic diagram shows the potential applications of induced pluripotent stem cell (iPSC). Fibroblasts or other cell types can be reprogrammed into iPSC. Afterwards, this iPSC can be used for generation of specialised cells which can be used for cell replacement therapies; otherwise, iPSC can be used for common disease modelling, drug and toxicology screening or basic biology studies [74].

1.2 The adult Liver: Anatomy and physiology

The liver is considered the largest internal organ in the body, weighing nearly 1,500 g. It is situated below the diaphragm in the right upper abdominal cavity and is protected by the rib cage. The liver is reddish-brown and is enclosed by a delicate connective tissue capsule

recognised as Glisson's capsule. It is divided into the right and left lobes by the falciform tendon that runs beside the umbilical fissure and attaches the liver to the anterior wall of the abdominal wall. The right lobe can be subdivided into anterior and posterior parts, whereas the left lobe is divided into a medial segment (quadrate lobe) and a lateral segment (caudate lobe) by the falciform ligament. Additionally, 60–70% of the liver mass is taken up by the right lobe, while the left lobe and caudate lobe make up the rest (Figure 1.4). The location of the liver interfacing with the digestive system facilitates its vital function in the processing of absorbed nutrients via the metabolism of proteins, carbohydrates and lipids. The liver is supplied by blood via a dual supply comprising the hepatic artery and the portal vein. The hepatic artery branches from the celiac artery (trunk) which also gives rise to the left gastric, splenic and common hepatic arteries. The hepatic artery delivers approximately 25% of the blood supply, while the portal vein delivers the rest of the blood supply. Portal veins deliver nutrients absorbed by the intestinal system to the liver, except the complex lipids which are transported primarily by lymphatics.

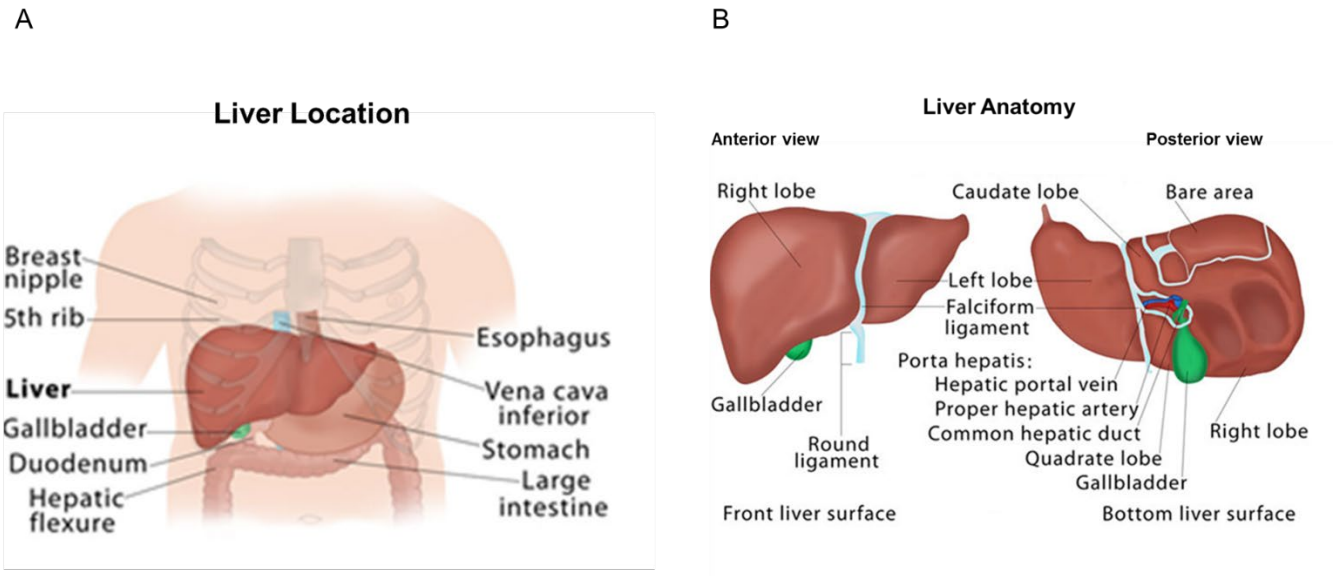

Figure 1.4 Liver location and anatomy diagram. A. The liver is the largest internal organ weighing approximately 1,500 g in the adult. It lies behind the rib cage in the upper right abdomen under the diaphragm and extends from the 5th rib to the bottom of the rib cage. B, The liver is multi-lobed in most mammalian species. In humans, the liver is mainly divided by falciform ligaments into two lobes, the right and left; the ligaments attach the liver to the abdominal wall and diaphragm. Two smaller lobes, the quadrate and caudate lobe are situated on the bottom side of the liver. [75]

1.2.1 Liver architecture

The liver consists of epithelial and mesenchymal elements arranged in microscopic functional unit near point(s) of blood entry through the portal tract and blood exit via the central veins. These structural and functional units are the lobules (first described by Kiernan) or the acinus (first described by Rappaport) [76,77](Figure 1.5). The human liver contains about one million lobules. Each lobule is about 1-2.5 mm in size, has a hexagonal shape consisting of hepatocyte plates which radiate outward from a central vein (a branch of hepatic vein) in the centre. Hepatocytes account for 78% of liver volume and constitute the dominant parenchymal cell type of the liver. They are typically arranged in cords that are one or two cells thick separated by sinusoids [78](Figure 1.5). The portal triads are regularly distributed at the apices of the lobule comprising an artery, a vein and a bile duct bundled all together by connective tissue. The blood flows from the hepatic artery, and portal vein into central veins among capillaries called the sinusoids (Figure 1.5) They are padded by endothelial cells in addition to Kupffer cells which are a specific population of cells belonging to the macrophage phagocytic system. The sinusoid endothelial lining is fenestrated to permit secure exchanging between the blood and hepatocytes via the space of Disse which is a compartment between the endothelial cells and hepatocytes that contains the blood plasma for exchange between blood and hepatocytes (Figure 1.6). In addition to the plasma, the space contains connective tissue and hepatic stellate cells (HSCs). The function of the HSCs is to control the sinusoidal blood flow and fibrogenesis, besides a prominent role for vitamin A storage [79]. The canaliculi surround each hepatocyte are generated by the tight junctions formed between neighbouring hepatocytes and are responsible for the gathering of bile salts and bile acids which are transported across the hepatocyte's apical surface (Figure 1.5). Bile assembled by the canaliculi is transported to the bile ducts in the portal triad and consequently carried to the gallbladder for storage. The lining of the bile ducts are cuboidal to columnar epithelium cells connected to a basement membrane [80] (Figure 1.5).

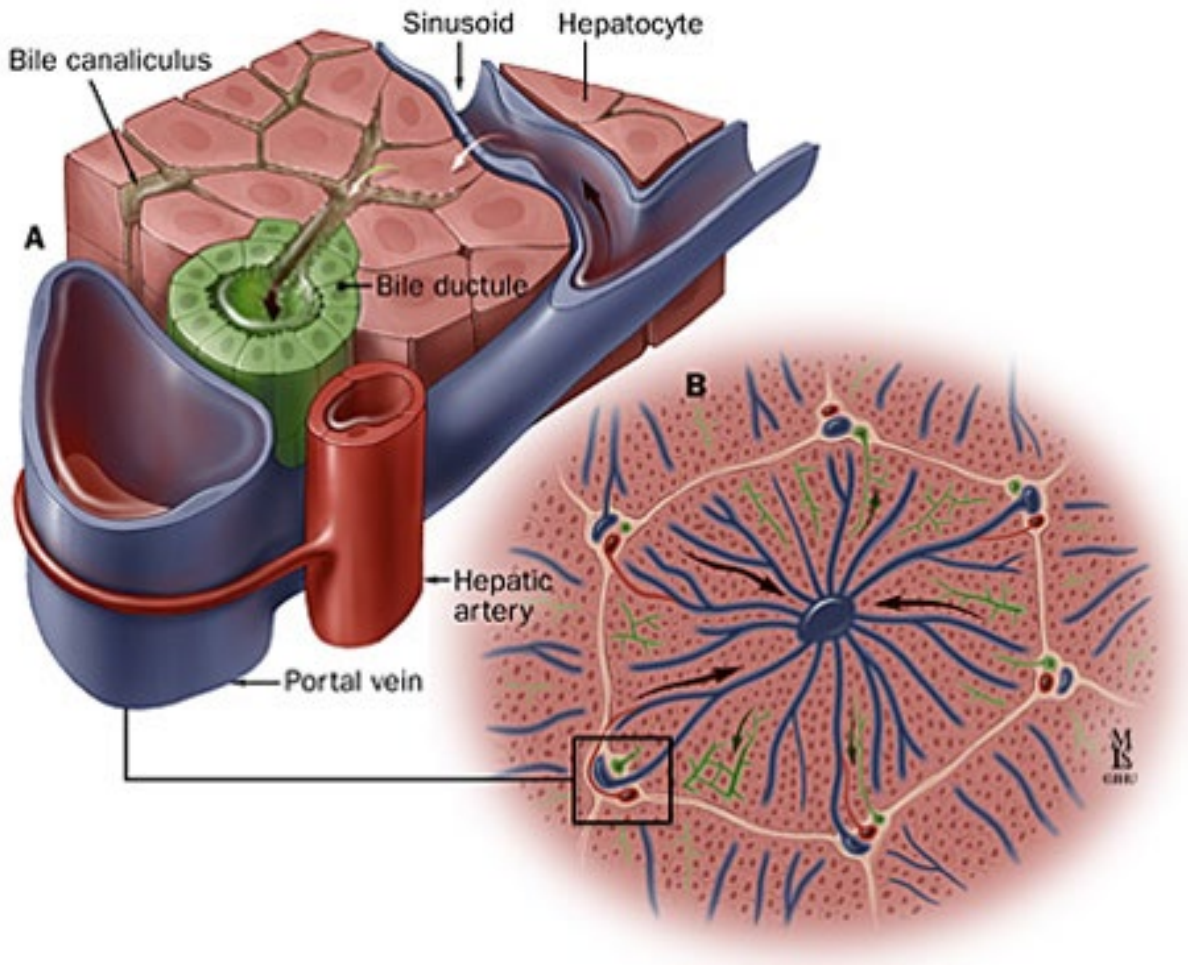

Figure 1.5 A schematic diagram of the hepatic lobule. The liver tissue made up of small lobules 1-2.5 mm in size. Each lobule consists of the central vein (a branch of the hepatic vein) surrounded by six pairs of vessels (branches of the portal the hepatic artery). A small bile duct accompanies each pair of blood vessels. The blood enters to the lobule through the portal vein and hepatic artery in the portal triad. The blood flows through the capillaries called the sinusoids into central veins. The bile is collected from the hepatic cells and carried out of the liver through bile ducts [81].

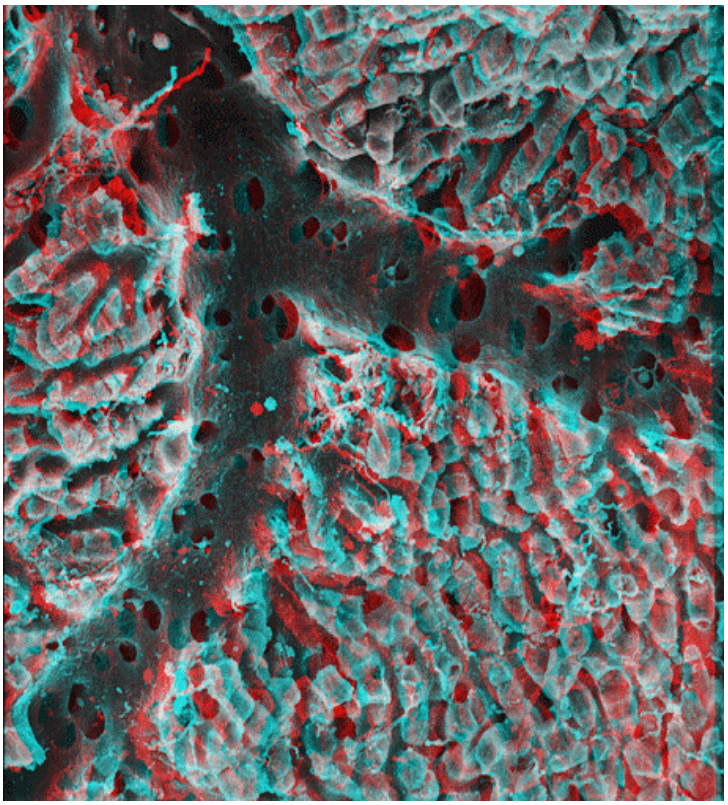

Figure 1.6The sinusoids. Electron microscopy image showing fenestrated sinusoids endothelial lining cells (grey), the hepatic plate (cyan) and connective tissue (red) [81].

1.2.2 Liver zonation

Jungermann et al. demonstrated that hepatocytes, although being histologically identical, were specialised, and perform a different function according to their site along the porto-central axis of the liver acinus, which is divided into zones corresponding to remoteness from the arterial blood supply [76]. The closest hepatocytes to the arterioles in zone 1 have an abundant supply of oxygen, whereas those in zone 3 are the farthest from the arterioles and have the most impoverished supply of oxygen. Zone 2 is presumed to be an intermediate environment. This arrangement also means that cells in zone one are the first cells exposed to blood-borne toxins absorbed into the portal blood from the small intestine [82,83]. Consequently, different pathologic processes lead to lesions that reflect acinar structure; for instance, necrotic hepatocytes at the periphery of the acinus. Acinar zones 1, 2 and 3 are parallel to the periportal, mid- and pericentral zones of the lobule, respectively. A distinctive gene expression profile exhibited by hepatocytes within each zone matches their metabolic compartmentalisation. For example, hepatocytes in zone-1 specialise in ammonia detoxification and gluconeogenesis, whereas the

zone-3 cells are committed to lipogenesis and glycolysis [84]. This zone-related heterogeneity of hepatocytes has been hypothesised as a consequence of the differential degree of exposure to oxygen, nutrition and gut-derived toxins [85]. For example, zone 3 hepatocytes mainly express cytochrome P450s, which allow xenobiotic metabolism (Figure 1.7). Xenobiotics require metabolism by Cytochrome P450 (CYP) which cause injury for most of the centrilobular area (zone three).

Even though, hepatocytes in the periportal (zone 1) are exposed first to xenobiotics absorbed by the gut, the ingestion of protoxins represents the majority of exposure to toxins and protoxins require enzyme-mediated conversion into a cytotoxic product. According to this fact, pro-toxin damage is found in the regions where the activating enzyme is expressed in addition to the lowest levels of oxygen in the centrilobular regions (zone 3), which may have an impact on the capability of cells to respond to and resist the injury. Therefore, hepatocytes are the more likely cell type damaged by hepatotoxins [86]. The evidence indicates that the gradient of WNT signalling that increases towards the central vein is thought to play a crucial role in modelling zonation. Consequently, WNT up-regulated genes are high in centrilobular regions and low in periportal regions (Figure 1.8) [87]. More recent studies on mice revealed that liver zonation is dependent on a β-catenin mechanism [88]. Thus, the upregulation of canonical WNT signalling in zone 3 might be critical for homeostatic renewal of hepatocytes in this zone [89].

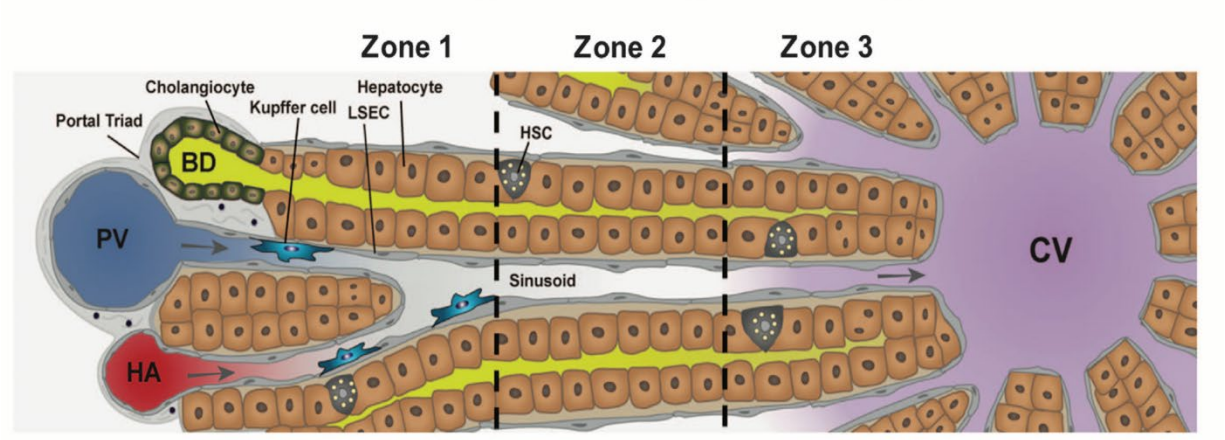

Figure 1.7 Liver cell plate acinus is divided into three zones. Zone 1 (periportal zone) surrounds the afferent vessels and the portal triad where hepatocytes are first exposed to the nutrient and oxygen-rich blood entering from the portal vein and hepatic artery. Zone 2 (intermediate zone) lies between zone 1 and zone 3. Zone 3 (centrilobular zone) where CYP450 expression is highest in hepatocytes surrounding the central vein [90].

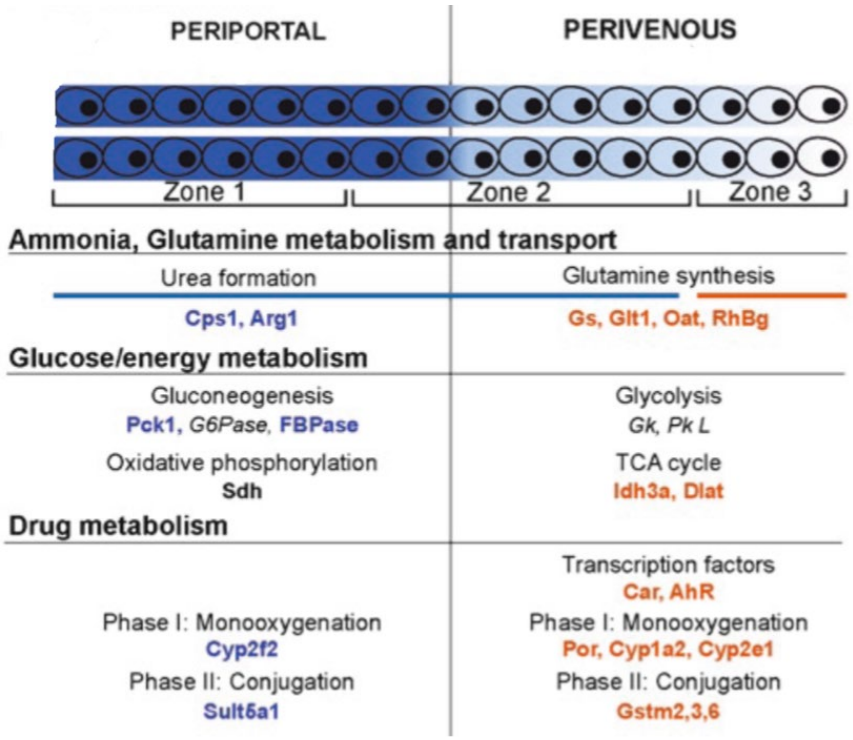

Figure 1.8 Liver zonated functions. The different metabolic functions located in different zones of the acinus include ammonia detoxification, glucose and energy metabolism, and xenobiotic metabolism. The proteins required for each type of zonal metabolism are demonstrated. The PV gene upregulated by WNT signalling are indicated in orange, while the PP genes down regulated by WNT signalling are shown in blue. Adapted from Colont et.al.(2011) [91].

1.2.3 Functions of the liver

The liver is a vital organ of the body, accountable for lots of chemical actions required by the body to survive. It is a gland because it produces chemicals which are used by other organs of the body. Therefore, the liver is considered both an organ and a gland. The human liver is believed to perform approximately 500 separate functions, most of these functions are performed in combination with other organs and systems. Most functions of the liver are carried out by the hepatocytes. These functions primarily include; metabolism of glucose, lipid, bilirubin, urea, detoxification of drugs and xenobiotics, production of serum proteins (such as albumin and clotting factors), storage of minerals and vitamins and secretion of bile, besides immunologic functions, as the liver contains cells involved in adaptive and innate immunity.

Gluconeogenesis or the synthesis of glucose from amino acids (alanine from muscle), pyruvate, and lactate is primarily carried out by the liver. Similarly, the liver performs glycogenesis which is glycogen synthesis from excess glucose for storage of glucose. In addition, glucose can be

produced from glycogen by glycogenolysis when the body requires it. Hence, the liver plays a crucial role in the maintenance of blood glucose levels which prevent hypoglycaemia maintaining glucose supply to the brain and other tissues for energy demands [92] The liver is the only organ capable of converting cholesterol to bile acids, which are necessary for the efficient absorption and transport of dietary lipid nutrients [93,94].

A further critical metabolic role of the liver is its active involvement in the detoxification and metabolism of xenobiotics and drugs due to the expression of drug metabolising enzymes (DMEs) in hepatocytes. These DMEs primarily act to modify lipophilic xenobiotics, absorbed from the gut, to create more excretable (through bile or urine) compounds by way of a three phase process — phase I xenobiotics modification, phase II xenobiotics conjugation and phase III further modification and excretion. In phase I, liver enzymes are accountable for the metabolism of xenobiotics by first activating them via oxidation, reduction, hydrolysis or hydration reactions. These chemical reactions add or expose functional groups such as -OH, -SH, -NH2 or –COOH on the substance [95], which facilitate the subsequent conjugation of hydrophilic groups by phase II conjugation enzymes. In humans, the majority of the drug oxidation in phase I reactions involves flavin-containing monooxygenases and the superfamily of CYP monooxygenases. Hepatic microsomal cytochrome P450 is a paradigm of a group of enzymes required for xenobiotic metabolism [96]. The primary drug metabolising P450 in the human liver is CYP3A4; it constitutes up to 60% of P450 enzymes in the liver and metabolises up to 75% of drugs metabolism [97]. The conjugation reactions in phase II include sulphation, methylation and glucuronidation for an additional increase in the solubility of oxidised metabolites. In phase III, the xenobiotic conjugates may be further metabolised in addition to the induction of the drug transporters in the membranes of hepatocytes, kidney, intestine cells and other tissues for excretion out of the body [98]

The liver also plays one more vital function in purifying the body from toxic substances by converting ammonia into a water-soluble compound known as urea. Ammonia is a toxic weak basic compound derived from the metabolism of amino acids. Severe liver injury results in the accumulation of ammonia which is toxic to the brain and other parts of the central nervous system (CNS). The ammonia detoxification process takes place primarily in the liver. This process is carried out through a cycle of biochemical reactions known as the urea cycle which consists of four enzymatic reactions: one in the mitochondria and three in the cytosol [99].

Liver cells

The hepatocyte is polygonal in shape. It measures approximately 25 to 40 μm and comprises a large amount of smooth endoplasmic reticulum in the cytoplasm, while most cells in the body have only small amounts. The cytoplasm contains abundant glycogen and is eosinophilic reflecting numerous mitochondria and a central nucleus (binucleate cells are also typical). The nucleus is round or oval, with dispersed chromatin and prominent basophilic nucleoli containing abundant rough endoplasmic reticulum [100]. All these features allow the hepatocytes to perform its crucial metabolic and synthetic functions, for instance protein synthesis and storage, synthesis of bile salts, detoxification of cholesterol and phospholipids, elimination of exogenous and endogenous substances, as well as induction of bile formation and secretion. Typically, hepatocytes are arranged in one or two cells thick cords separated by sinusoids. They form a critically important cell layer to separate the sinusoidal blood from canaliculus bile. The cell membrane of the hepatocyte faces the sinusoids basolateral and forms the biliary canaliculus with the next hepatocyte. Moreover, it has a portion next to the canaliculus that attaches laterally to the next hepatocyte. This position of hepatocyte between the blood plasma flow in the sinusoid and the bile in the canaliculus contributes to their proper organised polarity [101] (Figure 1.9).

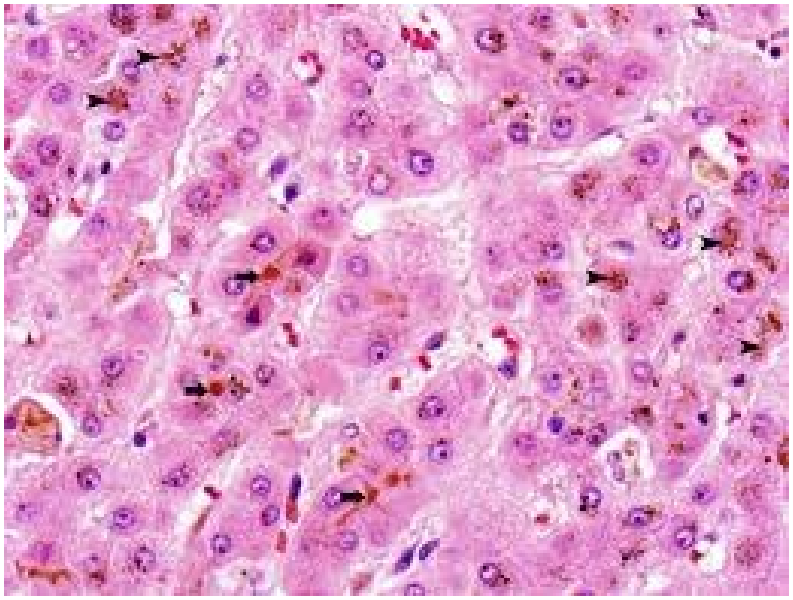

Figure 1.9Microscopic micrograph of H & E stained hepatocyte cords. Arrowheads show the accumulation of brown coarse granules of iron. Arrows illustrate the bile (greenish-brown) within biliary canaliculi that are situated between hepatocytes (H & E stain, magnification x500) [100].

Cholangiocytes or biliary epithelial cells (BECs) are epithelial cells lining the biliary tree which is a three-dimensional network of bile ducts. Cholangiocytes participate in the modification of the hepatic bile when it is conveyed through the biliary tree. They contribute to

bile modification by managed transportation of several ions, solutes and water via the cholangiocyte apical and basolateral plasma membranes. Several locally acting hormones mediate cholangiocyte fluid and electrolyte secretion [102]. Cholangiocytes also have a role in inflammatory responses; they interact with other liver cell types through the production of many growth factors, peptides and pro-inflammatory and chemotactic cytokines. [103].

Hepatic stellate cells (HSCs) are also known as vitamin A-storing cells, interstitial cells, fat-storing cells, lipocytes and Ito cells. HSCs are located in the space of Dissè between the hepatocytes and liver sinusoidal endothelial cells. They primarily function to store the majority of vitamin A in the body in lipid droplets as retinyl ester in the cytoplasm. Physiologically, these cells are quiescent and play important roles in the regulation of retinoid homeostasis. In pathological conditions such as in acute liver injury, the population of HSCs expand and increase their expression of alpha-smooth muscle actin. In chronic liver injury, HSCs lose vitamin A and synthesise an abundant extracellular matrix (ECM) elements like proteoglycan, glycosaminoglycan, collagen and adhesive glycoproteins, besides morphological changes from the HSCs star-like shape to that of fibroblasts or myofibroblasts shape [104]

Kupffer cells are liver-resident macrophages. They adhere to the sinusoidal side of endothelial cells and are found primarily in the periportal region of the liver [105]. This localisation allows them to act as the first line of protection against immunoreactive material transferred from the gut by the portal circulation. They stop the movement of these gut-derived immune-reactive substances from travelling beyond the hepatic sinusoid. Likewise, they maintain blood homeostasis through the phagocytosis of large particles and dead erythrocytes and microorganisms. While in many conditions such as toxin-induced fibrosis [106] and drug-induced liver injury [107], the Kupffer cells are protective. Additionally, the direct or indirect activation of Kupffer cells by toxic agents leads to the release of a group of inflammation mediators, reactive oxygen species and growth factors. This activation appears to account for the modulation of acute hepatocyte injury as well as chronic liver reactions such as hepatic cancer [108].

Liver sinusoidal endothelial cells (LSECs) form the walls of the hepatic sinusoids and comprise the highest proportion of non-parenchymal cells in the liver. They exhibit distinctive phenotypic and structural characteristics which discriminate them from the capillary endothelium found in other organs. LSECs are fenestrated by many pores of 100 to 150 nm diameters. This fenestration provides channels between the sinusoidal blood and the subendothelial space of Disse [79], as described previously in Section 1.2.1. Under normal physiological conditions, the fenestrations mediate the exchange of plasma, nutrients, lipids and

lipoproteins between hepatic sinusoids and hepatocytes [109,110]. LSECs show a high endocytic capacity in comparison to other endothelial cells mediated via distinct endocytosis receptors, giving them importance as the most efficient scavengers of blood-borne waste macromolecules and nanoparticles in the body [111].

1.3 Overview of liver development

1.3.1 Endoderm formation

In the early stages of development, the epiblast is differentiated from the ICM of the preimplantation blastocyst. The epiblast represents the source of the gastrula, i.e. the three germ layers; ectoderm, mesoderm and definitive endoderm (DE) [112]. When the pluripotent epiblast cells travel through the PS, DE is developed [113,114]. Subsequently, the multipotent endoderm gives rise to the epithelium of the gastrointestinal and the respiratory systems, as well as the glandular and ductal cells of the liver, pancreas, thyroid and thymus. In the earliest stages, studies discovered the requirement for high doses of the TGF-β family member Nodal for DE induction during gastrulation [113,115,116]. Nodal signalling motivates the expression of an array of endoderm transcription factors comprising the forkhead domain proteins Foxa1–3 and the HMG domain DNA-binding factor (Sox17). These transcription factors consecutively control a cascade of genes that direct cells to the endoderm lineage [117].

1.3.2 Endoderm patterning: making the foregut

Higher levels of nodal signalling are demanded by anterior endoderm fate than posterior endoderm cells. The expression of Foxa2 is also essential to make anterior definitive endoderm (ADE)[117,118]. After gastrulation, naive endoderm cells remain plastic and not yet dedicated to specific organ fates. After 48 hours, the endoderm germ layer develops a primitive gut tube. It is from this tube that the organ buds arise. During this time, the endoderm along the A-P axis gradually subdivides into foregut, midgut and hindgut domains by the action of a sequence of overlying growth factor signals from the adjacent mesoderm[119]. These domains which can give rise to several organs are distinguished by the expression of transcription factors, for example Hhex in the foregut, pancreatic and duodenal homeobox gene 1(Pdx1) in the midgut and Cdx in the posterior endoderm, distinguishing these domains which then give rise to several organs [120].

1.3.3 Foregut development requires repression of WNT/β-catenin and FGF4

Due to dynamic tissue movements during gastrula and early somite stages, the endoderm becomes proximal to various mesodermal tissues which produce the patterning factors. These factors comprise FGF, WNT and BMP ligands, and moreover, all of them appear to retain hindgut identity and block the foregut fate in the posterior [121,122] Experiments in Xenopus and chick propose that FGF4 and WNTs secreted from the posterior mesoderm prevent foregut fate and encourage hindgut development [123] (Figure 1.10). Experiments in Xenopus exhibited that preventing the activity of the canonical WNT effector β-catenin in posterior endoderm resulted in activation of Hhex expression and liver bud formation in the intestine [124]. Surprisingly a few hours after development, FGF and WNT signalling have contrasting effects and encourage hepatic development [125].

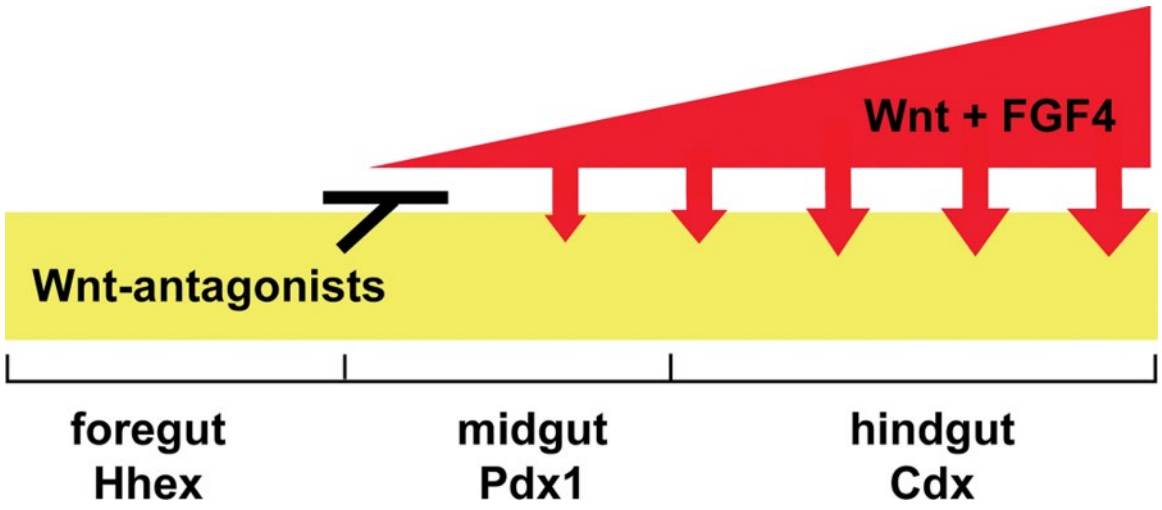

Figure 1.10 An outline of endoderm patterning by WNT and FGF

In the first gastrulation and somite phases: different WNT and FGF signalling through the A-P axis divides the primitive endoderm into foregut, midgut and hindgut progenitor areas expressing the different transcription factors Hhex, Pdx1 and Cdx as indicated. The data from the available literature suggest that WNT and FGF ligands are expressed progressively in the mesoderm (indicated in red) next to the endoderm (depicted by yellow) to prevent foregut formation and stimulate hindgut fate. Canonical WNT/β-catenin activity is expected to be repressed by WNT-antagonists expressed in the anterior endoderm [126].

1.3.4 Hepatic competence

In vivo, the foregut endoderm only can develop into the liver [127,128]. Initial foregut organogenesis is significantly impacted by the expression of transcription factors, such as Hhex,

GATA-binding proteins (Gata4–6) and Foxa2 [129]. This expression could explain the intrinsic hepatic competence. The liver-specific serum albumin gene expression has been identified to develop via three developmental stages. During the first stage, the nucleosomes appear tightly packed and the gene is in closed chromatin and transcriptionally inactive. In the second stage, the enhancer element of the gene is bound to Foxa and Gata transcription factors. One biochemical studies has shown that this binding is adequate to enhance chromatin accessibility by creating a locally open domain of nucleosomes [130], although it is insufficient to trigger the transcription of the gene [131]. In endoderm cells, this open chromatin domain encourages the competence of these hepatic genes to be transcribed. In the third stage, liver genes become activated in the hepatic endoderm due to the stimulus of different signals from the mesoderm, more transcription-factor-binding sites at the enhancer become occupied (C/EBP, CCAAT/enhancer binding protein, nuclear factor 1), as well as at the promoter which activates the albumin gene [114].

1.3.5 Hepatic induction by FGF and BMP

As mentioned previously, mesodermal signalling is crucial for endoderm patterning into discrete tissue areas. The organogenesis of the embryonic gut tube is affected by FGF signalling in different ways. Studies on mice propose different thresholds of FGF signalling released from the cardiac mesoderm resulting in the production of liver, pancreas and lung lineages from the progenitor cells of the ventral foregut. *In vitro* experiments performed on mice showed that applying the recombinant FGF signalling in moderate doses, induced liver-specific gene expression [132]. In other studies using mice, the cells of the septum transversum mesenchyme, which are a distinctive mesoderm cell type, are found close to the ventral endoderm and influence the hepatic induction. Using an inhibitor of BMPs and a mouse Bmp4 null mutation, it was realised that BMP signalling triggered by the septum transversum mesenchyme is essential to exclude pancreatic fate and to stimulate liver genes in the endoderm [133]. BMPs influence the levels of the GATA4 transcription factor and act similarly to FGF signalling produced from the cardiac mesoderm. This information indicates that the specification of the endodermal domain for the liver is controlled by coincident signalling from specific mesodermal suppliers [133] (Figure 1.11). Signal transduction analysis revealed that FGF signals induce hepatic gene expression by means of MAP kinase, whereas the hepatic growth is regulated by PI3 kinase [134].

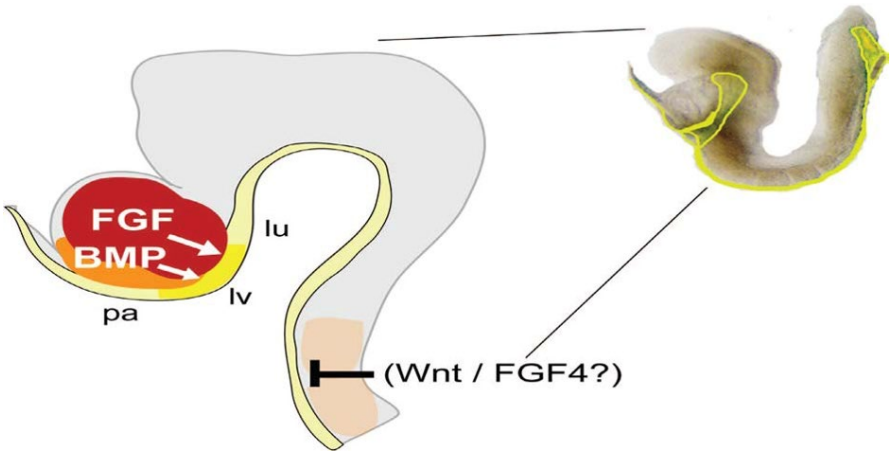

Figure 1.11 Hepatic induction. The figure demonstrates the anterior segment of an e8.25 of the mouse embryo in the 2–4 somite phase (lateral view). The grey indicates the growing head. The yellow demonstrates the DE which is forming a foregut pocket. The liver (lv) in a part of the ventral foregut is triggered by BMP signals produced from the septum transversum mesenchyme (orange) and the FGF from cardiogenic mesoderm (red). Hepatic fate is specified, while foregut endoderm will express liver genes, such as Albumin after the 5–7 somite stage. Different doses of FGF appear to provoke ventral pancreas (pa) and lung (lu) from the progenitors of the foregut. In the dorsal endoderm, FGF4 and WNT signals from the axial mesoderm block hepatic fate [126].

1.3.6 Liver bud morphogenesis and growth

After FGF and BMP signals have specified the hepatic endoderm from the septum transversum and cardiac mesenchyme, the hepatic epithelium begins to express liver-specific genes, for instance α- fetoprotein (Afp), Hnf4α , albumin and becomes columnar in shape, the contiguous basement membrane ruptures and the hepatoblasts (hepatic precursors) proliferate and move to the nearby stroma and develop the liver bud. Transcription factors (such as Hhex, Hnf6/Onecut1, Onecut2, Prox1 and Gata4/6) are essential to stimulate the morphogenesis of the liver bud. Hepatoblast migration, proliferation and survival are regulated by paracrine signals from hepatic mesenchyme and endothelial cells including FGF, BMP, WNT, HGF, TGF-β and retinoic acid (RA) in addition to the transcription factor such as by hepatocyte nuclear factor 4 (Hnf4α), T-box transcription factor (Tbx3) and Hlx [135].

1.3.7 Hepatocytes and biliary epithelial cells differentiation

Hepatoblasts are bi-potential, expressing genes related to both adult hepatocytes which marked by albumin and Hnf4α and cholangiocytes which marked by cytokeratin-19, in addition to foetal liver genes like Afp. Their differentiation into hepatocytes or cholangiocytes depends on their sites. Those cells located adjacent to the portal vein mesenchyme are encouraged to

differentiate into cholangiocytes by a Notch-mediated process, while the cells located more in-depth in the parenchyma produce hepatocytes [135]. In response to the mesenchyme signals (possibly TGFβ and WNTs), hepatoblasts adjacent to the portal mesenchyme down regulate pro-hepatic factors *HNF4α*, *Tbx3* and *C/EBP* and increase expression of BEC transcription factors *OC1/HNF6*, *OC2* and *HNF1β*. Continued signalling from the periportal mesenchyme (Notch, EGF and HGF) are essential for ductal plate remodelling. In comparison, hepatoblasts in the parenchyma not exposed to periportal mesenchyme signals, activate the expression of hepatogenic factors. Subsequently, factors such as oncostatin M (OSM), glucocorticoids, hepatocyte growth factor (HGF) and WNT promote hepatocyte maturation [126]

1.4 Liver disease and regeneration

1.4.1 Liver disease and cirrhosis

Liver disease causes around 2 million mortalities each year worldwide; specifically, 1 million caused by viral hepatitis and hepatocellular carcinoma HCC and 1 million owing to complications with cirrhosis. At present, cirrhosis is the 11th most frequent reason for fatality worldwide, whilst liver cancer is the 16th most common cause of fatality; together, they account for 3.5% of all deaths internationally. Worldwide, approximately 2 billion people drink alcohol, and more than 75 million suffering from alcohol-use disorders and are endangered by alcohol-related liver disease. Roughly 2 billion adult people are overweight or obese, and more than 400 million are diabetics; which places them at risk of non-alcoholic fatty liver disease as well as hepatocellular carcinoma. The global predominance of viral hepatitis remains elevated; however, drug-induced liver injury keeps increasing as a leading trigger of acute hepatitis. Liver transplantation is the second most common solid organ transplantation and just less than 10% of global transplantation requests are met at existing rates (Table 1.1) [136].

Liver cirrhosis is characterised by replacement of liver tissue by dense fibrous scar tissue as well as a continued stimulus for regeneration, which results in widespread distortion of standard hepatic architecture and a transformation to a nodular architecture [137]. Hepatocytes primarily in zone 3 are more likely to be exposed to hepatic pro-toxins which results in necrosis. Signals from damaged cells generate Kupffer cell activation which in turn release a range of chemokines and cytokines that result in activation of both resident and circulating leucocytes [138,139]. In response to the injury, several alterations in the liver architecture along with changes in the expression of adhesion proteins in sinusoidal endothelial cells that results in loss of fenestrae take place. This injury results in a conversion of hepatic stellate cells into

myofibroblasts, which proliferate and secrete extracellular matrix proteins and fibrosis. In the acute conditions and under some chronic conditions, fibrosis may be reversible. However, if the liver damage continues to re-occur through repeated acute incidents within a particular period of time, the resolution, myofibroblast increase in numbers leading to a distorted hepatic architecture and vascular structure by the formation of fibrous scar tissue, eventually developing into cirrhosis and liver failure [140].

Unfortunately, the treatment options for most of the hepatic diseases are limited. Up to now, the majority of the treatments for chronic liver disease have been directed at the causing agent: for instance, there are several active antiviral agents as therapies for hepatitis B and C. Likewise, there are many immunosuppressive agents which are given for immune-driven disease, such as autoimmune hepatitis. Even though these agents regularly have a beneficial effect on the degree of fibrosis, researchers are currently focusing on the development of drugs that are precisely developed to interfere with fibrosis. As the disease is only associated with general symptoms like malaise and fatigue, the risk of developing liver cirrhosis or hepatocellular carcinoma, consequently liver failure is increased. For end-stage liver disease, the only available option for treatment is orthotopic transplantation. Hepatocyte transplantation is the alternative to whole organ transplantation for patients with hepatic failure or hereditary liver disease.

	Cirrhosis and the liver			HCC	
	Worldwide rank	Mortalities (000s)	% of total mortalities	CDR (per 100,000 population)	Mortalities (000s)
World	11	1,162	2.1	15.8	788
Pacific & East Asia	13	328	2.0	14.4	547
Central Asia & Europe	17	115	1.2	12.7	78
Caribbean & Latin America	9	98	2.7	15.6	33
North Africa & Middle East	8	77	3.5	18.2	24
North America	12	50	1.7	14.0	27
South Asia	10	314	2.5	18.0	38
Sub-Saharan Africa	16	179	1.9	17.9	42

Table 1.1 Worldwide deaths related to liver cirrhosis and liver cancer 2015.
Adapted from Asrani (2019)[136].

1.4.2 Liver regeneration

The liver performs crucial physiological functions and the malfunctions of the liver directly threaten life. Hence, the liver retains an exceptional regeneration capacity after injury. The organ can maintain homeostasis via either the replication of mature cells or the differentiation of stem cells. The synthetic and metabolic functions of the liver are predominantly performed by hepatocytes. Therefore, the default pathway in response to mild-to-moderate acute liver injury is for hepatocyte-mediated liver regeneration. In conditions such as massive hepatocyte loss or severe viral hepatitis which result in mature hepatocytes replication impairment, the response to these severe injuries is associated with activation and expansion of adult hepatic progenitor cells (HPCs) [141,142,143]. HPCs existence in normal liver are characterised by expression of surface markers involving epithelial cell adhesion molecule (EpCAM), CD13 and CD133 [144]. HPCs also express markers of both biliary epithelial cells (K7, K19 and K14) and hepatocytes lineages (K8, K18, C-met and albumin) [145,146].

The origin of HPCs has been much debated; traditionally they are thought to be small epithelial cells of the bile duct situated in the canal of Hering, the structures that reside between the intrahepatic bile ducts and hepatocyte-lined canaliculi [147](Figure 1.12). Similarly, early investigations suggested an extrahepatic origin such as bone marrow [148]. It has been suggested that HPCs may originate from HSCs, as they express the same genes as undifferentiated cells in rats and contain many similar signalling pathways [149]. More recent studies suggest that HPCs may originate from the dedifferentiation of mature hepatocytes or bile ductular epithelial cells in response to liver damage, proposing that the conversion from hepatocytes or bile ductular epithelial cells to HPCs is a reversible process after recovery from injury [150]. Moreover, in addition to the canal of Hering at least three more discrete niches have been determined: intralobular bile ducts, periductal cells and peribiliary hepatocytes.

Due to the lack of expression of a unique HPCs specific marker, the understanding of mechanisms originating bidirectional differentiation capacity of HPCs is inadequate. It is expected that the interaction between different constituents of HPCs niche is the vital factor controlling the self-renewal, activation, maintenance and differentiation capacity of the HPCs. Therefore, the potential of HPCs to contribute to liver regeneration could be related to the type and the severity of liver injury [151,152,153].

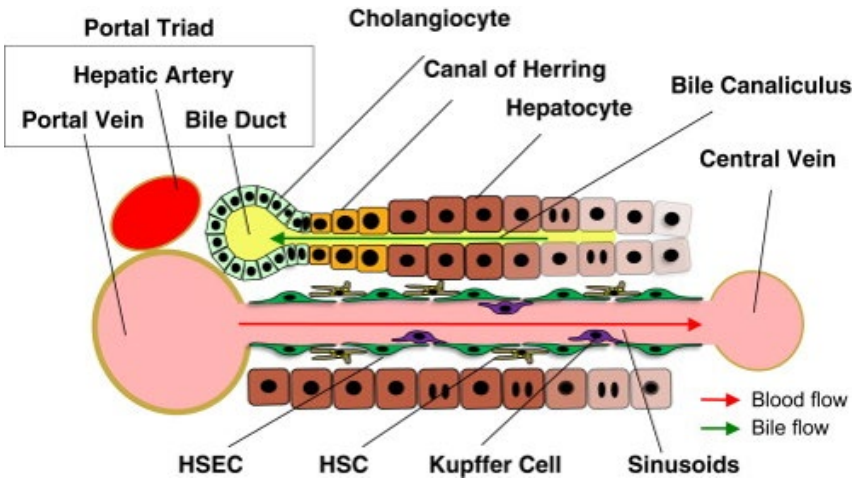

Figure 1.12 Schematic overview of liver lobule demonstrating the site of the canal of Hering. The Canal of Hering is located in the junctional region between the hepatocytes and bile ducts [154].

1.5 Transdifferentiation of pancreas to liver

1.5.1 Pancreas anatomy and physiology

The pancreas is a tapered 6-inch long gland that is located behind the stomach across the back of the abdomen. It extends through the abdomen from the curved part of the duodenum to the spleen. The pancreas' head is connecting to the duodenum and it is the broadest region of the organ. The organ extends laterally to the left and slightly narrowing forming the body of the pancreas. The narrow, tapered region extends from the body of the organ into the left side of the abdominal cavity close to the spleen is called the tail of the pancreas [155](Figure 1.13).

The pancreas consists of exocrine and endocrine glandular tissue. Therefore, it is categorised as a heterocrine gland. The exocrine tissue forms approximately 99% of the pancreas mass. It is organised into several small groups recognised as acini, which are small collections of exocrine cells surrounding tiny ducts to form a raspberry-like structure. The acini exocrine cells secrete digestive enzymes which are excreted to the acini ducts. The products of many acini run into the largest pancreatic duct formed by joining the ducts of numerous acini [156] (Figure 1.13). The exocrine part of the pancreas performs a significant role in food digestion. The partially digested food is discharged slowly from the stomach into the duodenum in the form of a chyme, which is a thick, acidic liquid.

Acini of the pancreas secrete pancreatic juice to be released into the duodenum to accomplish the chyme's digestion. Pancreatic juice is a blend of salts, water, bicarbonate, as well as several

digestive enzymes. The pancreatic juice contains bicarbonate ions which act to neutralise the acidity of chyme to protect the wall of the intestine in addition to the generation of a proper environment for the pancreatic enzymes to function [157]. The pancreatic enzymes specialise in digesting certain compounds that exist in chyme; such enzymes include amylase, trypsin, chymotrypsin, carboxypeptidase, lipase and nucleases [158].

The endocrine tissue makes up 1% of the weight of the pancreas and it secretes hormones into the bloodstream. It consists of small collections of cells known as islets of Langerhans. Numerous capillaries flow through each islet to convey hormones to the other parts of the body. Alpha and beta cells are the main types of endocrine cells which make up the islets (Figure 1.13). The endocrine portion of the pancreas act to regulate the glucose homeostasis in the bloodstream. The glucose levels in the blood must be maintained within specific borders to secure a steady source of glucose nourishing the cells of the body, although not to excess, as glucose could damage organs such as the kidney. The pancreas produces glucagon and insulin hormones in order to control blood sugar. The glucagon is secreted by the alpha cells. It increases blood glucose concentrations by motivating the liver and adipose tissue to breakdown the glycogen and triglycerides respectively into glucose to be released into the blood [159].

Moreover, insulin is secreted by the beta cells which reduces blood glucose concentrations following a meal by increasing the taking of glucose by the liver, muscle and adipose tissues. Insulin promotes the storage of absorbed glucose in the forms of the glycogen in the muscles and liver and triglycerides in adipose tissue [160].

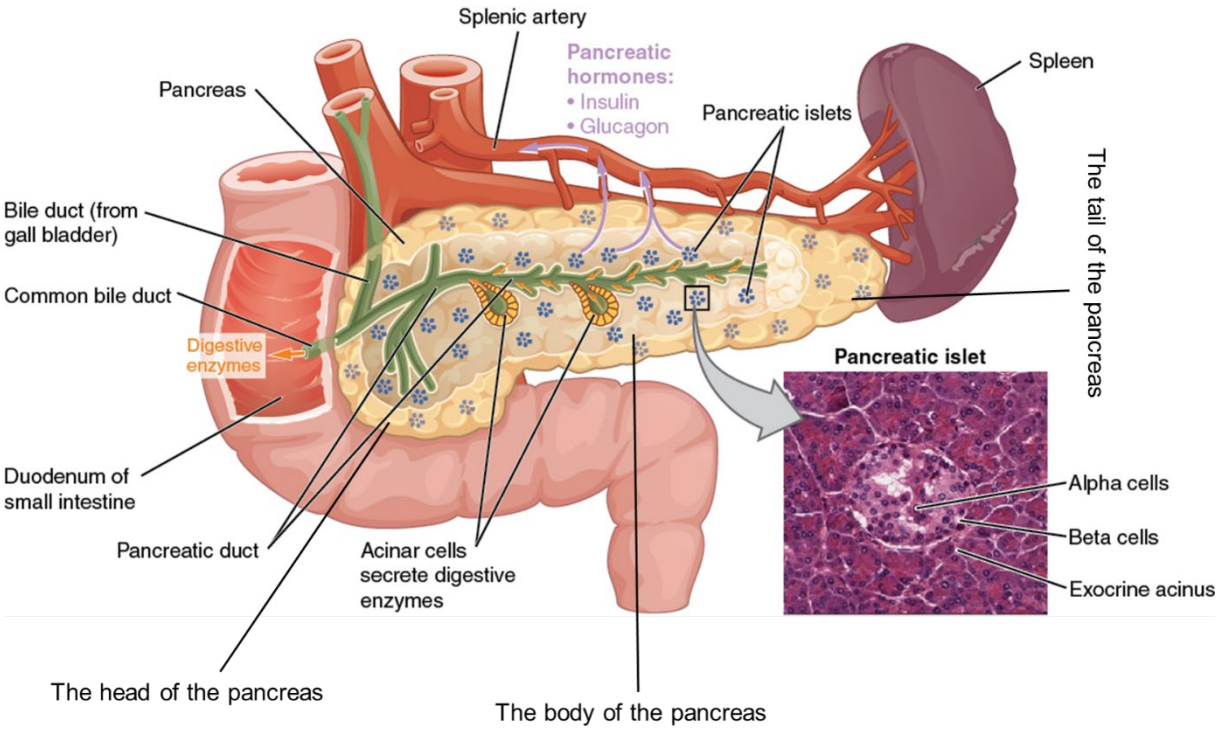

Figure 1.13 An illustration of the anatomy of the pancreas. The pancreas crosses the abdomen laterally and superiorly toward the left side. The most broad part of the organ lies in the bend of the duodenum is called the head (right side). The body of the pancreas is the tapered part extending up slightly (left side). The end close to the spleen is the organ, the tail. It consists of two types of glands: the exocrine gland made of small clusters of acinar cells and secretes digestive enzymes which are released via a network of ducts joined to form the main pancreatic duct. Additionally, the endocrine gland, made up of the islets of Langerhans, secretes hormones into the bloodstream [161].

1.5.2 Overview of signals defining hepatic and pancreatic progenitors

Many genetic approaches have revealed that the pancreas and liver cells are derived from the endoderm germ layer after hours of endoderm development. The endodermal epithelium folds to the anterior of the gut tube to create the foregut and to the posterior to create the hindgut. Primarily, general suppression of fibroblast growth factor 4 (FGF4) and mesodermal WNT signalling in the foregut permits liver and pancreas induction. In the ventral foregut, bone morphogenetic protein (BMP) from septum transversum mesenchyme cells and FGF from the cardiac mesoderm promote the liver programme and suppress the pancreas programme [114]. Subsequent morphogenetic movements assist in foregut closure. During this process, the undifferentiated cells of lateral ventral endoderm avoid the pancreas inhibitory FGF because they move caudal to the cardiac domain and can initiate ventral pancreatic development. The liver and ventral pancreas bud are characterised by the expression of Hex [162,163]. Activin and FGF signals from the notochord block sonic hedgehog (Shh) signalling within the dorsal foregut endoderm allowing the pancreatic programme [164].

After activation of gene expression for the liver or pancreas, the epithelium of the endoderm changes to a columnar appearance. The cells of hepatic and pancreatic endoderm then migrate to the adjacent mesenchyme making tissue buds which become vascularised and proliferate [162]. Therefore, the embryonic development of the liver and pancreas are similar and may explain the observed transdifferentiation of cell types in adulthood.

1.5.3 The trans-differentiation

Throughout embryogenesis, neighbouring tissues that develop in a shared cell layer will possess similar combinations of transcription factors specifying their fate. Tissues develop by varying the expression of a small number of transcription factors [165,166]. This close developmental relationship is giving the cells of these tissues the ability to interconvert in some cases of chronic tissue damage and regeneration [167]

The term metaplasia is used to describe the conversion of cells or tissue from one phenotype to another and can comprise the direct transformations of differentiated cells as well as stem cells [165,166]. In human pathology, the term metaplasia has been extensively used to define the unpredicted exhibition of unrelated tissues in ectopic sites [168], for instance, the appearance of patches of intestinal epithelium in the stomach [169]. In contrast, transdifferentiation is described as an irreversible switching of the cells that already differentiated to another phenotype, which signifies the loss of one phenotype and the acquisition of another [170]. The term 'transdifferentiation' was first proposed by Selman and Kafatos to explain a change in cell differentiation when they observed a switch in cell type during metamorphosis in the silk moth [171].

1.5.4 Transdifferentiation of pancreatic cells into hepatocytes in vivo

Several pathological and experimental conditions lead to the transdifferentiation of pancreatic cells to hepatocytes. In 1981, Scarpelli and Rao used a methionine-deficient diet protocol to stimulate pancreas injury and regeneration in a Syrian golden hamster and observed hepatocytes in the regenerating pancreas, their observation was confirmed by detecting a variety of morphological features in addition to the expression of albumin and peroxisomes [172]. Since then, various protocols have been used for the *in vivo* induction of hepatocyte in the pancreas, for example, the use of peroxisome proliferators treatment (e.g. ciprofibrate) [173,174] or particular carcinogens [175] and epithelial cells transplantation [176]. The copper-depletion protocol is perhaps the most widely examined *in vivo* model of the hepatic metaplasia of the pancreas [175,177,178]. Such a model is extremely reproducible *in vivo*. For example, hepatocytes may be induced in

the pancreas of adult rats kept for 7–9 weeks on a copper-deficient diet supplemented with a copper-chelating agent. This results in a near total loss of pancreatic acinar cells and formation of numerous foci of hepatocytes during the recovery stage. Moreover, the liver cells in some animals occupied more than 60% of pancreatic volume within weeks 6–8 of recovery [177]. The copper-deficient protocol results in the expression of HNF-1, HNF-3a, HNF-3b, HNF-4, C/EBPa and C/EBPβ in the pancreas of copper-depletion rat [178,179].

Several of these transcription factors are mutual to both pancreas and liver [180] and it appears doubtful that factors typically found in both pancreas and liver tissues would be responsible for the transdifferentiation. However, the liver-enriched transcription factors LETFs (C/EBPβ) is not naturally expressed in the pancreas. Utilising *in vitro* model (treatment of organ cultures of mouse embryonic pancreas with DEX), show that it DEX is associated with an elevation of expression of the transcription factor C/EBPβ (CCAAT/ enhancer-binding protein β) and a reduction of the transcription factor Pdx-1. DEX also induces the appearance of hepatocyte-like cells in organ cultures of the pancreas, based on the expression of liver markers, albumin, α1-antitrypsin and transthyretin. These findings suggested that C/EBPβ is a crucial component that discriminates between the liver and pancreatic differentiation programme [181]. Several different cell origins for pancreatic hepatocytes have been suggested by using *in vivo* model systems ; specifically, the suggested origins include acinar, endocrine or ductular cells [174,176,182]. For example, using peroxisome proliferators induced hepatocytes in the pancreas of an adult male when added to their diet. Uricase-containing crystalloid nucleoids, specific for rat hepatocyte peroxisomes, existed in pancreatic hepatocytes. These structures assisted the detection of cells with hybrid cytoplasmic characteristics of pancreatic acinar and endocrine cells and hepatocytes. Such cells are assumed to represent a transitional stage in which pancreas-specific genes are being repressed while liver-specific ones are simultaneously expressed. The presence of exocrine and/or endocrine secretory granules in transitional cells suggests that acinar/intermediate cells represent the precursor cell from which pancreatic hepatocytes are derived [174].

since the embryonic development of the liver and pancreas are induced from the adjacent area in the foregut endoderm [183]. This suggests that the difference in developmental specification of the liver and pancreas refers to the expression of only a few genes which also means the possibility to induce the conversion of liver into the pancreas (reverse transdifferentiation).

The transdifferentiation of liver into the pancreatic exocrine tissue has been observed in animal experiments and certain human pathologies. It has been demonstrated in the livers of rats after

treatment with polychlorinated biphenyls [184], in the liver of fish treated with chemical carcinogens [185] or in the human liver of a patient with hepatic carcinoma [186]. Moreover, the hepatocytes have been reversely transdifferentiated into pancreatic cells by adenoviral-mediated expression of PDX1 which induced the conversion of hepatocytes into insulin-producing pancreatic β-like cells in mice with budding β-cells to ameliorate Type 1 diabetes mellitus [187,188].

These finding offered evidence regarding the origin of pancreatic hepatocytes. However, the difficulties in using the whole-animal experiments such as the ethical concern in addition to the requirement of time-consuming protocols and very high cost involved in breeding and housing has pushed the experts to use the pancreatic AR42J-B13 cells to establish the cell lineage experiment and to investigate the molecular and cellular basis of the transdifferentiation of pancreas to liver. In contrast to whole animal studies, cell lines offer several advantages, such as they are cost-effective, easy to use, provide an unlimited supply of material and bypass ethical concerns associated with the use of animal tissue. More advantages of using the pancreatic AR42J-B13 cells to establish the cell lineage experiment instead of the whole animal are ensuring that the starting populations are clearly defined and markers used to mark the cells remain exclusively in the original cells and their progeny and will not diffuse to the neighbouring cells.

1.5.5 Trans-differentiation of B-13 cells to hepatocyte (B-13/H cells)

The AR42J is a cell line isolated from adenocarcinoma of an azaserine-treated Wistar/Lewis rat [189]. Azaserine is a natural antibiotic initially isolated from Streptomyces fragilis [190] that causes cytotoxicity in cells. Only one intraperitoneal inoculation of 30 mg azaserine per kg body weight is efficient to induce adenoma and consequently carcinoma in rats several months after exposure, primarily in the pancreas [191]. The AR42J is an exocrine pancreatic adenocarcinoma cell line used currently in basic exocrine pancreas research [192]. They were isolated from tumour cells produced from the rat azaserine studies and were re-transplanted into untreated rats of the same species by intraperitoneal and subcutaneous injections up to five times [189] (Figure 1.14). The generated AR42J cell line was observed to express high levels of pancreatic exocrine enzymes such as amylase [193]. The AR42J-B-13 (B-13) cell line is a sub-clone of the AR42J cell line which was subcloned by the Kojima lab in 1996 and stimulated to produce insulin-secreting β-like cells after treatment with activin A and HGF [194,195].

In 2000, Shen and colleagues observed that the B-13 cells go through an overwhelming alteration in the phenotype from the pancreatic exocrine-like cell to an hepatocyte-like-

cells(B13/H cells) in response to the glucocorticoid dexamethasone (DEX) treatment [196]. A sequence of reports after this discovery conclusively verify this information and reveal that B-13/H cells express a diversity of hepatocyte-specific genes or hepatocyte enriched, comprising glucose-6-phosphatase, albumin, transferrin, transthyretin [197] and cytochrome P450 [198]. The expression of many hepatocyte-specific genes can be observed within ~3 days of DEX treatment including UGT, transferrin and CYP2E1, whereas albumin expression is not detected until later, at around day 9, showing the full transdifferentiation event takes time [199]. A distinct characteristic of B-13/H cells is that they are exhibiting afunctional capacity that is quantitatively similar to freshly isolated rat hepatocytes (Figure 1.15). This feature is essential for *in vitro* cell models for studying toxicity mechanisms and possibly using the model to screen for drug and chemical toxicity [200].

To date, the data propose that the B-13 may be corresponding to a pancreatic or liver progenitor cell based on it trans-differentiation from the phenotype of B-13 acinar cells straight to the hepatocyte-like B-13/H phenotype. Utilising a B-13 cell line stably transfected with a green fluorescent protein (GFP) gene controlled by a promoter (trans-activated in exocrine pancreas cells), data demonstrated that following treatment with glucocorticoid, B-13/H cells were detected expressing both GFP and hepatocyte markers. This observation suggests that the mechanism of altered differentiation is likely a direct conversion from "differentiated" pancreatic exocrine cell type into a hepatocyte and excludes the reversion to a plastic progenitor-like intermediate. However, more recent limited evidence suggests that B-13 cells may be turned to form a ductal phenotype in response to glucocorticoid and EGF [201]. This conversion suggests that B-13 cells have a potency similar to hepatoblasts or may possess an endodermal progenitor phenotype, although a variety of cells *in vitro* are reflecting apparent response like epithelial-mesenchymal transition (EMT), to which the apparent plastic nature of B-13 could refer [202], even if B-13 cells entering (or are able under certain circumstances to enter) a transient plastic state prior to conversion to B-13/H cells remains ambiguous.

Despite the fact that many liver-enriched transcription factors have been involved in trans-differentiation to B-13/H, as mentioned previously (C/EBPß), which were expressed in the pancreas of copper-depletion rats has been identified as the critical component in trans-differentiation [203]. More importantly, Shen et al. (2000) found that transfection of C/EBPβ into B-13 cells can trigger the trans-differentiation into B13/H cells, while the dominant-negative form of C/EBPβ can inhibit this process. This observation suggests that C/EBPβ is an essential candidate for switching the pancreatic phenotype to the liver [181]. The data from literature demonstrated that DEX treatment results in suppression of WNT signalling and subsequent

expression of C/EBPβ [204]. Therefore, the role of WNT signalling in trans-differentiation has been examined.

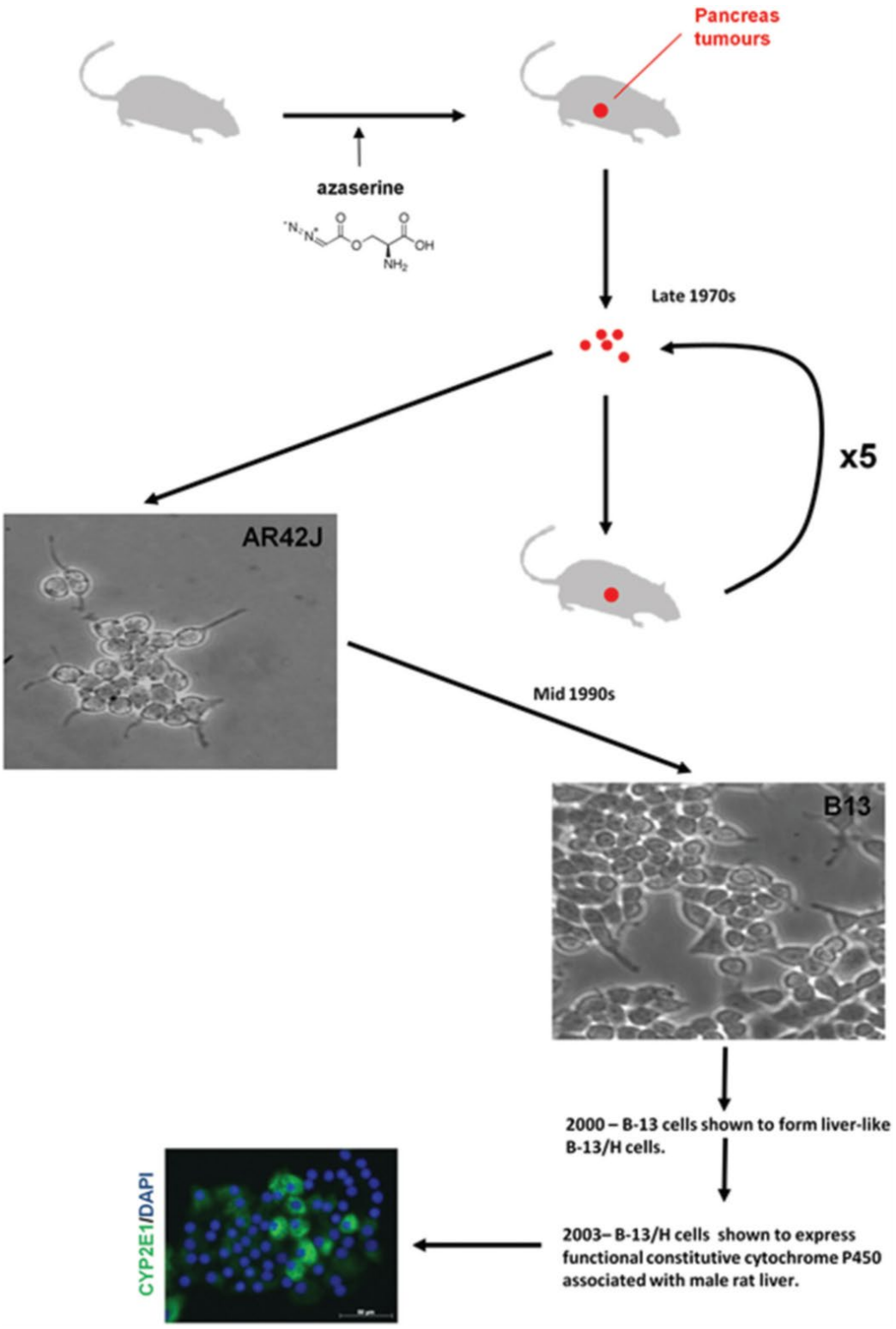

Figure 1.14 Origin and isolation of the AR42J and AR42J-B13 (B-13) cell lines. Light micrographs of AR42J cell line and b-13 as indicated (Upper panels), fluorescence immunocytochemical staining showing cytoplasmic staining of the CYP2E1, DNA stained with DAPI DNA to identify the nucleus in B-13/H cells (lower panel)[200].

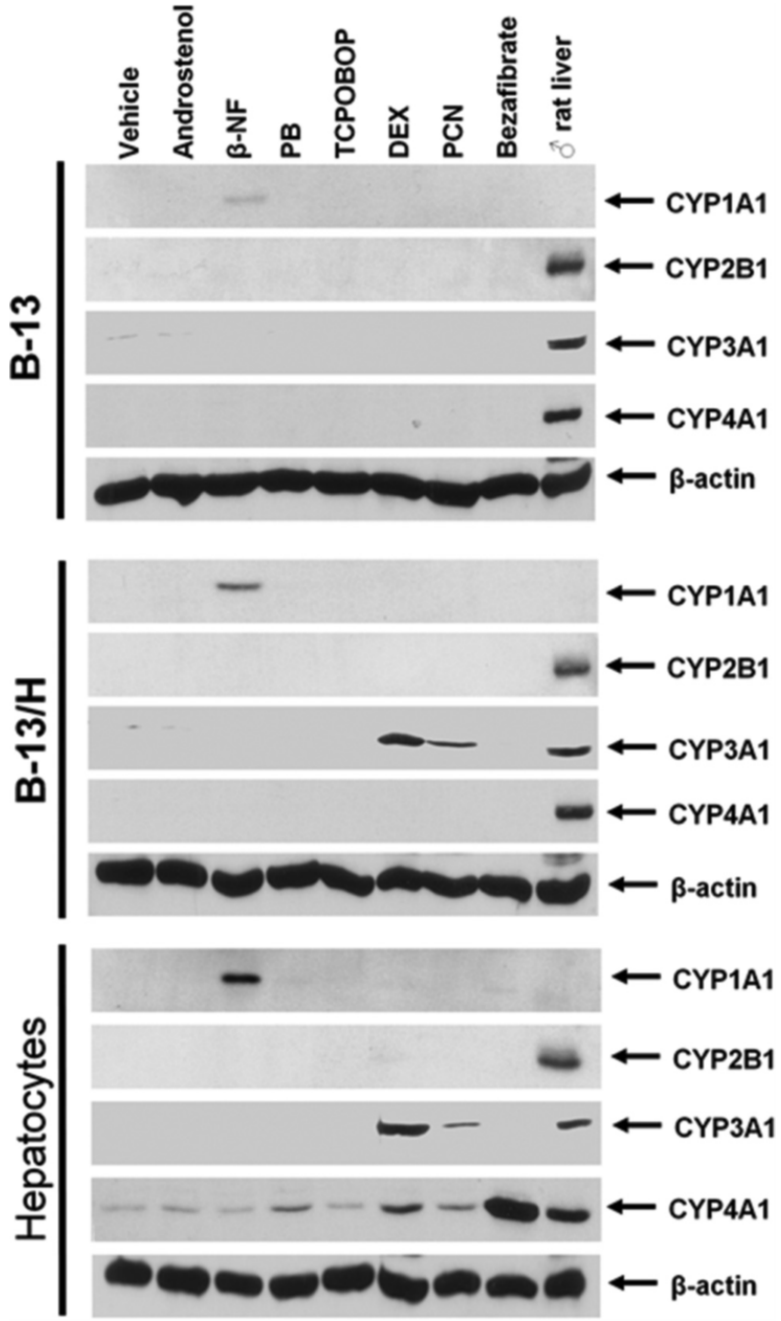

Figure 1.15 Western blotting analysis of the indicated proteins after induction of hepatic phenotype. *In vitro* induction of cytochrome P450s in B-13, B-13/H and rat hepatocytes. B-13, B-13/H and rat hepatocytes in culture were treated daily for 3 days with cytochrome P450 inducers (androstenol, 5 μM; β-naphthoflavone [β-NF], 20 μM; phenobarbitone [PB], 1 mM; 1,4-Bis-[2-(3,5dichloropyridyloxy)]benzene,3,3',5,5'-Tetrachloro-1,4-bis(pyridyloxy)benzene [TCPOBOP], 1.5 μM DEX, 10 μM; pregnenolone 16α carbonitrile [PCN], 2 μM or bezafibrate 250 Mm. [200]

1.5.6 Role of the WNT/β-catenin pathway in the transdifferentiation of B-13 cells into B-13/H cells

The WNT signalling pathway is a highly conserved signalling pathway across multiple species from Drosophila to humans [205]. Initially, discovered for its role in carcinogenesis, then for its function in early development controls including cell fate defining, proliferation, migration and body axis patterning. Additionally, the WNT signalling pathway also controls tissue regeneration in the adult. The pathways of WNT signalling are a set of signal transduction pathways which start with proteins that deliver signals into a cell through cell surface receptors via specific proteins. The pathways involve a diverse family of secreted lipid-modified signalling glycoproteins which work as ligands to trigger the discrete WNT pathways via paracrine and autocrine routes [206]. WNT signalling launches when a WNT protein combines into a frizzled (Fz) family receptor [207] co-receptors like lipoprotein receptor-related protein (LRP)-5/6 and receptor tyrosine kinase (RTK) may be involved besides the interaction between the Fz receptor and the WNT protein [208]. As soon as the receptor is activated, a signal is conveyed to Dishevelled (Dsh), which is a phosphoprotein found in the cytoplasm. The conduction of this signal is via a direct interaction between Fz and Dsh. Subsequently, the WNT signal can turn-off into several pathways. The three most studied WNT signalling pathways are the noncanonical planar cell polarity pathway, the noncanonical WNT/calcium pathway and the canonical WNT pathway. As their names indicate, these pathways belong to one of two groups: canonical or noncanonical. The canonical pathway implies the protein β-catenin while the noncanonical pathway works independently [209].

It has been documented that the canonical pathway plays a role in B-13 cells transdifferentiation into B-13/H cells. It is mediated by ligand binding to Frizzled and LRP (5/6) receptors resulting in the cytoplasmic gathering of β-catenin and β-catenin pass on to the nucleus. In the nucleus, it interacts with T cell factor (TCF)/lymphatic enhancement factor (LEF) for regulation of different target genes expression [205,210] In the absence of WNT, β-catenin would not accumulate in the cytoplasm as it would be degraded by the destruction complex which is composed of the following proteins: adenomatosis polyposis Coli (APC), Axin, protein phosphatase 2A (PP2A), casein kinase 1α (CK1α) and glycogen synthase kinase 3(GSK3)[211,212]. It degrades β-catenin by directing it for ubiquitination. Then, the degraded β-catenin are sent to the proteasome to be digested [213]. In contrast, in the presence of the WNT ligand, it binds the Frizzled (Fz) receptor and its co-receptor (LRP6) or its close relative LRP5. As a consequence, the destruction complex function is disturbed. This function disturbance is attributable to the formation of a

WNT-Fz-LRP6 complex together with the recruitment of the scaffolding protein Dishevelled (Dsh) outcomes in the phosphorylation and activation of LRP6 and the recruitment of the Axin complex to the receptors. These actions inhibit Axin-facilitated β-catenin phosphorylation. Moreover, this permits β-catenin to accumulate, stabilise and travel to the nucleus to act as transcription cofactor beside the TCF/LEF (T-cell factor/lymphoid enhancing factor) transcription factors to induce WNT target gene expression [213] (Figure 1.16).

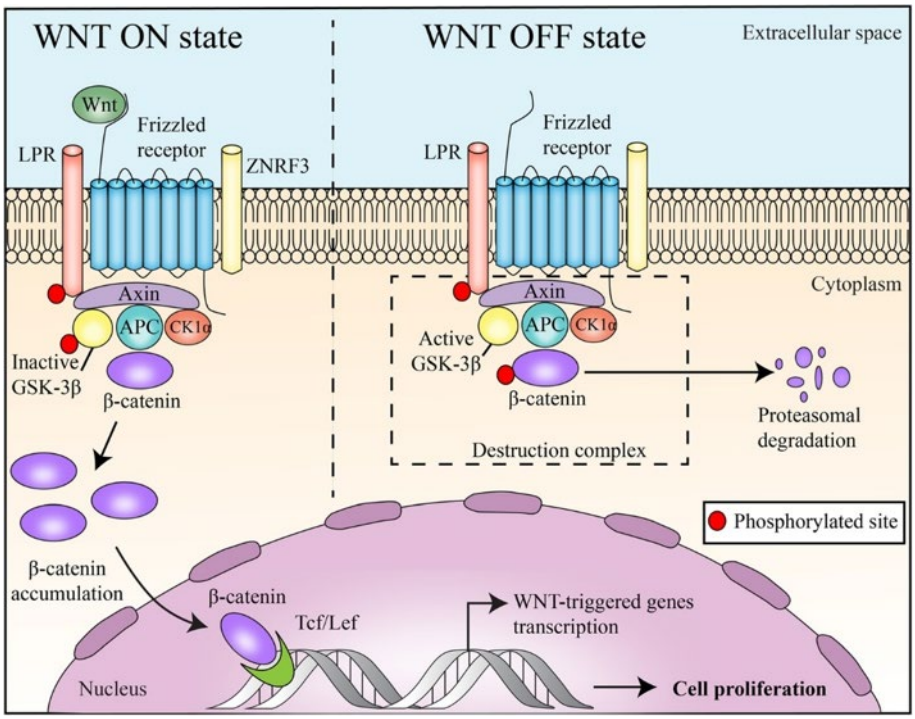

Figure 1.16 The canonical WNT/β-catenin pathway. WNT proteins are binding to frizzled receptors and the LRP co-receptor (WNT ON state) forming WNT-frizzled-LRP5/6 complex act to suppress the activity of glycogen synthase kinase-3β (GSK-3β). This prevents phosphorylation of downstream molecules allowing β-catenin to stabilise and accumulate within the cytoplasm prior to translocating to the nucleus and activating gene expression of the target genes. In the absence of the WNT ligand (WNT OFF state), the destruction complex of β-catenin (axin, APC, CK1α and GSK 3β) will phosphorylate β-catenin targeting it for ubiquitination subsequent proteasomal degradation [210].

As mentioned previously in this section, WNT signalling is essential in organ development [214]. Moreover, the WNT/β-catenin pathway is predicted to play a role in liver development in addition to hepatocyte zonation in the adult liver [215,216] as discussed in Section 1.2.2. Focusing on canonical WNT signalling pathway, the expression analysis of its elements presented that AR42J B-13 cells are expressing the WNT ligands (WNT1, WNT2b, WNT3a and WNT5a) mRNAs and that the levels were repressed by DEX treatment. Furthermore, it has been

demonstrated that DEX treatment in AR42J B-13 cells results in down-regulation of frizzled receptors (Fzd) and up-regulation of both DKK (Dickkopf-related protein 1) and sFRP (secreted Frizzled-related protein)[217]. This finding predicts that B-13 cells conversion into B-13/H cells by DEX may be induced by the suppression of the WNT signalling pathway.

Moreover, in 2010, Wallace et al. found that DEX treatment induced a transient loss of constitutive WNT3a expression, resulting in an activation of GSK3β (glycogen synthase kinase 3β) and consequent beta-catenin phosphorylation and loss of its nuclear localisation [218]. Similarly, it is indicated that Tcf/Lef transcriptional activity was high in B-13 cells and furthermore, that this activity decreases with DEX treatment. Twenty-four hours of treatment with DEX was adequate to inhibit Tcf/Lef activity to a level parallel to that after treatment with the Tcf/Lef inhibitor quercetin (Figure 1.17) [218]. Additionally, siRNA knockdown of beta-catenin in B13 cells was sufficient to enhance DEX dependent transdifferentiation, whereas transfection with a mutant beta-catenin protein (a non-degradable version of β-catenin) prevented dexamethasone-mediated transdifferentiation [218]. β-Catenin acts as an activator for the transcription factors Tcf (T-cell factor)/Lef (lymphoid enhancer factor) and loss of cellular β-catenin is followed by a reduction in Tcf/Lef transcriptional activity. Although treatment of B13 cells with the Tcf/Lef inhibitor (Quercetin) resulted in induction of C/EBPβ, indicating that C/EBPβ is repressed by Tcf/Lef activity, the Tcf/Lef inhibitor did not promote transdifferentiation into B-13/H cells but did potentiate glucocorticoid-mediated transdifferentiation. Thus, inhibition of Tcf/Lef alone was not adequate to induce transdifferentiation of B13 cells into B13/H cells[218]. This data suggests that although it was evident that DEX treatment results in suppression of WNT signalling and subsequent expression of C/EBPβ, the connection between DEX and the WNT/β-catenin pathway needs to be identified.

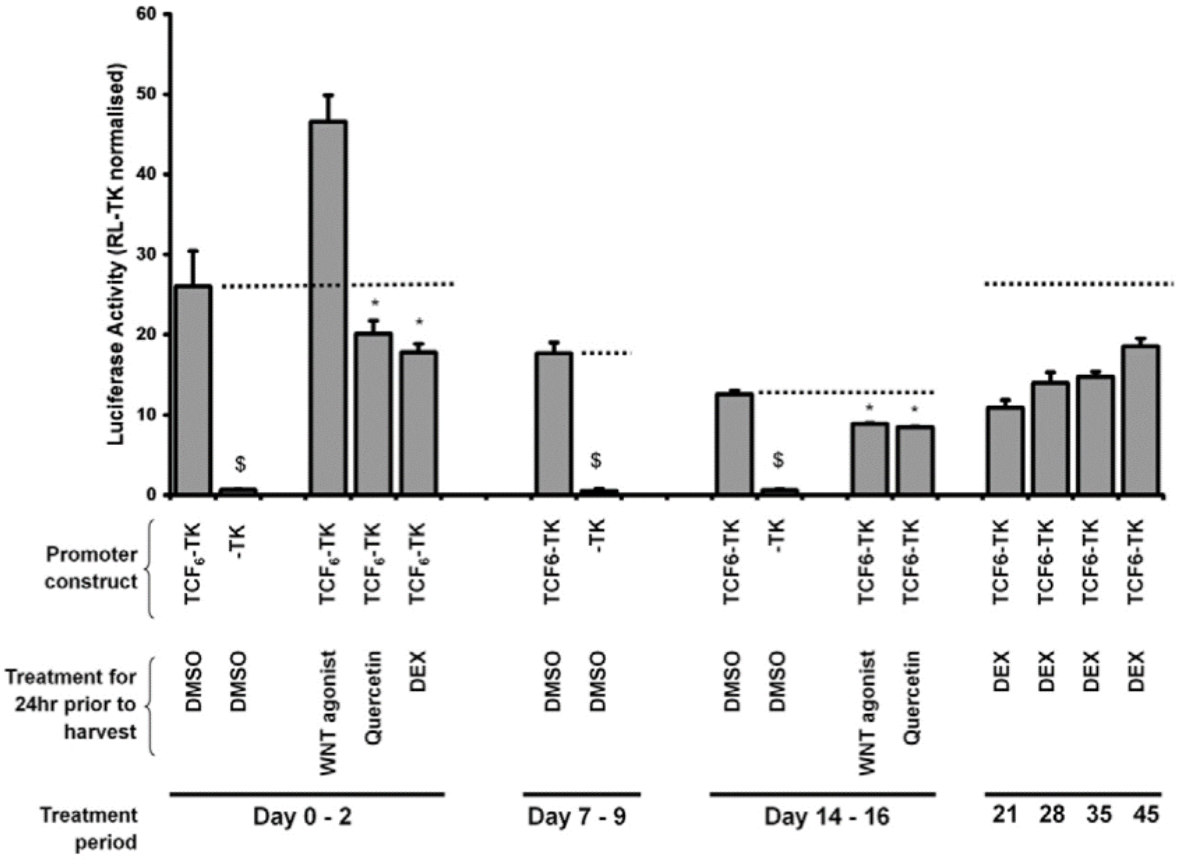

Figure 1.17 B-13 cells into B-13/H cells transdifferentiation is linked with suppression of Tcf/Lef transcriptional activity. B-13 cells were treated with DEX and transfected with the demonstrated constructs. After 24 hours of DEX treatment, the medium was changed and the cells were treated with 100 nMWNT agonists, 50μM quercetin and 10nMDEX. The cells were harvested 24 hours later. 0.1% (v/v) DMSO treatment was used as a vehicle control. Normalised luciferase activity versus cells transfected with TK$or TCF6-TK* during the same treatment. Significantly different with a p-value <0.05 using ANOVA (two-tailed) and ANOVA (two-tailed)[218].

1.5.7 Glucocorticoids in transdifferentiation of pancreas to liver

Glucocorticoids are endogenous adrenal hormones. They were discovered in the 1940s as extracts of the adrenal cortex. Their levels in the blood are controlled by the hypothalamus-pituitary-adrenal (HPA) axis [219,220]. The primary physiological function of glucocorticoids is the regulation of general metabolism. In response to stress, high levels of glucocorticoids promote gluconeogenesis, lipolysis and protein and amino acid degradation [220]. Glucocorticoids also regulate fluid and electrolyte homeostasis as they promote diuresis. Besides, they have a general anti-inflammatory effect, which allows them to be used as therapeutic agents [221]. Although glucocorticoids also have multiple effects on foetal development, their circulating

levels are low in the embryo and foetus because the placental enzymes, such as 11β-hydroxysteroid dehydrogenase [HSD2] inactivate glucocorticoids by metabolising them into inactive yields. Consequently, foetal levels only rise as the foetal HPA axis develops [222,223]. This increase in circulating foetal glucocorticoid perhaps significantly participates in cell differentiation and tissue maturation, most particularly stimulating maturation of the lung as well as the production of the surfactant essential for extrauterine lung function [224]. The effects of glucocorticoid are mediated by glucocorticoid Receptors (GR) and mineralcorticoid receptors (MR)[225]. It has been reported that the GR facilitates the response to glucocorticoid in B-13 cells and induces the process of transdifferentiation [226]. DEX which is a synthetic glucocorticoid has been commonly employed in generating B-13/H cells [166]. It is more specific for GR than lots of natural glucocorticoids and less rapidly metabolised. Additionally, GR antagonists inhibit B-13 cells transdifferentiation into B-13/H cells [226]. Other classes of steroids (e.g. oestrogens) are not able to stimulate the trans-differentiation of B-13 cells into B-13/H cells [200,227]. Although glucocorticoids also activate the MR [228], glucocorticoid-dependent trans-differentiation to the B-13/H cell is not blocked by MR antagonists. Besides, B-13 trans-differentiation does not occur in response to mineralocorticoids [226].

As mentioned in a previous section (1.5.4), several observations over the years have stated *in vivo* manifestation of hepatocyte-like tissue in pancreatic exocrine, in response to a range of pathological conditions. Later reports have been directed to study the effects of glucocorticoid on pancreatic exocrine tissue differentiation. *In vitro* studies have demonstrated that glucocorticoid treatment results in the conversion of both rodent and human embryonic acinar cells into hepatocyte-like cells [181,229]. Although the functionality of these pancreatic hepatocyte-like cells needs to be quantitatively compared to liver hepatocyte, then it would be arguable whether such cells could be defined as hepatocytes. However, the in-vitro environment in which the cells were cultured could influence this quantitative comparability which means that the cells could have the potentiality to form functional hepatocytes in the appropriate environment (such as *in vivo*). Moreover, studies in both rodents and humans verify this [217,227]. In a study conducted by Wallace et al. (2009), using *in vivo* models, they demonstrated that pancreatic acinar cells of adult rats had been converted into cells that express liver-levels of CYP2E1 after treatment with high dose glucocorticoid for just a few weeks [217].

In a transgenic mouse with high circulating endogenous glucocorticoids, many of the clinical features of Cushing's disease are evident. Cushing's disease results from an adrenocorticotropic hormone-secreting pituitary tumour that leads to excess secretion of adrenocorticotropic hormone (ACTH). This excess secretion of ACTH stimulates secretion of cortisol by the

adrenal glands, resulting in supraphysiological levels of circulating cortisol. The pathophysiological levels of cortisol are associated with hypertension, diabetes, obesity, and early death [230]. In the pancreas of many mice at 21 weeks of age there was significant liver-levels of hepatocyte gene expression [231]. This observation demonstrates that *in vivo* pathologically high levels of glucocorticoids alters the healthy pancreas to a hepatocyte-like phenotype showing equivalent levels of hepatocyte gene expression. Later analyses also indicate that the pancreas of adult patients maintained at high levels of systemic glucocorticoid treatment expressed hepatocyte levels of hepatocyte expressed genes [227].

1.5.8 The role of Serine/threonine protein kinase (SGK1) in glucocorticoid-dependent transdifferentiation of B-13 cells to B-13/H cells

Serum and glucocorticoid-regulated kinases (SGKs) are also known as Serine/threonine protein kinases. SGK1 is a member of the Protein kinase superfamily; AGC kinases which include protein kinase A, protein kinase G and protein kinase C. Multiple isoform variants exist of most AGC kinases, adding to the complexity of this family [232]. Physiologically, SGK1 functions to regulate sodium salt re-absorption by the kidney [233]. Sgk1 exhibits a broad distribution in the tissues.

In situ hybridisation studies localised Sgk1 mRNA in several epithelial and nonepithelial cells in the brain [234], eye [235] lung [234], liver [236], ovary [237], pancreas [238] and kidney [239]. Little is known concerning the distribution of the Sgk isoforms at the protein level which may refer (at least in part) to the fact that the existing antibodies are not isoform-specific and thus, may detect different Sgk isoforms. Moreover, Sgk1 is an unstable protein with a rapid turnover/half-life of approximately 30 minutes [240]. Rapid degradation of Sgk1 occurs through its ubiquitination and degradation by the proteasome [240]. Although Sgk isoforms are expressed in numerous tissues and cell types, the function of Sgk1 in aldosterone-dependent control of sodium ion (Na+) homeostasis is the most-studied role of these kinases concerning the transportation of epithelial ions [241]. The kidneys perform a vital role in keeping Na+ homeostasis. Excretion of Na+ in urine requires strict regulation to retain a constant extracellular volume during different dietary Na+ consumption and extrarenal Na+ losses [241]. In the kidney, the expression of Sgk1 is induced by aldosterone which binds to the MR. Sgk1 then translocates into the nucleus and becomes phosphorylated via the PI-3K pathway, leaving SGK1 functionally active as a kinase which results in phosphorylation of the ubiquitin ligase Nedd4-2. Consequently, there is inhibition of epithelial Na+ channel (ENaC) ubiquitylation, internalisation and degradation in the endosomal/lysosomal system [241]. In addition to this indirect action of Sgk1 on the ENaC cells abundant availability, it was suggested that Sgk1 could increase the activity of the ENaC

channel by direct interaction with the ENaC channel [242] and phosphorylation of α-ENaC subunits [243]. In the kidney, HSD11B2 rapidly oxidises the glucocorticoid to the inactive metabolite, thus preventing illicit activation of the mineral corticoid receptor by glucocorticoids which ensures that the main activation of MR is in response to mineralocorticoid and not glucocorticoid levels [244].

Despite a clear functional role for SGK1 in the kidney, Sgk1 is induced by a vast spectrum of stimuli in addition to glucocorticoids, mineralocorticoids [245] and serum. These stimuli include cell shrinkage and swelling [246], TGF-β[247], chronic viral hepatitis [236], vitamin D3 [248], glucose [249], fibroblast growth factor (FGF)[250], platelet-derived growth factor (PDGF) [250], heat shock [251] and oxidative stress [251]. As SGK1 provokes stress in response to low salt levels to promote salt re-absorption, the effect of Sgk1 gene knockout in mice has only been noticed when the mice are forced onto a low salt intake [252,253]. Recently, SGK1 has been shown to play a role in cell differentiation [254,255]; however, there is no apparent phenotype – developmental identified. In comparison, the role for SGK1 in B-13 cells conversion into B-13/H cells has been extensively studied and identified.

In 2011, Wallace and colleagues suggested that GR activation by DEX treatment in B-13 cells induces a marked increase in the serine/threonine kinase SGK1 before induction of C/EBPβ [256]. A microarray study measured the levels of approximately 5000 transcripts in B-13 and compared them to those in B-13/H cells. In this study, SGK1 was identified as the highest induced transcript in B-13/H cells in response to glucocorticoid treatment [217]. This observation provided a potential mechanism by which DEX treatment of B-13 cells could induce transdifferentiation/conversion via the WNT/β-catenin pathway, suggesting that SGK1, at least partially, phosphorylates the WNT signalling protein messenger β-catenin as an element of the mechanism that precedes stimulation of transcription factors such as CEBP-β [166,218] (Figure 1.18). Further studies confirmed that the plasmid vector-mediated expression of either of SGK1 isoforms which are identical except for alternative N-terminal domains (SGK1c and SGK1f) alone, resulted in the transdifferentiation of B-13 into B-13/H cells and inhibition of Tcf/Lef activity [256].

Wallace et al. showed that inhibition of SGK1 expression by siRNA resulted in abrogation of dexamethasone-induced transdifferentiation. The *in vitro* experiment showed that recombinant SGK1 was efficient to phosphorylate recombinant β-catenin on the residues that target β-catenin for ubiquitination and degradation [256]. The process of β-catenin phosphorylation would be predicted to down-regulate the WNT signalling pathway *in vivo*. As mentioned previously

(Section 1.5.6), WNT signalling activity was high in B-13 cells, confirmed by a WNT signalling responsive promoter-reporter gene construct (top flash). Inhibition of WNT by over-expression of a mutant β-catenin or siRNA to knockdown β-catenin expression alone led to Cebp-β induction and trans-differentiation/conversion of B-13 cells into B-13/H cells [218]. These findings suggest that Sgk1 isoforms may provide the link between GR activation and the WNT signalling pathway. This crosstalk could result in upstream Cebp-β induction and trans-differentiation/conversion. It is unlikely to be operational in normal cells and operates only in pathological conditions, for instance, chronic high glucocorticoid levels.

In 2016, Fairhall et al. discovered that continuous and pulse exposing of B-13 cells to DEX was sufficient to induce a robust increase in Sgk1c mRNA transcripts expression levels from undetectable levels in B-13 cells. Remarkably, expression of Sgk1c mRNA persisted 14 days later involving after pulse exposure to glucocorticoid. Moreover, this high induction Sgk1c mRNA transcripts was prevented by 5-azacytidine or by histone deacetylase inhibitors which propose that exposing B-13 cells to glucocorticoid-associated with a Gr-dependent pulse in DNA methylation and probably other epigenetic alterations such as histone modifications results in constitutive expression of Sgk1c and irreversible conversion of B-13 cells into B-13/H cells [257]. Understanding and application of these mechanism(s) could be used to generate a human equivalent B-13/H cell which could be used for drug and chemical toxicity screening as an alternative to primary human hepatocytes.

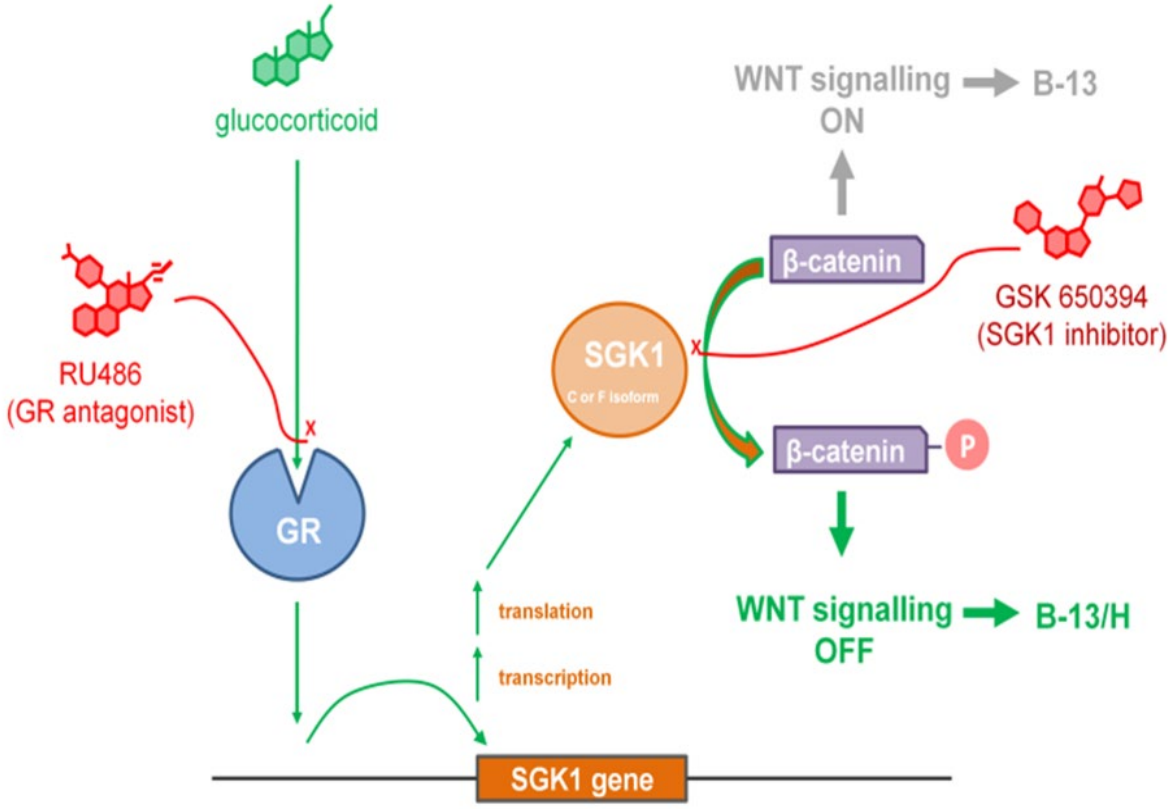

Figure 1.18 Schematic diagram of suggested mechanism of B-13 cells conversion / trans-differentiation into B-13/H cells [200]

1.6 Pluripotent derived hepatocyte-like cells

Hepatocyte transplantation has recently turned into an option for orthotopic liver transplantation for the treatment of life-threatening metabolic liver diseases and acute liver failure [258]. Besides their therapeutic capability, primary human hepatocytes are used to study the molecular and genetic features of human liver disease. Additionally, they offer a fundamental tool for drug toxicity screens and the discovery of new pharmaceuticals that can treat a broad group of metabolic diseases. However, the potential to use primary hepatocytes either for basic research or for therapeutic purposes has also been frustrated by the lack of donors and their affinity to quickly dedifferentiate and lose most hepatic functions following growth in a tissue culture condition [259]. Besides, they are challenging to cryopreservation [260]. The mature hepatocyte is patterned by the de-differentiation in reactions to the *in vitro* culture environment. De-differentiation may be initiated immediately after the cells isolation and probably induced by various factors, for example cell density, cell-matrix interactions, cell-cell interactions, deficiency of hormonal regulators and other factors *in vitro* [261] [262,263]. Under regular culture conditions such as culture on plastic, most of the original hepatocyte phenotype might be lost within a few days of culture.

The need to expand primary hepatocytes purified from donor's livers could be avoided by using stem cells for hepatocytes production. In 2007, human hepatic stem cells isolated from adult livers appeared to be beneficial *in vivo* when they were transplanted back into a mouse model of liver injury [264]. In 2009, mesenchymal stem cells from human adipose tissue were differentiated into hepatocyte-like cells *in vitro* and were determined to be able to engraft and express hepatic specific proteins when transplanted in mouse liver [265]. However, the quantity of adult stem cells that should be extended *in vitro* and differentiated remains a drawback to these approaches. Human pluripotent stem cells (i.e., hESCs and hiPSCs) constitute a substitute supply of hepatocytes to elucidate the deficiency of liver cells for cells based therapy. Unlike adult stem cells, ESCs and iPSCs can proliferate indefinitely without loss of potency. Several studies have depicted the differentiation of hESCs into cells that display hepatic characteristics [266]. Similarly, iPSCs provide an alternative approach that avoids the arguments associated with the utilisation of human embryos to acquire pluripotent ES cells and they could supply autologous hepatocytes.

Karim Si-Tayeb et al. (2010), is the first report demonstrating that mouse iPS cells can be used to generate hepatocyte-like cells efficiently [267]. In this decade, hepatocyte differentiation technology has predominantly been improved. Several hiPSC differentiation protocols that mimic developmental processes and lead to hepatocyte-like cells with increasing efficiency were published and reviewed by Yiangou et al. [268] . Most of the hepatocyte differentiation protocols can be divided into three differentiation steps: DE differentiation, hepatoblast differentiation and hepatocyte maturation. In general, each of these differentiation steps is performed using growth factors and cytokines known to be necessary for liver development. Specifically, this involves the application of growth factors at defined times in order to differentiate the stem cells from pluripotency to endoderm induction, hepatic lineage specification and finally, maturation.

The first step of differentiating pluripotent stem cells to DE cells is critical in hepatocyte differentiation. The critical part of this step includes exposing cells to activin A and BMP4 [269,270,271,272]. Various protocols established the supplementation of the medium with high concentrations of Activin A to promote the endoderm formation from pluripotent stem cells [268]. The efficiency of endoderm formation can be enhanced through modulating the WNT pathway either by supplementing recombinant WNT protein (or adding small molecules mimicking WNT, such as Chir99021) or by inhibition of GSK3-beta. Additionally, inhibition of PI3-kinase using small molecules LY294002 can enhance the efficiency of endoderm formation [269,273,274]. FGF2 and BMP4 are considered as initiators of the differentiation into DE and their addition during the first 24-48 hours of differentiation may be further promote endoderm formation [275]. Both, WNT and FGF are required for the normal formation of the primitive streak, as mentioned in Section 1.3.3 [276]. However, extended WNT3a exposure causes loss of hepatocyte differentiation capability [277] as repression of WNTs in the ADE is essential for liver development. After the DE differentiation, hepatoblast differentiation can be enhanced by repression of the WNT/b-catenin pathway [278]. These facts propose that the operating time of WNT3a treatment should be precisely regulated in order to achieve an efficient DE differentiation. The resulting endoderm progenitors described by some protocols can be retained for a prolonged period while preserving their ability to differentiate into a variety of endodermal derivatives [279,280,281]. It has been observed that foregut cells could be frozen after five pas-sages and then thawed to be expanded for at least five additional passages without any loss in gene expression profiles or observable loss of proliferation capacity [280].

Cai et al. (2007), reported that the combination of FGF4 and BMP2 efficiently induced hepatoblast differentiation from DE cells [282]. Brolen et al. used the mixture of BMP2/4 and FGF1/2/4 for the hepatoblast differentiation [283]. Importantly, a low concentration of FGF2 has been shown to enhance the hepatocyte differentiation, while an intermediate or high concentration of FGF2 enhanced pancreatic or intestinal differentiation, respectively [284]. According to this finding, the concentration of FGF should be controlled.

For maturation of hepatocyte progenitors to hepatocyte-like cells, researchers recapitulated the physiological environment during perinatal and neonatal life. Therefore, the majority of the existing protocols use a particular hepatocyte maintenance medium supplemented with HGF and OSM in addition to DEX, which is known to induce expression of mature hepatic specific genes reviewed in [285]. The longer the cells are subsequently grown in these conditions, the more their metabolic activity appears to increase. This stage of functional maturation can last up to 20–30 days with some protocols without DEX [52,283,286] and for 7-20 days with DEX [287]. Hepatocytes produced from hPSCs express the critical transcription factors and functional markers, for instance hepatocyte nuclear factor 4 alpha (HNF4A), hepatocyte nuclear factor 6 (HNF6), CCAAT/enhancer-binding protein alpha (CEBPa), Prospero homeobox protein 1 (PROX1), Transcription factor GATA-4, ALB and CYP3A4. These hepatocyte-like cells were also shown to have liver-specific functions such as albumin secretion, glycogen synthesis, urea production, low-density lipoprotein (LDL) uptake and limited cytochrome P450 activity [52,267,283,286].

Although human ES/iPS derived hepatocyte-like cells show various hepatic functions, the drug metabolic capacities in these cells are lower than those in primary human hepatocytes. Human ES/iPS derived hepatocyte-like cells also express high levels of immature hepatocyte markers, for example AFP, proposing a remaining immature/foetal phenotype [288,289]. The characterisation of human hepatocyte-like cells functionality includes evaluating mature liver-specific features that include albumin, urea, and fibrinogen synthesis, phase 1 and 2 metabolic enzyme activity (with specific substrates), and induction of drug metabolism enzyme and transporter (DMET) expression in response to specific inducers [279,290].

1.7 Improving differentiation of iPSCs to hepatocyte-like cells

The rapid dedifferentiation and immaturity of pluripotent derived hepatocyte-like cells have resulted in extensive attempts to manipulate the *in vitro* environment to generate or preserve hepatic functionality. These attempts include using co-culture systems in which paracrine

influence is added or coculturing different supportive cell types. Pan et al. (2016), efficiently generated functional hepatocyte-like cells from mouse liver progenitor cells via indirect co-culture with immortalised human hepatic stellate cells (Pan et al., 2016).

Another commonly used method to promote cellular maturation is the three dimensional (3D) culture method [291,292]. Yamashita et al. (2018), have established a method for bulk production of hepatocyte-like cells exploiting a 3D cell culture bioreactor that enabled them to achieve homogenous hepatocyte-like cells on a billion scale (>109 cells). Some hepatocyte markers genes such as alpha-1 antitrypsin, cytochrome (CYP) 1A2, CYP2D6 and HNF4a have higher expression levels in 3D-cultured hepatocyte-like cells in comparison to 2D-cultured hepatocyte-like cells [292]. The flow culture method in which a continuously perfused system is applied, was also used and resulted in the retention of *in vivo*-like hepatocyte phenotype and metabolic function [293] Moreover, in several approaches, transcription factors that are expressed in several developmental stages have been expressed in various differentiation steps of iPSCs to hepatocyte-like cells. Recombinant adenoviral vectors have been used to express SOX17 [294], HEX [295] and HNF4a [296] to improve the differentiation to definitive endoderm, hepatoblasts and hepatocyte-like cells, respectively.

1.8 Adenoviral vectors for gene transfer

Adenovirus-based vectors are commonly used as gene delivery vehicles for transduction of different cell types, specifically for quiescent, differentiated cells, in basic research and gene therapy applications. The significant advantages of using adenovirus-based vectors are that they provide the most efficient gene transfer among other viral vector systems for a wide variety of cell types. Additionally, it has a very efficient nuclear entry mechanism. Notably, they can transfer genes into both proliferating and quiescent cells [297]. Regarding the production, it can be produced in high titers (> 10^{12} pfu/ml). In addition, adenovirus DNA does not integrate into the host cell genome [298]**.** Recent improvements in the development of adenoviral vectors have brought significant advancement concerning problems like target cell specificity, long-term expression of the transgene, immunogenicity and toxicity *in vivo*.

1.8.1 Adenovirus Structure and biology

Since the first isolation of adenovirus from adenoid tissue in 1953 [299], to date approximately 57 different human serotypes have been identified [300]. Type 2 and 5 are the most commonly studied adenovirus serotypes, both of which are the basis of the recombinant expression system in

research today. Adenovirus is a non-enveloped virus with a linear, double-stranded DNA genome of 30-40 kb. Its nucleocapsid made up of 252 proteins in the form of 3 main types: hexon, fibre and penton based proteins [300] (Figure 1.19). Hexon based proteins are the structural basis of adenovirus and the major capsid protein. Both the fibre and penton based proteins are for receptor binding and internalisation of the adenovirus into host cells [301].

The adenovirus capsid is accountable for the primary virus attachment to the cellular receptor, the coxsackie- and adenovirus receptor (CAR)[302]. Following initial attachment via CAR, the RGD-motif -motif in the penton based protein attaches to cell surface integrin receptors (αvβ1, αvβ3, or αvβ5), which act as a secondary or internalisation receptor. This step triggers the virus uptake by the host cell via endocytosis [303]. After the endosomal uptake of the virus and release into the cytoplasm, the capsid of the virus is dismantled leading to the delivery of the core protein-coated viral genome to the nucleus. Inside the nucleus, the viral genes are expressed via the host cell's replication machinery [304] (Figure 1.20). In the nucleus of infected cells, the virus genome is replicated and assembled, and mature viruses leave the host cell via disintegration. In contrast to other viruses, adenovirus DNA is not integrated into the host genome and remains in an episomal state [305].

Episomes are non-integrated [306] extrachromosomal closed circular DNA molecules that may be replicated in the nucleus [306]. The immediate early E1A gene is the first gene to be expressed once the adenovirus enters a host cell. The E1A gene is essential for adenovirus replication. Moreover, they encode a transactivator for the transcription of the delayed early genes in E1B, E2, E3 and E4 transcription units. The expression of these transcription units genes will modify a group of cellular genes in the host cell to facilitate adenovirus replication [307]. The structural organisation of the Ad genome is shown in (Figure 1.21). Replication of the viral genome, which rely on 'inverted terminal repeats' (ITRs) of 100–140 bp in length at each end of the genome which contains cis-acting elements (origin of replication) and one copy of the terminal protein (TP) covalently attached to each 5' (prime) end as an initiation primer, starts approximately 5–6 h after infection [307]. Recognising the adenovirus replication cycle has allowed researchers to employ the vector to develop replication-defective (RD Ad Vector) versions for use in research.

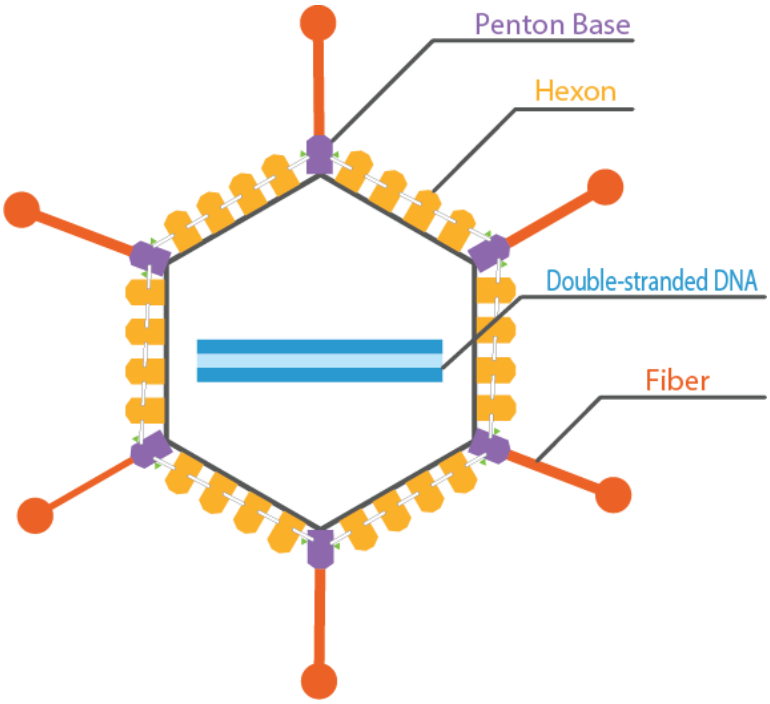

Figure 1.19 Adenovirus Structure [308]

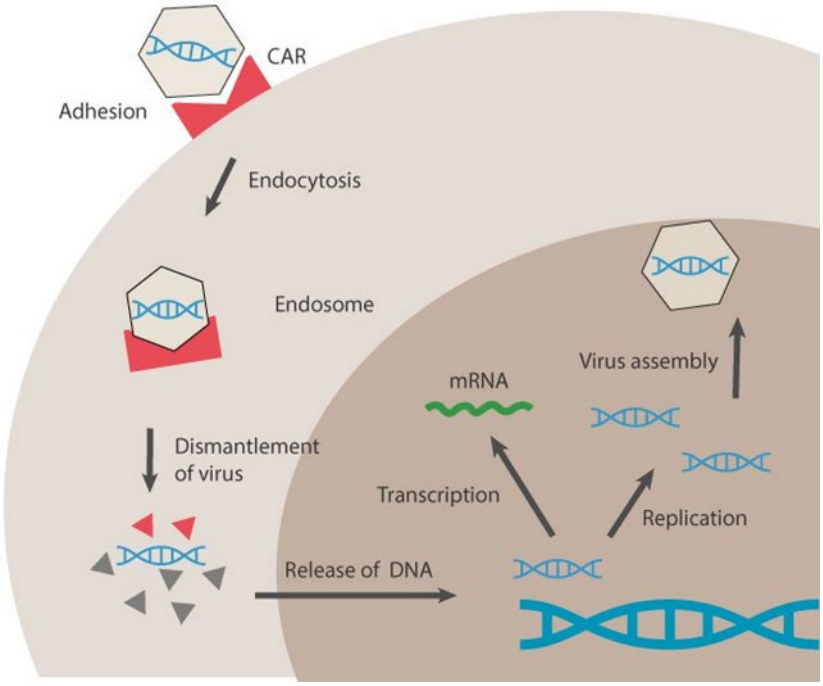

Figure 1.20 Transduction of Adenovirus [308]

1.8.2 Replication- deficient adenovirus vectors

Recombinant adenovirus expression vectors manipulate the low pathogenicity of the virus and the high nuclear transfer efficiency to deliver genes to the host cell. Most adenovirus vectors used in research are derived from adenovirus serotype 5 (Ad5). Replication-deficient can be produced by inserting or substituting the gene of interest into three regions of the viral genome: a region in E1, E3 and a short region between E4 and end of the genome (Figure 1.21). First-generation vectors are based on the replacement of the E1 gene region with the transgene or therapeutic gene to be delivered to the cell of interest, with a highly active promoter like cytomegalovirus (CMV) promoter to motivate the expression of transgenes [301]. As the E1 gene is essential for replication, the vector does not replicate in these cells under normal conditions. First-generation vectors can have an additional deletion in E3 which is dispensable for viral replication in cell culture, which make the total transgene capacity of these vectors up to 8kb. In order to propagate the recombinant virus that lacks E1 transgene expression, a complementing producer cell line, such as HEK293 which is a well-known cell line prepared by Frank Graham in 1977 is used [309]. This cell line stably expresses the viral E1A and E1B proteins and thereby provides the essential E1 proteins for adenovirus replication. Despite the E1 and E3 deletion, evidence from animal experiments and human clinical studies demonstrated that viral genes are still expressed at low levels in cells transduced with first-generation vectors which can cause direct toxicity and immune response *in vivo*. This issue has led to the construction of ‘‘second-generation’ adenovirus vectors featured by additional deletions or inactivation (e.g., temperature-sensitive mutants) of E2 [310] and/or E4 [311] functions, which have improved transgene persistence and decreased inflammatory response in some studies; however, it did not ultimately solve the immunogenicity problem. The advantage though is that the second generation recombinant vectors can accommodate bigger transgene sizes.

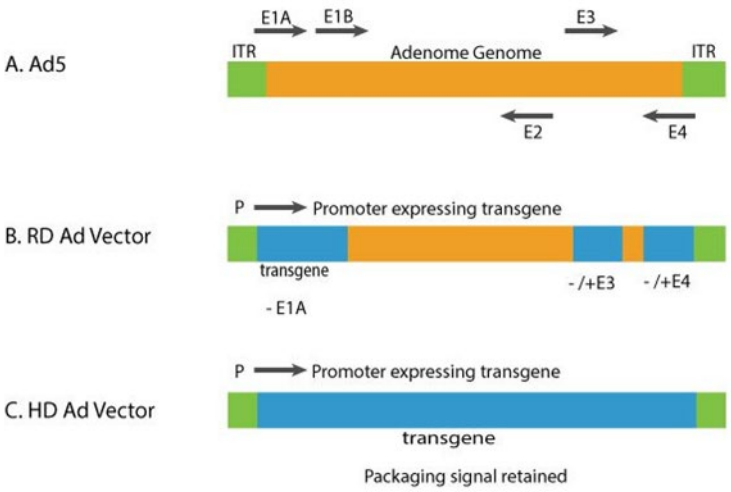

Figure 1.21 Schematic of the genome of adenovirus type 5 (Ad5) and Ad5 based Replication-defective vector [308]

1.9 Project aim and hypothesis

A common difficulty encountered with stem cell-derived differentiated cells *in vitro* is their maturation into fully differentiated phenotypes that quantitatively reflect the function of cells *in vivo* or directly after isolation from tissues. An example of this problem is the hepatocytes. Several reasons result in the immaturity of stem cell-derived hepatocyte-like cells. These include sub-optimal differentiation protocols, a sub-optimal *in vitro* environment and aberrant levels of regulating factors. These issues have resulted in extensive attempts to manipulate the *in vitro* environment to generate and/or preserve hepatic functionality.

Numerous genetic approaches have revealed that the liver and pancreas cells are specified from the endoderm and regulated by a number of signalling pathways and transcription factors.

Genetic studies revealed that they have a close developmental relationship which explains the *in vivo* transdifferentiation of pancreatic cells to hepatocyte-like cells and AR42JB-13 cells to B-13/H cells in response to dexamethasone *in vitro*. Moreover, *in vitro* transdifferentiation of B-13 cells is dependent on a transient suppression of Wnt signalling followed by induction of SGK1 via interactions with the GR.

The project hypothesises that adenoviral-mediated expression of SGK1F will promote a mature hepatic phenotype in B-13/H cells and iPSCs derived hepatocyte-like cells. Accordingly, this project aims to:

1. Examine the effect of the adenoviral-mediated expression of SGK1F on B-13 cells transdifferentiation into B-13/H cells.
2. Investigate if SGK1F expression is upstream of β-catenin phosphorylation and WNT signalling changes in B-13 cells.
3. Exploit the effect of SGK1F on B-13 cells and employ it on iPSCs directed toward hepatocyte-like-cells to potentiate their differentiation into hepatocytes (liver cells) so that their function more closely resembles human hepatocytes.

Chapter 2. **Materials and Methods**

2.1 Materials

Ethical authorisation for human liver tissue and hepatocyte isolation was gained via the Newcastle Biobank (https://www.ncl.ac.uk/biobanks/) with over-arching ethical permission from the Newcastle & North Tyneside 1 Research Ethics Committee. WNT signalling reporter constructs "Topflash" and "Fopflash" were purchased from Addgene

AdV-GFP was kindly offered by Dr Audrey Brown (Newcastle University). Professor Matthew Wright (Newcastle University, UK) provided The pFLAG-CMV2 SGK1F construct which encoded 2-241 amino acids of flagged protein [256] and was sub-cloned into adenovirus to produce a replication deficient AdV-SGK1F by Vector Biolabs (Eagleville, PA). AdV-null was kindly provided by Philip Probert (PhD student Newcastle University, UK). AD3 cells were grown in 6 well plates by Rachel Wilson and Charlotte Candlish from Professor Lyle Armstrong's laboratory (Institute of Genetic Medicine, Newcastle University, UK). The isolation of human hepatocytes was performed by Ibrahim, Tarek Abdelghany and Alistair Leitch from the Wright lab

2.2 Cell Culture

2.2.1 Rat pancreatic progenitor cells

AR42J-B-13 Cells were generously provided by Philip Probert (PhD student Newcastle University, UK). B-13 cells culture was routinely performed using low glucose (1g/L) Dulbecco's Modified Eagle's Medium (DMEM) supplemented with 10% (v/v) foetal calf serum (FCS), 100units/ml penicillin, 100µg/ml streptomycin and 0.584g/L L-glutamine. Cells were retained in a humidified atmosphere at 37°C, 5% CO_2 in the air. Cell culture media was changed every 2-3 days. DEX treatment was used to transdifferentiate B-13 Cells into B-13/H by adding the 1000-fold molar ethanol solvated stocks. 0.1% (v/v) ethanol vehicle was used as the control treatment.

2.2.2 HepG2 Cells

The cell line (Hep G2) is a cell line that has been isolated from a liver biopsy sample belonging to a 15-year-old Caucasian male diagnosed with a well-differentiated hepatocellular carcinoma [312]. The cells secrete a variety of proteins such as α 1-antitrypsin, α2-macroglobulin, albumin, and transferrin. HepG2 cells were cultured in DMEM containing 10 % (v/v) FCS, 100units/ml

penicillin, 100µg/ml streptomycin and 0.584g/L L-glutamine. Media was subsequently changed every 2-3 days and cells were sub-cultured when 90-95% confluent, as described in Section 2.2.1 using 2x Trypsin- Ethylenediaminetetraacetic acid (EDTA) (Sigma), as explained in Section 2.2.7.

2.2.3 MCF-7

MCF-7 cell line is a human breast adenoma cell line isolated from the pleural effusion from a 69-year-old female experiencing a breast adenocarcinoma. Some features of differentiated mammary epithelium are exhibited by this cell line. MCF-7 cells were cultured in DMEM- (Sigma D5546 1000mg/L glucose) containing 10 % (v/v) FCS, 100 units/ml penicillin, 100µg/ml streptomycin and 0.584g/L L-glutamine. Additionally, the media was changed every 2-3 days.

2.2.4 HEK293

Sarah Armour (PhD student, Newcastle University, UK) kindly provided human embryonic kidney 293 (HEK293) cells. The cells were routinely seeded into six-well plates at 1 x 105 cells/well and cultured in low glucose (1g/L) DMEM supplemented with 10 % (v/v) FCS, 100units/ml penicillin, 100µg/ml streptomycin and 0.584g/L L-glutamine until approximately 80% confluent.

2.2.5 AD3 (iPSCs)

AD3 cells are human iPSCs reprogrammed from dermal fibroblast (Lonza) isolated from a 37-year-old female using a CytoTune-iPS 2.0 Sendai Reprogramming Kit (Invitrogen) which includes three vector preparations: Klf4–Oct3/4–Sox2, cMyc, and Klf4, as described in Neganova et al. (2009 & 2016) [313,314]. AD3 were grown in 6 well plates, transferred to the Wright laboratory and differentiated into hepatocyte-like cells, as described by Hannan et al. (2013) [52].

2.2.6 Primary human hepatocytes

Collagenase perfusion was used for the isolation of human hepatocytes from liver tissue, as described by Diaz et al. (1990) [315]. It is donated after circulatory death of 60 years old patient. The liver is weighing 1900 g with high Liver Injury and cholestatic marker.

Cells were received, plated in 6 well plates and were cultured in Williams' Medium E supplemented with 50 µg/ml gentamycin, 0.584g/L L-glutamine, 100units/ml penicillin, 100µg/ml streptomycin 100nM insulin and incubated at 37ºC, an atmosphere air of 5% CO_2.

2.2.7 Cell passage

When adherent cells reached 75-95% confluence, they were sub-cultured. The medium was completely removed from the cells and washed once in phosphate buffered saline 8.0g/L NaCl; 0.2g/L KCl; 0.2g/L KH2PO4,1.15g/L Na2HPO4) pH 7.4. Cells were incubated with 1 x Trypsin-EDTA (Sigma), diluted in 1x phosphate buffered saline (PBS) (5ml per T75 flask and 0.5ml per well of six-well plate) and incubated at 37°C and 5% $_{CO2}$ for 5-15 minutes. The culture vessel was then tapped gently to promote cell detachment which was confirmed by light microscopy and the trypsin was inactivated by adding an equal volume of FCS- containing culture media to the cell suspension. Cells suspension was then transferred to a 50 ml centrifuge tube (Fisher, Loughborough, UK). Cells were then centrifuged at 2000rpm for 5 minutes. The supernatant was discarded, and the cells re-suspended in fresh medium. The cells were then seeded as required for cell maintenance or kept frozen for cell storage.

2.2.8 Long term cell storage

Stocks for all cell lines were routinely frozen and stored long-term in -80°C or in liquid nitrogen. As soon as cells reached ~80% confluent, they were detached from the cell culture vessel and pelleted by centrifugation, as previously described in 2.2.7. After removing the supernatant, the pellet was re-suspended in freezing medium (10% Dimethyl sulfoxide (DMSO) and 90% FCS), typically 2ml per T752 flask. The suspension was then aliquoted into sterile cryovials (1ml/tube). Cryovials were placed in a Mr Frosty cooling device (Thermo Scientific, Loughborough, UK) which was prefilled with isopropanol and pre-chilled at - 80°C. Mr Frosty freezes cells at a rate of approximately 1°C per minute for optimal cell survival. Cryovials were left overnight, and then they were either transferred to the storage box at -80°C or retained for long term storage submerged in liquid nitrogen.

2.2.9 Cell stock revival

For the revival of frozen cells, cryovials were taken out from the storage box and rapidly defrosted in a water bath pre-warmed to 37°C. Once thawed, the cryovial contents were carefully pipetted into 50ml of fresh warmed culture medium in a falcon tube. The cells were then centrifuged at 600rpm for 4 minutes and the supernatant removed. The cell pellets were

re-suspended in fresh media and transferred to a culture vessel (cells were initially seeded into small culture vessels, e.g. 6-well plates). Subsequently, the cells were incubated under standard conditions, as outlined in the cell culture section (see 2.2), until the cells had adhered to the culture flask (overnight). The culture medium was then aspirated. The medium was changed the following day.

2.2.10 Determining cell number

Following the trypsinisation and the pellet preparation, as described in Section 2.2.7, cells were re-suspended in a defined volume of medium (1-10ml). 1 volume aliquot of cell suspension was added to 1 volume of trypan blue (0.4% w/v in PBS), gently mixed and loaded into a haemocytometer counting grid with just enough cell suspension such that no liquid falls down the side gulleys. Using the microscope under normal illumination, the number of cells in 4-16 small squares was counted (depending on cell density). Three counts were taken per sample and averaged. The number of viable cells which excluded trypan blue (i.e. colourless cells) per ml of original suspension was then calculated as follows:

$$no.of\ cells\ per\ ml = average\ of\ cells\ count \times 2 \times \frac{16}{no.of\ squares\ counted} \times 10^{-4}$$

The cell suspension was then diluted as necessary based on the count as follows:

$$\text{volume of the cells suspension needed (}\mu\text{l)} = \text{number of cells needed} / \text{no. of cells counted per ml of original suspension} \times 1000$$

Cells were then sub-cultured in 6 or 24 well plates at the desired density and incubated in an incubator at 37°C and 5% CO_2 under humidified conditions.

2.2.11 Cells viability test by trypan blue exclusion

To assess the cells' viability, 200ul of trypan blue (0.4% (w/v) was added to 2ml of cell media in 6 well plates and then aspirated off after 10 seconds had passed. Live cells which have intact plasma membrane exclude trypan blue stain, whereas dead cells fail to exclude it staining them blue. Cell photos were then taken using an OPTIKA bright-field microscope and imaged with a BUC2 Camera connected to a TOSHIBA computer set up with ScopeImage 9.0 software and ImageJ cell counter was used for counting the number of trypan blue positive (dead) and negative colourless cells (viable) cells. The number of non-viable cells and the total cell number in random views of fields were calculated and used to determine the percentage viability as follows:

$$\% \text{ Of cells viability} = \frac{\text{no. of viable cells}}{\text{total no. of cells}}\ x100$$

2.2.12 Adenoviral production and titration.

Replication-deficient adenovirus was produced via HEK293 cells routinely seeded into six-well plates at 1 x 10^5 cells/well and cultured, as described in 2.2.4, until approximately 80% confluent. Viral stocks were serially diluted typically between 10 x 10^{-4} - 10^{-9}. The medium was removed from the HEK293 cells and 300 µl of each adenoviral dilution added to each well. The plate was gently rocked to ensure coverage of all cells by the viral solution and returned to the incubator for 1 hour. During this incubation, 5% agarose solution in PBS was dissolved by heat and cooled to 45°C separately with a culture medium. After the hour of incubation for infection, the viral dilutions were aspirated from the cells, 5% agarose solution was diluted to 0.5% in the culture medium. In addition, 2 ml of this solution was added per well and left to set. Once set, a further 2 ml of culture medium was added per well and the cells typically cultured for 7-10 days. The medium was discarded, and cells were then stained with neutral red (0.03% (w/v) in PBS) for 2 hours. The viral titre was determined from the number of plaques counted as follows:

$$\frac{\text{no. of plaques}}{\text{dilution factor x } 0.3} = pfu/ml$$

2.2.13 Multiplicity of infection (MOI) determinations

For the determination of MOI in any particular cell type, typically cells were expanded to approximately 80% confluence and infected with a serially-diluted range of titred AdV-GFP. Infected cells were then returned to the incubator. Cultures were examined daily using a fluorescent microscope for up to 4 days and the percentage of cells positive for green fluorescent protein (GFP) determined from 5 randomly selected fields. The titre and the number of cells was used to estimate the MOI as below:

$$\text{MOI} = \frac{\text{the virus titre X the virus volume resulted in} > 85\ \% \text{ infection rate}}{\text{no. of cells per ml}}$$

2.2.14 Adenovirus protocol for Infecting Cells

A day before infection, cells were sub-cultured into six-well plates to give approximately 50% confluency. An appropriate volume of titred virus suspension is added to the media to infect the cells based on the MOI of the cell line and the number of cells seeded. The adenovirus used either AdV-SGK1F encoding human SGK1F, AdV-null, AdV-GFP or AdV-NTCP. Uninfected

cells were included as controls. The cells were in some cases re-infected – with MOI altered as necessary – based on the extent of any apparent toxicity to previous infections in order to optimise both expression and cell viability. Cells cultured as outlined in (cell culture). To determine the amount of virus or plaque forming unit (PFU) to be added for a particular MOI, the following formula was used:

$$\text{Total no. of PFU needed} = \text{no. of cells x desired MOI}\ .$$

Subsequently, to calculate the total volume (ml) of the virus suspension needed to reach the desired dose, this formula was used:

$$\text{Total volume (ml)of virus needed} = \frac{\text{no. of PFU}}{Virus\ titre}$$

2.3 Plasmid DNA constructs and cells transfection

2.3.1 Competent cell (TOP10) transformation

Top 10 cells (Invitrogen, Paisley, UK) were transformed with the Plasmid of interest that propagate the DNA. TOP10 cells were stored at -80°C. When required, they were defrosted on ice and 50-100ng of plasmid DNA was combined in the vial and left on ice for 30 minutes. The cells were shocked by heating in a water bath at 42°C for 30 seconds without shaking, before being transferred to ice. 250 µl of super optimal broth (20mM glucose, 10mM NaCl, 2.5mM KCL, 10mM MgCl2, 10mM MgSO4, 2% tryptone and 0.5% extract of yeast) was added to the vial and retained in a 37°C incubator shaking at 225 rpm for 1 hour to allow cells to recover. The transformed cells (50-200 µl) were spread onto Luria broth (LB) (LB-10g NaCl, 10 g Tryptone, 5 g yeast in 1 litre dH_2O) agar plates containing the appropriate selection agent (kanamycin 25µg/ml or ampicillin 100µg/ml) and incubated over night at 37°C. The next morning a colony was picked and placed into 5 ml of LB with antibiotics as required and placed at 37°C in a shaking incubator at 220rpm overnight. The following day the cells were subjected to either mini- or maxi-prep or frozen, as described in, 2.3.2, 2.3.3 and 2.3.4 respectively.

2.3.2 Miniprep purification of plasmid DNA

Miniprep purification kits (Qiagen, Southampton, UK) were used for the purification of all plasmid DNA constructs following the manufacturer's protocols. After alkaline lysis of the bacterial cell walls, the purification process continued with the adsorption of plasmid DNA onto a permeable silica membrane under high salt conditions [316]. Additionally, 5 ml of culture was centrifuged in Eppendorf tubes at 16,000 g for one minute. The supernatant was discarded and

250 µl of buffer P1 (containing RNase) was mixed with the pellet to remove any ribonucleic acid (RNA) contamination. This step was followed by adding 250 µl of buffer P2 (highly concentrated salt buffer containing (SDS sodium dodecyl sulphate). The tube was mixed to produce a clear solution and 350 µl of buffer N3 then was added (containing acetic acid to neutralise alkaline lysis buffer) and immediately inverted to mix. The solution was centrifuged at 16,000 g for 10 minutes resulting a white pellet. The supernatant was then carefully removed and pipetted into a Qiaprep spin column and centrifuged once again for 1 minute at 16000 g. The flow-through was discarded, and 500 µl of buffer PB dispensed into the column, which was then centrifuged again as before, and the supernatant removed. The column was again centrifuged at 16,000 g for 1 minute after adding 750 µl of buffer PE to remove excess salt and the flow through disposed of. The column centrifuged once more for 1 minute to remove the deposits. Then, the column was transferred to a sterile and nuclease-free water (50 µl) added directly to the column membrane. The column was left to stand for 1 minute then centrifuged for 1 minute at 16,000 g to elute the plasmid DNA. Plasmid DNA was then quantified by a spectrophotometer, as described in 2.4.2

2.3.3 Maxiprep purification of plasmid DNA

Maxiprep relied on the same theory as the miniprep but designed to produce larger yields. A maxi-prep was performed using the Qiagen Maxiprep kit to purify large quantities of plasmid DNA (up to 500µg). An overnight culture of 500 ml culture flasks was divided into 50 ml centrifuge tubes and then centrifuged for 10 minutes at 6,000 g. The pellets were re-suspended and combined in one tube. The bacteria pellet was then lysed by adding 10 ml of buffer P1 and 10 ml P2 and mixed by inversion. The solution was allowed to remain for 5 minutes and 10 ml of buffer P3 (pre-chilled on ice) was then added and mixed by tube inversion. After this step, the lysate was transferred to a QIA filter cartridge and was kept at room temperature for 10 minutes. Subsequently, the lysate was then applied to a Qiagen-tip 500 column that had been equilibrated by the addition of 10 ml of buffer QBT left to drain through. The supernatant was left to enter the column after which the column was rinsed twice with 30 ml of buffer QC. The flow-through was discarded. Then the plasmid DNA elution and precipitation was performed by the addition of 15 ml of buffer QF into a 50ml centrifuge and 10.5 ml of absolute isopropanol respectively. The sample was inverted to mix then centrifuged at 6,000g at 4°C for 30 minutes. The supernatant was removed, and the pellet washed with 70% ethanol. After another centrifugation step (6,000g for 30 minutes at 4°C), all the supernatant was aspirated, and the DNA pellet left to air dry for 10 minutes. The pellet was then re-suspended in nuclease-free water and quantified as described in 2.4.2

2.3.4 glycerol stocks storage of DNA plasmids

TOP10 cells transformed with plasmid DNA were stored long-term as glycerol stocks at -80°C. 500µl of an overnight culture picked from a single colony was diluted 1:1 (v/v) with sterile LB media containing 30% (v/v) glycerol then transferred to a cryovial, labelled and frozen long term at -80°C. When required, previously stored bacteria were thawed, and a small sample (20-30µl) streaked out on an agar plate augmented with a proper antibiotic such as ampicillin to select for transformed bacteria. After incubation overnight at 37°C, a single colony was picked from the plate and grown overnight in LB, with antibiotics as required, and plasmid DNA purified using a miniprep (2.3.2) or maxiprep (2.3.3).

2.3.5 TOPflash/FOPflash plasmid transfection and dual luciferase assay

WNT signalling reporter constructs M50 Super 8xTOPFlash and control plasmid Super 8XFOPFlash were obtained from Addgene. The TOPFlash construct is a luciferase reporter of beta-catenin-mediated transcriptional activity. The construct backbone is the PTA-Luc vector, which delivers a minimal promoter driving expression of the firefly luciferase gene. M50 Super 8x TOPFlash reporter plasmid contains 7 copies of TCF/LEF binding sites (AGATCAAAGGgggta) which were cloned into the Mlu1 site of this vector, TCF/LEF binding site in CAP letters and a spacer in lower case, separating each copy of the TCF/LEF site. This plasmid was published as M50 Super 8x TOPFlash, however the plasmid contains only 7 TCF/LEF sites. (Figure 2.1). Clone M51, Super8XFOPflash is the appropriate control plasmid which has mutant TCF/LEF binding sites (

Figure 2.2). Top10 cells from Invitrogen (Paisley, UK) were transformed with the plasmid of interest to generate DNA. Miniprep and maxiprep purification of plasmid DNA were performed following the Qiagen protocol.

Prior to transfection with plasmids, B-13 cells were sub-cultured onto 24 large plates using standard culture medium. The following day, 30 - 50% confluent cells that are actively dividing were used and two plasmid stocks were prepared (TOPFLASH and Luciferase containing reporter gene: RL-TK). A transfection with 6:1 fixed ratio for experimental to control plasmid DNA vectors were employed to control the transfection efficiencies between wells. (i.e. so that ratio of luciferase to the renilla vector will be identical in all transfected wells). For the 24 well plates, the total DNA concentration should be 0.34µg/well. Using Lipofectamine™ 2000 transfection Reagent (Promega), cells were transfected according to previously optimised protocol. DNA was diluted in 17.3 µl serum-free media (DMEM), mixed by tapping and left for 5 mins at room

temperature (RT). Then, 3.5 µl of lipofectamine reagent was diluted in 17.3 µl serum-free media (DMEM), mixed by means of tapping and left for 5 mins at RT. The two dilutions were then combined 1:1 and left for 20 mins at RT. Next, 34 µl/well was dispensed and incubated for 24 hours. At this point, cells were treated daily according to the experiment set up and examined to check the plasmid toxicity. Cells were harvested up to 72 hours after transfection.

Following the manufacturer's instructions, a Dual-Luciferase Reporter Assay kit from Promega was used to assess the activity of WNT signalling in cells transiently transfected with renilla and or firefly luciferase constructs. (TOP/FOPFLSH and RL-TK). Dual reporter systems work to increase experimental accuracy where two individual reporter enzymes are simultaneously expressed. The dual luciferase® assay utilises the luciferase activities of both firefly (photinus pyralis) and renilla (renilla reniformis, sea pansy) detecting the activities of both sources respectively (Figure 2.3). The difference in the structure of the two luciferase enzymes allows discrimination between their bioluminescence. Transfected cells were washed twice in 1 x PBS before 1 x passive lysis buffer (5 x stock diluted 1:4 with dH2O) was added to each well (100 µl/well of 24 well plate) and shaken on an orbital shaker for 15 minutes to disrupt the cell membrane and lyse the cells. Luciferase assay reagent (LAR II) was prepared by resuspending the luciferase assay substrate with the luciferase assay buffer. Then, 100 µl of LAR II was pipetted into a polypropylene tube and 100 µl of cell lysate added and mixed. The activity of the luciferase was measured by a luminometer. Firefly luciferase activity was then quenched using a pre-diluted stock of stop and glo reagent containing the substrate for renilla luciferase. The luciferase activity of the RL-TK was subsequently measured and recorded. For all transfections, the relative luciferase of the experimental plasmid DNA construct (e.g. TOPFLASH) was normalised to RL-TK levels by dividing the firefly measurement by the renilla value. Data was expressed as a fold change in luciferase activity in response to individual treatments.

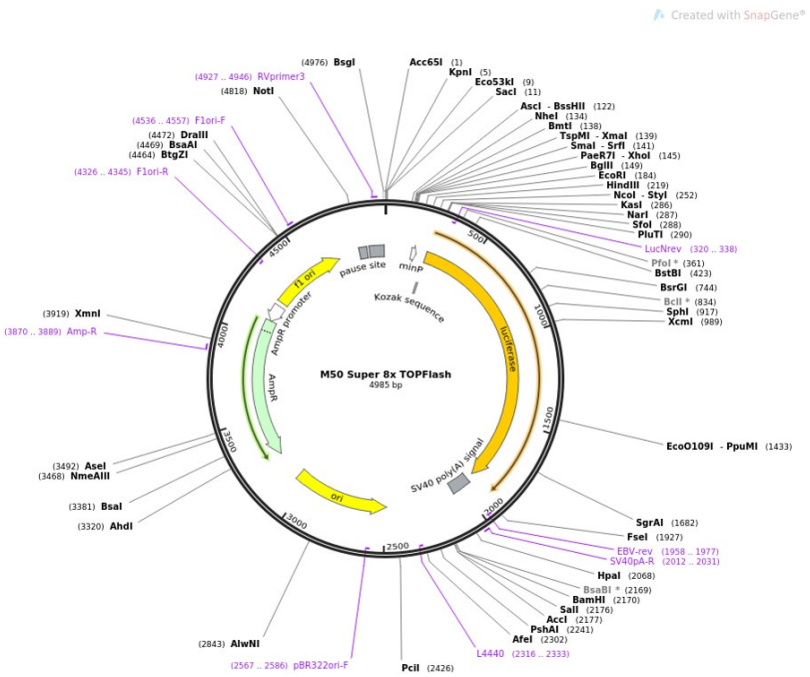

Figure 2.1 Sequence Map for M50 Super 8x TOPFlash. (addgene plasmid #12456)[317]

Figure 2.2 Sequence Map for M51 Super 8x FOPFlash (TOPFlash mutant). (addgene plasmid #12457)[318]

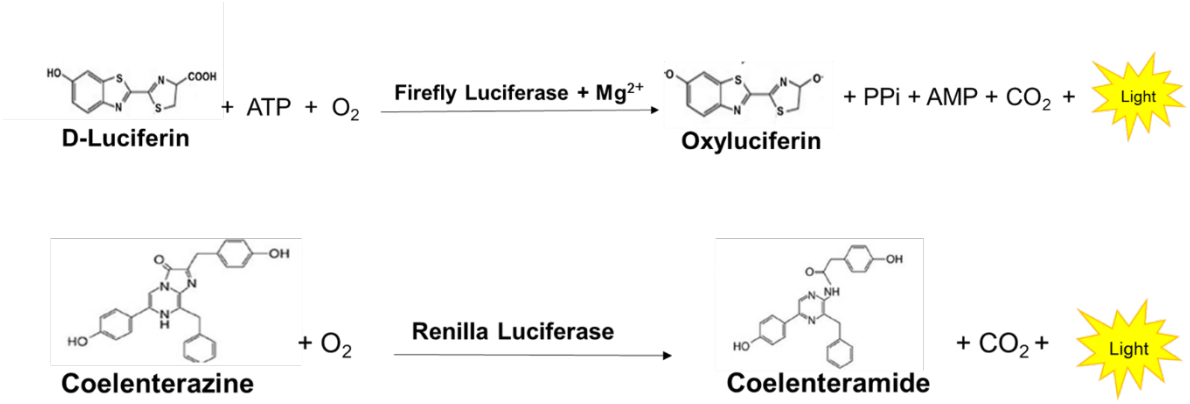

Figure 2.3 Firefly and Renilla luciferases bioluminescent reactions. Fireflies emit light via a chemical reaction in which luciferin is converted to oxyluciferin by the action of luciferase enzyme (upper panel). Renilla luciferase converts coelenterazine into coelenteramide. The energy released by this reaction is in the form of light (lower panel).

2.4 Reverse transcription polymerase chain reaction (RT-PCR) and real-time reverse transcription PCR (qRT-PCR)

2.4.1 RNA isolation

The medium was aspirated prior to washing the cells in PBS before isolation of the total RNA using TRIzol (Invitrogen), according to the manufacturer's protocol. After the PBS wash, 1ml of TRIzol was added directly to the cells in the well and left on an orbital shaker for 5 minutes. The TRIzol was then transferred to RNAse free Eppendorf tubes. After a 5 minute incubation, 200 µl of chloroform was added and mixed by inversion. The mixture was then centrifuged at 16,000 g for 15 minutes to promote the formation of an aqueous phase, interphase and organic phase. RNA partitions in the aqueous phase, whereas DNA and proteins are localised to the interphase and organic phases. The aqueous phase was transferred to a new tube and 500 µl of isopropanol was added to precipitate the RNA. Then, the tube was mixed by inversion and left to stand on ice for 15 minutes. To pellet the RNA, the tube was centrifuged at 16,000 g for 10 minutes. The isopropanol was aspirated off and 1 ml of 70% ethanol used to wash the pellet. The samples were centrifuged again as before, and all the ethanol removed. After 5-10 minutes of air drying at room temperature, the pellets were re-suspended in RNase free water. The RNA was then quantified and frozen at -80°C until required.

2.4.2 RNA and DNA quantification

For the determination and quantification of RNA or DNA in samples, their absorbance at 260nm was measured using a Nanodrop 2000 spectrophotometer (Thermo Scientific) using RNase free water as the blank. The purity of the samples was measured by calculating the OD260/OD280 ratio. For pure nucleic acid samples, this should be between 1.8-2.1. Lower ratios suggest contamination, possibly by phenol or protein. The peak absorbance at 270nm rather than 260nm indicates significant phenol contamination which contribute to overestimation of nucleic acid concentration. After determining the quantity of RNAs. RNA samples were routinely diluted to 200ng/µl and 5ng/µl for RT-PCR and qRT-PCR respectively.

2.4.3 1st strand synthesis and reverse transcription of RNA

Reverse transcription was performed using the RNA-dependent DNA polymerase M-MLV (Moloney Murine Leukemia Virus reverse transcriptase), essentially following the manufacturer's guidelines (Promega). To create complementary deoxyribonucleic acid (cDNA), RNA was diluted to a starting concentration of 200ng/µl. Additionally, 4µl of RNA (800ng) was incubated with 1 µl (50ng/µl) of random primers (Promega) at 95°C for 3 minutes. Samples were placed on ice. Master mix containing (per tube) 4 µl of 5x RT buffer (50mM Tris- HCl (pH 8.3 @ 25°C), 75mM KCl,3mM MgCl2 and 10mM DTT), 8 µl dH2O, 2 µl of 10mM dNTP's and 1 µl of MMLV was prepared on ice and added to each tube (15 µl total volume per reaction). The RNA was left for one hour at 42°C for optimal cDNA synthesis. Samples were stored at -20°C.

2.4.4 Primers Design

Forward and reverse PCR primers pairs were typically designed to amplify specific desired DNA sequences. The NCBI database (www.ncbi.nlm.nih.gov) was used to download nucleotide sequences of the required DNA sequences. Primer-blast was then used to design primer sequences for RT-PCR. PCR primers designed to flank the region of interest, range in length from 15–30 bases and contain 40–60% (G + C). Sequences that had minimal complementarity with themselves were avoided because they might produce an internal secondary structure. The 3 -ends of the primers were designed not be complementary to avoid the production of primer-dimers which deplete primers from the reaction and result in an unwanted polymerase reaction that competes with the desired reaction. Preferably, both primers had similar content of G and C to result in nearly identical melting temperatures (Tm= 2 ^{o}C x (A + T) + 4 ^{o}C x (G + C); in this way, both primers should anneal roughly at the same

temperature. The annealing temperature of primer pairs is calculated as Tm -5°C. (For the List of primers used for PCR see Appendix A).

2.4.5 Polymerase chain reaction (PCR)

PCR relies on thermal cycling which involves many cycles of repeated heating and cooling allowing for DNA melting, primer annealing and polymerase enzymatic replication of the DNA templates. Primers are explicitly designed to target genes of interest allowing selective amplification of the target DNA. During the reaction, the DNA generated from earlier cycles can act as a target itself allowing the DNA to be exponentially amplified. Taq polymerase is the DNA polymerase enzyme that was used in the PCR reaction to amplify short segments of DNA.

For PCR reactions, 1 µl of cDNA (40ng) was added to each reaction tube along with 20 µl of PCR master mix which contained (per tube): 10 µl 2x go-Taq green master mix (Taq DNA Polymerase, 1.6mM dNTPs, 3mM MgCl2 and reaction Buffers), 6 µl dH2O, 2 µl of 10pmol/µl of up and downstream primers. PCR procedures were optimised for each set of primers. The standard PCR procedure was as follows:

Initial denaturation	95°C	1 minute
Then 30-35 cycles of:		
Denature	95°C	1 minute
Anneal	depends on primer design	1 minute
Elongate	73°C	1.5 minute
Final elongation	73°C	8 minutes
Hold	4°C	

PCR products were then visualised by running them out on an agarose gel (1- 2% dependent on amplicon size) and viewed under U.V light.

2.4.6 Agarose gel electrophoresis

Due to the presence of sugar-phosphate in the backbone of the DNA, the DNA is negatively charged. When DNA fragments are placed within an electric field, they migrate towards the

positive electrode. All DNA migrates towards the anode; however, larger nucleic acid fragments migrate slower through the polymerised agarose gel. Agarose gel electrophoresis was used to separate DNA fragments by size. To resolve DNA fragments greater than 400bp, a 1% agarose gel was used, whereas for amplicons smaller than 400bp, a 2% agarose gel was used.

The gels were prepared by dissolving (1-2% (w/v) agarose powder in TAE (40mM Tris, 20mM acetic acid, 1mM EDTA) by means of heating and allowed to cool enough to hold before 5µg/ml ethidium bromide was added. Ethidium bromide is a nucleic acid inserting agent; upon exposure to UV light it fluoresces and allows nucleic acid samples to be visualised. Gels were then cast in a casting stand and a comb added to form wells. Subsequently, this was then left to set before electrophoresis. Once set, the gel was placed into the gel tank which was filled with 1 x TAE buffer and 10 µl of the reaction was loaded into an agarose gel alongside 100bp or 1Kbp DNA ladder (New England Biolabs). Agarose gels were run for approximately 45-60 minutes at 90 volts. Once amplicons were resolved, they were imaged using a G: BOX transilluminator and bundled software.

2.4.7 Total RNA isolation for qRT-PCR

For qRT-PCR, High Pure RNA Isolation Kits were used (Roche), which included treatment of RNA with DNase, according to the supplier's instructions. Prior to running the TaqMan Gene Expression Assays, total RNAs were isolated to be used as a template for synthesis of single-stranded cDNA. Working solutions were prepared as directed in the producer’s manual. Cells were suspended in 200 µl PBS and 400 µl Lysis/-Binding Buffer (4.5 M guanidine-HCl, 50 mM Tris- HCl, 30% Triton X-100 (w/v), pH 6.6) was added and vortexed for 15 seconds and the entire sample was pipetted into the upper reservoir of a filter tube and centrifuged for 15 seconds at 8,000 × g. Afterwards, the flowthrough liquid was discarded and 90 µl DNase incubation buffer (1 M NaCl, 20 mM Tris-HCl and 10 mM MnCl2, pH 7.0) per sample was pipetted and added to 10 µl DNase. Next, the solution was mixed, pipetted on the upper reservoir of the filter tube and incubated for 15 mins at +15 to +25° C. 500 µl Wash Buffer I (5 M guanidine hydrochloride and 20 mM Tris-HCl, pH 6.6 (25° C); final concentrations after addition of 20 ml absolute ethanol was added to the upper reservoir of the filter tube and centrifuged 15 seconds at 8,000 × g. The flowthrough was discarded, the filter tube was combined with the collection tube and 500 µl Wash Buffer II (20 mM NaCl, 2 mM Tris-HCl, pH 7.5 (25°C) was poured into the upper reservoir of the assembly of the filter tube and centrifuged for 15 seconds at 8,000 × g. Subsequently, 200 µl of wash buffer II was then added to the upper reservoir of the filter tube assembly and centrifuged for 2 min at maximum speed

(approx. 13,000 × g) to remove any residual wash buffer. The filter tube was then inserted into a clean, sterile 1.5 ml microcentrifuge tube to elute the RNA: Next, 50 µl of elution buffer was dispensed to the upper reservoir of the filter tube and centrifuged for 1 min at 8,000 × g. The eluted RNA was directly quantified, as previously described in 2.4.2 and used either in RT or at –80°C for later analysis.

2.4.8 qRT-PCR protocol

The relative expression of the genes of concern was compared between samples using TaqMan Gene Expression Assays for quantitative analysis. qRT-PCR works in a similar manner to standard PCR by amplifying sequences of interest though it was using TaqMan Universal PCR Master Mix (The mix contains Taq DNA Polymerase, reaction buffer, dNTP mix with dUTP instead of dTTP). Likewise, a gene-specific primer and probe mixture (predeveloped TaqMan Gene Expression Assays), contains two unlabelled primers (1× final concentration is 900 nM per primer; 20× stock concentration is 18 µM per primer). The TaqMan® MGB probe (1× final concentration is 250 nM; 20× stock concentration is 5 µM). TaqMan® MGB probes contain a reporter dye (6-FAMTM) linked to the 5′end of the probe, a minor groove binder (MGB) at the 3′ end of the probe in addition to a nonfluorescent quencher (NFQ) Figure 2.4

The assay process (Steps 1 to 4 in Figure 2.4) occurs in every cycle during PCR amplification. The system depends upon the transfer of fluorescent energy between a reporter and a quencher. The TaqMan Minor-groove binding (MGB) oligonucleotide probe is covalently bonded to a fluorescent reporter. The TaqMan - (MGB) probe anneals specifically to a complementary sequence between the forward and reverse primer sites (Step 1). In these probes, a moiety that binds to the minor groove of dsDNA is covalently bonded to the 3' end of the probe, in addition to the quencher, providing increased stability for the probe-template duplex and increasing the annealing temperature. When the probe is intact (Steps 1 and 2), the closeness of the reporter dye to the quencher dye results in repression of the reporter fluorescence. As the DNA polymerase extends the template from the primer in a 5' to 3' direction, it cleaves only probes that are hybridised to the target (Step 3). The cleavage of the reporter dye from the quencher dye results in increased fluorescence by the reporter. The increase in fluorescence occurs if the target sequence is complementary only to the probe and is amplified during PCR. The fluorescence from the reporter dye is directly proportional to the number of amplicons generated. The polymerisation of the strand continues, however because the 3` end of the probe is blocked, no extension of the probe occurs during PCR (step 4).

The TaqMan Gene Expression Assays applied are targeting the following human transcripts (OCT4, Hs04260367_gH; SOX2, Hs01053049_s1; SOX17, Hs00751752_s1; HEX, Hs00242160_m1; FOXA2, Hs00232764_m1; HNF4α, Hs00230853_m1; AFP, Hs01040598_m1; CYP1A2, Hs00167927_m1; CYP3A4, Hs00604506_m1; CYP3A7, Hs02511627_s1; CPS1, Hs00157048_m1; Albumin, Hs00609411_m1). The probe fluoresces once bound to double-stranded DNA (dsDNA). By the end of each cycle, the level of fluorescence is determined and used to calculate the amount of dsDNA present, thus allowing the amount of transcript of the target gene to be determined, relative to other samples. In a final volume of 20 µl the quantitative real-time PCR (qPCR) reaction mix was prepared by mixing TE buffer (0.5 µl), PCR grade water (7 µl), Taq man master mix (10 µl), TaqMan gene expression assay (0.5 µl) and 2 µl of 5ng/µ of each cDNA sample per well in an optical 96 well reaction plate. Each reaction was repeated in triplicate. The plates were sealed using optical film, vortexed gently and centrifuged at 250 g to collect the reaction mixture at the bottom of each well. Afterwards, the DNA was amplified using an Applied Biosystems 7500 Fast Thermocycler using standard ramp rate and the following Thermal cycling conditions:

Stage	**Temp (°C)**	**Time (mm:ss)**
Hold§	**50**	**2:00**
Hold	**95**	**10:00**
Cycle (50 Cycles)	**95**	**0:15**
	60	**1:00**

Transcript levels between treatments were determined using the comparative ΔΔCt method by normalising to 18S ribosomal RNA (18S rRNA)) as housekeeping control to account for any variations in the RNA template between samples. For more reliable results it would be better to include control samples without reverse transcriptase treatment to check for any contamination.

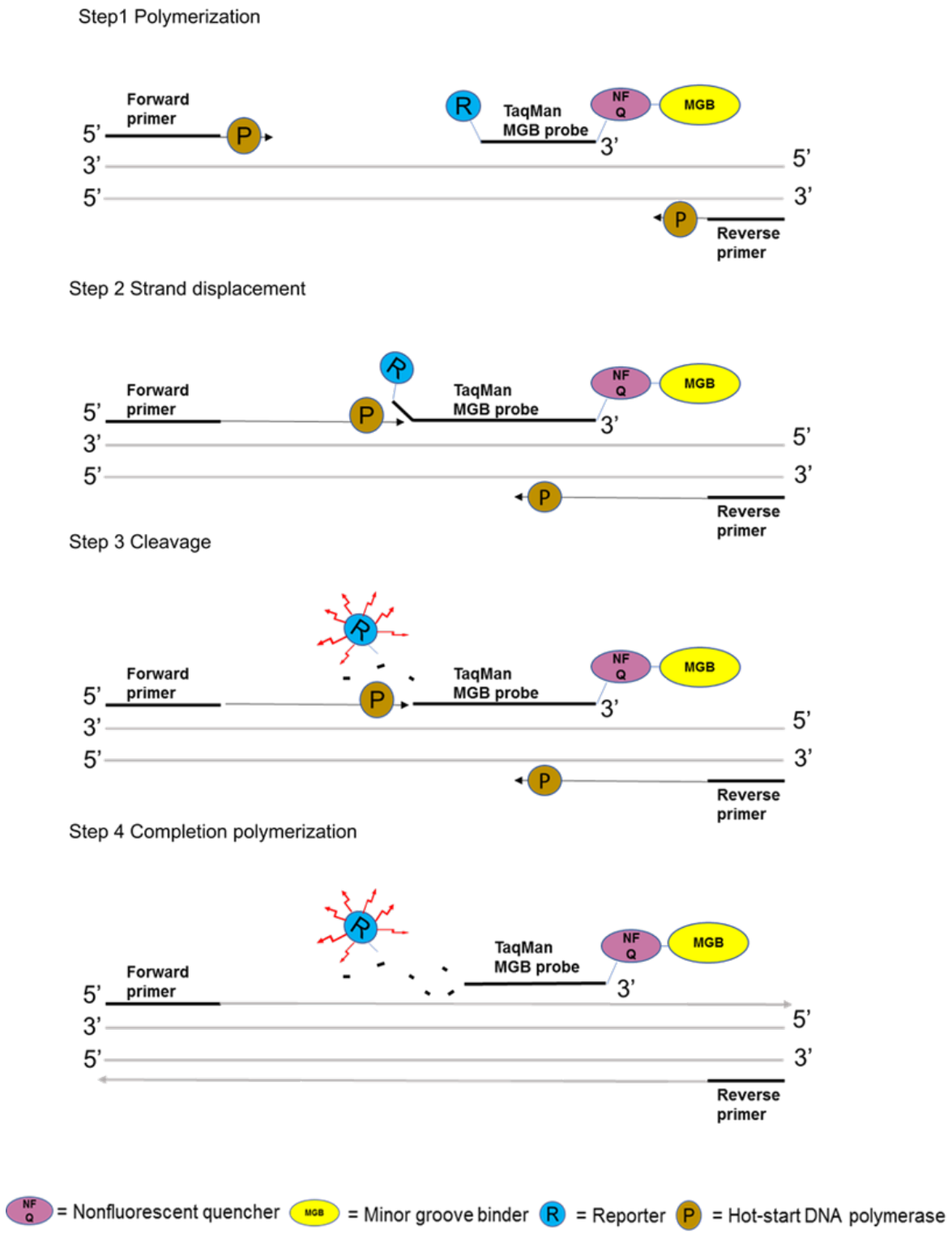

Figure 2.4 Schematic illustrations of TaqMan PCR. (Step 1) During polymerisation, the TaqMan probe containing a reporter dye (R) and a quencher dye (Q) specifically anneals to one strand of the DNA template between forward and reverse PCR primers. (Step 2) During amplification, the fluorogenic probe is displaced by Taq polymerase; (Step 3) and then cleaved, releasing the reporter dye; (Step 4) after cleavage, the shortened probe dissociates from the template allowing polymerisation of the strand to complete. Fluorescence is relative to the amount of amplification product accumulated Adapted from Medhurst 2000 [319]

2.5 Protein isolation, quantification and analysis

2.5.1 Tissue lysate preparation

Rat liver tissue was snap frozen in liquid nitrogen then stored at -80°C until required. When needed, it was thawed on ice and rinsed in PBS to remove any blood. The tissue was then homogenised in 20mM Tris (pH 7.5). Protein concentration was then quantified by Lowry assay described in 2.5.3 and stored until required at -80°C.

2.5.2 Preparation of cell lysate

Cultured cells were washed twice in 1x PBS then scraped into 1ml (per well of 6 well plates) of PBS. The samples were then transferred to a clean Eppendorf tube and centrifuged 13,000 rpm for 10 minutes and the pellet re-suspended in a known volume of 20mM Tris (pH 7.5). Samples were then quantified by Lowry assay (2.5.3), aliquoted and frozen at -80°C until needed.

2.5.3 Lowry protein assay

The Lowry assay was performed to determine protein concentration [320]. The mechanism is that under alkaline conditions, copper reacts with peptide bonds. The addition of Folin-Ciocalteu reagent (FCR) produces a blue colour. The intensity of the colour is relative to the amount of protein present at 750 nm. With the use of protein standards, the concentration of protein in samples can therefore be easily calculated. Assay buffers were prepared fresh each time. Buffer ABC was made up as follows: Lowry A (2% (w/v) Na2CO3 and 4% (w/v) NaOH), Lowry B (2% (w/v) sodium tartrate) and Lowry C (1% (w/v) CuSO4) were combined at a ratio of 100:1:1 (v:v:v). Folin's reagent (Fluca, Switzerland) was diluted 1:1 in distilled water prior to use. BSA was used as the protein standard and was made up in 20mM Tris (pH 7.5) in concentrations ranging from 0-20mg/ml from a 20mg/ml stock diluted into dH2O. Then, 5 µl of each standard and sample was diluted with 50 µl of dH2O and 1 ml of ABC buffer. The diluted samples were briefly vortexed and left at room temperature for 10 minutes. Subsequently, 100 µl of diluted Folin's reagent was added to each sample, mixed and incubated for 30 minutes. The samples were then transferred to 1 cm plastic cuvettes, and the absorbance at 750 nm was determined for each sample by a spectrophotometer. OD750 was measured using the 0mg/ml standard to blank. The OD750 of the standards was plotted against the concentration and used to calculate the protein concentrations of samples using the equation $y = m\chi + c$.

2.5.4 Sodium-dodecyl sulphate polyacrylamide gel electrophoresis (SDS- PAGE)

In 1970, Laemmli first described the use of the SDS-PAGE method to separate proteins by their molecular weight [321]. The proteins are initially denatured to polypeptide chains by heating in the presence of SDS and the reducing agent DL-dithiothreitol (DTT) which breaks any disulphide bonds in the secondary, tertiary and quaternary structure. Sodium-dodecyl sulphate polyacrylamide gel electrophoresis (SDS-PAGE) depends on utilising sodium SDS which is an anionic detergent. When an electric difference is applied to SDS bound polypeptides, they migrate towards the anode (due to the binding of negatively charged SDS) via the polyacrylamide gel at a rate proportional to their molecular weight, which allows for separation of proteins in a solution.

Regarding the SDS-PAGE, gels were cast between two glass plates held together with clamps and sealed at the bottom. Resolving gels (9%) were composed of 9% bis-acrylamide, 375mM Tris-HCl (pH 8.8), 0.1% (w/v) SDS, 0.05% (w/v) ammonium persulphate and 0.05% (v/v) tetramethylethylenediamine (TEMED). The ammonium persulphate and TEMED were added last as they catalyse the polymerisation of the acrylamide. After pouring the resolving gel, 100 µl of isopropanol was layered on top to eliminate air bubbles and to produce a straight edge between the separating and stacking gel. Once set (within 1 hour), the isopropanol was washed off with distilled water. The stacking gel consisted of 4% acrylamide/bis (w/v), 125mM Tris (pH 6.8), 0.1% (w/v) SDS, 0.1% (w/v) ammonium persulphate and 0.1% (w/v). TEMED was immediately poured over the resolving gel and a comb inserted into the polymerising gel to form wells. Once set, the glass plates were unclamped and either stored in electrode running buffer (25mM Tris, 0.1% (w/v) SDS and 192mM glycine, pH 8.3) at 4°C for 2-3 days or placed in a gel tank filled with electrode running buffer for immediate use.

2.5.5 Sample preparation for gel electrophoresis

To prepare the protein samples for SDS-PAGE gel electrophoresis. They were diluted to 1-2µg/µl in reducing loading buffer (62.5mM Tris buffer pH 6.8, 10% v/v glycerol, 2% w/v SDS, 100mM DTT and 0.02% w/v bromophenol blue and denatured by heating to 95°C for 5 minutes. Typically 20 µg of protein was loaded per well alongside a ladder containing coloured proteins of known molecular weights (ColorBurst Electrophoresis Marker, molecular weight 8-220kDa). Electrophoresis was run at 100V until the migrating front reached the stacking/resolving interface at which point the voltage was increased to 160V. Once the samples had passed through the entire length of the gel, the proteins were transferred to nitrocellulose for Western blotting (described in 2.5.6).

2.5.6 Western blotting

Western blotting is the process of specific proteins detection utilising SDS-PAGE and immunodetection. After the protein samples have been separated by electrophoresis, filter paper and nitrocellulose membrane (Thermo-Scientific) were cut to the same gel size and dipped in pre-chilled transfer buffer (25mM Tris, 192mM glycine and 20% (v/v) methanol, pH 8.3). Then, the plates were removed, and the gel transferred to the nitrocellulose membrane. The gel and nitrocellulose membrane was sandwiched between filter paper and a scrubbing pad on both sides in a transfer cassette, placing the nitrocellulose membrane close to the anode. The cassette was placed in a tank filled with pre-chilled transfer buffer and an ice block. The transfer was run for 2 hours at 100V. Once the transfer had occurred, nitrocellulose membranes were washed twice with 1 xTBS-T (0.2M NaCl, 20mM Tris, and 0.05% v/v Tween 20, pH7.4) to remove any excess methanol. The membranes were then blocked in 3% (w/v) skimmed milk powder in TBS-T for 1 hour at room temperature or 16 hours at 4°C to block non-specific antibody binding. After blocking, the membranes were washed 3x 5 mins each in TBS-T, before immunodetection. The nitrocellulose membranes were then incubated in primary antibody (diluted in 0.3% (w/v) skimmed milk powder in TBS-T, (see Table 2.1 for dilutions) for 1 hour at room temperature or 16 hours at 4°C. After primary incubation, nitrocellulose membranes were washed 3x 5 mins in a 1xTBS-T buffer followed by incubation with the appropriate species-specific horseradish peroxidase (HRP) -conjugated secondary antibody diluted in 0.3% (w/v) skimmed milk powder in TBS-T before the nitrocellulose membrane was rewashed as before.

To detect the proteins of interest, enhanced chemical luminescence reagents ECL (Thermo-scientific) was used. 1 ml of reagents 1 and 2 were mixed and added to the membrane and left for 30 seconds. ECL is a chemiluminescent able to bind to the HRP conjugated on the secondary antibody allowing detection of proteins. The membrane was then blotted with tissue paper to remove excess ECL and wrapped in saran wrap in a film cassette. CL-Xposure films (Thermo scientific) were exposed to the nitrocellulose membrane in a dark room at different times (dependent on antibodies used), then developed using an automated developer (RP X-OMAT, Kodak, Hertfordshire, UK). Following development, the position of the ladder proteins was marked on the film. Nitrocellulose membranes in some cases were re-probed for an additional protein. After the initial probing, membranes were stripped by washing for 1 hour at room temperature in TBS-T, changing the TBS-T every 10 minutes. The membranes were then blocked and probed again as before.

2.5.7 Fluorescence immunocytochemistry

Cells cultured either in 6 well plates or in the NUNC® chamber were washed twice in PBS then permeabilised with 2 ml of ice-cold absolute methanol at 4°C for 10 minutes. The methanol was then aspirated, and the cells washed twice with PBS before fixation in 2 ml of fixative solution (0.2% (v/v) glutaraldehyde and 2% (v/v) formaldehyde in PBS, pH 7.4). After 15 minutes at room temperature, the cells were incubated with 5% (v/v) FCS in PBS for 10 minutes to block non-specific binding of antibodies. After washing twice in 10mLs of PBS, the cells were incubated with the primary antibody diluted in PBS (see Table 2.1 for antibody details and dilutions) for 1 hour at RT followed by extensive washing in PBS, which was followed by incubation with the suitable secondary antibody at room temperature for 20-30 minutes.

Secondary antibodies incubation was conducted in the dark, i.e., slides were covered in foil). Replicate wells stained identically except for incubation with no primary antibody were routinely included to determine the background level of fluorescence (no 1o Ab control). After extensive washing in PBS, the cells were incubated with the DNA intercalator 4',6-diamidino-2-phenylindole (DAPI, 6µg/ml in PBS) for 20 minutes to identify cell nuclei. The cells were washed three times with PBS before and stored in 5 ml of PBS at 4°C in the dark before visualisation. For double staining, the cells were stained sequentially. They were reblocked with 5% (v/v) FCS in PBS for 10 minutes and washed twice in 10mLs of PBS. This was followed by incubation for 1 hour with a second primary antibody diluted in PBS.

The second primary antibody was raised in a species different from that of the first primary antibody (i.e., the first primary antibody was raised in a rabbit and the second primary antibody was raised in a mouse). This was followed by washing in PBS and incubation at room temperature for 20-30 minutes with a second secondary antibody conjugated with a fluorophore label that has a different colour from that of first secondary antibody (i.e. the first secondary antibody was anti rabbit IgG- fluorescein isothiocyanate (FITC) conjugated (green) and the second secondary antibody was anti-mouse IgG- Alexa fluor 568 conjugated (red). This was subsequently followed by rinsing in PBS-and counterstaining with DAPI for 20 minutes at room temperature. Finally, chambers were removed from the slides before coverslips were mounted using vectashield (anti-fade) and sealed with clear nail varnish. Slides were visualised by fluorescence confocal microscope.

Table 2.1 List of antibodies employed in Western blot and immunocytochemistry analysis

Antigen	Molecular mass (kDa)	Dilution	Comments and source
Primary antibodies			
AFP	n/a	1:100 ICC	Mouse monoclonal IgG to alpha 1 Fetoprotein (ab3980)
Albumin	60	1:3000 WB	Rabbit polyclonal IgG from ICN (0855715).
Albumin	n/a	1:100 ICC	Mouse monoclonal anti albumin (sc-271605)
β-actin	44	1:3000 WB	Monoclonal anti β-actin antibody produced in mouse sigma (A54410)
Cytochrome P4502E1	50	1:1000 WB 1:100 ICC	Rabbit polyclonal IgG Cytochrome P4502E1, Abcam (28146)
CPS-1	160	WB 1:2000 ICC 1:100	Rabbit polyclonal IgG to CPS1 (ab3682)
Cytokeratin 19	n/a	1:100 ICC	Rabbit polyclonal IgG to Cytokeratin 19 (ab484632)
-β-catenin	95	1:1000 WB	Rabbit polyclonal IgG to beta Catenin, Abcam (ab 6302)
β-catenin phosphorylated	95	1:1000 WB	Mouse monoclonal to beta Catenin phosphorylated at serine 33 and 37, Abcam (ab11350)

Antigen	Molecular mass (kDa)	Dilution	Comments and source
DDDDK tag	48.9	1:2000 WB 1:200 ICC	Anti-DDDDK tag mouse antibody, Abcam (ab72469)
SGK	55	1:1000 WB 1:200 ICC	SGK mouse Ab (sc-377360)
Secondary antibodies			
Anti-rabbit IgG	n/a	1:3000 WB	HRP-conjugated goat anti-rabbit IgG , Sigma (A6154)
Anti-mouse IgG	n/a	1:3000 WB	HRP-conjugated goat anti-mouse IgG, Dako (P0447)
Anti-rabbit IgG	n/a	1:3000 ICC	FITC-conjugated sheep anti-rabbit IgG, Dako (F7512)
Anti-mouse IgG	n/a	1:3000 ICC	TRITC conjugated rabbit Anti-Mouse IgG (whole molecule) - SIGMA T2402

(abbreviations: ICC - immunocytochemistry, IWB – Western blot, IgG -immunoglobulins, HRP-horse radish peroxidase)

2.6 SGK1 activity assay

2.6.1 Buffer preparation

1. 5X Reaction Buffer A: 200mM Tris [pH 7.5], 100mM MgCl2 and 0.5mg/ml BSA
2. 4X Kinase Buffer: 4X Reaction Buffer A + 200µM DTT =2µl/ml)
3. 4X Kinase Buffer D: by adding 4% DMSO
4. 1X Kinase Buffer: by diluting the 4X Kinase Buffer

5. 1X Kinase Buffer D: by diluting 4X Kinase Buffer D

6. 1X Kinase Buffer (5% DMSO): by diluting the 4XKinase Buffer and adding 5% DMSO

2.6.2 SGK1 assay protocol

The ADP-Glo Kinase Assay is a luminescent kinase assay which determines the amount of adenosine diphosphate (ADP) produced by a kinase reaction; ADP is changed into adenosine triphosphate (ATP), which is changed into light by Ultra-Glo Luciferase. The luminescent signal positively relates to kinase activity. 500ng/ml of cells lysate were prepared. Next, 20 µl kinase solution was made by mixing 13.33µl of (500ng/ml) of cells lysate, 5 µl kinase buffer D (4X Reaction Buffer A + 200µM DTT) and 1.67 µl of H20 per samples. Additionally, the substrate mix was prepared by mixing 4X Kinase Buffer D, 100µM ATP (the 10x used to create the standard curve) and AKT Substrate (1mg/ml) in ratio 1:1:2. A kinase reaction was performed by adding 14 µl of 2.5X ATP/Substrate Mix into 20 µl of kinase solution, mixed for two mins and incubated for 40 minutes at room temperature. After the kinase reaction was completed, an equal volume of ADP-Glo Reagent was added and incubated for 40 minutes to terminate the kinase reaction and deplete the remaining ATP. Second, the kinase detection reagent was added and incubated for 30 to 60 minutes at room temperature to simultaneously convert ADP to ATP and allow the newly synthesised ATP to be measured using a luciferase/luciferin reaction Figure 2.5. The generated light was measured using a luminometer. The luminescence was correlated to ADP concentrations by using an ATP-to-ADP standard curve. The samples used to generate an ATP-to-ADP standard were created by combining the appropriate volumes of ATP and ADP stock solutions (Table 2.2). Making a standard curve that represents the luminescence corresponding to the conversion of ATP to ADP based on the ATP concentrations used in the kinase reaction.

%ADP	100	80	60	40	20	10	5	4	3	2	1	0
%ATP	0	20	40	60	80	90	95	96	97	98	99	100

Table 2.2 Percent Conversion of ATP to ADP Represented by the Standard Curve

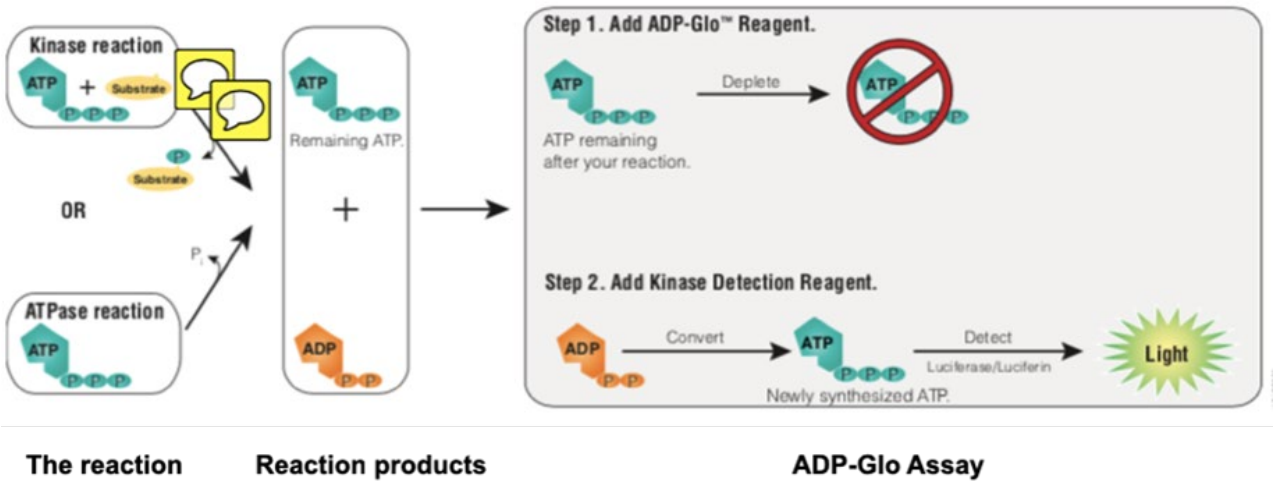

Figure 2.5 The ADP-Glo assay principle. The assay comprised two steps. The first step (after the kinase or ATPase reaction) is the addition of the ADP-Glo™ reagent which ends the kinase reaction and depletes any remaining ATP (40-minute incubation time). The second step adds the kinase detection reagent which converts ADP to ATP and generates light from the newly synthesised ATP using a luciferase-luciferin reaction, is 30–60 minutes incubation time according to the ATP concentration used in the kinase reaction). The light produced is proportional to existing ADP and, consequently, kinase or ATPase activity [322].

2.7 Differentiation of IPSCs (AD3 cells) into hepatocyte-like cells.

2.7.1 Reagent set up

All media and reagents were purchased from Gibco unless stated

CDM-PVA medium

Chemically defined medium: Poly Vinyl Alcohol (CDM-PVA) medium was prepared for maintenance of human induced pluripotent stem cells and differentiation to endoderm. For 500 ml, 0.5 grams of Poly Vinyl Alcohol (PVA) (Sigma) was dissolved in 5 ml of sterilised distilled water by gradual heating in a water bath till 90ºC and mixed with 245 ml of Iscove's Modified Dulbecco's Medium (IMDM). This was then sterilised using 0.22 µm filtration device and added to 250 ml of DMEM-F12 before adding 5mL Concentrated lipids 20 µL Thioglycerol (Santa Cruz), 350 µL Insulin, (Roche) 250µL Transferrin(Roche), 100units/ml penicillin, 100µg/ml streptomycin (Sigma). The medium was stored in 4ºC to be used up to four weeks after preparation and should to be warmed to 37 °C before use. For maintenance of hPSCs, 10ng/ml of recombinant Human/Mouse/Rat Activin A Protein(Activin A) (R&D systems), 10ng/ml recombinant Human FGF basic Protein (bFGF) (R&D system) was freshly prepared

by adding 1 µl of 100µg/ml stock per 10ml of CDM-PVA medium. For cell differentiation to endoderm CDM-PVA media was freshly prepared by mixing 10 ml of CDM-PVA media with 10 µl of 100µg/ml stock Activin A (100ng/ml), 10 µl of 100µg/ml stock bFGF (100ng/ml), 1 µl of 100µg/ml stock of recombinant Human Protein BMP4 (ThermoFisher Scientific) (10ng/ml), 2 µl LY294002 of (Promega) 50mM stock solution (10µM) and 7 µl of 4.29793mM CHIR99021(Sigma) (3µM)

RPMI-B27

Roswell Park Memorial Institute (RPMI) 1640 Medium supplemented with B27 (RPMI-B27) was prepared for differentiation of ADE and hepatoblast specification. For 500 ml of RPMI, B27 supplement was freshly prepared by mixing 0.05 mg Vitamin A acetate (sigma) (0.1mg/L), 0.2125 g bovine serum albumin (BSA) (based on serum albumin concs of 0.35-0.5g/L), 5 ml ITS supplement (1:100 dilution) that consists of 1.0 mg/ml recombinant human insulin, 0.55 mg/ml human transferrin and 0.5 µg/ml sodium selenite at the 100x concentration, 450 mg D-galactose(Sigma) (900mg/L), 0.95 mg Ethanolamine HCl (1.9mg/L), 3.95 ml of L-Cartinine HCl (2mM) (Sigma), 5 ml concentrated lipids (1:100 dilution) which is a concentrated lipid emulsion formulated to substitute foetal bovine serum in cell culture, 0.04 mg Putrescine 2HCl (0.08mg/L) (Sigma), 5 µl of 10mM Triiodothyronine (T3) and 5 mg reduced glutathione (10mg/L).

Subsequently, B27 supplement was added to 490 ml RPMI 1640 in addition to 5 ml Non-Essential Amino Acids (NEAA) which were supplemented for cell culture medium to increase cell growth and viability. NEAA is constituted of 10mM glycine, 10mM L-alanine, 10mM L-asparagine, 10mM L-aspartic acid, 10mM L-glutamic acid, 10mM L-proline and 10mM L-serine. Additionally, 100units/ml of penicillin and100µg/ml streptomycin were also added to RPMI-B27. The medium was stored at 4 °C for up to 3 weeks and warmed up to 37 °C before use. For differentiation to Anterior Definitive Endoderm (ADE), RPMI-B27 + Activin A was freshly prepared by mixing 10 ml of RPMI-B27 with 5 µl of 100µg/ml stock of Activin A (50ng/ml). For hepatoblast specification, RPMI-B27 + BMP4 and FGF10 was freshly prepared by adding 1 µl of 100µg/ml stock of BMP4 (20ng/ml) and 0.5 µl of 100µg/ml stock of FGF10 (ThermoFisher Scientific) (10ng/ml)

HBM+OSM+HGF

Hepatocyte Basal Medium (HBM) from Lonza (CC-3199 was used for maturation of hepatoblast into hepatocyte-like cells. 100units/ml penicillin, 100µg/ml streptomycin was added to 500 ml of HBM and per 10ml of HBM, 3 µl of 100µg/ml stock of recombinant human OSM (PEPROTECH), (30ng/ml) and 5 µl of 100µg/ml stock of HGF (PEPROTECH) 50ng/ml were added when required.

2.7.2 The procedure for AD3 cells differentiation toward hepatocyte-like cells

Upon receiving iPSCs ad3 cells, cells were cultured with freshly prepared CDM-PVA with 100ng/ml Activin A and 100ng/ml b FGF. After 24 hours, the cells were washed with calcium- and magnesium-free PBS (137 mM NaCl, 27 mM KCl and 100 mM phosphate pH 7.4). The cells were then treated with freshly prepared CDM-PVA media containing 100ng/mL activin-A, 100ng/mL FGF2, 10ng/mL bone morphogenetic protein 4 (BMP4), 10µM LY294002 and 3µM CHIR99021 for 24 hours. This was followed by freshly prepared CDM-PVA with 100ng/mL activin-A, 100ng FGF2, 10ng/mL BMP-4 and 10µM LY294002 for 24 hours to produce a culture enriched for definitive endodermal cells (DE) [52] (DEF ENDODERM d3). DE cells represent the earliest precursors for all endodermal organs. The culture medium was then changed to RPMI-B27 medium containing 100ng/mL activin-A and 100ng/mL FGF2 to promote the formation of anterior definitive endodermal cells [52].

From days five to seven, cells were treated daily with RPMI-B27 differentiation medium with Activin-A (50 ng/ml). At this time ADE specification takes place (ANT DEF ENDODERM d8).). These cells represent a common progenitor between the liver, pancreas, lung and thyroid. At day 8, hepatic differentiation was induced by replacing the medium with RPMI-B27 differentiation medium containing 20ng/mL BMP4 and 10ng/mL fibroblast growth factor (FGF10). The medium was changed daily for the subsequent four days leading to cell cultures enriched with hepatoblasts (HEPATOBLASTS d12). Formation of hepatocyte-like cells was subsequently promoted by culturing hepatoblasts in basal hepatocyte medium (Lonza CC-3199) containing 30ng/Ml OSM and 50ng/mL HGF. The medium was changed every two days (HEPATOCYTE-LIKE dX).

2.8 Image analysis

Cells were viewed using an OPTIKA bright-field microscope and imaged with a BUC2 Camera connected to a TOSHIBA computer set up with ScopeImage 9.0 software. Fluorescently stained cells were imaged using either a Zeiss fluorescence (Cambridge, UK) or a Nikon SP2 laser scanning confocal (Kingston-upon-Thames, UK) microscope. AdV-GFP infected cells were imaged by confocal microscope (Leica). The cells were counted using ImageJ. Percentage of the GFP fluorescence cells determined. The threshold for positive staining was specified and kept constant for each batch of stained slides.

2.9 Statistics

Data in this project were analysed using SPSS statistical software version 19 (IBM, Armonk, NY, USA). To determine the statistically significant differences between groups, the mean values of the groups were analysed using one way ANOVA and the Student's 2-tailed t-test. Despite the hypothesis test used, significance was achieved where $p<0.05$.

Chapter 3. **Investigating the role of SGK1 in B-13 trans-differentiation to B-13/H cells**

3.1 Introduction

The B-13 pancreatic cell line is a progenitor cell line with a unique capacity to generate hepatocyte-like (B-13/H) cells after exposure to glucocorticoid hormone alone [198,200]. The mechanism(s) controlling the conversion/trans-differentiation of B-13 cells to B-13/H cells could therefore be used to stimulate/maintain differentiated phenotype in stem cell-derived specialised cells.

In the Tg (Crh) mouse model of Cushing's disease, which produces a prevalent expression of hepatocyte-specific gene expression in the acinar pancreas by 21 weeks of age, Sgk1c was induced from undetectable levels in the pancreas [226,231]. A further study in 2013, demonstrated that the human pancreas contained hepatocyte levels of hepatocytes marker genes after long-term systemic treatment with glucocorticoid and culturing human acinar cells with glucocorticoid also results in expression of hepatocyte-specific genes. These modifications were associated with an induction in the expression of the SGK1F variant [227]. Moreover, a previous study identified that *Sgk1* is significantly upregulated in B-13 cells when treated with glucocorticoid, most noticeably an alternatively transcribed variant c. Transfecting B-13 cells with expression vectors encoding the different human *SGK1* variants demonstrated that SGK1C and the human-specific F variant converted B-13 cells into hepatocytes without glucocorticoid treatment. In addition, kinase-dead (KD) mutant SGK1C and SGK1F proteins failed to induce expression of CYP2E1 or albumin in contrast to the wild-type equivalents.

All these findings suggest that the kinase function of SGK1C and F isoforms are essential for promoting the trans-differentiation of B-13 cells to B-13/H cells [226]. Thus, expression of SGK1 was considered as a potential future route to promoting the maturation of human iPSC-derived hepatocytes. An adenoviral vector system was selected given that liver cells are readily infected by adenovirus and the human *SGK1F* cDNA sequence was chosen because i) the intention was to work with human iPSCs and it encodes a human-specific sequence; ii) previous data suggested it functioned in B-13 cells, which were to be used to test functionality prior to moving into limited iPSCs resources and iii) avoid the use of SGK1C ensured that any complications with endogenous *Sgk1c* could be avoided (i.e., it would be evident that any influence on the B-13 cells was associated with ectopic gene expression).

3.2 DEX induced the conversion of B-13 into B-13/H and SGK1 induction

B-13 cells have been observed to transdifferentiate from a pancreatic exocrine-like cell to an hepatocyte-like-cell (B13/H cells) in response to DEX treatment[323].To examine the effect of DEX on the conversion of B-13 cells into B-13/H cells and the induction of SGK1, B-13 cells were treated with 10 nM DEX for 14 days. Changes in cells morphology were readily observed. The size of DEX treated B-13 cells increased and their shape changed from round spherical to a flattened polygonal shape indicating the change in cells phenotype (Figure 3.1**)**.To confirm the trans-differentiation of the cells into hepatic phenotype, fluorescence immuno-cytochemical staining was used to detect the expression of the hepatocyte-specific genes, such as carbamoyl phosphate synthase (*CpsI*) cytochrome P450 (*Cyp2e1*) and *Albumin* [324].Figure 3.2 illustrates the marked expression of Cps1 and moderate to low expression of Cyp2e1 and Albumin proteins respectively. Moreover, using the standard glucocorticoid-dependent differentiation protocol (14 days treatment with 10nM DEX, fluorescence immunocytochemistry results demonstrated expression of both CpsI and Sgk1 in B-13/H cells, with higher punctate staining (likely due to the mitochondrial localization of CpsI) correlating with cells expressing the highest levels of Sgk1 protein (Figure 3.3).

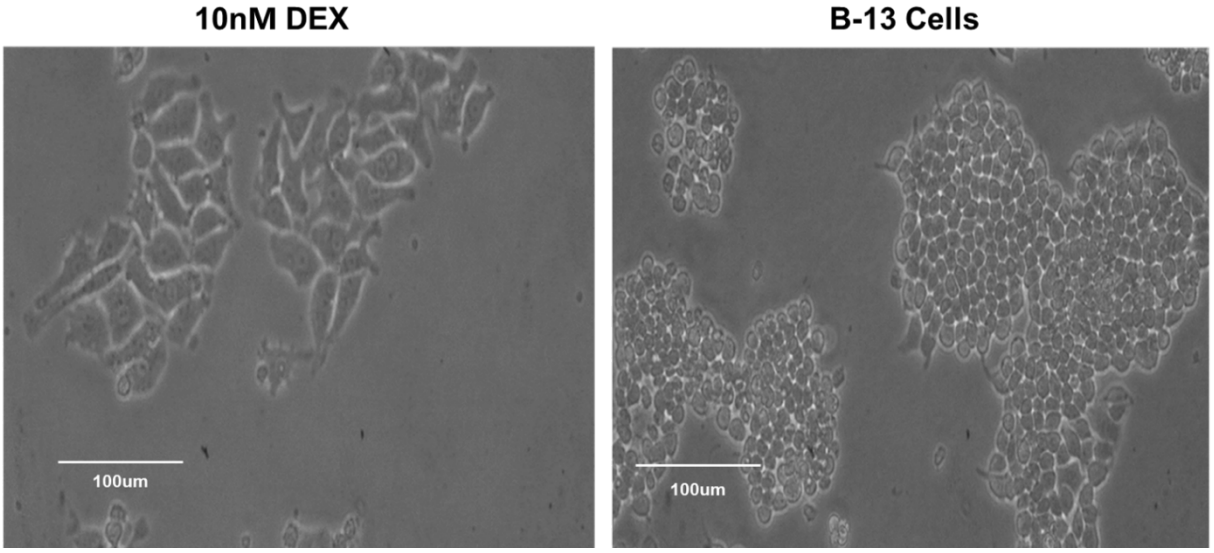

Figure 3.1 10 nM DEX induced morphological alterations of B-13 cells into B-13/H cells phenotype. B-13 cells treated with 10nMDEX for 14 days. A Photomicrograph of B-13 cells were taken before and after treatment with 10 nM DEX. Data are typical for several separate experiments.

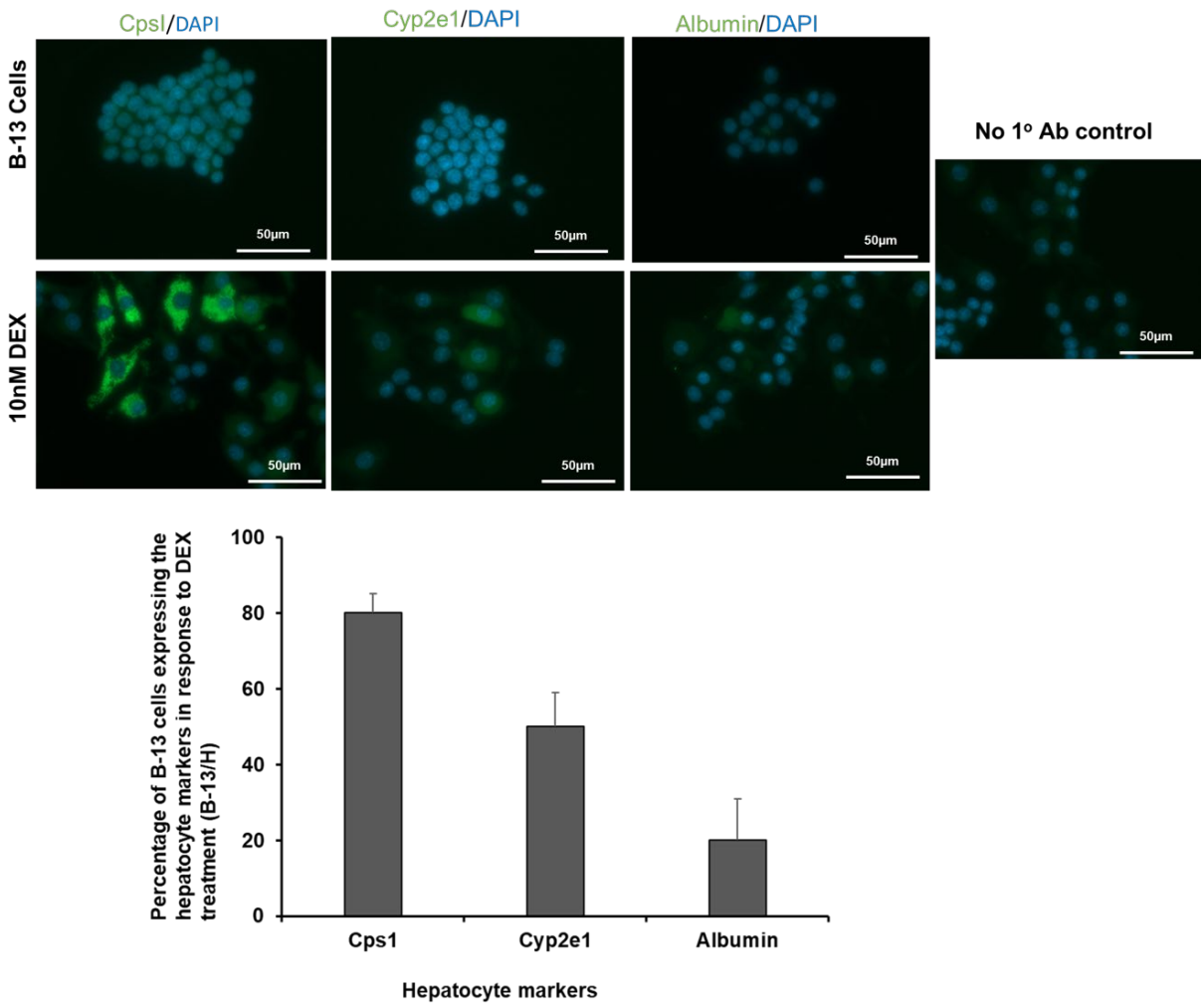

Figure 3.2 10 nM DEX induced the conversion of B-13 into B-13/H. B-13 cells were treated with 10nM DEX for 14 days (to generate B-13/H cells) and cells fixed. The detection of hepatocyte markers for indicated protein expression (green) determined by immunocytochemistry with DAPI (blue) for identification of nuclei (upper panel). Percentage of B-13/H cells expressing Cps1, Cyp2e1 and albumin proteins were quantified (lower panel). Data are typical of 4 separate experiments. All images were taken under identical spectral conditions and processed identically.

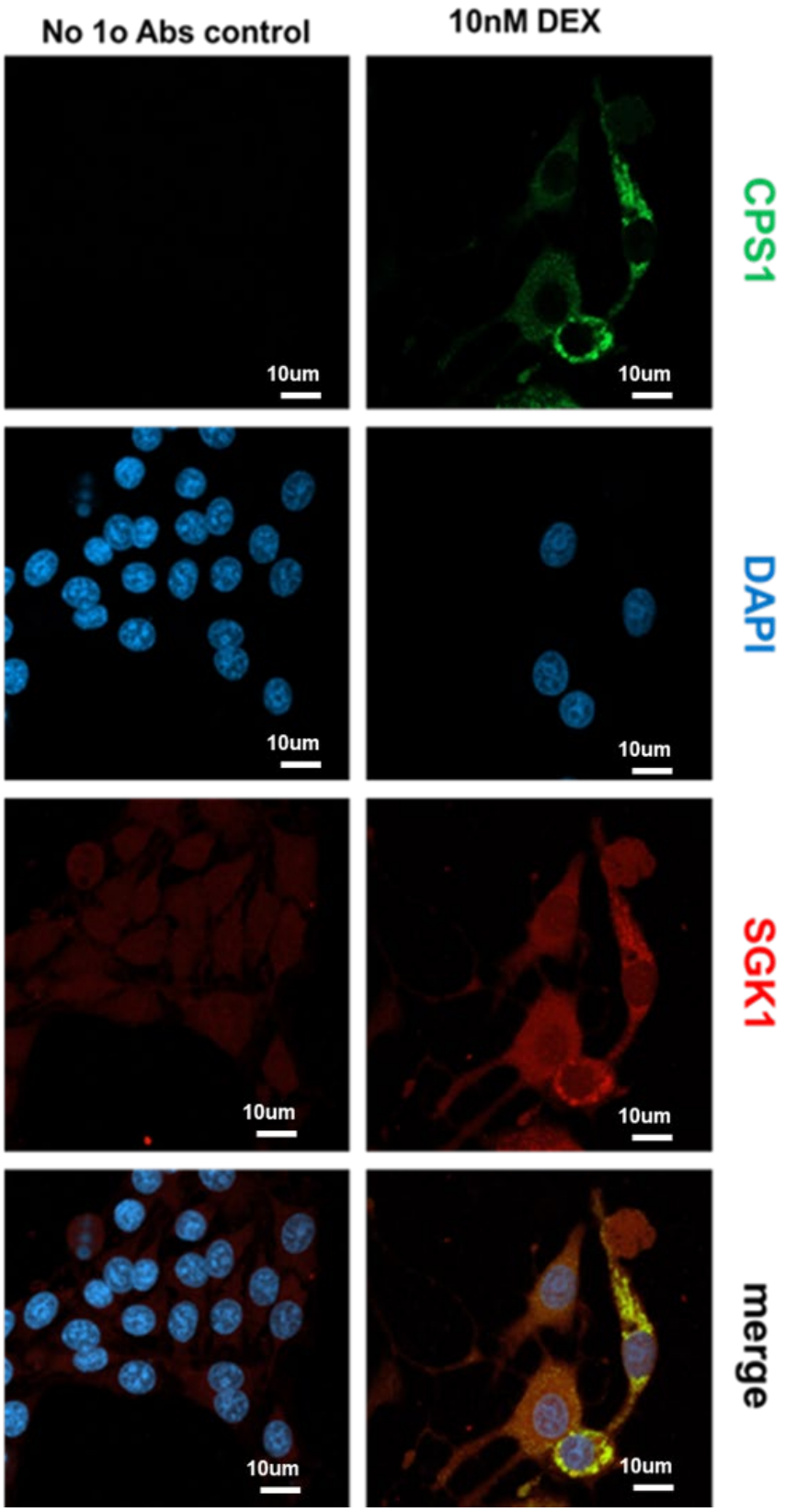

Figure 3.3 10 nM DEX induced the conversion of B-13 into B-13/H and SGK1 induction. Confocal images of B-13/H cells produced via exposure to10nM DEX glucocorticoid and examined for the expression of CpsI and Sgk1. Data are typical of 4 separate experiments. All

images were taken under identical spectral conditions and processed identically.**Adenovirus efficiently infected B-13 cells but impacted on cell viability**

To increase the likelihood that a significant proportion of cells express SGK1F, an adenoviral vector system was employed and to optimise the efficiency of B-13 infection with the adenovirus, B-13 cells were infected AdV-GFP at different multiplicity of infections (MOIs). B-13 and B-13/H cells were infected with MOI 0, MOI 1, MOI 5, MOI 10 and incubated for 24 hours. Cells were imaged by fluorescence microscopy and infected cells identified by means of their expression of the fluorescent GFP protein. The mean percentage of GFP positive cells per random fields of view were calculated. As presented in Figure 3.4 A&B the rate of infection was proportional to the MOI and resulted in more than 80% of B-13 and B-13/H cells being infected with an adenovirus encoding green fluorescent protein (AdV-GFP) at an MOI of 15. Trypan blue viability test was conducted to assess the B-13 and B-13/H cells viability post 6 days of infection with different MOIs of AdV-GFP. The percentage of cells excluding trypan blue dye was high in control cells or cells infected with a low MOI of 1, though marked toxicity was observed at MOIs of 10 and 15 in B-13 cells and MOI 15 in B-13/H cells as demonstrated in Figure 3.5 A & B. Therefore, an MOI of 1 was chosen to infect cells over an extended 14 day period, with repeated infection every 2 days. As judged by GFP expression, the infection at an MOI of 1 resulted in moderate (~20%) infection with minimal toxicity, repeated infection at an MOI of 1 was employed to maximise the proportion of cells infected, whilst reducing toxicity (Figure 3.6**).** This approach was successful for roughly 10 days but typically, significant toxicity after this time was observed, which limited the scope for testing the effects of SGK1F expression.

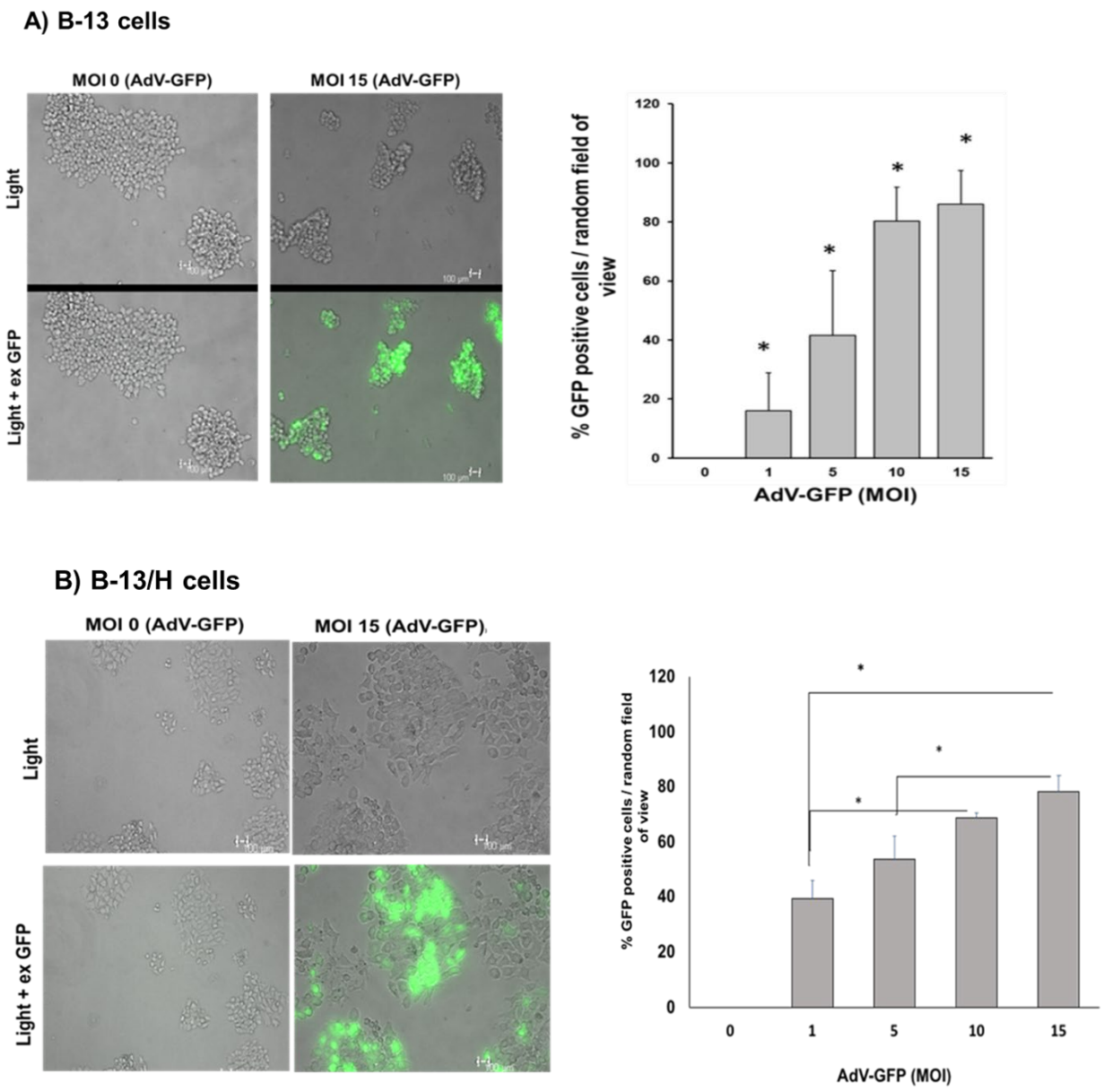

Figure 3.4 Infecting B-13 and B-13/H cells with AdV-GFP results in more than 80% infection and expression of GFP rate. A, B-13 cells were infected with AdV-GFP at the indicated MOI. left panel: typical view of B-13 cells after 24 hours post infection as indicated. right panel: the mean percentage and SD of cells expressing GFP determined by fluorescence microscopy from 3 randomly selected views from the same experiment. B, B-13/H cells were infected with AdV-GFP at the indicated MOI. Left panel typical view of 14 days DEX treated B-13 cells (B-13/H) after 24 hours post infection as indicated. Right panel: mean and SD percentage GFP positive cells from 3 randomly selected fields of view from the same experiment. Data are the mean and SD of 3 determinations from the same experiment. Data typical of 3 separate experiments. *Significantly different infection ($P < 0.05$) from uninfected cells using one way ANOVA followed by a Tukey post hoc test.

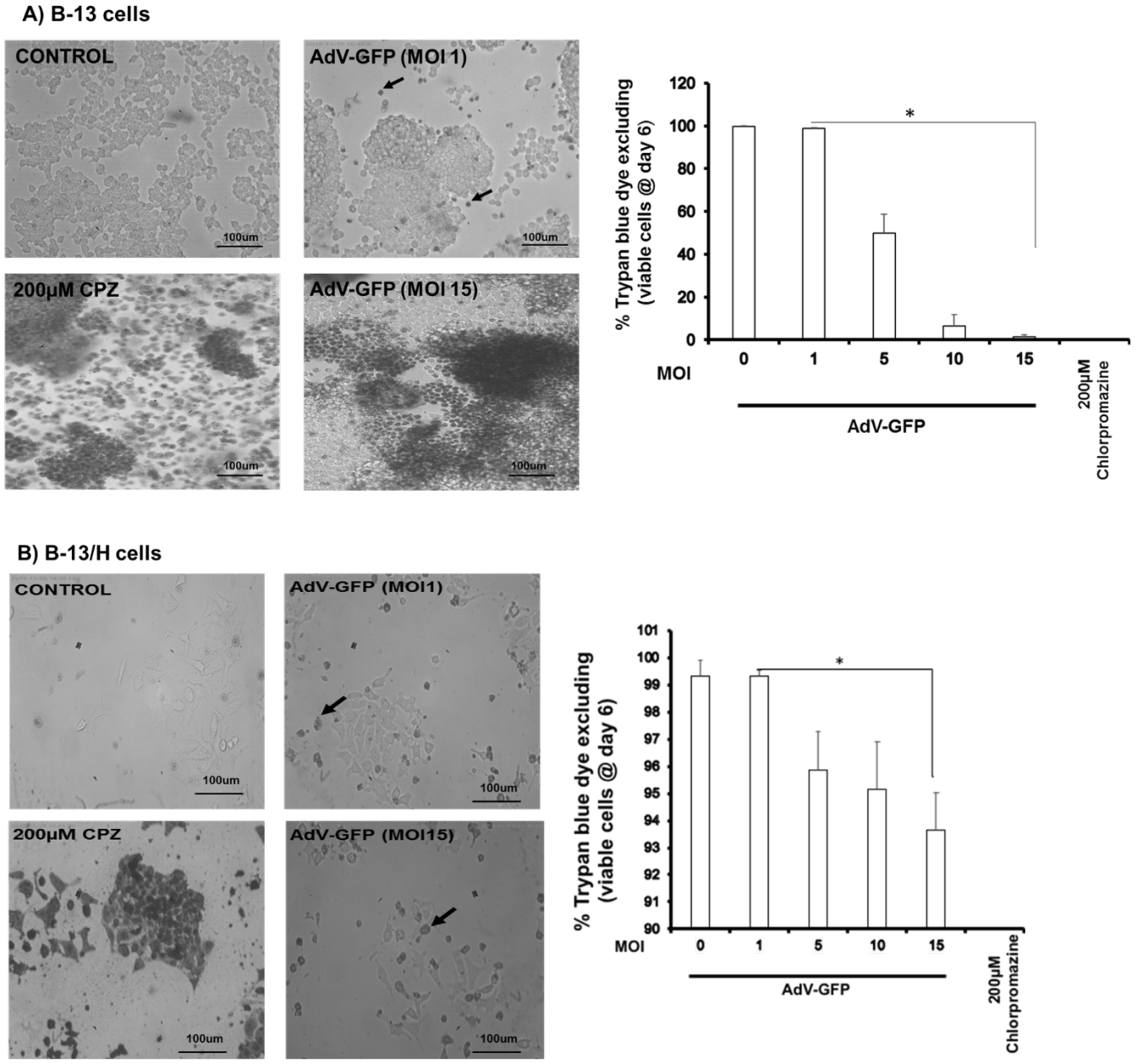

Figure 3.5 Infecting B-13 and B-13/H cells with AdV-GFP impacted on cell viability. B-13 and B-13/H cells were infected with AdV-GFP at the indicated MOI :(A) Left panel: photomicrographs of B-13 cells infected or treated as indicated for 6 days and stained with trypan blue as a marker for cell viability (excludes dye); Right panel: trypan blue exclusion; data are the mean and SD of 3 determinations from the same experiment. (B) Left panel, photomicrographs of 14 days DEX treated B-13 cells (B-13/H) infected or treated as indicated for 6 days and stained with trypan blue as a marker for cell viability (excludes dye); right panel: trypan blue exclusion. Data are the mean and SD of 3 determinations from the same experiment. *Significantly different trypan blue exclusion ($P < 0.05$) from uninfected cells using oneway ANOVA followed by a Tukey post hoc test. Data typical of 3 separate experiments. The arrows in the figures indicating the dead cells (trypan blue stained).

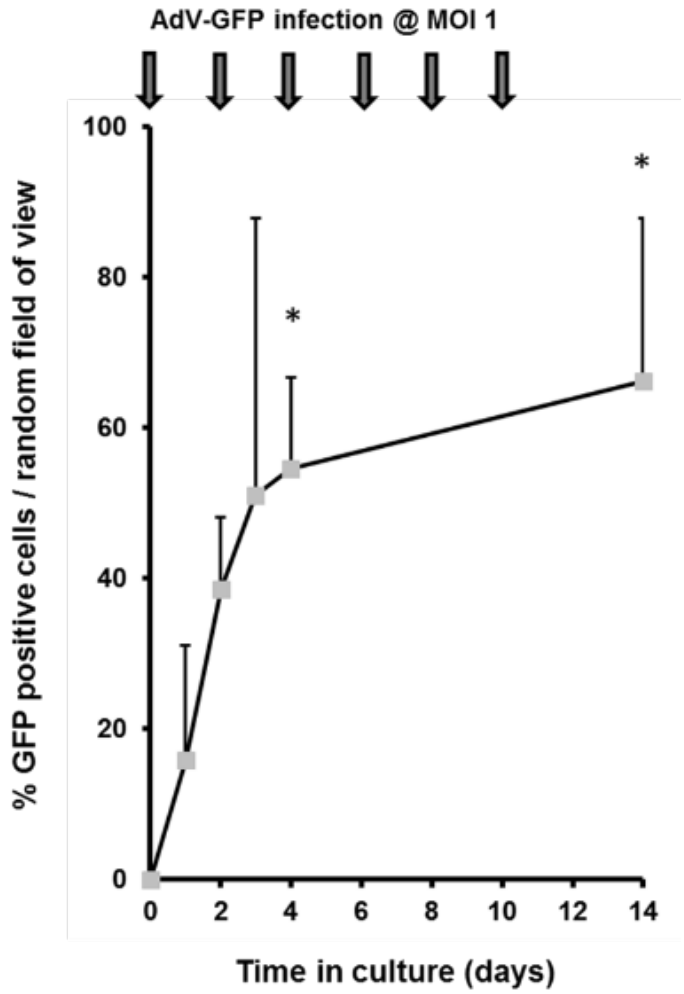

Figure 3.6 Effect of repeated infection of B-13 cells with AdV-GFP at MOI 1 on the expression of GFP. B-13 cells were infected at an MOI of 1.0 as indicated by the arrows and the mean percentage and SD of cells expressing GFP determined by fluorescence microscopy from 3 randomly selected views. Data typical of 3 separate experiments. *Significantly different ($P < 0.05$) from time zero uninfected cells using one way ANOVA followed by a Tukey post hoc test**.**

3.4 Infection of B-13 cells with AdV-*SGK1F* results in expression of SGK1 kinase activity

To determine the functionality of *SGK1F* expressed in B-13 cells, B-13 cells were infected repeatedly at an MOI 1 with AdV-*SGK1F* for 14 days (in the absence of DEX). Cell

lysates were made from day 0, 2, 4, 6 and 14 and 500ng/ml concentration of protein was prepared from each sample. After incubating the sample with 100 µMATP and 1mg/ml AKT substrate, SGK1 activity versus the times cultured with MO 1 of AdV-*SGK1F* was measured using the ADP-Glo Kinase Assay that measures ADP formed from a kinase reaction; ADP is converted into ATP, the levels of which are determined using light emitted by Ultra-Glo Luciferase. As can be seen from **A,** AdV-*SGK1F* infection resulted in detectable increases in Sgk1/SGK1F kinase activity. Employing fluorescence immunocytochemistry technique exhibited widespread increased expression of Sgk1/SGK1F in infected remaining viable cells (Figure 3.7B) and co-expression of CpsI with SGK1F-expressing cells (determined specifically using the N terminal tag sequence cloned into the protein (Figure 3.8**).**

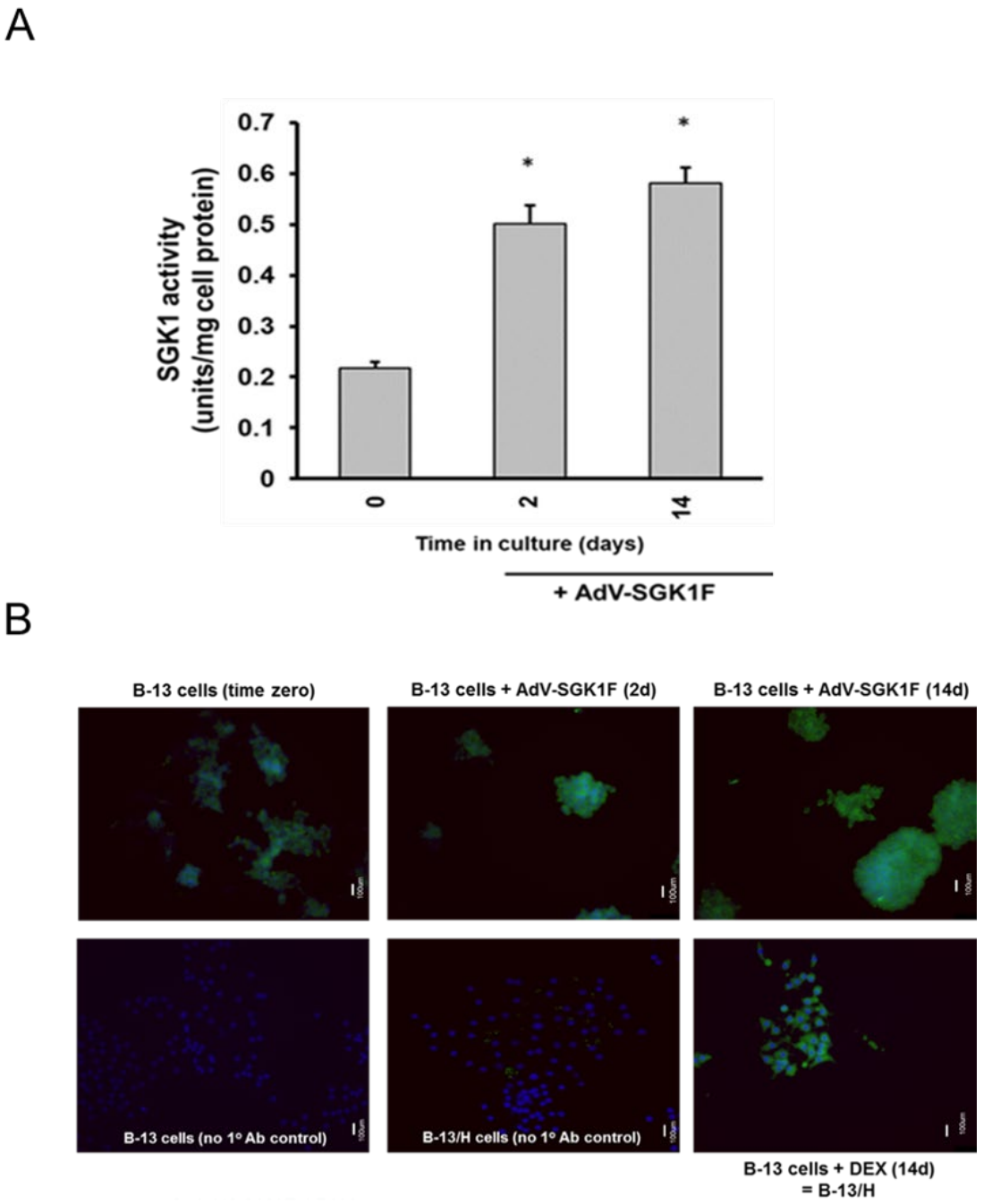

Figure 3.7 Expression of B-13-derived Sgk1 and AdV-SGK1F in B-13 cells. A: SGK1F/Sgk1 kinase activity in B-13 cells infected with AdV-SGK1F. Infection with AdV-SGK1F results in an increase in SGK1 kinase activity. B-13 cells were repeatedly infected with AdV-SGK1F at an MOI of 1 and SGK1 kinase activity determined in cell extracts, as outlined in the methods section. Data are the mean and SD of 3 replicates from the same experiment, typical of 3 separate experiments. *Significantly different ($P < 0.05$) from time zero uninfected cells using one way ANOVA followed by a Tukey post hoc test. B: Immunocytochemical detection of SGK1 expression. B-13 cells were repeatedly infected with AdV-SGK1F at an MOI of 1, cells fixed and Sgk1/SGK1F expression (green) determined by immunocytochemistry with DAPI (blue) for identification of nuclei. Data typical of 3 separate

experiments. All images were taken under identical spectral conditions and processed identically

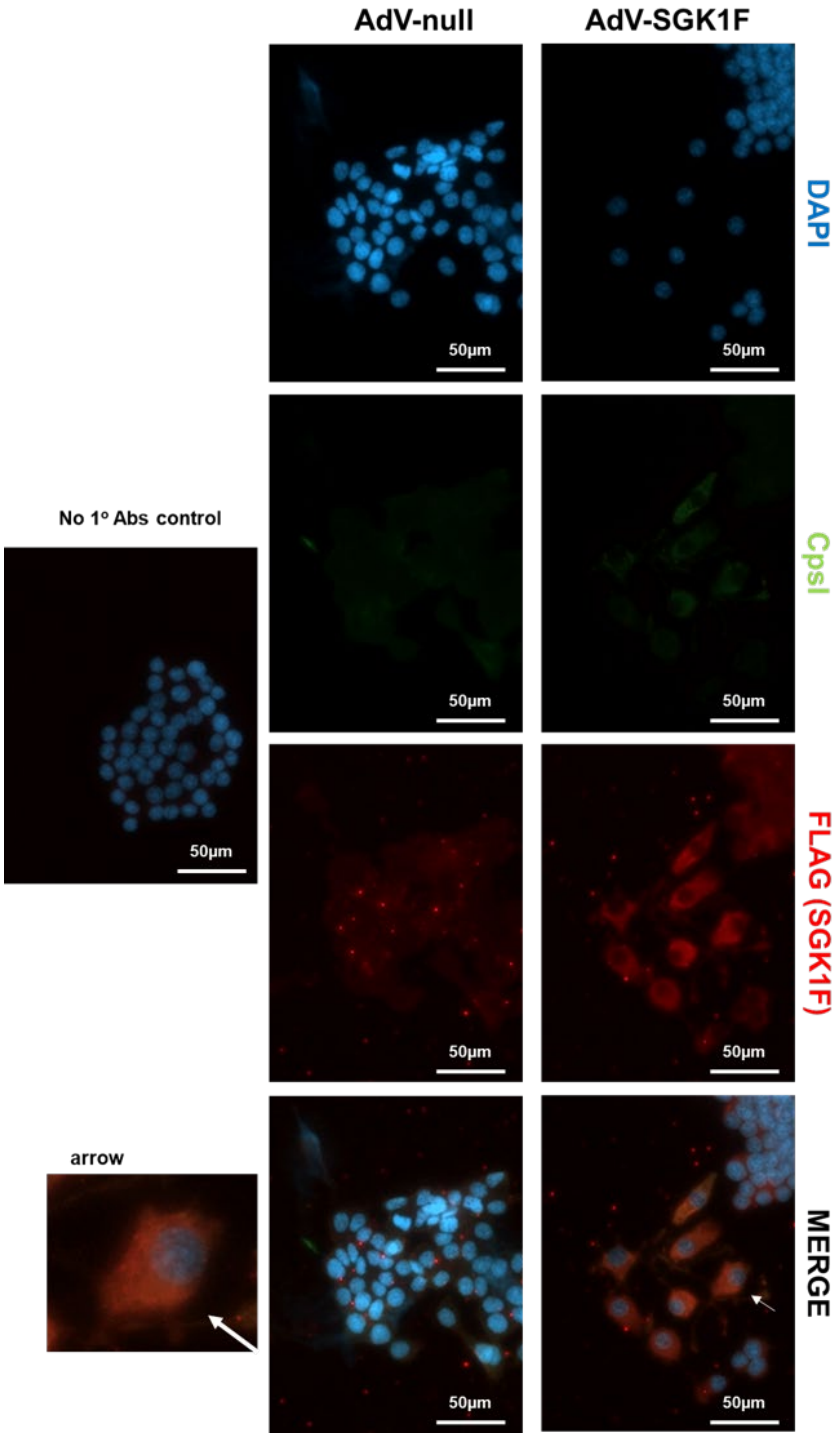

Figure 3.8 Immunocytochemical detection of CpsI and SGK1-F expression in B-13 cells.

B-13 cells were repeatedly infected with AdV-SGK1F using repeated infection at an MOI of 1 for 14 days, cells fixed and the co expression of CpsI (green) and SGK1F tag (red) determined by immunocytochemistry with DAPI (blue) for identification of nuclei. Data typical of 3 separate experiments. All images were taken under identical spectral conditions and processed identically. Panel labelled "arrow" is an expanded view of the cell identified by an arrow in the lower right hand panel.

3.5 Adenoviral-mediated expression of SGK1F induces the conversion of B-13 cells into B-13/H cells without the addition of glucocorticoid

To examine the effect of SGK1F, B-13 cells were infected over 8 days with AdV-*SGK1F* (MOI of 5) or a control adenovirus (AdV-null) by employing the repeated infection strategy in B-13 cells (in the absence of DEX) to maximise infection and SGK1F expression and minimise cell death, although this also resulted in a degree of cell death. B-13 cells were also separately treated with 10nM DEX with/without AdV-*SGK1F*.RT- PCR using primers designed for h-*SGK1F*, *Cyp2e1* and *CpsI*. Double bands can be seen in RT-PCR for *Cps1* Figure 3.9 which could be due to nonspecific bands formed by the primer-template DNA binding. This nonspecific binding of the primer could be eliminated by increasing the annealing temperature.

The adoption of an hepatocyte-like phenotype by B-13 cells in response to AdV-SGK1F infection was confirmed by detection of liver-enriched and liver-specific gene transcripts *Cyp2e1* and *CpsI* respectively, similar to cells treated with DEX for (Figure 3.11A). The observations were further confirmed by examining protein expression by Western blotting and immunocytochemistry. Western blot analysis demonstrated that the expression of the SGK1F/Sgk1 protein was higher in cells infected with AdV-*SGK1F*. In addition, albumin protein was expressed by B-13 cells infected with AdV-*SGK1F*. Expression was low compared to the expression by B-13 cells treated with a combination of DEX and AdV-*SGK1F*. Cps1 protein was clearly expressed by B-13 cells treated with a combination of DEX and AdV-*SGK1F* and barely detectable by B-13 cells infected with AdV-*SGK1F*. However, Cyp2e1 protein was not detected by Western blot analysis yet was expressed by B-13 cells treated with a combination of DEX and AdV-*SGK1F* (Figure 3.10**).** B-13 cells were repeatedly infected with AdV-*SGK1F* (MOI of 5) for 10 days or treated with 10nM DEX for 14 days (to generate B-13/H cells) and cells fixed immunocytochemistry was performed to determine liver marker protein expression using anti-rat Cyp2e1and anti-rat CpsI (Figure 3.11**).** There was readily detectable expression for CpsI in the majority of the cells and weak expression for Cyp2e1 hepatic markers in B-13 cells infected with AdV-*SGK1F*. Infection with AdV-*SGK1F* also resulted in morphological alteration of B-13 cells from small round cells with low cytoplasm to nucleus ratio to hepatocyte-like cells with high cytoplasmic to nuclear ratio. This change in cell morphology resembles the change in B-13 cells in response to DEX treatment **(**Figure 3.12**)**.

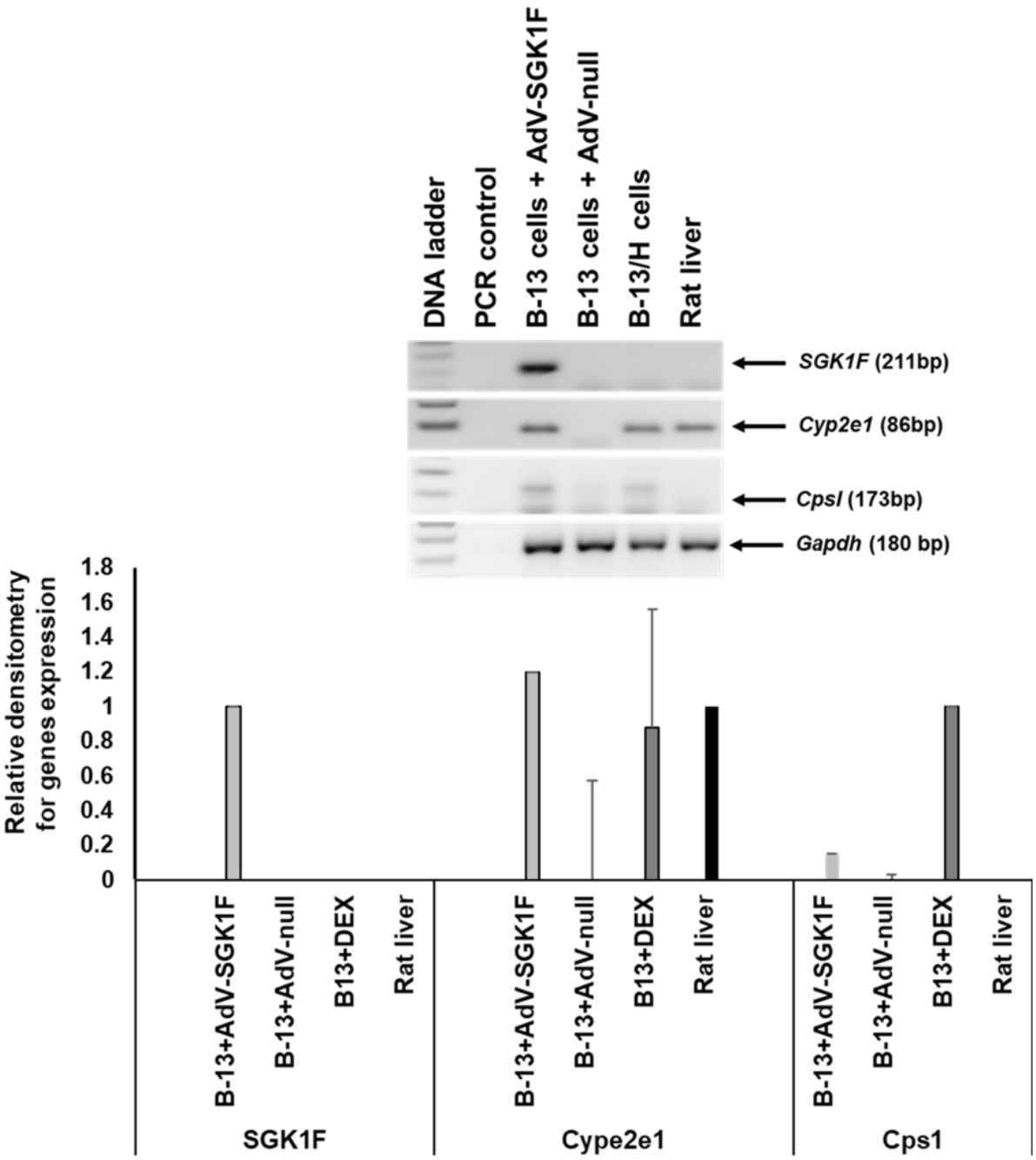

Figure 3.9 Infecting B-13 cells with AdV-SGK1F leads to the expression of hepatic markers.

B-13 cells were repeatedly infected with the indicated AdV before total RNA was isolated at day 8 and transcript expression determined by RT-PCR, as outlined in the methods section. Gapdh was used as a housekeeping gene. Upper panel demonstrates the bands separated by gel electrophoresis, which quantified using ImageJ software in the lower panel.

Data are typical of 3 separate experiments.

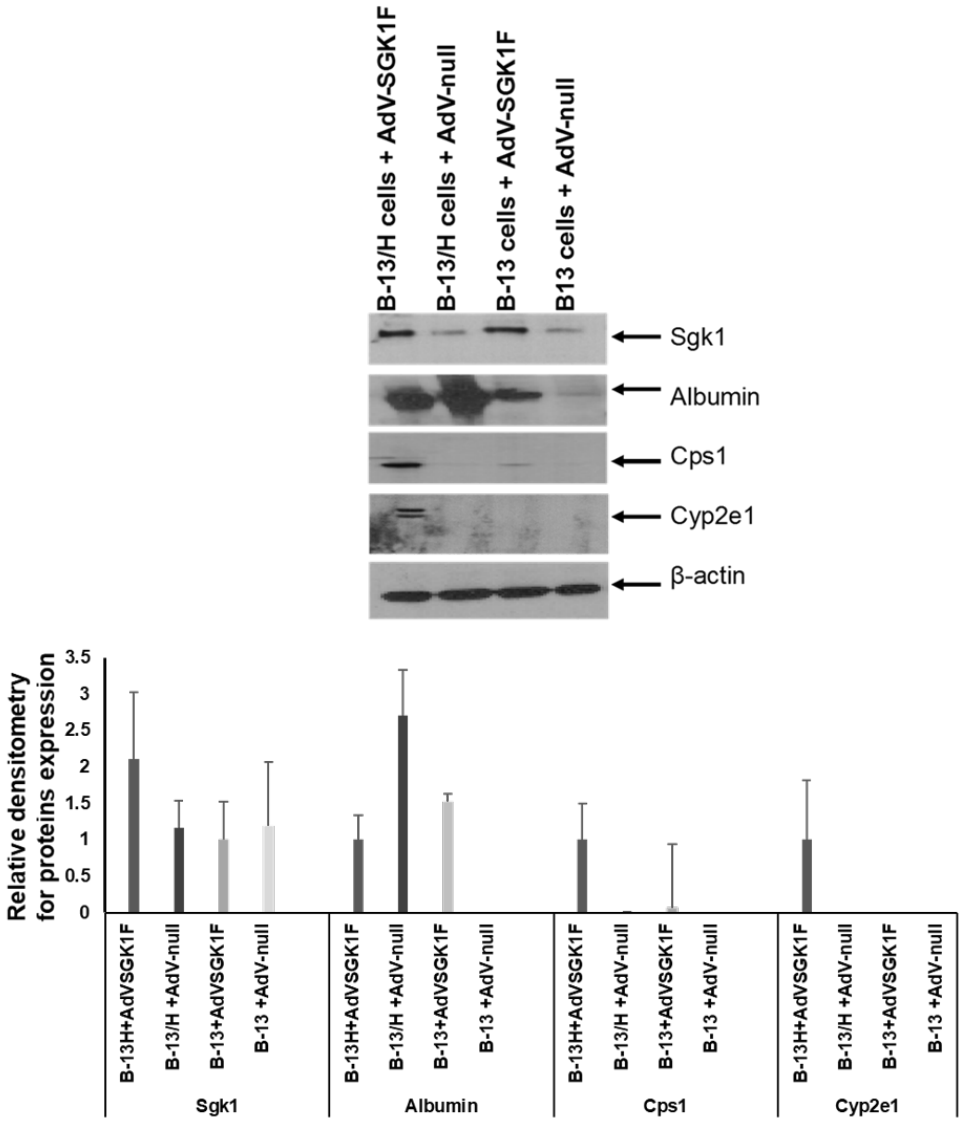

Figure 3.10 Infecting B-13 cells with AdV-SGK1F leads to the expression of hepatic markers. Western blot analysis of protein expression. B-13 cells were repeatedly infected with the indicated AdV before indicated protein expression was determined by Western blotting at day 8. β-actin protein was used as loading control. Western blot results in the upper panel were quantified using ImageJ software in the lower panel. Data are typical of 3 separate experiments.

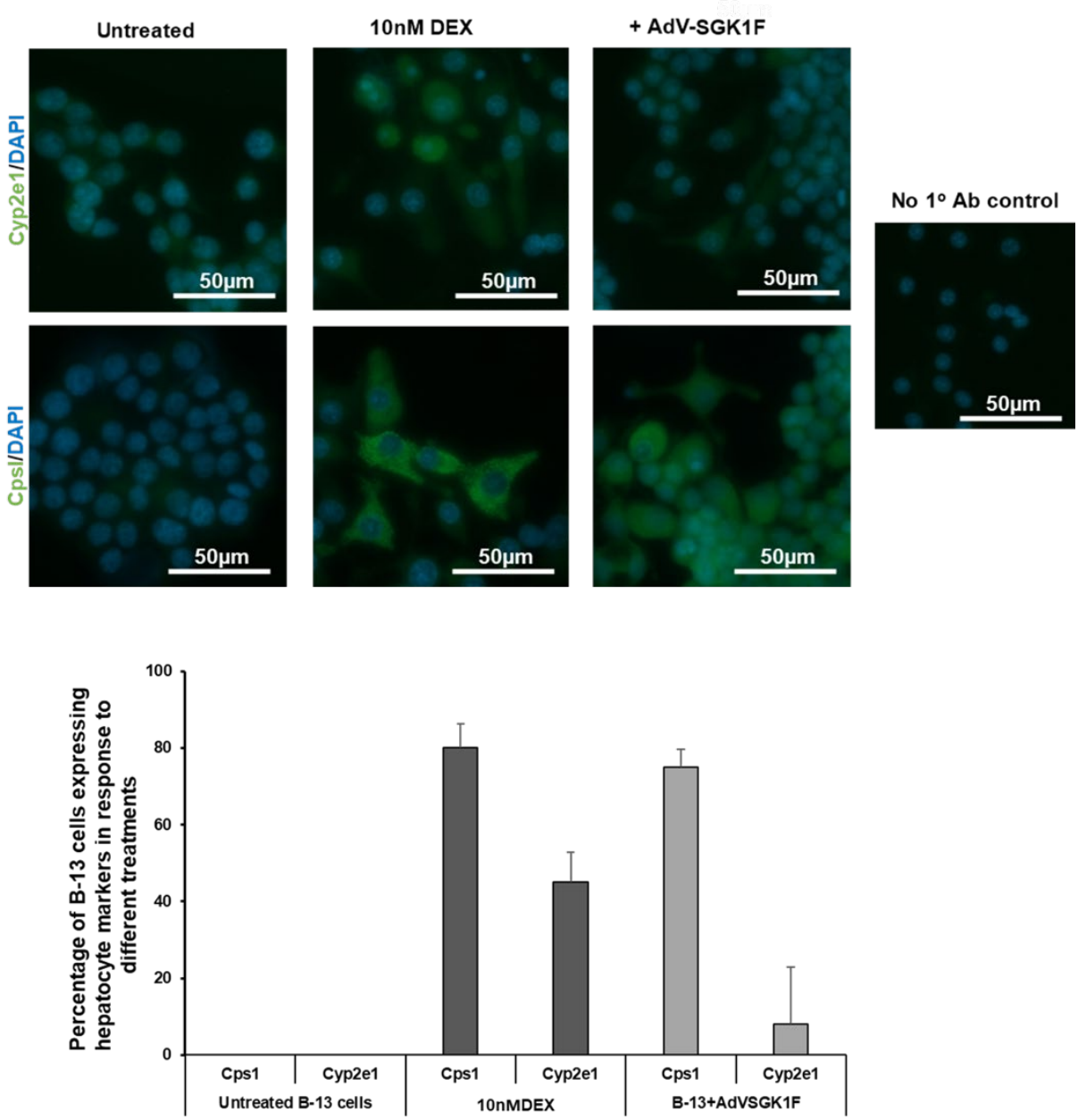

Figure 3.11 Immunocytochemical detection of CpsI and Cyp2e1 expression in DEX treated B-13 cells and AdV-SGK1F infected cell.syle B-13 cells were repeatedly infected with AdV-*SGK1F* (MOI of 5) for 10 days or treated with 10nM DEX for 14 days (to generate B-13/H cells) and cells fixed and indicated protein expression (green) determined by immunocytochemistry with DAPI (blue) for identification of nuclei (upper panel). Percentage of cells expression of hepatocyte proteins in response to the indicated treatment was determined (lower panel). Data are the mean and SD of 3 replicates from the same experiment, typical of 3 separate experiments. All images were taken under identical spectral conditions and processed identically.

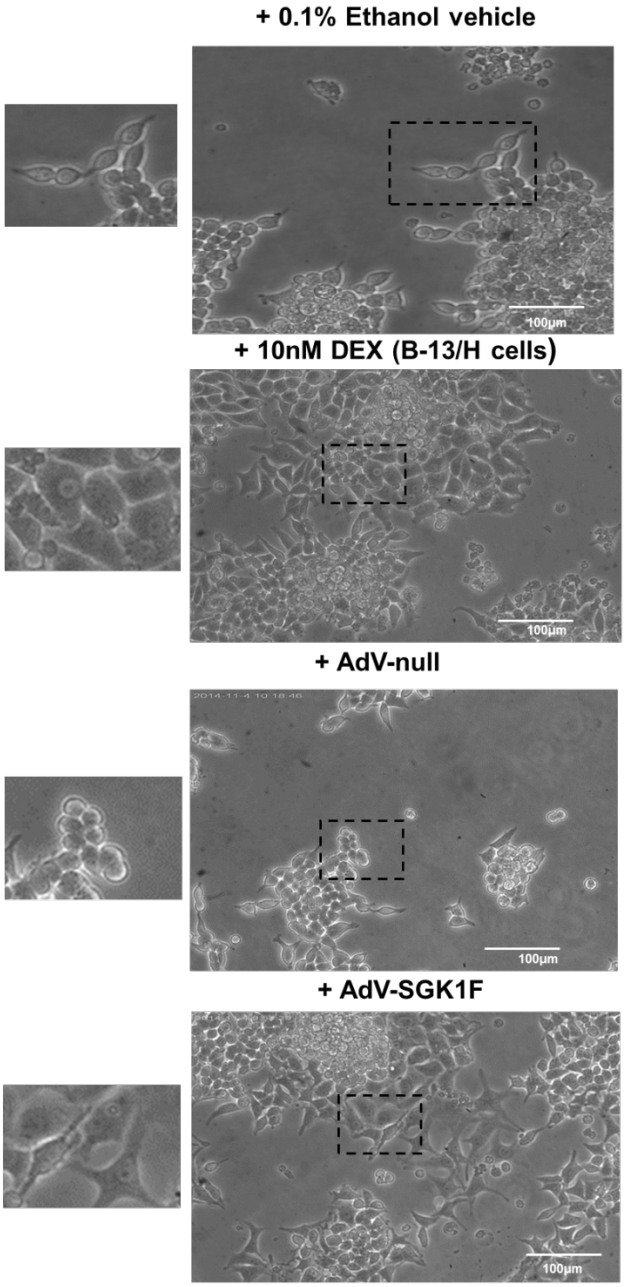

Figure 3.12 Morphology of B-13 cells after infection with AdV-*SGK1F*. Infecting B-13 cells with AdV-*SGK1F* leads to a morphological change into the B-13/H phenotype Light micrographs of B-13 cells infected with the indicated AdV (MOI of 5) or treated with 10nM DEX for 14 days (B-13/H cells). Ethanol vehicle-treated appears identical to AdV-null treated cells. Dotted squares demonstrate the area of cells magnified in the small squares.

3.6 Sgk1 inhibitor and glucocorticoid receptor antagonist (Ru486) prevent the conversion of B-13 cells treated with 10nM DEX or AdV-SGK1F into B1-13/H

To determine whether Sgk1 kinase activity is essential in B-13 conversion into B-13/H cells, B-13 cells were treated with 10nM DEX, 100nM GSK 650394 (an Sgk1 kinase inhibitor)

and 10μM Ru486 (glucocorticoid receptor antagonist). RNA was isolated after 7 days and it was established that 100nM GSK 650394 prevented the morphological change observed in response to DEX and inhibited DEX-dependent expression of the liver marker gene Cyp2e1 (Figure 3.13). Figure 3.14 compares the effect of B-13 cells infected with either AdV-*SGK1F* or AdV-*null* (AdV-control) at an MOI 5 and treated with ethanol vehicle, DEX (10nM DEX), glucocorticoid receptor antagonist (10 μMRU486) or the SGK1 antagonist GSK 650394 (100nM GSK). The cells were treated for 8 days prior to analysing hepatic marker expression at the protein level by way of Western blotting. Cell morphology confirms that over-expression of SGK1F induced a trans-differentiation of B-13 cells to B-13/H cells without the addition of glucocorticoid. Supporting the information obtained from RT-PCR of the previous experiments, only cells treated with DEX or a combination of DEX and AdV-*SGK1F* expressed the liver markers proteins albumin and Cyp2e1 as demonstrated in Figure 3.14 (middle panel and lower panel). Thus, Sgk1 kinase activity appears to be important in the trans-differentiation process of B-13 into B-13/H cells.

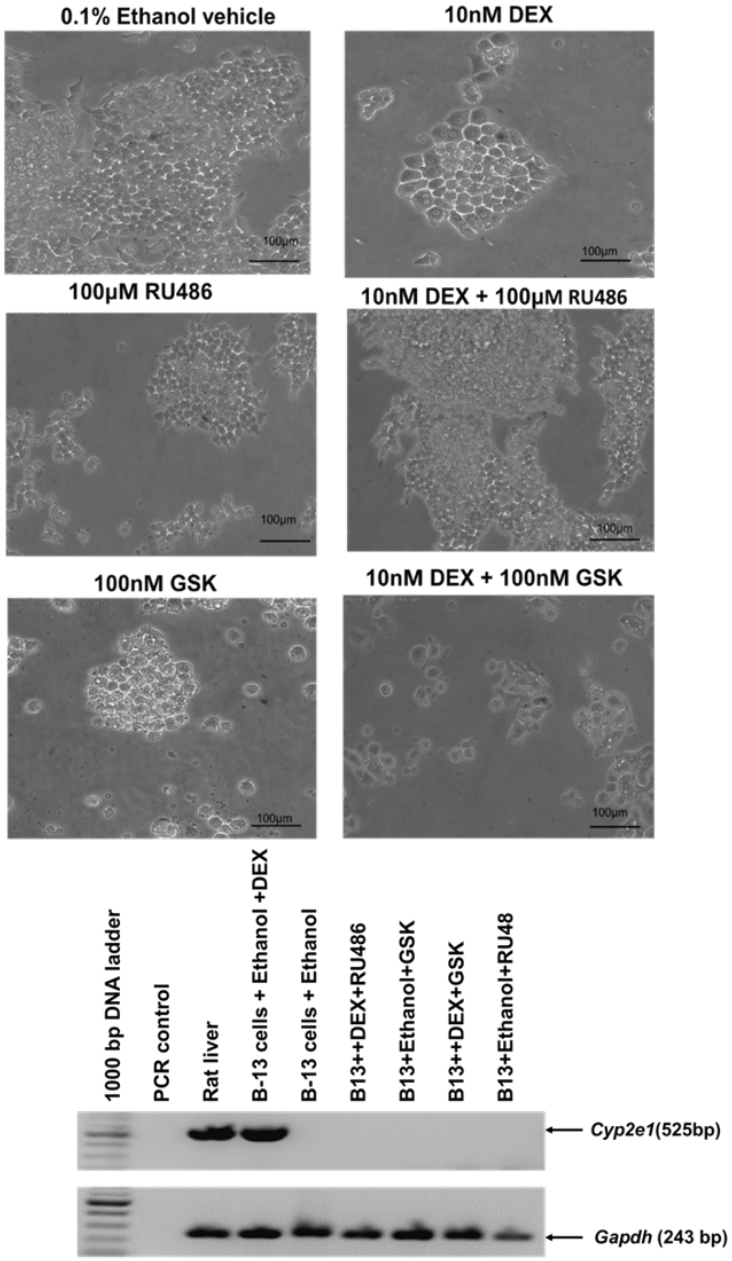

Figure 3.13 SGK1F kinase activity is important in trans-differentiation of B-13 cells to B-13/H cells. B-13 cells were treated with DEX, sgk1 inhibitor or glucocorticoid antagonist as indicated. Upper panel, light micrographs of B-13 cells after treatment with 10nM DEX and/or 100nM SGK1 inhibitor (GSK 650394), 10 µM RU486 (glucocorticoid antagonist) in addition to 0.1% ethanol vehicle for 7 days. Lower panel: RT-PCR analysis for gene expression for the liver marker (Cyp2e1) was performed as outlined in the methods section. Total RNA was

isolated on day 7. Gapdh was used as a house keeping gene. Data are typical of 3 separate experiments

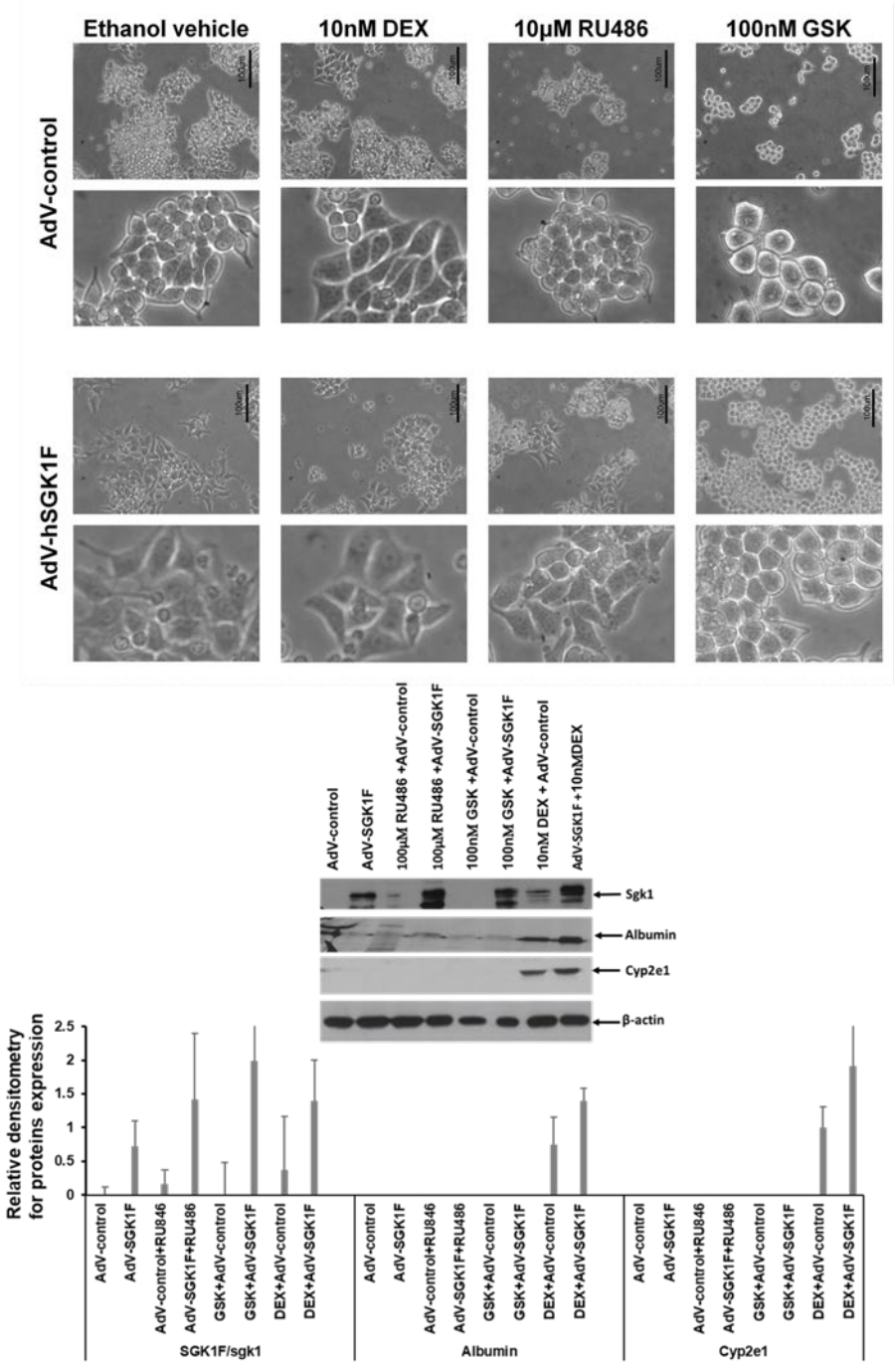

.

Figure 3.14 SGK1F kinase activity is important in trans-differentiation of B-13 cells to B-13/H cells. B-13 cells were infected with an adenovirus encoding the human SGK1F isoform (AdV-*SGK1F*) or a control adenovirus encoding NTCP (AdV-control) and treated with 0.1% ethanol vehicle, 10nM DEX, 100nM SGK1 inhibitor (GSK 650394) or 10 μM RU486 (glucocorticoid antagonist) as indicated. Morphology was examined after 5 days. Upper panel: light micrographs of B-13 cells after treatment with the indicated treatment. Middle panel: protein expression, B-13 cells were treated with the indicated treatments before indicated protein expression was determined by Western blotting at day at 8. Percentages of indicated

proteins expression in response to the indicated treatment were quantified using ImageJ software (lower panel). β-actin protein was used as loading control. Data are typical of 3 separate experiments.

3.7 B-13 conversion to B-13/H cells in response to DEX is primarily associated with glucocorticoid receptor activation and an induction of Sgk1 activity

Mineralcorticoid receptors **(**MR) are known to regulate the induction of sgk1 in the kidney [233]. To determine whether Sgk1 induction in B-13 cells is associated with glucocorticoid receptor activation in response to DEX – rather than or in association with the MR activation, B-13 cells were cultured in serum-free media for 1 day. RNA at time zero sample was isolated. Subsequently, B-13 cells were treated with ascending gradients of DEX and mineralocorticoid hormone; aldosterone (ALD) (1nM 10 nM 100 nM). After 3 days, RNA was isolated and a concentration of 500ng/ml of protein was prepared from cells lysate from each treatment. Primers for the detection of rat Sgk1 transcript isoforms were designed (*sgk1a, sgk1b, sgk1x2*) including a recently identified Sgk1 -like sequence (*LOC*). RT-PCR results confirmed that *sgk1a, sgk1b, sgk1c* are all induced in B-13 cells treated with 100nM DEX, *sgk1x2* was expressed constitutively and induced in cells treated with DEX.

There was no expression of the liver marker Cyp2e1 which could be explained by the limited exposure time and low level of *Sgk1c* expression at this stage. However, in ALD treated cells, only *Sgk1a* was induced in B-13 cells treated with 10nM ALD. Similarly, *Cyp2e1* expression was not detected (Figure 3.15). In addition, Sgk1 kinase activity was examined. SGK1 activity versus ascending gradient of DEX and ALD was measured using the ADP-Glo Kinase Assay that measures ADP formed from a kinase reaction; ADP. The luminescent signal showed a significant difference between ethanol vehicle-treated cells and cells treated with different gradients of DEX and ALD, however, the signal does not correlate with sgk1 isoform expression detected by RT-PCR, which might be due to the non-specificity of this assay to detect the phosphorylation produced by Sgk1, as it might detect phosphorylation resulting from the action of other kinases in the cells (Figure 3.16). Furthermore, an additional experiment was performed to assess the effect of DEX and ALD on B-13 conversion into B-13/H cells. B-13 cells were treated with an ascending gradient of DEX and ALD (1nM ,10nnM, 100nM) for 14 days. Proteins were isolated for Western blotting for liver markers (Cyp2e1, Cps1). The results demonstrate that only DEX converted B-13 into B-13/H cells (Figure 3.17 upper panel). However, a limited number of cells treated with 100nM ALD morphologically revealed the hepatocyte-like phenotype. This may be associated with the high concentration of ALD and activation of the GR (Figure 3.17 lower panel). These observations suggest that SGK1a induced

by both DEX and ALD is not involved in the trans-differentiating process of B-13 into B1-13/H cells as only DEX resulted in B-13 conversion into B1-13/H.

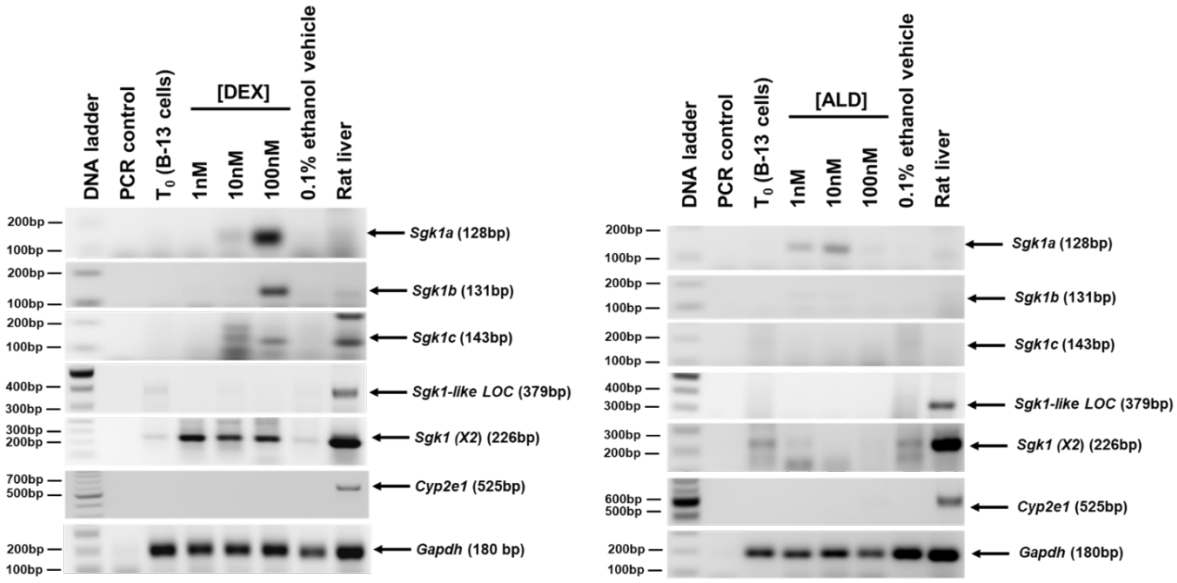

Figure 3.15 Conversion of B-13 to B-13/H cells is associated with an induction of Sgk1 kinase activity. RT-PCR for the indicated transcripts. B-13 cells were treated with serum free media for 24 h, then treated with the indicated concentration of DEX (left panel), ALD (right panel) or ethanol control vehicle for 3 days as outlined in the methods section. Gapdh was used as a house keeping gene.

Table 3.1 RT-PCR summary of results for *Sgk1* isoforms expression in B-13 cells, DEX and ALD treated B-13 cells

	B13 control	DEX	ALD	Rat liver
Sgk1a	n/d	↑	↑	Detectable
Sgk1b	n/d	↑	n/a	n/d
Sgk1c	n/d	↑	n/a	n/d
Sgk like (loc)	low	transient	n/a	detectable
Sgk1 x2	low	(GR)	transient	detectable

		Weak MR	(GR &MR)	

n/d= not detectable, n/a= no or weak effect

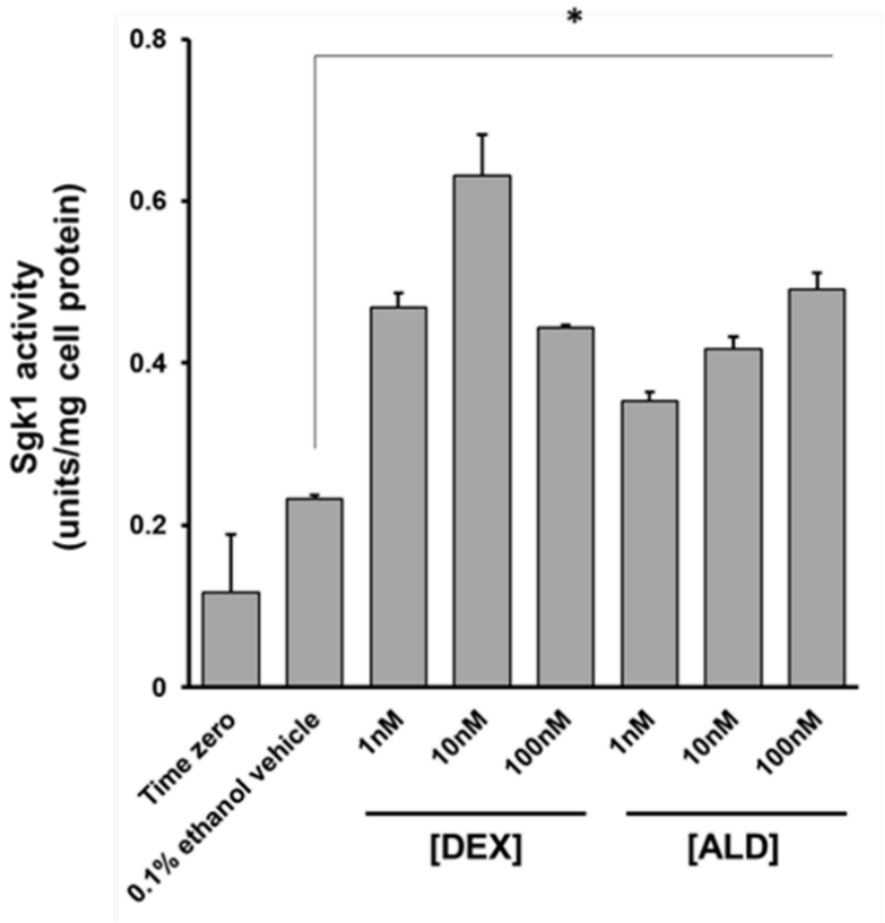

Figure 3.16 DEX and ALD treatment is associated with an induction of Sgk1 kinase activity in B-13 and B-13/H. Skg1 kinase activities in B-13 cells treated for 3 days with the indicated concentration of DEX or ALD. Data are the mean and SD of 3 separate determinations from the same experiment. *Significantly different ($P < 0.05$) from ethanol vehicle treated cells using oneway ANOVA followed by a Tukey post hoc test.

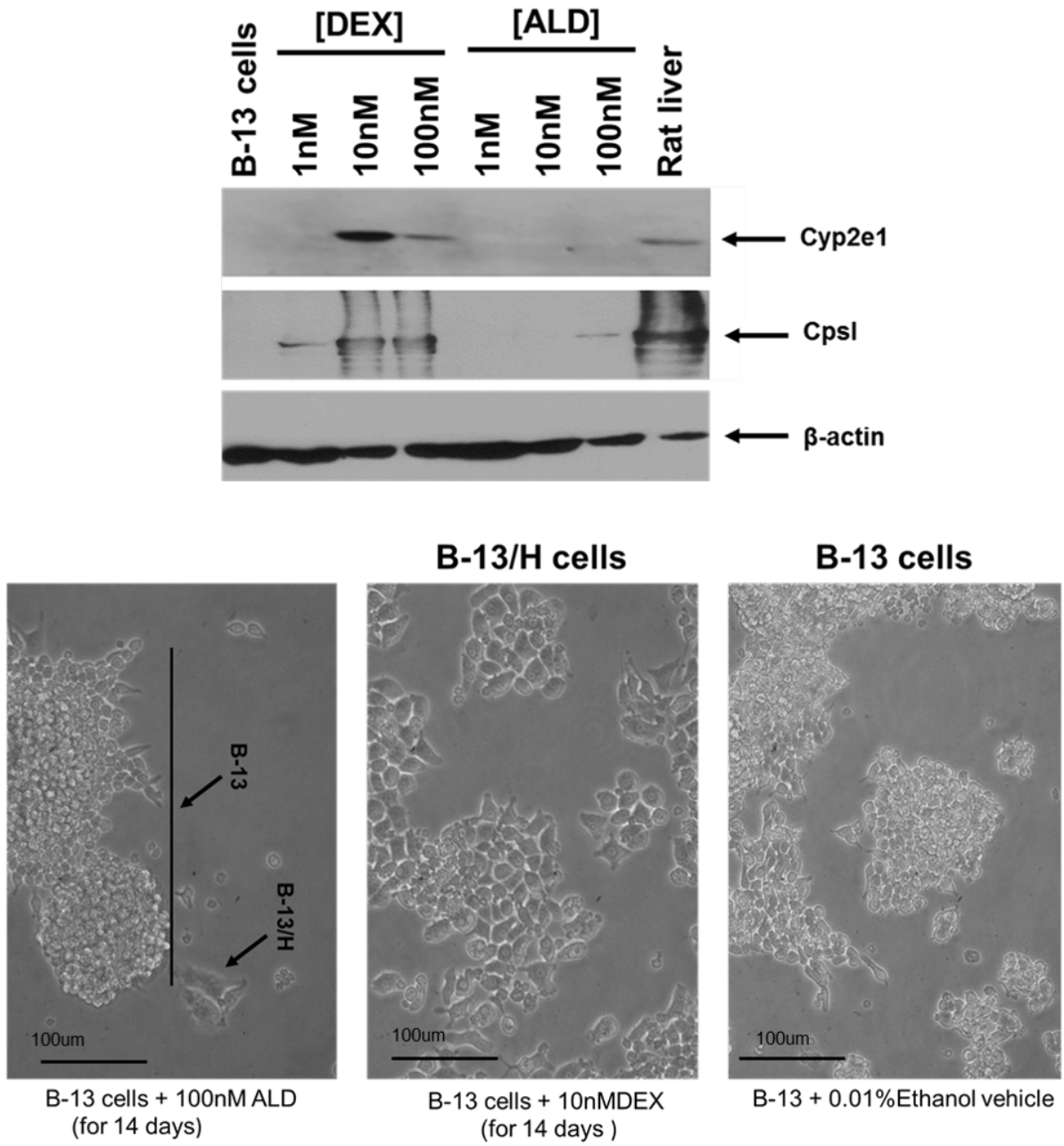

Figure 3.17 Conversion of B-13 to B-13/H cells is associated with an induction of Sgk1 kinase activity. C: Western blot for the indicated proteins after treatment for 14 days with the indicated concentration of DEX or ALD (20 μg protein/lane). β-actin protein was used as loading control (upper panel). The data are typical of 3 separate experiments. Lower panel: photomicrographs of cells treated as indicated, typical of at least 3 separate experiments.

3.8 Treating B-13 cells with different growth factors has no effect on *Sgk1* expression and B-13 cells conversion into B-13/H cells

Given that some growth factors induce Skg1, one might expect growth factors could replace DEX – and therefore potentially turn B-13 cells into B-13/H cells. To test this possible effect, B-13 cells were cultured in serum-free media for 24 h to synchronise the cells. RNA from time zero sample was isolated. Cells were then treated for 3 days with: 0.0 % (v/v) FCS as the negative control: 1% (v/v) FCS, 5% (v/v) FCS, 10% (v/v) FCS, 5% (v/v) FCS+10ng/ml epidermal growth factor (EGF), a growth factor that acts a potent mitogenic factor for B-13 cells (Probert et al., 2014) and 5% (v/v) FCS + 30ng/ml OSM, an interleukin-6 family cytokine, which has been found - in combination with glucocorticoid – to promote the maturation of stem cell derived-hepatocytes [325]. Morphologically, growth factors did not change cells to hepatocyte-like cells. Interestingly, OSM has shown an impact on B-13 cells size (Figure 3.18 left panel). Moreover, increasing the FCS concentration resulted in an increase in B-13 cell replication (Figure 3.18 left panel), the increase in replication was determined visually by an apparent increase in cell number, but was not quantified. RT-PCR results did not detect any Sgk1 isoforms expression (Figure 3.18 right panel). Treating B-13 cells with 10ng/ml EGF and 30ng/ml OSM for 14 days did not results in B-13 cell conversion into B-13/H cell as shown in RT-PCR results (Figure 3.19), there is no expression of liver markers genes (*albumin* and *cyp2e1*).

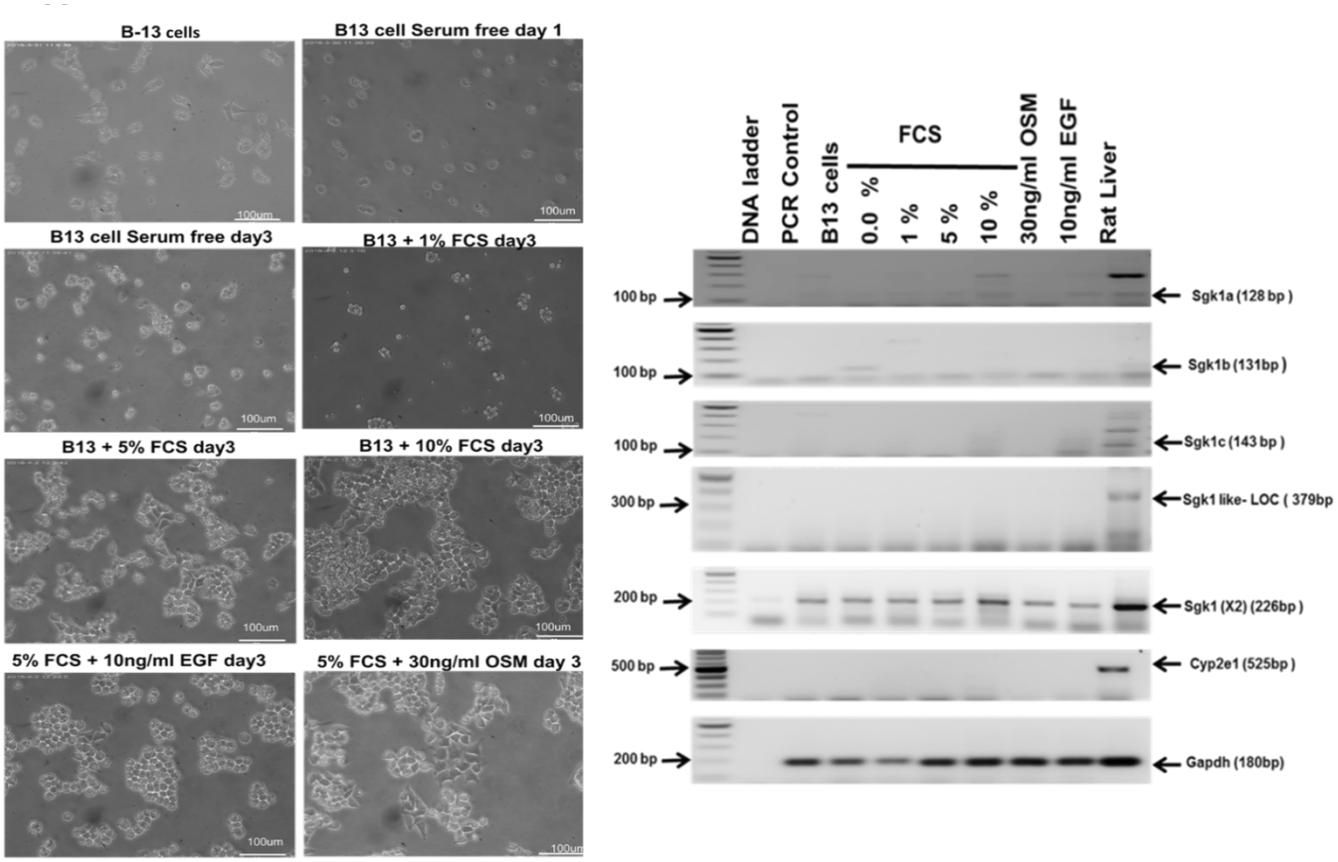

Figure 3.18 Treating B-13 cells with different growth factors has no effect on Sgk1 induction. B-13 cells were treated with serum free media for 24 h, then treated with 0.0 % (v/v) FCS as the negative control: 1% (v/v) FCS, 5% (v/v) FCS, 10% (v/v) FCS, 5% (v/v) FCS+10ng/ml EGF and 5% (v/v) FCS + 30ng/ml OSM. A: photomicrographs of cells treated as indicated. B: RT-PCR for the indicated transcripts and a summary table for the results.

Table 3.2 RT-PCR summary of results for *Sgk1* isoforms expression in B-13 cells treated with serum free and different growth factors.

	10%FCS control	SF	FCS	OSM	EGF	Rat liver
Sgk1a	n/a	n/a	n/a	n/a	n/a	**Detectable**
Sgk1b	n/a	n/a	n/a	n/a	n/a	n/a
Sgk1c	n/a	n/a	n/a	n/a	n/a	**Detectable**
Sgk like (loc)	n/a	n/a	n/a	n/a	n/a	**detectable**
Sgk1 x2	n/a	n/a	n/a	n/a	n/a	**detectable**

n/d= not detectable, n/a= no or weak effect

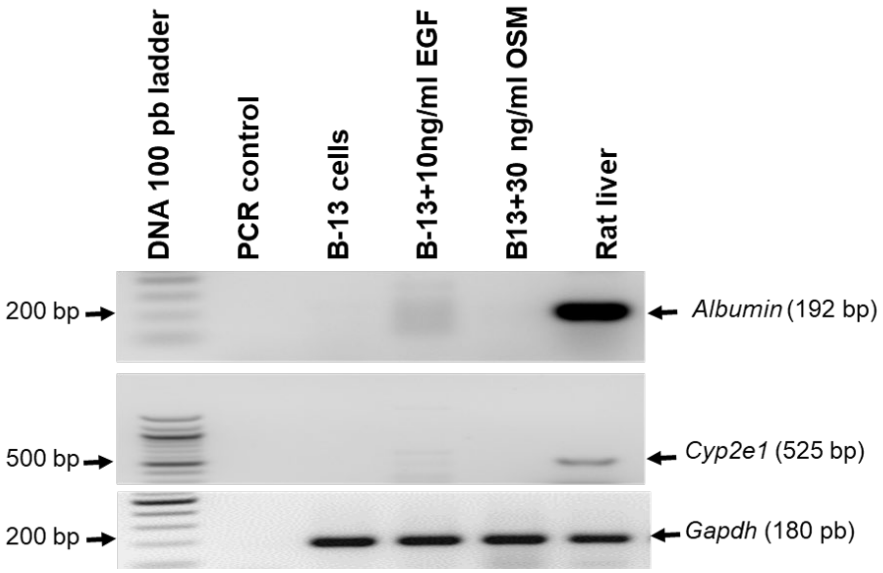

Figure 3.19 Treating B-13 cells with different growth factors has no effect on B-13 conversion into B-13/H. C: B-13 cells were treated with 10ng/ml EGF, 30ng/ml OSM for 14 days: RNA was isolated, and RT-PCR was performed for the detection of liver marker genes (*Albumin and Cyp2e1*). Data are typical of 3 separate experiments.

3.9 Chapter discussion

The transdifferentiation of B-13 cells into B-13/H cells after 14 days of exposure to DEX results in qualitative and quantitative similar gene expression similar to that of primary hepatocytes[197]. Understanding the mechanism(s) controlling the conversion/trans-differentiation of B-13 cells to B-13/H cells could be used to stimulate/maintain differentiation phenotype in stem cell-derived specialised cells. The data in this chapter demonstrate that adenoviral-mediated SGK1F expression in B-13 cells induces their differentiation into B-13/H cells similar to their response to exposure to glucocorticoid. The mechanisms involved in B13 cell transdifferentiation into B13/H cells still requires further investigation. The rat *Sgk1* gene is currently known to encode 3 validated mRNA transcripts and possibly 1 further transcript [NCBI database, see also Table 3.3 **.** and appendix B]. All 4 transcripts encode an identical core amino acid sequence and differ only in their N terminal amino acid sequences. It is not known whether the *Sgk1* isoforms have different functions, however, only the rat *Sgk1c* transcript appears to be irreversibly induced in B-13 cells after exposure to glucocorticoid [326]. This suggests that endogenous Sgk1c may be responsible for its differentiating effects in B-13 cells. This is supported by the high expression of the murine orthologue in pancreatic tissue from mice with high circulating endogenous glucocorticoids (these mice experience a conversion of the pancreatic exocrine tissue into hepatocyte-like cells [231].

Wallace et al. (2011), used the plasmid transfection technique to direct the expression of a series of human *SGK1* expression constructs. Their data demonstrated that expression of either the human *SGK1C* (orthologous to the c form in rat) or *SGK1F* (which has no orthologue in the rat) isoforms alone resulting in transdifferentiation of B-13 cells. In another experiment, it was found that kinase-dead (KD) mutants of SGK1C and SGK1F proteins failed to inhibit Tcf/Lef transcriptional function or induce expression of CYP2E1 or albumin in comparison to the wild-type parallels [226]. These findings suggest that the kinase function of SGK1C and SGK1F is essential for promoting B-13 transdifferentiation, Based on this, the cDNA for this transcript was cloned into a replication-deficient adenoviral genome. The rationale for focusing on SGK1F was also driven by the knowledge that the pancreas from a patient treated for many decades with systemic glucocorticoid experienced a degree of hepatic differentiation and also contained high levels of SGK1F mRNA transcripts [227].

In this approach, replication-deficient recombinant adenoviruses were used to introduce the genetic material (SGK1F) into B-13 cells. There are numerous advantages to using adenovirus to insert genetic material into host cells. These viruses can be used to infect many mammalian

cell types. Moreover, recombinant adenoviruses can also be used to infect various sensitive cells with low MOI and to obtain a high proportion of infected cells [307]. Adenovirus vector genomes carrying gene of interest constructs can mediate homologous recombination with target loci in a cellular genome at efficiencies 103–104-fold higher than plasmid constructs **[327].** The efficiency of B-13 infection with the adenovirus was optimised. B-13 cells were found to be readily infectable with AdV-*GFP*, but marked toxicity was observed at MOIs of 10 and 15. Therefore, an MOI 1 was chosen to infect cells over an extended 14 day period, with repeated infection every two days or MOI 5 for the shorter period (8 days with repeated infection every two days). AdV-*SGK1F* overexpression was used to investigate the role of SGK1 in B-13 trans-differentiation to B-13/H cells. MOI 5 was used every two days to maximise infection and expression, although this also resulted in a degree of cell death. Due to this, cells infected with MOI 5 were not cultured after the initial infection for more than eight days. However, B-13 cell transdifferentiation to B-13/H cells was seen morphologically and was detected by RT-PCR for the expression of liver transcript marker genes such as *Cyp2e1* and *Cps1*.

Western blot detection of SGK1F/Sgk1 protein expression demonstrated that SGK1F/Sgk1 protein was higher in cells treated with AdV-*SGK1F*. Additionally, albumin protein was expressed by B-13 cells infected with AdV-SGK1F. Expression was low compared to the expression by B-13 cells treated with a combination of DEX and AdV-*SGK1F*. Cps1 protein was clearly expressed by B-13 cells treated with a combination of DEX and AdV-*SGK1F* and barely detectable by B-13 cells infected with AdV-*SGK1F*. However, the Cyp2e1 protein was not yet detected by Western blot analysis and it was expressed by B-13 cells treated with a combination of DEX and AdV-*SGK1F*. Furthermore, 100nM GSK 650394 (an Sgk1 kinase inhibitor), which has never been tested before, was used to examine whether Sgk1 kinase activity is important in B-13 conversion into B-13/H cells. It was observed that 100nM GSK 650394 prevented the morphological change observed in response to DEX and inhibited DEX-dependent expression of the liver marker *Cyp2e1*. Supporting this information, only cells treated with DEX or a combination of DEX and AdV-*SGK1F* expressed the liver markers proteins albumin and Cyp2e1. Thus, Sgk1 kinase activity appears to be important in the trans-differentiation process of B-13 into B-13/H cells.

The RT-PCR results for different *Sgk1* transcripts showed that *Sgk1a*, *Sgk1b* and *Sgk1c* isoforms are expressed by cells treated with 100nM DEX. In comparison to ALD treated cells, only *Sgk1a* was expressed by B-13 cells treated with 10nM ALD. In both treatments, *Cyp2e1* expression was not detected, which could be explained by the low Sgk1 level at this stage (3 days). Sgk1 kinase activity from the same DEX and ALD treated cells, which has never been

examined, was measured. The luminescent signal exhibited a significant difference between ethanol vehicle-treated cells and cells treated with different gradients of DEX and ALD. However, the signal does not correlate with Sgk1 isoform expression detected by RT-PCR, which might be due to non-specificity of this assay to detect the phosphorylation produced by Sgk1 only, it might detect phosphorylation by other kinases in the cells. Another possible reason is that the sgk1 transcription to mRNA had occurred but significant translation to protein had not occurred at the time of sampling.

The effect of 14 days treatment of DEX or ALD on B-13 conversion into B-13/H cells was assessed by WB analysis. The results demonstrate that only DEX converted B-13 into B-13/H cells. However, few numbers of cells treated with 100nM ALD, morphologically show the hepatocyte-like phenotype. That might be caused by using a high concentration of ALD which might result in the activation of the GR. These observations suggest that *Sgk1a* induced by both DEX and ALD is not involved in the trans-differentiating process of B-13 into B1-13/H cells and indicates the involvement of *Sgk1c*. Synchronised B13 cells were treated with different growth factors, such as serial concentrations of FCS, EGF and OSM to investigate their effect on Sgk1 induction and B-13 conversion to B-13/H cells. RT-PCR results did not detect any Sgk1 isoform expression. The data also revealed the failure of the natural MR agonist ALD to convert B-13 cells into B-13/H cells except with a very high concentration (100nM ALD). These data support the idea that the effect of DEX on transdifferentiation are mediated primarily through the GR [226].

The data in this chapter show that B13 cells are readily infected with adenovirus. However, marked toxicity was observed with high MOIs. The data also suggest that Sgk1 activity is crucial in B13 conversion into B-13/H cells following DEX treatment. The data also demonstrated that adenoviral-mediated *SGK1F* expression in B-13 cells induces their differentiation into B-13/H cells, similar to their response to exposure to glucocorticoid. Accordingly, SGK1F is implicated in the transdifferentiation of B-13 cells into B-13/H hepatocyte-like cells. Further investigation is essential to understand the mechanism of B-13 conversion into B-13/H and how Sgk1 is involved in the process, as this could offer an insight into potential ways to manipulate stem cells differentiation to generate hepatocytes *in vitro* for a wide range of uses, from toxicological screening to hepatocytes transplantation.

Table 3.3 Rat and human Sgk1 proteins. **Underlined sequence, flag sequence. For raw sequence data Appendix B.**

Rat					Human			
Transcript	**NCBI #**	**N terminal amino acid sequence encoded** **(total amino acids in protein; theoretical molecular weight)**	**Trivial name**		**Transcript**	**NCBI #**	**N terminal amino acid sequence encoded** **(total amino acids in protein; theoretical molecular weight)**	**Trivial name**
Sgk1 isoform 1	NM_001193568	MGEMQGALARARLESLLRPRHKKRVEAQKRSESVLLSGL (445; 50627 Da)	Sgk1b		SGK1 isoform 4	NM_001143678	MGEMQGALARARLESLLRPRHKKRAEAQKRSESFLLSGL (445; 50623 Da)	SGK1B
Sgk1 isoform 2	NM_001193569	MREEALRSPWK (417; 47626 Da)	Sgk1c					
Sgk1 isoform 3	NM_019232	MTVKTEAARSTLTYSRMRGMVAILI (431; 49024 Da)	Sgk1a		SGK1 isoform 1	NM_005627	MTVKTEAAKGTLTYSRMRGMVAILI (431; 48942 Da)	SGK1A

Rat					Human			
Transcript	**NCBI #**	**N terminal amino acid sequence encoded** **(total amino acids in protein; theoretical molecular weight)**	**Trivial name**		**Transcript**	**NCBI #**	**N terminal amino acid sequence encoded** **(total amino acids in protein; theoretical molecular weight)**	**Trivial name**
					SGK1 isoform 5	NM_001291995	MTVKTEAAKGTLTYSRMRGMVAILI (387; 43811 Da)	
Sgk1 isoform X1	XM_006227723	MVNKDMNGFPVKKCSAFQFFKKRVRRWIKSPMVSVDKHQSPNLKYTGPAGVHLPPGEPDFEPALCQSCLGDHTFQRGMLSPEESRSWEIQPGGEVKEPCNHANILTKPDPRTFWTSDDP (525; 59721 Da)			SGK1 isoform 2	NM_001143676	MVNKDMNGFPVKKCSAFQFFKKRVRRWIKSPMVSVDKHQSPSLKYTGSSMVHIPPGEPDFESSLCQTCLGEHAFQRGVLPQENESCSWETQSGCEVREPCNHANILTKPDPRTFWTNDDP (526; 59903 Da)	SGK1D
					SGK1 isoform 3	NM_001143677	MSSQSSSLSEACSREAYSSHNWALPPASRSNPP	SGK1C

Rat					Human			
Transcript	**NCBI #**	**N terminal amino acid sequence encoded** **(total amino acids in protein; theoretical molecular weight)**	**Trivial name**		**Transcript**	**NCBI #**	**N terminal amino acid sequence encoded** **(total amino acids in protein; theoretical molecular weight)**	**Trivial name**
							AYPWATRRMKEEAIKPPLK (459; 52119 Da)	
					-	GenBank: CAR58098.1	MKPSKRFFISPPSST (421; 47910 Da)	SGK1F
					-	-	MDYKDDDDKKPSKRFFISPPSST (429; 48905 Da)	AdV-encoded SGK1F

Chapter 4. **Investigating if SGK1F expression is upstream of β-catenin phosphorylation and WNT signalling changes in B-13 cells**

4.1 Introduction

WNT signalling is known to be involved in liver development [328,329,330,331] and also to regulate zonal hepatocyte gene expression in the adult liver [332]. High glucocorticoid levels lead to the conversion of B-13 cells onto B-13/H cells as a result of a process that involves the transient repression of WNT signalling upstream of the induction of C/EBP-β [218]. However, the mechanism by which glucocorticoid mediates WNT signalling repression is obscure. An earlier study revealed that B-13 transdifferentiation is mediated via the glucocorticoid receptor and not the mineralocorticoid receptor [227]. In addition, microarray data has indicated that the transdifferentiation of B-13 cells into B-13/H cells results in a significant (>100-fold) increase in Sgk1 mRNA transcripts in B-13/H cells. In contrast, few changes were detected in the expression levels of mRNAs encoding other components of the WNT and PI3K signalling pathways [197].

Initial work by Wallace et al. (2011) has demonstrated that β-catenin phosphorylation and reductions in the levels of β-catenin are early upstream events in relation to C/EBP-β induction and B-13 transdifferentiation to B13/H cells. When the effects of SGK1C, SGK1F or SGK1A (as a control) transfection on β -catenin was examined, it was found that SGK1C and SGK1F expression resulted in phosphorylation of β-catenin and reduced levels of total β-catenin, while the SGK1A isoform had no influence. In the same study-, they demonstrated that purified recombinant SGK1 was incubated with purified recombinant β-catenin and that phosphorylation was examined by Western blotting. β - catenin phosphorylation only occurred when SGK1 and ATP were present which determined that SGK1 could directly phosphorylate β- catenin [226].

For a better understanding, the mechanism(s) regulating the conversion/trans-differentiation of B-13 cells to B-13/H cells and whether Sgk1c/F cross-talks with the WNT signalling pathway based on distal Tcf/Lef transcriptional activity, Tcf/Lef-dependent luciferase expression (Topflash) was used to examine the effect of DEX and AdV-SGK1F expression on WNT signalling activity. Also in this approach, Western blot analysis was used to investigate if DEX and SGK1F are upstream of β-catenin phosphorylation in B-13 cells.

4.2 Trans-differentiation of B-13 cells into B-13/H cells is associated with a repression of WNT signalling based on a repression in Tcf/Lef transcriptional Activity.

To determine whether treatment of B-13 cells with DEX results in WNT signalling repression, the influence on Tcf/Lef transcriptional activity was examined. B-13 cells were treated with DEX (10 nM and 100 nM), 50 μM WNT antagonist (quercetin), ethanol and DMSO as vehicle controls and transfected with TCF-TK promoter construct (T cell factor reporter [TOPFLASH] plasmid and renilla reporter plasmid RL-TK in the 6:1 ratio. Additionally, B-13 cells were also transfected with a control vector (FOPFLASH) containing identical sequences except for the concatamer of Tcf/Lef binding response elements and RL-TK construct in the 6:1 ratio as a plasmid negative control. After 24 hours, cells were harvested and luciferase and renilla activities determined. Figure 4.1 shows that treatment with 10nM DEX significantly suppressed WNT signalling based on reduced relative TopFlash luciferase activity (~50% of constitutive level) reflected in B-13 cells treated with 10nM DEX in comparison to ethanol vehicle-treated cells (p value= 0.009). Moreover, increasing concentration to 100 nM DEX led to more repression in WNT signalling with p-value = 0.001 in comparison to ethanol control. Treatment of 50 μM quercetin suppressed ~70% of basal TopFlash luciferase activity, p-value =0.003 in comparison to DMSO control.

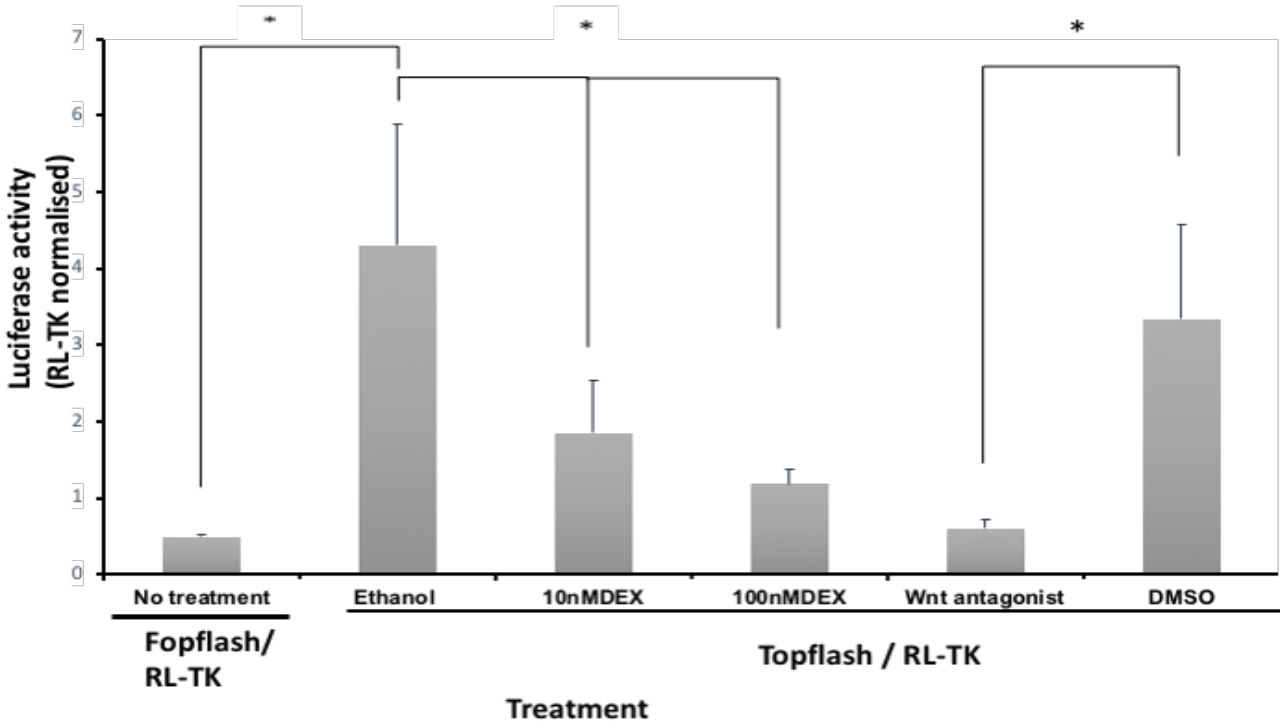

Figure 4.1 Treatment of B-13 cells with DEX repressed WNT signalling and Tcf/Lef transcriptional activity. B-13 cells were seeded in 24 well plates at a density of 50,000 cells/well for 24 hours. Then, cells were treated with the following treatments: DEX (10 nM and 100 nM), which were added to the medium from a 1000-fold concentrated stock in ethanol. Ethanol treatment as a control 50 μM WNT antagonist (quercetin) was added to the medium from a 1000-fold concentrated stock in DMSO. DMSO treatment as control was 0.1% (v/v) DMSO, B-13 cells with DMEM only. 48 hours later, all treated cells were transfected with TCF-TK promoter construct (T cell factor reporter plasmid TOPFLASH) and renilla reporter plasmid RL-TK in the 6:1 ratio. B-13 cell without DEX treated with mutated copy of TCF (FOPFLASH) and RL-TK construct in the 6:1 ratio as a plasmid negative control. After 24 hours, cells were harvested, and dual luciferase assay was carried. Data are the mean and standard deviation of six replicates from the same experiment. Significantly different (P<0.05) using one way ANOVA (Dunnet test). Similar results were obtained in three independent experiments.

4.3 Treatment of B-13 cells with DEX resulted in β -catenin depletion and phosphorylation.

In order to confirm the inhibitory effect of DEX on the WNT/β-catenin signalling pathway as observed by luciferase assay and to investigate DEX treatment upstream of β-catenin phosphorylation, the stability of β-catenin was examined. B-13 cells were treated with 10nM DEX, 100nM DEX, 50 μM WNT antagonist (tcf/lef inhibitor) for 14 days. Protein extracts were isolated and protein assay was performed. Western blotting analysis was performed for phosphorylated β-catenin, total beta-catenin and β-actin. The results showed that there was a depletion of total β-catenin levels in cells treated with DEX and WNT antagonist compared to B-13 cells treated with the ethanol vehicle only. Ser33- and Ser37- phosphorylated β-catenin was detected in B-13 cells treated with 10nM and robust expression of phosphorylated β-catenin was detected in 100nM DEX treated cells (Figure 4.2). To examine the effect of DEX on β-catenin phosphorylation and total β-catenin level in a time less than 14 days (which has never been investigated), B-13 cells were treated with 10nM DEX and 0.1% ethanol vehicle for 10 days only. Western blot analysis showed that Ser33- and Ser37- phosphorylated β-catenin was detected in B-13 cells treated with 0.1% ethanol vehicle and 10nM DEX. However, there is no complete loss of total beta-catenin protein compared to the complete loss of total beta-catenin protein in B-13 treated for 14 days with DEX (Figure 4.3).

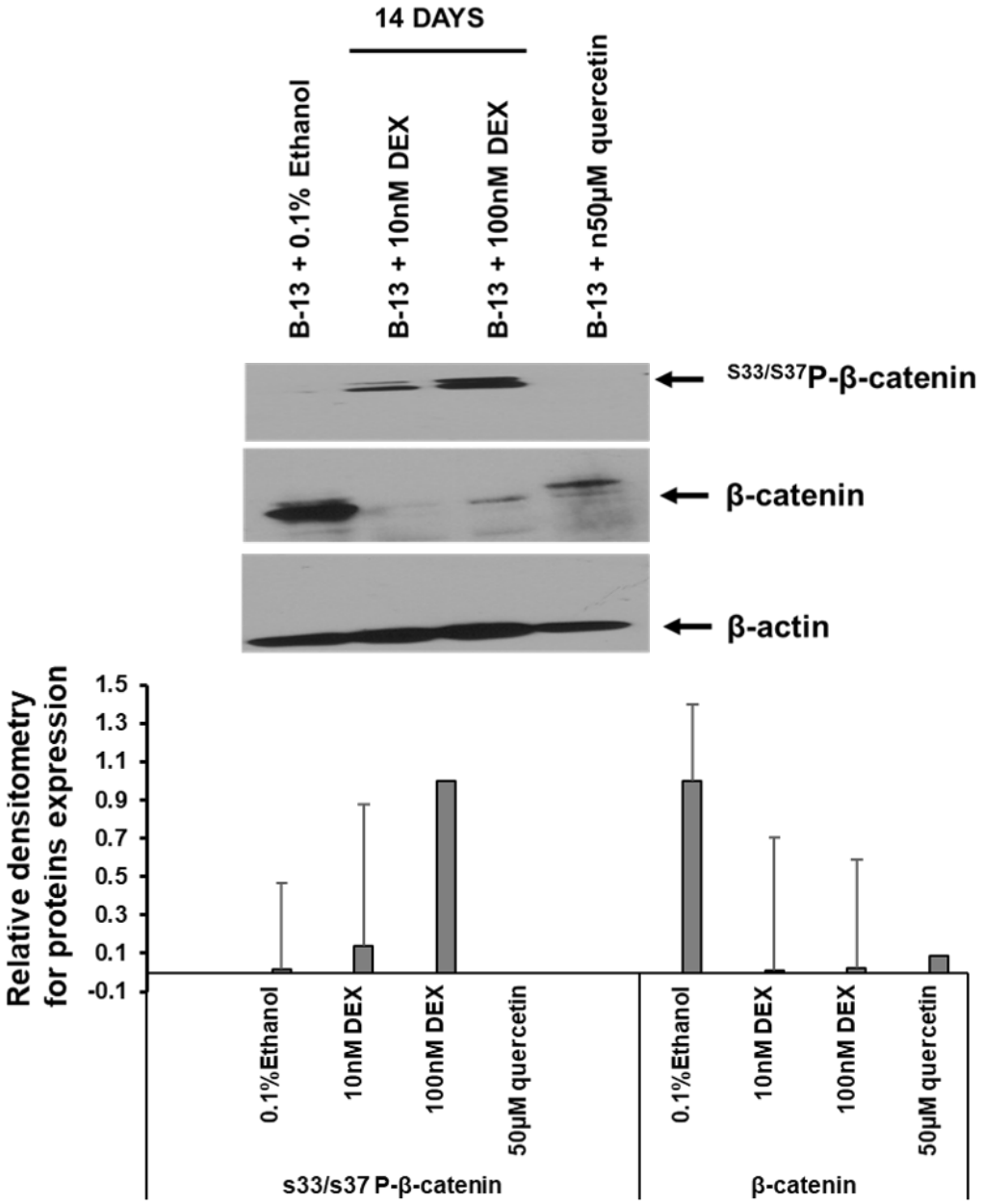

Figure 4.2Treatment of B-13 cells with DEX upstream for beta-catenin depletion and phosphorylation. Cells were treated for 14 days with the indicated treatments: 0.1% ethanol, DEX (10 nM,100nM) and quercetin (50 μM). Total cell lysates were collected and subjected to western blotting to analyse the stability of β-catenin protein and β-catenin phosphorylation, while β-actin was measured as the loading control (upper panel). The proteins expression level were quantified using ImageJ software in the lower panel. All data typical of at least three separate experiments.

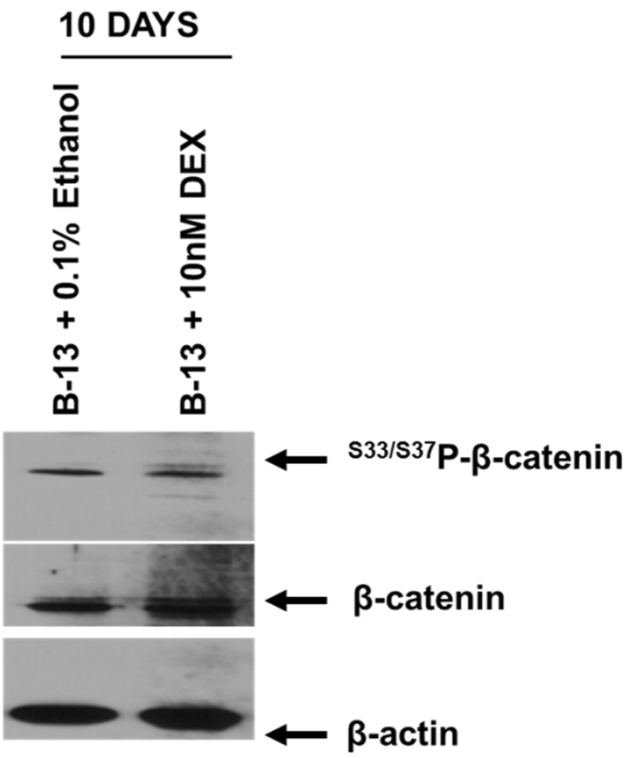

Figure 4.3 Treatment of B-13 cells with DEX upstream for beta-catenin depletion and phosphorylation. Cells were treated for 10 days with indicated treatment: 0.1% ethanol and 10nMDEX. Western blots were performed for the indicated protein at the indicated time of culture to analyse the stability of β-catenin protein and β-catenin phosphorylation, while β-actin was measured as the loading control. All data typical of at least three separate experiments.

4.4 Trans-differentiation of B-13 cells into B- 13/H cells is dependent on glucocorticoid interaction with the glucocorticoid receptor

To confirm that the GR is involved in changes in WNT signalling, B-13 cells were treated with 100nM DEX, 10μM RU486 (GR antagonist), 100nM DEX + 10μM RU486 and ethanol as a control. 48 hours later, cells were transfected with the TOPFLASH construct (and renilla reporter plasmid RL-TK in 6:1 ratio) or FOPFLASH (and RL-TK construct in 6:1 ratio, used as a plasmid negative control). After 24 hours, cells were harvested, and a dual luciferase assay was carried out. Figure 4.4 demonstrates that treating cells with 100nM DEX resulted in WNT signalling reduction with p-value =0.008. However, adding RU486 (GR antagonist) to 100nM DEX led to non-significant difference in WNT signalling when compared to DEX treated cells with p value= 0.719. Surprisingly, RU486-only treated cells showed markedly decreased WNT signalling with P value=0.008. The reduction in WNT signalling in B-13 cells treated with RU486 only, could be due to activation of other nuclear receptors contacted by RU486.

To determine whether other nuclear receptors known to be contacted by RU486 are responsible for the suppression of WNT activity in B-13 cells when treated with RU486, the potential role of the progesterone receptor (Pgr) and pregnane x receptor (PXR) were examined. RT-PCR was first performed to determine whether they are expressed. The data in Figure 4.5 (upper panel) exclude a role for PXR as it is expressed by B-13/H cells only. However, Pgr was found to be expressed in both B-13 and B-13/H cells Figure 4.5 (middle and lower panel). Further investigations were conducted to examine if progesterone exposure would convert B-13 into B-13/H cells. B-13 cells were treated with different concentrations of progesterone (10nM,100nM and1μM) and 10nM DEX for 14 days. Photomicrographs were taken and RT-PCR performed for the liver marker Cyp2e1. The results in Figure 4.6 show that progesterone exposure did not convert B-13 into B-13/H cells. According to the cell morphology, there is no morphological phenotype change in B-13 cells treated with progesterone and RT-PCR results showed that treatment of cells with progesterone (10nM,100nM and1μM) failed to induce liver marker gene *Cyp2e1*.

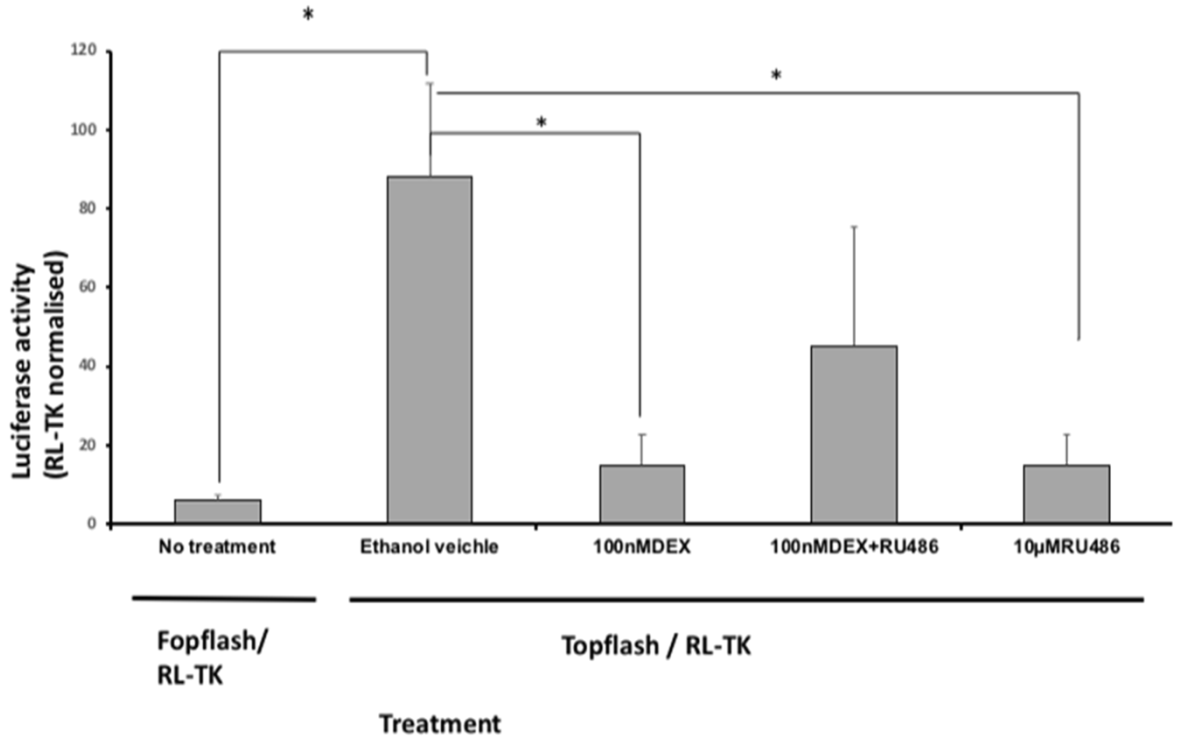

Figure 4.4 Treatment of B-13 with DEX and glucocorticoid antagonist (RU486) increased WNT signalling and Tcf/Lef transcriptional activity in comparison to DEX treated cells. B-13 cells were seeded in 24 well plates with a density of 30,000 cells/well for 24 hours. Then, cells were treated with the following treatments: 100 nM DEX, which was added to the medium from a 1000-fold concentrated stock in ethanol. 0.1% (v/v) ethanol as a control, 10 μM RU486 (GR antagonist) was added to the medium from a 1000-fold concentrated stock in ethanol, 100 nM DEX+ 10 μM RU486 and DMDEM only. 48 hours later, all treated cells transfected with TCF-TK promoter construct (T cell factor reporter plasmid TOPFLASH) and renilla reporter plasmid RL-TK in the 6:1 ratio, except B-13 cell with DMEM medium only treated with a mutated copy of TCF (FOPFLASH) and RL-TK construct in the 6:1 ratio as a plasmid negative control. After 24 hours cells were harvested, and dual luciferase assay was carried out. Data are the mean and standard deviation of six replicates from the same experiment. Significantly different ($P<0.05$) using one way ANOVA (Dunnet test).

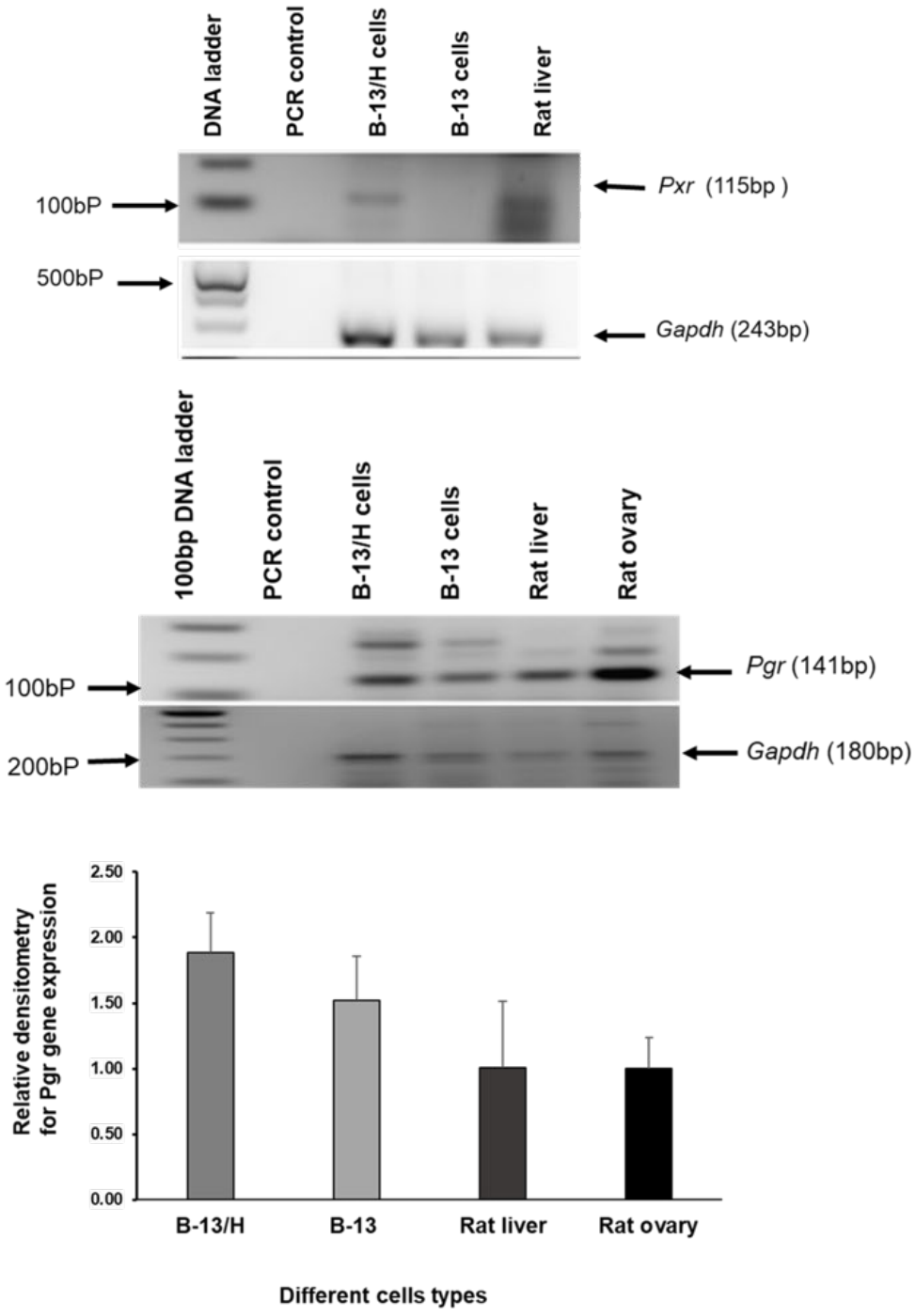

Figure 4.5 Several other nuclear receptors bind glucocorticoids. To define if there are other nuclear receptors that might react, glucocorticoids rather than GR: B-13 cells were treated with 10 nM DEX for 9 days, and RNA was isolated from B-13/H, B-13 and cell extracts from rat liver and ovary tissues were used as controls. RT-PCR was performed for r- PXR (upper panel)and r –Pgr (middle panel). RT-PCR results for Pgr were quantified using ImageJ

software, Gapdh was used as a loading control. All data typical of at least three separate experiments.

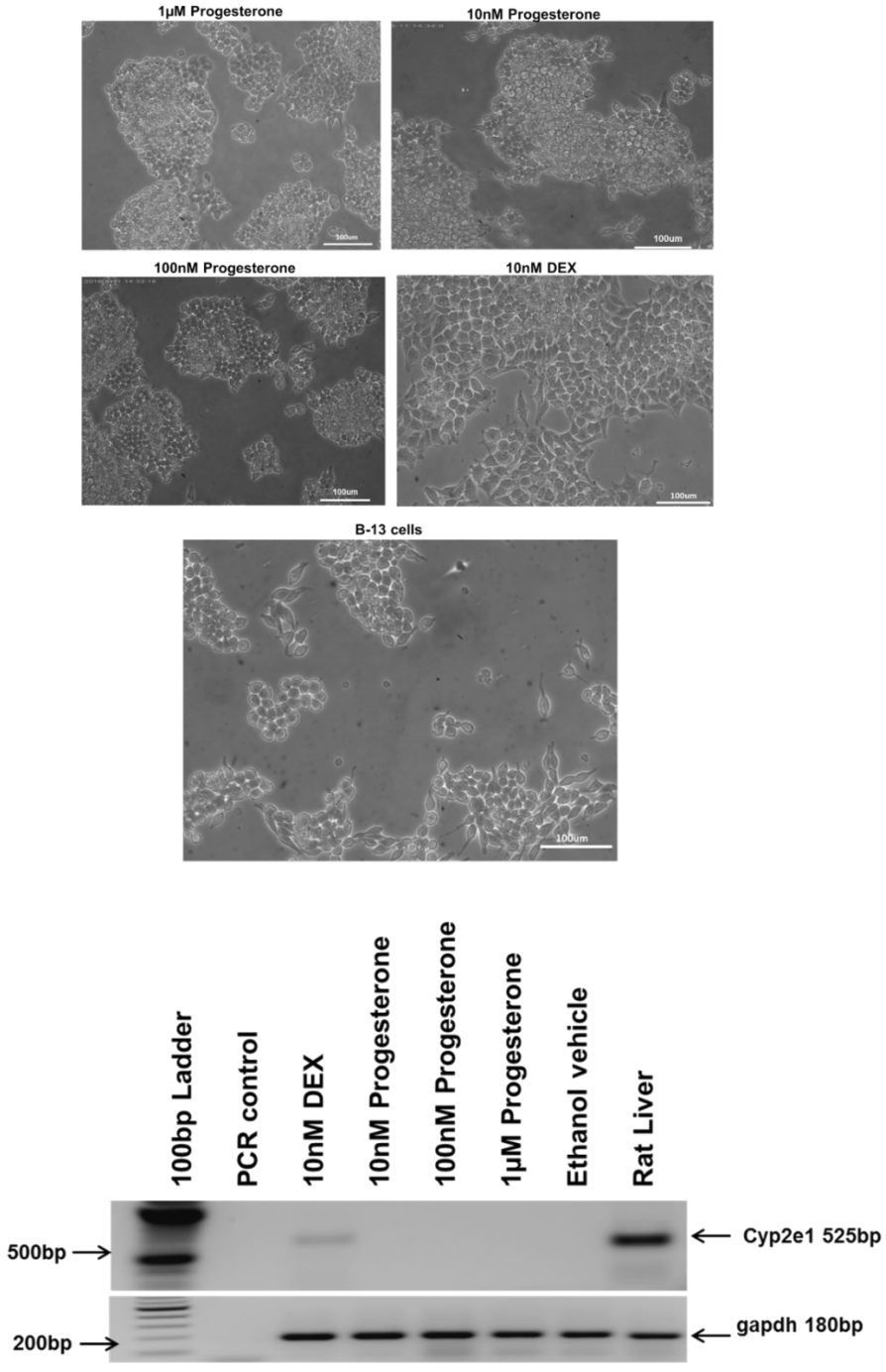

Figure 4.6 Trans-differentiation of B-13 cells into B- 13/H cells is dependent on glucocorticoid interaction with the glucocorticoid receptor. B-13 cells were treated with different concentrations of progesterone (10nM,100nM,1μM) and 10nM DEX for 14 days. Photomicrograph pictures (upper panel) and RT-PCR for the liver marker cyp2e1(lower panel), Gapdh was used as a loading control. All data typical of at least three separate experiments.

4.5 Treatment of B-13 with DEX and SGK1 inhibitor did not increase WNT signalling in comparison to DEX-treated cells

To determine whether SGK1 kinase activity is involved in the regulation of WNT signalling in B-13 cells, B-13 cells were seeded in 24 well plates with a density of 2500 cells/well for 72 hours. Then, cells were treated with the following treatments: 10nM DEX was added to the medium from a 1000- fold concentrated stock in ethanol, ethanol treatment as a control and 500nM SGK1 inhibitor (GSK 650394) was added to the medium from a 1000-fold concentrated stock in DMSO, 10nM DEX + 500nM SGK1 inhibitor. 48 hours later, cells were transfected with TOPFLASH (and renilla reporter plasmid RL-TK in the 6:1 ratio) or FOPFLASH (and RL-TK construct in the 6:1 ratio as a plasmid negative control). After 24 hours, cells were harvested, and dual luciferase assay was carried out. Figure 4.7 shows that treating cells with 10nM DEX reduced the WNT signalling with p-value = 0.01 when compared to ethanol vehicle control treated cells. Treating cells with a combination of 10nM DEX and 500nM SGK1 inhibitor has not significantly increased the signal when compared to10nM DEX treated cells (p-value 0.966). Likewise, there was no significant difference when compared to DMSO treated cells.

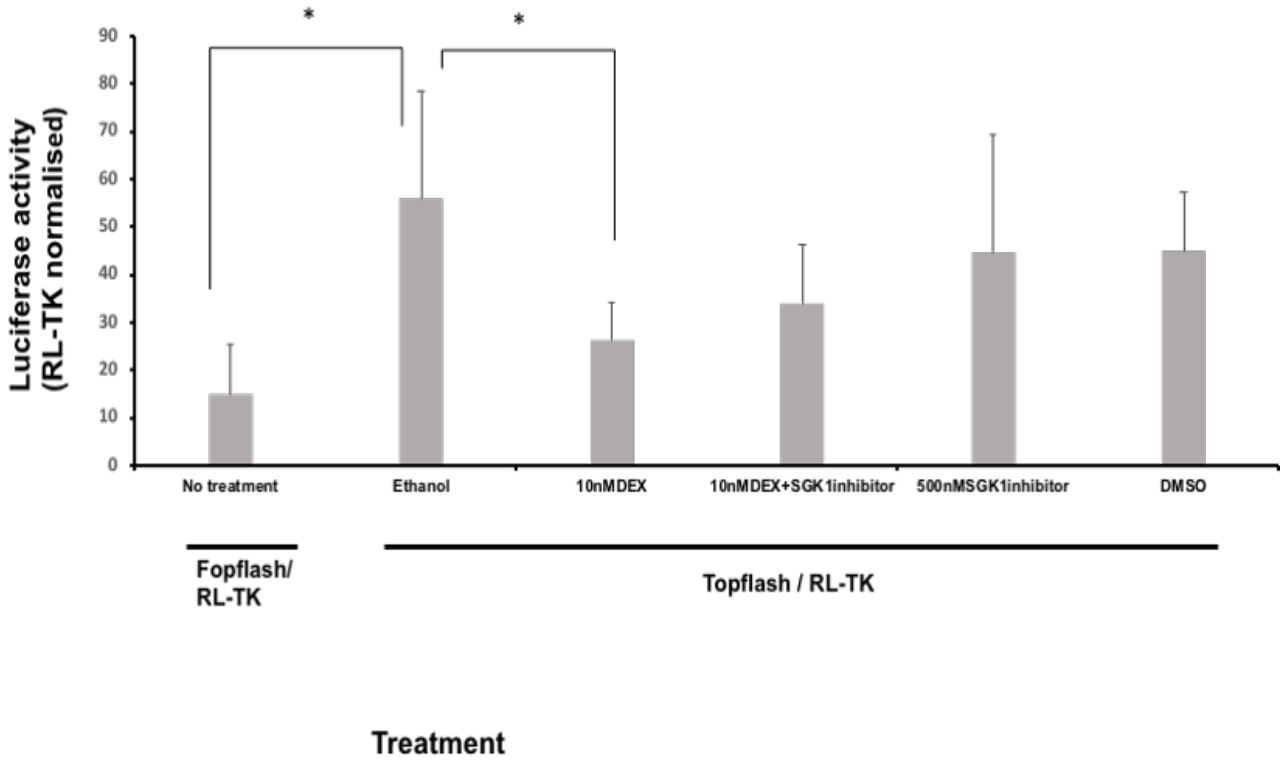

Figure 4.7 Treatment of B-13 cells with DEX and SGK1 inhibitor (GSK 650394) did not increase WNT signalling in comparison to DEX-treated cells. B13 cells were seeded in a 24 well plate with a density of 2500 cells/well for 72 hours. Then, cells were treated with the following treatments: 10nM DEX, which was added to the medium from a 1000-fold concentrated stock in ethanol. Ethanol treatment as a control. 500nM SGK1 inhibitor (GSK 650394) which was added to the medium from a 1000-fold concentrated stock in DMSO. 10nM DEX+ 500nM SGK1 inhibitor. 48 hours later, cells were transfected with TCF-TK promoter construct (T cell factor reporter plasmid TOPFLASH) and renilla reporter plasmid RL-TK in the 6:1 ratio, b13 cell treated with DMEM medium only were transfected with a mutated copy of TCF (FOPFLASH) and RL-TK construct in the 6:1 ratio as a plasmid negative control. After 24 hours cells were harvested, and dual luciferase assay was carried out. Data are the mean and standard deviation of six replicates from the same experiment. Significantly different ($P<0.05$). Using the one way ANOVA (Dunnet test). All data typical of at least three separate experiments.

4.6 Over-expression of SGK1F repressed WNT signalling and resulted in β-catenin phosphorylation

To further test the role of Sgk1 kinase activity in B-13 cells and WNT signalling, B-13 cells were infected with AdV-SGK1F and the effects on WNT signalling examined using TOPFLASH and FOPFLASH. B-13 cells were transfected with either TOPFLASH or FOPFLASH, both with RL-TK to normalise for transfection efficiencies. After 24 hours, cells were then infected with either AdV-SGK1F or AdV-GFP (as control) at an MOI of 5. After a further 24 hours, luciferase and renilla activities were determined. Figure 4.8 shows that infection of B-13 cells with AdV-SGK1F resulted in suppression of WNT signalling activity .Moreover, to investigate if SGK1F overexpression resulted in β-catenin phosphorylation, B-13 cells were infected every 2 days with AdV-SGK1F (MOI 5) or the control AdVs (AdV-GFP, AdV-null) at an MOI of 5 over a 4 day period. Protein was isolated from each treatment after 4 days, and protein assay was performed. Western blot analysis was performed using 20µg protein/lane of protein for β -catenin phosphorylated, total β-catenin and the β-actin as a loading control. The results in Figure 4.9 clearly reveal that infection of B-13 cells with AdV-SGK1F resulted in changes in the ratio of β-catenin/phosphorylated-β-catenin, however the total β-catenin was still detectable in AdV-SGK1F infected cells. In contrast, phosphorylated β-catenin was undetectable in B-13 cells infected with AdV-GFP or AdV-null.

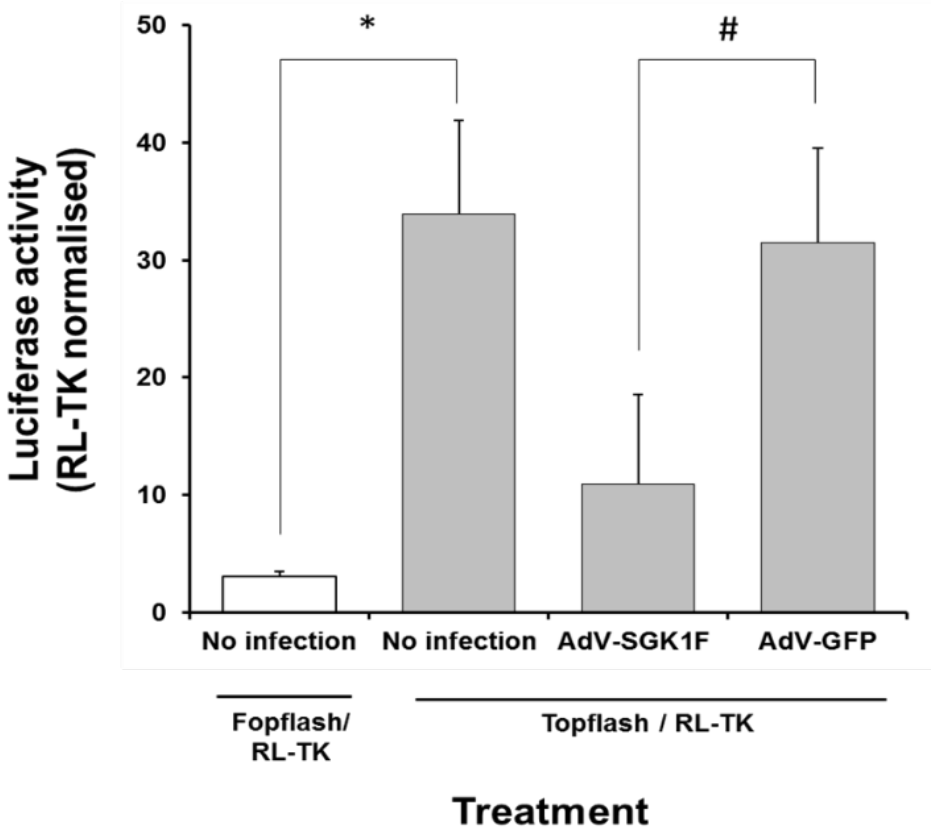

Figure 4.8 Infecting B-13 cells with AdV-SGK1F leads to reduction in Tcf/Lef (WNT signalling) transcriptional activity. B-13 cells were transfected with a mixture of the indicated reporter gene constructs as indicated. After 24 hours, cells were then infected with the indicated AdV at an MOI of 5. After a further 24 hours, cells were lysed and the levels of luciferase and renilla determined, as outlined in the methods section. Data are the mean and SD of 5 separate determinations from the same experiment, typical of 3 separate experiments. Significantly different ($p < 0.05$) normalized luciferase activity versus (*) Foplash or (#) AdV-GFP infected cells using the Student's T test (two tailed).

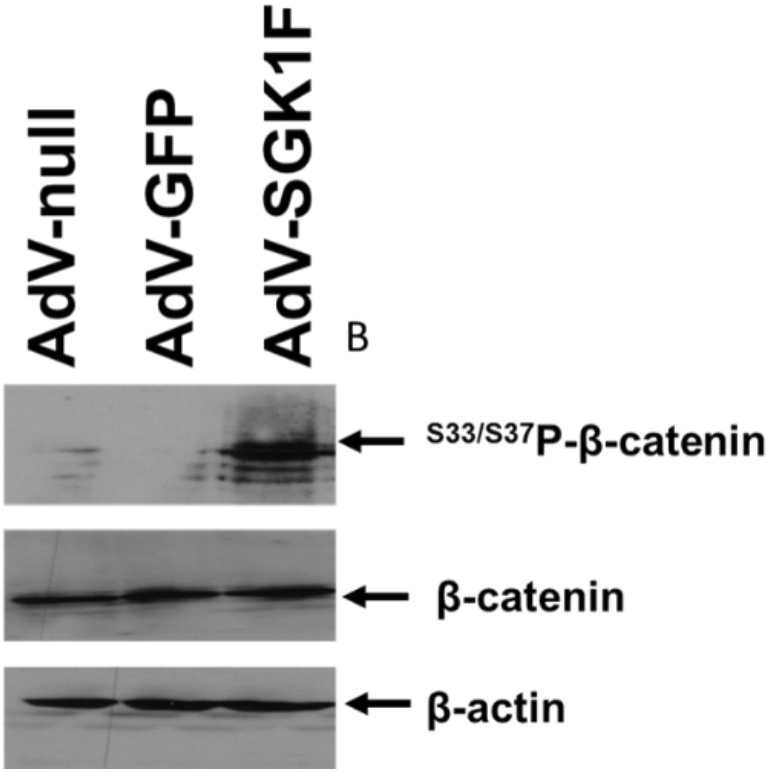

Figure 4.9 Phosphorylation of β-catenin in B-13 cells in response to AdV-SGK1F infection. B-13 cells were repeatedly infected with AdV-*SGK1F* or the control AdVs (AdV-*GFP*, AdV-*null*) at an MOI of 5 over a 4 day period before expression levels of the indicated proteins were determined by Western blot (20µg cell protein/lane), β-actin was used as a loading control. Data typical of 3 separate experiments

4.7 Chapter discussion

WNT signalling is a passive signalling pathway in adult liver tissue and regulates the expression of several genes in the liver [332]. The WNT signalling concentration gradient is high in centrilobular regions and low in periportal regions. Additionally, WNT up-regulates genes such as glutamine synthetase (Gs); *Idh3a* isocitrate dehydrogenase 3a; *Dlat* dihydrolipoamide. S-acetyltransferase and *Gstm* glutathione S-transferase mu, cyp1a2 and cyp2e1. Genes down-regulated by WNT signalling include Cps1 and arginase 1 (Arg1), Phosphoenolpyruvate carboxykinase 1 (pck1), fructose bisphosphatase (FBPase), Cytochrome P450 2F 2(Cyp2f2) and sulfotransferase (Sult5a1)[91]. Wallace et al. (2010), demonstrated that B-13 cells express the WNT3a protein and have high WNT signalling activity. Treatment with DEX caused a temporary loss of WNT3a expression, which was linked to a reduction in WNT signalling activity and the subsequent transdifferentiation of B-13 cells into hepatocyte-like B-13/H cells. Their data suggested that suppression of WNT signalling by glucocorticoid is a vital mechanism controlling B-13 transdifferentiation, furthermore, knockdown of the intracellular WNT messenger protein β-catenin replaced DEX and also generated rapid transdifferentiation [218].

The data in this chapter confirm that B-13 cells treated with the 10nM DEX treatment resulted in a significant decrease in WNT signalling. Moreover, increasing the concentration to 100nM DEX led to more repression in WNT signalling in comparison to the ethanol control. The data also indicate that 50 μM quercetin inhibited WNT signalling. Quercetin has been observed to lack the ability to promote transdifferentiation into B-13/H cells but to potentiate glucocorticoid-mediated transdifferentiation [218]. The mechanism by which glucocorticoid mediates WNT signalling repression has not therefore been fully explained. There are only a few investigations studying the interaction of glucocorticoids with WNT signalling, which appear to depend on the cell type assessed. It has been shown that glucocorticoid exposure reduces the expression of β-catenin in pituitary cells [333] and inhibition of β-catenin expression by DEX promotes the differentiation of mesenchymal progenitor cells into adipocytes [334], while it does not influence osteoblasts [335].

In B-13 cells, it has been detected that there is a constitutive WNT3a expression and moreover, after 14 days of 10nM DEX treatment, glucocorticoid treatment resulted in phosphorylation and depletion of β-catenin and loss of β-catenin nuclear localisation, besides significant reductions in T-cell factor/lymphoid enhancer factor (Tcf/Lef) transcriptional activity before obvious changes in phenotype into hepatocyte-like (B-13/H) cells. A reoccurrence of higher Tcf/Lef transcriptional activity was noted along with the re-expression of WNT3a in B-13/H

cells. β-catenin knockdown alone was substituted for glucocorticoid-dependent transdifferentiation. Overexpression of a mutant β-catenin protein blocked glucocorticoid-dependent suppression of Tcf/Lef activity and resulted in inhibition of transdifferentiation [218].

The data in this chapter also confirms that in addition to the DEX effect on WNT signalling repression, β-catenin phosphorylation was also was resulted. In a previous work by Fairhall and colleagues, it has been shown that B-13 transdifferentiation is mediated via the glucocorticoid receptor and probably not by the mineralocorticoid receptor [227]. In this study, treating cells with 100nM DEX resulted in significant reduction of WNT signalling transcriptional activity. Meanwhile, as demonstrated in the previous chapter, the GR antagonist mifepristone (RU486) prevented transdifferentiation of B-13 into B-13/H cells. However, adding RU486 to 100nM DEX did not result in a significant difference in WNT signalling transcriptional activity when compared to DEX-treated cells. Surprisingly, RU486 treated cells exhibited markedly decreased WNT signalling. The reduction in WNT signalling in B-13 cells treated with RU486 only could be due to weakly acting nuclear receptors responding to the high concentration of RU486. Therefore, the expression of the Pgr and PXR, which are known to be contacted by RU486 was examined. Pgr was found to be expressed in both B-13 and B-13/H cells. However, progesterone exposure failed to convert B-13 into B-13/H cells. As shown in the flowchart Figure 4.10), antagonising the progesterone receptor with RU486 should have the same effect as DEX on WNT signalling. However, while both RU486 and DEX repressed WNT signalling, only DEX converted B-13 cells into B-13/H cells. DEX exposure might result in epigenetic changes, for instance the up-regulation of Gr mRNA expression and increased expression and translation of a functional N-terminally truncated Gr protein that shows increased nuclear localisation in B-13/H cells [326]. This effect of DEX could explain its influence on B-13 trans-differentiation into B13/H cells.

Data in this chapter demonstrate a novel regulatory role for Sgk1 (SGK1F) in WNT signalling changes and suggested that SGK1F overexpression is upstream of β-catenin phosphorylation changes. The likelihood is therefore that the conversion of B-13 cells into B-13/H cells in response to glucocorticoid is associated with Sgk1 induction and WNT signalling changes. The mRNA expression of WNT related genes and WNT signalling inhibitors genes (Dkk1, DDKK3 and sFRP), could be assessed using real-time PCR. The changes in genes at protein levels can be validated by Western blotting. Understanding the mechanisms is essential to recognise the cellular differentiation of stem cells, progenitor cells and terminally differentiated cells.

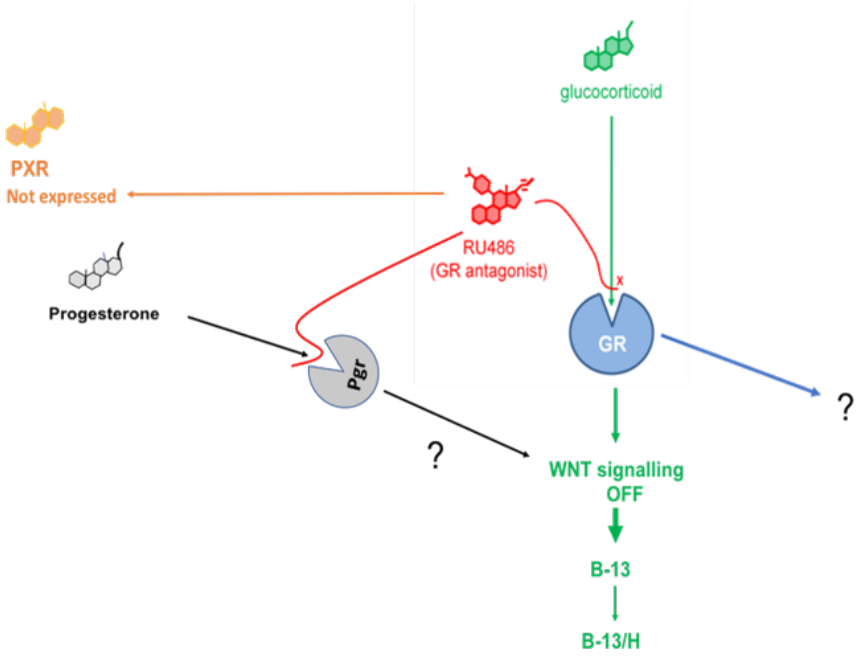

Figure 4.10: Schematic diagram illustrates the effect of glucocorticoid antagonist (RU486) on GR and Pgr and their effect on WNT signalling and B-13 cells conversion into B-13/H cells.

Chapter 5. **Conversion of human iPSCs into human hepatocyte-like cells**

5.1 Introduction

Liver transplantation and hepatocyte transplantation are effective treatments against chronic liver failure, acute liver failure and hereditary liver disease [336]. In addition, *in vitro* toxicity assays using human hepatocytes is currently the gold standard for accurate assessment of drug toxicity and safety [337]. However, several factors limit hepatocyte utility. Hepatocytes do not proliferate *in vitro* and therefore cannot be expanded *in vitro*. Furthermore, culture results in dedifferentiation and loss of function [338,339,340]. Moreover, their sources are limited, which results in difficulty in obtaining the ample quantities required for large-scale drug toxicity screening [341,342]. A disadvantage of using human hepatocellular carcinoma cell lines (such as HepG2 cells), is that they do not correctly reflect hepatic function [343]. In addition, animal models can be used, but they introduce the problem of inter-species differences [344]. Therefore, hepatocyte-like cells generated from hESCs and iPSCs are expected to provide an alternative model for drug toxicity screening and hepatocyte transplantation.

Hepatocyte differentiation technology has improved over the years and it has become possible to generate ESCs/iPSCs-derived human hepatocyte-like-cells that have drug metabolic capacity and responsiveness to specific treatment, as these cells could be used for diseases modelling. This suggests that human ESCs/iPSCs-hepatocyte-like-cells may be a useful model for drug toxicity assays. However, they still have an immature phenotype in most of the differentiations experiments [268]. As mentioned in section 1.7 of this dissertation there are some attempts to manipulate the *in vitro* environment to generate or preserve hepatic functionality[293,345]. Thus, further improvements in hepatic differentiation technology will be required before human ESCs/iPSCs-derived hepatocyte-like-cells can be a worthwhile alternative to primary human hepatocytes in drug toxicity prediction and screening. Unpublished studies in the laboratory conducted by (Wallace and Wright, unpublished data) investigated the effect of plasmid-driven human SGK1 expression on ES cell differentiation and maturation into hepatocyte-like-cells. Cells were transfected with SGK1F, SGK1C or SGK1A after 7 days of differentiation. The transfections did not result in any detectable alteration in hepatocyte-like-cells differentiation. In another experiment, cells were transfected with SGK1F, SGK1C, SGK1A just before day 11 of differentiation. The transfections did not result in any detectable alteration in mature hepatocyte differentiation. However, it was not considered a robust test because transfection rates were extremely low.

Induced pluripotent stem cells (iPSCs) are generated by reprogramming somatic cells to a pluripotent state by the introduction of specific factors [46,47]. In this approach, iPSCs received from Prof. Lyle Armstrong (Institute of Genetic Medicine, Newcastle University) were reprogrammed using a Sendai reprogramming kit. This kit includes three vector preparations: polycistronic Klf4–Oct3/4–Sox2, cMyc, and Klf4 for iPSC derivation from adult dermal fibroblasts (AD3 cells). Following a natural path of development hiPSCs (AD3) were differentiated into hepatocyte-like cells according to the protocol by [52]. The effect of AdV-SGK1F overexpression on hepatocyte-like cells maturation was examined at different stages of differentiation. The effect of AdV-SGK1F overexpression on adult human hepatocytes dedifferentiation were examined also. As SGK1 is a glucocorticoid-induced gene, the effect of glucocorticoid exposure (1μMDEX) at the hepatoblast stage of differentiation, was also examined.

5.2 The initial protocol employed

Following a natural path of development, hiPSCs (AD3) were initially differentiated into hepatoblasts according to the protocol by Hannan et al. (2013) [52] (Figure 5.1 upper panel). On day 1 the RT-PCR result shows expression of stem cells marker OCT4 (Figure 5.2). Cells were cultured with CDM-PVA with Activin-A (100ng/mL) and b FGF (100ng/mL) and incubated for 24 hours for the pluripotency maintenance. The next day, cells were washed with DPBS and differentiation was induced by treating cells with freshly prepared CDM-PVA containing Activin-A (100ng/mL), bFGF (100ng/mL), BMP-4 (10ng/mL), LY294002 (10μM), CHIR99021 (3μM) for a further 24 hours. Then, the medium was replaced with freshly prepared CDM-PVA with Activin-A (100ng/ mL), bFGF (100ng/mL), BMP-4 (10ng/mL) and LY294002 (10μM). This change in media induced endoderm specification over the next 24 hours [52]. Cells were incubated for 24 hours only and the medium replaced with freshly prepared RPMI- B27 medium containing Activin-A (100ng/mL) and bFGF (100ng/mL). This change in media creates endoderm commitment over the next 24 hours which can be detected by the increase in cell size (Figure 5.1 lower panel) and expression of endoderm marker (sox17) , even though pluripotency marker (OCT4) expression was still detectable by RT-PCR after 4 days (Figure 5.2). Next, the medium was replaced with RPMI-B27 differentiation medium with Activin-A (50 ng/ml). After 3 days of daily medium changes, hepatic specification was induced by treating cells with RPMI-B27 differentiation medium with Activin-A (50 ng/ml) and FGF10 (10ng/mL) for 3 days. It should be noted that foregut endoderm is reported to be specified over this period, according to the protocol issued by Hannan et al (2013) [52]. It can be seen from Figure 5.1 (lower panel) day 12 that the cells take on a polygonal shape and organise into an

epithelium with canaliculi-like structures (indicated by the white arrow) and a dark cytoplasm. After 12 days, hepatic specification was determined by the expression of alpha-fetoprotein (AFP) (Figure 5.2). Cells were treated with hepatocyte basal medium supplemented with OSM (30ng/mL) and HGF (50ng/mL), and the media was replaced every two days. RT-PCR results demonstrate that cells expressed the hepatoblasts marker (AFP) and ductal marker (CK19) after 15 days, although no expression was detected by RT-PCR of albumin or CYP2E1 at this stage of differentiation (Figure 5.2). Immunocytochemical staining showed an expression of CK19, AFP and a weak expression of albumin after 16 days of differentiation (Figure 5.3 A,B&C).

These data demonstrate that the cells only achieve an immature phenotype. In the subsequent differentiation trials the hiPSCs (AD3) were subjected to prolonged maturation protocol as described in Figure 5.4 . The RT-PCR results revealed a marked reduction in pluripotency markers OCT4 and SOX2 after day 7 and were completely absent at day 26; a clear expression of DE marker SOX17 at day 5, expression of ADE marker HHEX at day 5, FOXA2 at day 5-26. The cells still show an immature phenotype through expression of AFP and CYP3A7, although mature liver genes albumin expression is detected (Figure 5.5).

Q-RT-PCR was employed to provide a more quantitative determination in the progression of cultured AD3 cells toward hepatic lineage, which is widely seen to occur by means of four stages (endoderm, anterior definitive endoderm, hepatoblast and hepatocyte-like). The expression of specific genes markers for each differentiation stage was examined. Q-RT-PCR for the progression of cultured AD3 cells toward hepatic lineages from day 1 to day 26 showed significant expression of pluripotency genes (OCT4, SOX2) at day 1. After three days of differentiation, the cells continued to express the same level of pluripotency markers and scarcely detectable amounts of the endodermal marker gene SOX17. On day 7, the cells displayed a significant level of endodermal marker SOX17 expression; the pluripotency markers gene expression levels were now very low in comparison to SOX17. HEX and FOXA2 transcript levels were detectable at this stage; however, the hepatoblast marker gene AFP was not detected at this stage. Expression of hepatoblast marker genes was detected by day 12. After 26 days, pluripotency and endodermal markers were not expressed although the levels of AFP were diminished. The liver transcription factor HNF4α was detected along with low levels of the mature hepatocyte marker (CYP3A4). These data indicate that a prolonged differentiation protocol (26 days) resulted in a diminished level of hepatoblasts marker and suggested the expression of mature hepatocyte markers may require an inducer or prolonged protocol beyond 26 days to be detectable (Figure 5.6). The aim was to track the differentiation stage to confirm the cells are differentiating from the pluripotent stage (day0-1) into endoderm (days 3-5), ADE

(days 5-7), hepatoblasts (days 8- 12) and hepatocyte-like-cells (days 12-29). Sometimes the RNA concentration selected was too low or lack purity, which required some flexibility around the day of culture used for some analyses.

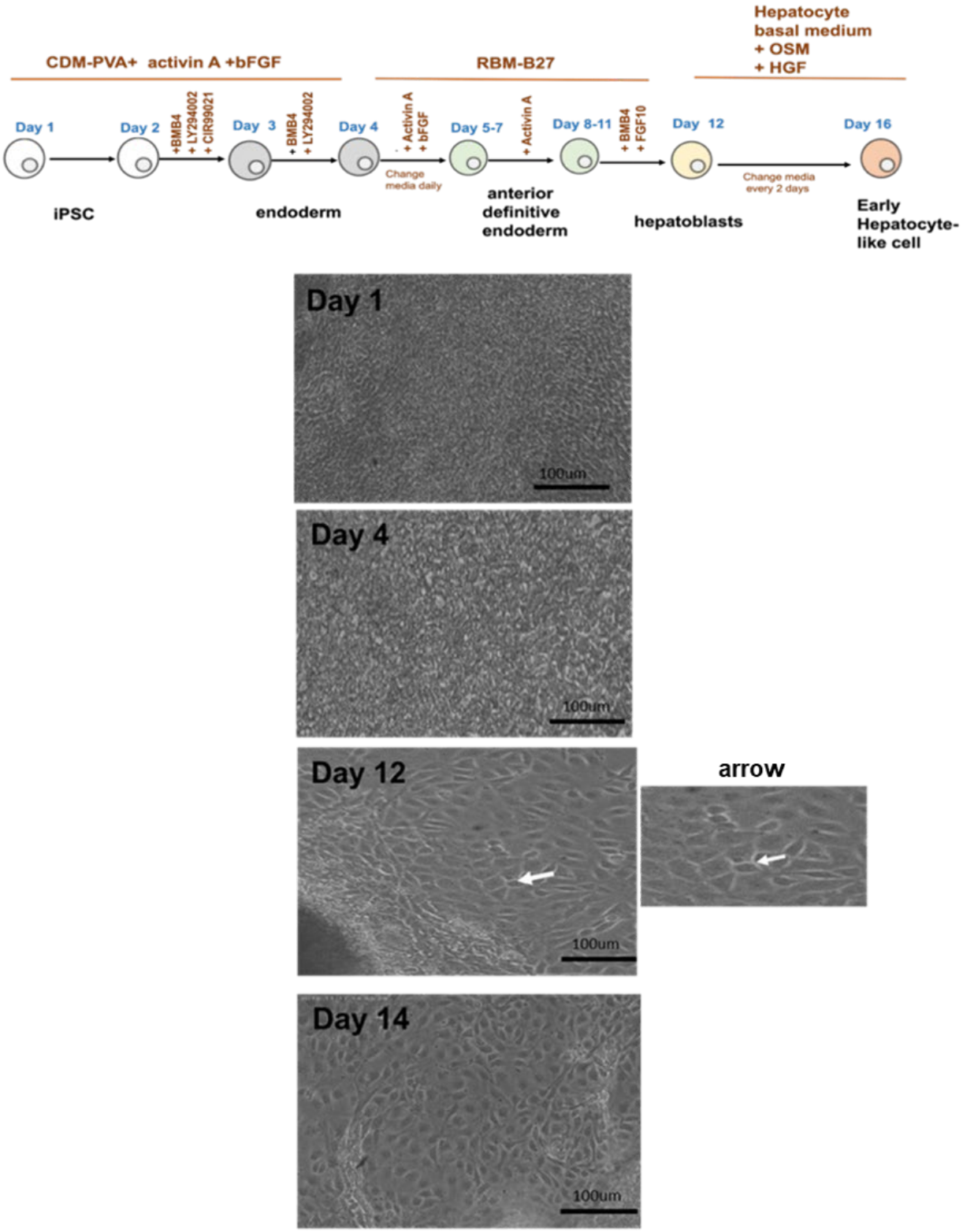

Figure 5.1 Initial protocol employed for iPSCs (AD3) differentiation into hepatocyte- like-cells. Flow chart outlining the growth factors and media used for the generation of mature

hepatocyte (upper panel). In the lower panel, iPSCs (AD3) differentiate into hepatocytes (white light/phase contrast pictures): Following a natural path of development hiPSCs (AD3) were differentiated into hepatic endoderm (hepatoblasts): Day 1 bright field picture demonstrating tightly packed colonies of Pluripotent cells with well-defined borders showing a high nuclear to cytoplasmic ratio. By the end of the day 4, definitive endoderm commitment can be detected by the increase in cell size and migration of cells away from the original colony. At days 12 and 14 hepatoblasts display polygonal shape and organised into an epithelium with canaliculi-like structures (indicated by the white arrow) and a dark cytoplasm. Data are typical for at least 3 separate experiments. Panel labelled “arrow” is an expanded view of the cell identified by an arrow at day 12.

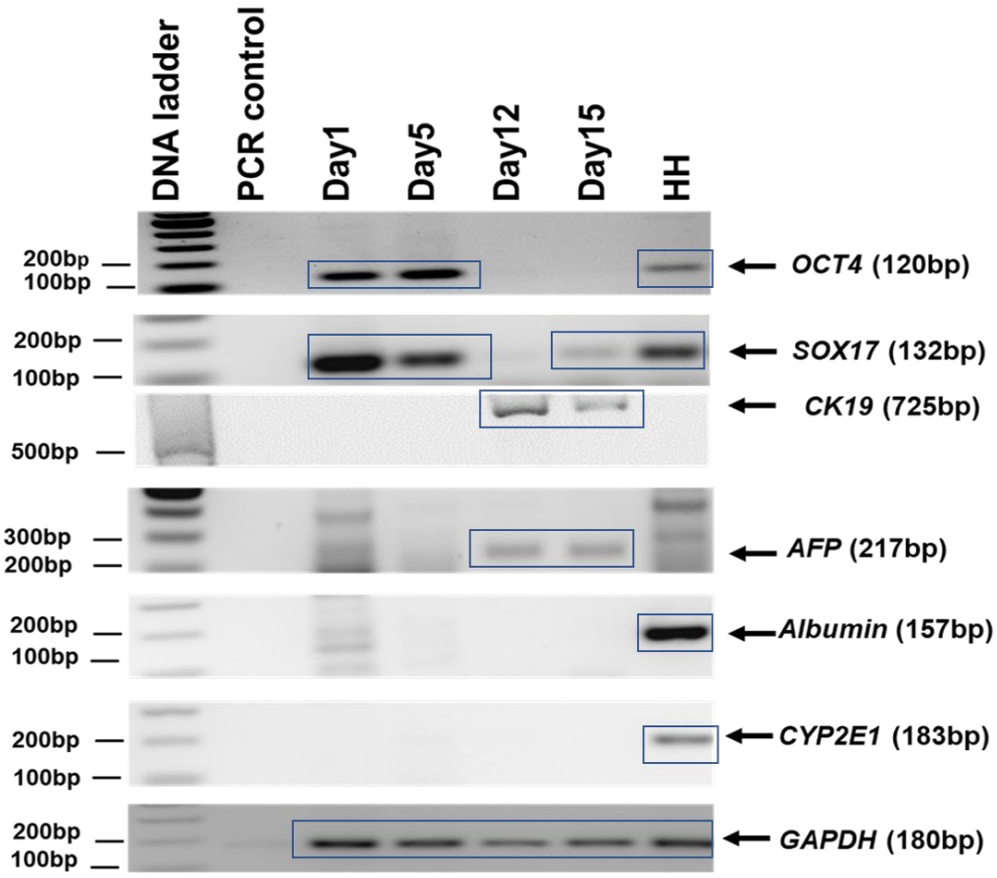

Figure 5.2 Initial protocol employed for iPSCs (AD3) differentiation into hepatocyte- like-cells.

RT-PCR for indicated genes, Gapdh was used as loading control; mRNA isolated from differentiated AD3 cells at different stages of differentiation as indicated. mRNA also isolated from human hepatocytes and used as a control. Data are typical for at least 3 separate experiments.

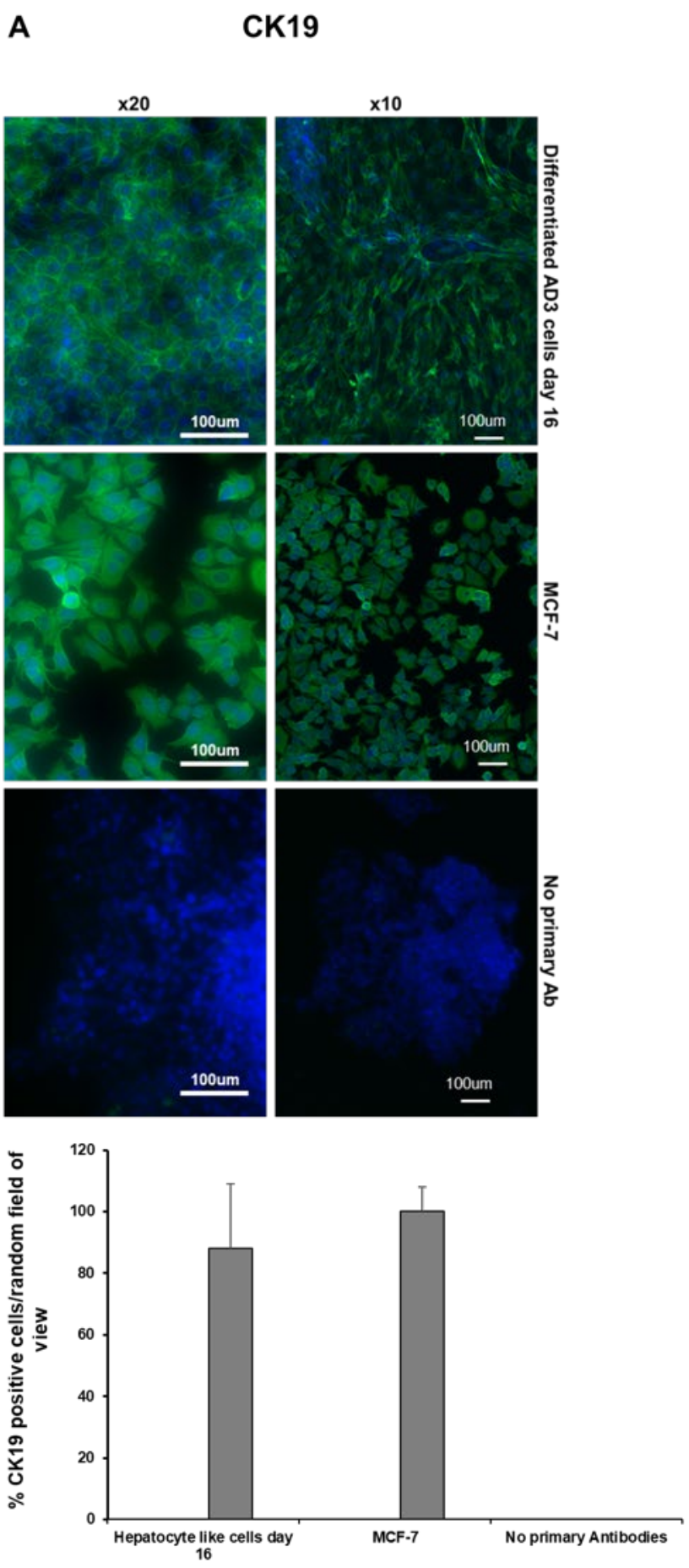
A
CK19
x20
x10
Differentiated AD3 cells day 16
MCF-7
No primary Ab
100um
% CK19 positive cells/random field of view
120
100
80
60
40
20
0
Hepatocyte like cells day 16
MCF-7
No primary Antibodies

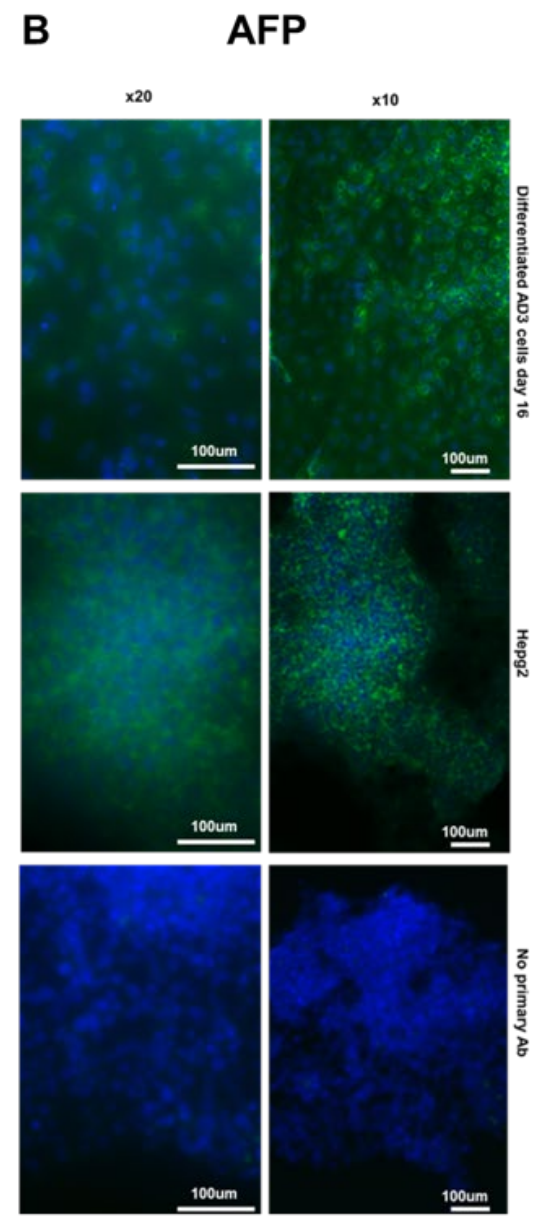
B
AFP
x20
x10
Differentiated AD3 cells day 16
Hepg2
No primary Ab
100um

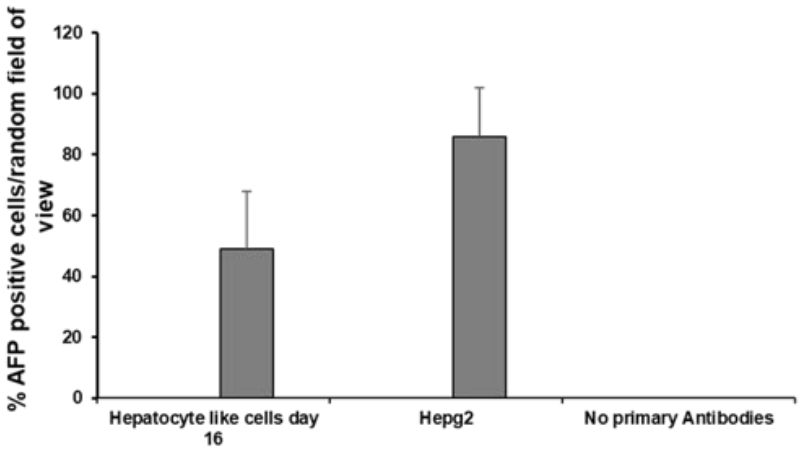
% AFP positive cells/random field of view
120
100
80
60
40
20
0
Hepatocyte like cells day 16
Hepg2
No primary Antibodies

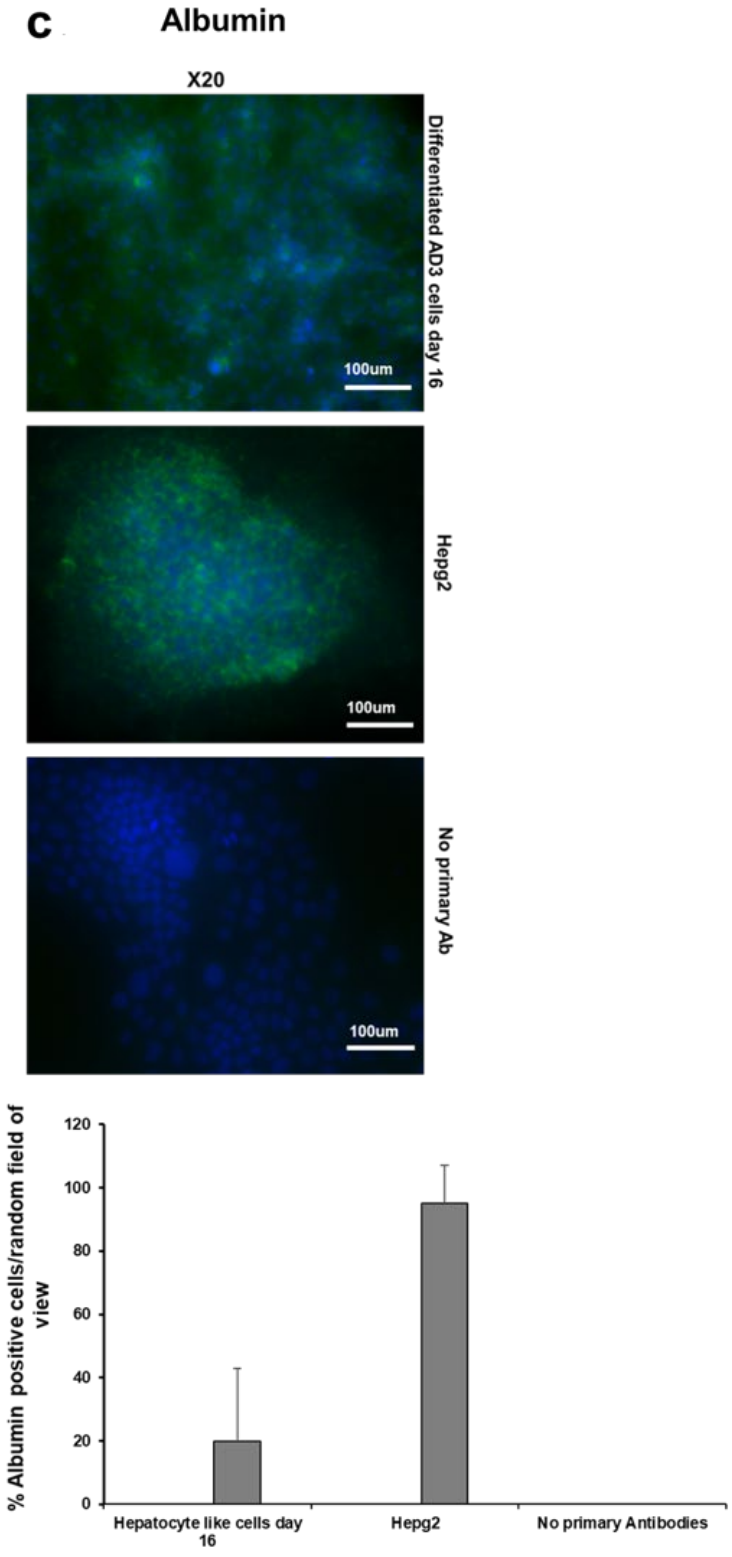

Figure 5.3 Initial protocol employed for iPSCs (AD3) differentiation into hepatocyte- like-cells. Confocal images of AD3 cells directed to differentiate into hepatocyte-like-cells: cells were fixed after 16 days of differentiation into hepatocyte-like-cells and examined alongside positive control cells for the expression of (A) CK19, (B) AFP and (C) Albumin. Data are mean and SD for at least 3 separate experiments. All images were taken under identical spectral conditions.

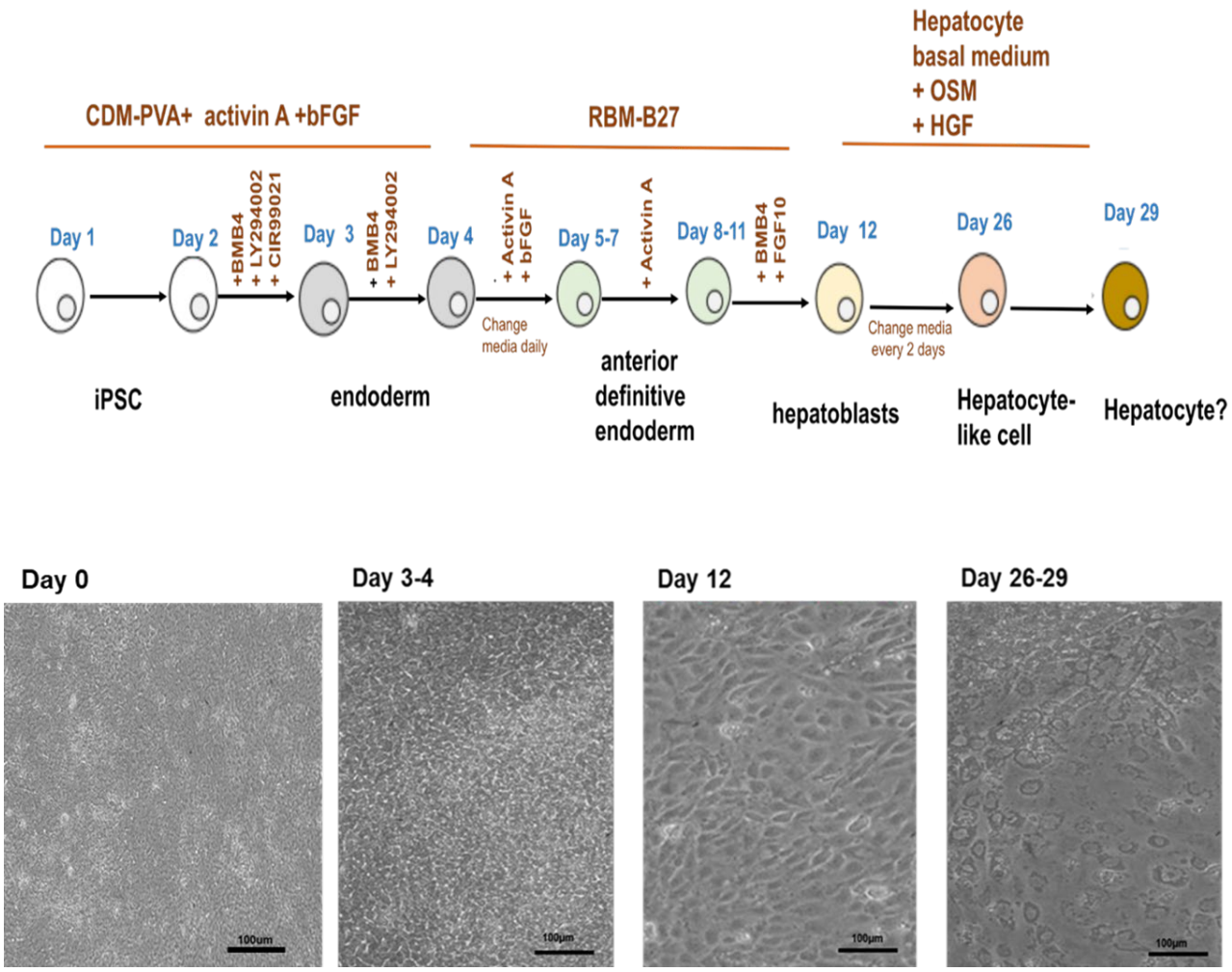

Figure 5.4 Final protocol employed to direct iPSCs toward hepatocyte-like cells. Schematic diagram depicting the protocol (Hannan et al., 2013) employed to direct iPSCs toward hepatocyte-like cells (upper panel). light micrographs of iPSCs at different stages – as indicated - of differentiation to hepatocyte-like cells. Results typical of 10 separate experiments.

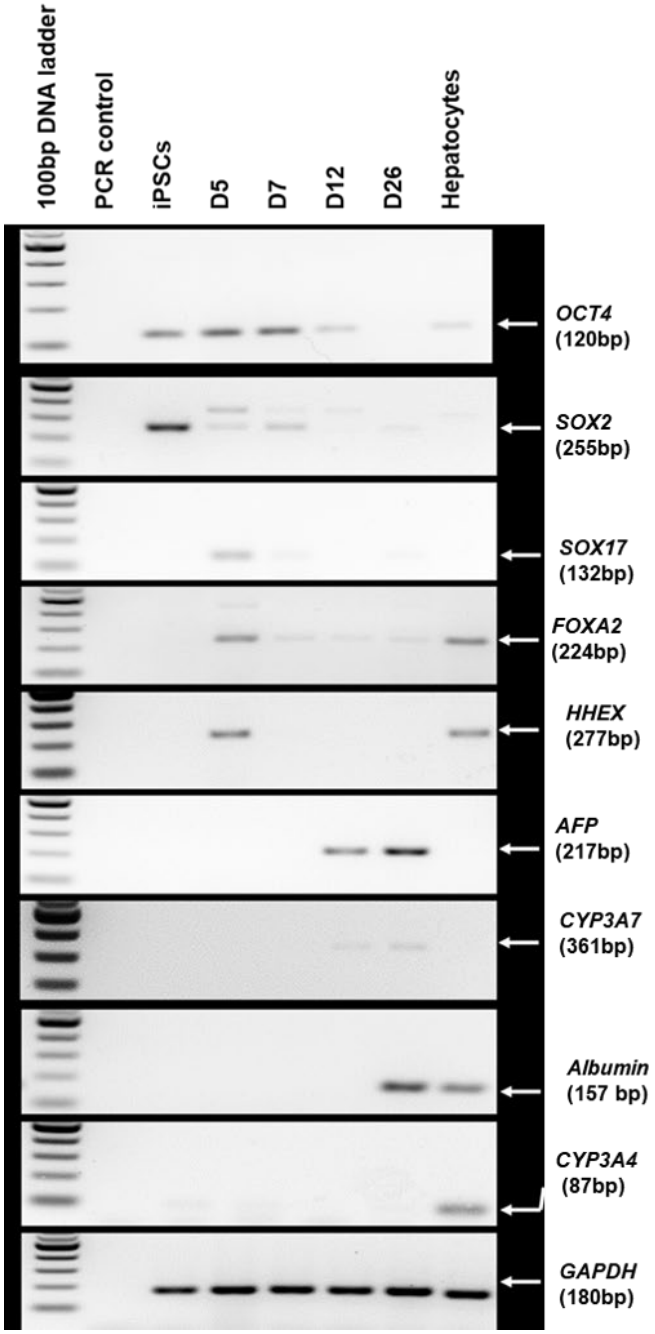

Figure 5.5 Final protocol employed to direct iPSCs toward hepatocyte-like cells. RT-PCR for selected transcripts in iPSCs at different stages of differentiation to hepatocyte-like cells. GAPDH was used as loading control. Results typical of 10 separate experiments.

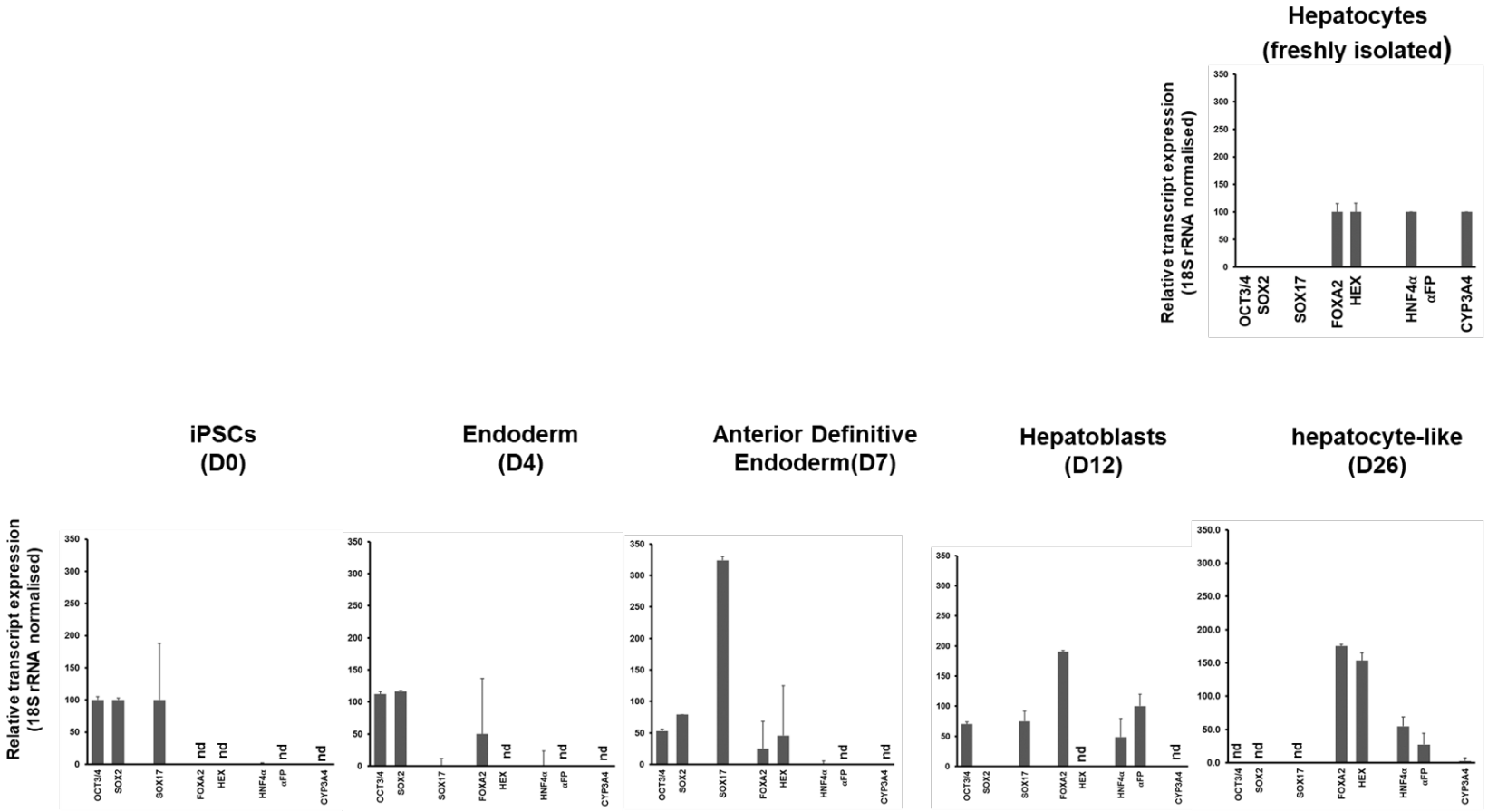

Figure 5.6 Q-RT-PCR for the progression of cultured AD3 cells toward hepatic lineages from day 1 to day 26. AD3 cells (iPSCs) were differentiated into hepatocyte-like cells for 26 days. qRTPCR results showed expression of (OCT4 and/or SOX2) at days 1-12. DE marker gene expression (SOX17) at day 1 and day 7. ADE markers (HEX and FOXA2) transcript levels were also detectable at day 7. Expression of hepatoblasts marker genes (AFP) was detected at day 12. After 26 days, pluripotency and endodermal markers are completely absent, AFP were diminished. hepatoblasts marker (AFP) and liver transcription factor HNF4α were detected with scarcely any detection of mature hepatocyte marker (CYP3A4). Data are represented as mean±standard deviation using ΔΔCt method.

5.3 Functionality of AdV-GFP, AdV-SGK1F in AD3 cells (iPSCs) at different stages of differentiation into hepatocyte-like-cells

In order to examine the efficiency of iPSCS derived hepatocytes infected with the adenovirus, hepatocyte-like-cells were subjected to the hepatocyte differentiation protocol outlined in the methods section and schematically described previously in Figure 5.4 . At day 1, cells were repeatedly infected with AdV-GFP at MOI 20. Limited trial and error suggested that that this approach gave the best infection rates whilst limiting losses in cell viability. Cells expressing GFP were determined by fluorescence microscopy from 3 randomly selected views up to 3 days later. Figure 5.7 demonstrates that infection of differentiating iPSCs (from day 1) at a MOI of 20 gave rise to low infection rates typically in the mean range of 7% by day 3. Infecting cells with AdV-SGK1F at day 1, when the cells are at a pluripotent/early transition to an endoderm stage of development resulted in low levels of expression of a protein immunoreactive to the mouse anti-SGK1 antibody (Figure 5.8). However, the size of this protein (~ 57 kDa) differed to the predicted size of the tagged SGK1F protein (48.9 kDa), the protein may be aberrantly modified post translationally (e.g. phosphorylation) which is a common issue with iPSCs. Also, the loading control protein (β-actin) is higher in the AdV-SGK1F infected sample, which could interfere with the detection of low levels of SGK1F. Increased total protein loading in this sample would help to obtain a clearer – more quantitative - SGK1F protein band.

Infecting cells with AdV-GFP at days 4-5, when the cells are transiting between the endodermal/anterior definitive endoderm stages of development at an MOI of 20 was able to give rise to infection rates typically in the mean range of approximately 70% by day 7, based on GFP expression (Figure 5.9). Infection with AdV-SGK1F during this period gave rise to the robust expression of a protein in the range of the predicted 48.9 kDa size for the tagged SGK1F protein (Figure 5.10). Infecting cells with AdV-GFP at day 26, when the cells are at the post-hepatoblast/foetal hepatocyte (hepatocyte-like) stage of development - at a MOI of 20 - was able to give rise to infection rates typically in the mean range of approximately 80% by day 29, based on GFP expression (Figure 5.11) and robust expression of the 48.9 kDa tagged SGK1F protein (Figure 5.12).

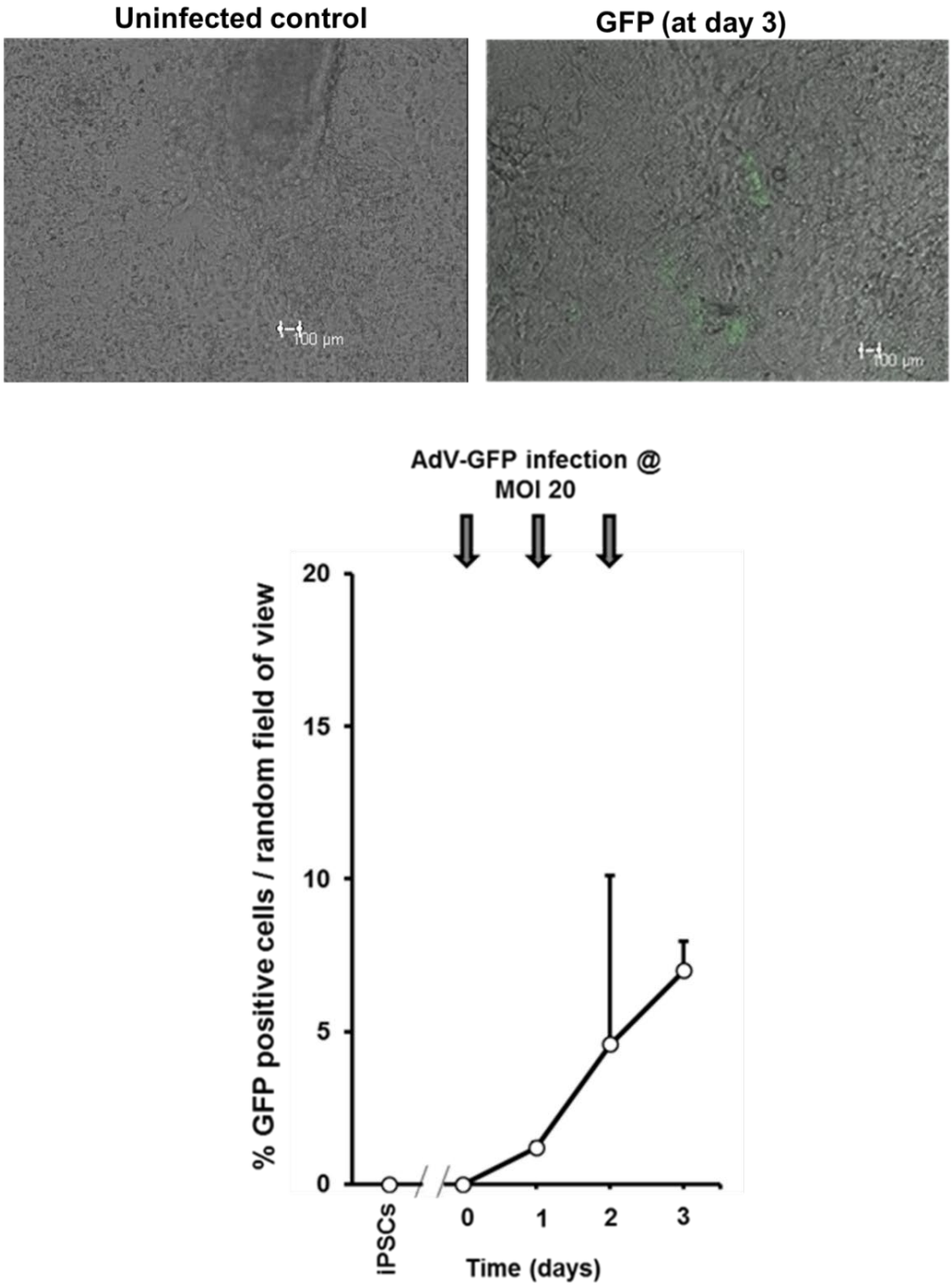

Figure 5.7 Early infection (at day 1) of iPSCs with AdV-GFP resulted in low infection rate. Effect of repeated infection of iPSCs after 1 day of differentiation with AdV-GFP on the expression of GFP. iPSCs were infected at a MOI of 20.0 and the mean percentage and SD of cells expressing GFP determined by fluorescence microscopy from 3 randomly selected views up to 3 days later. Typical views shown. Data typical of 3 separate experiments.

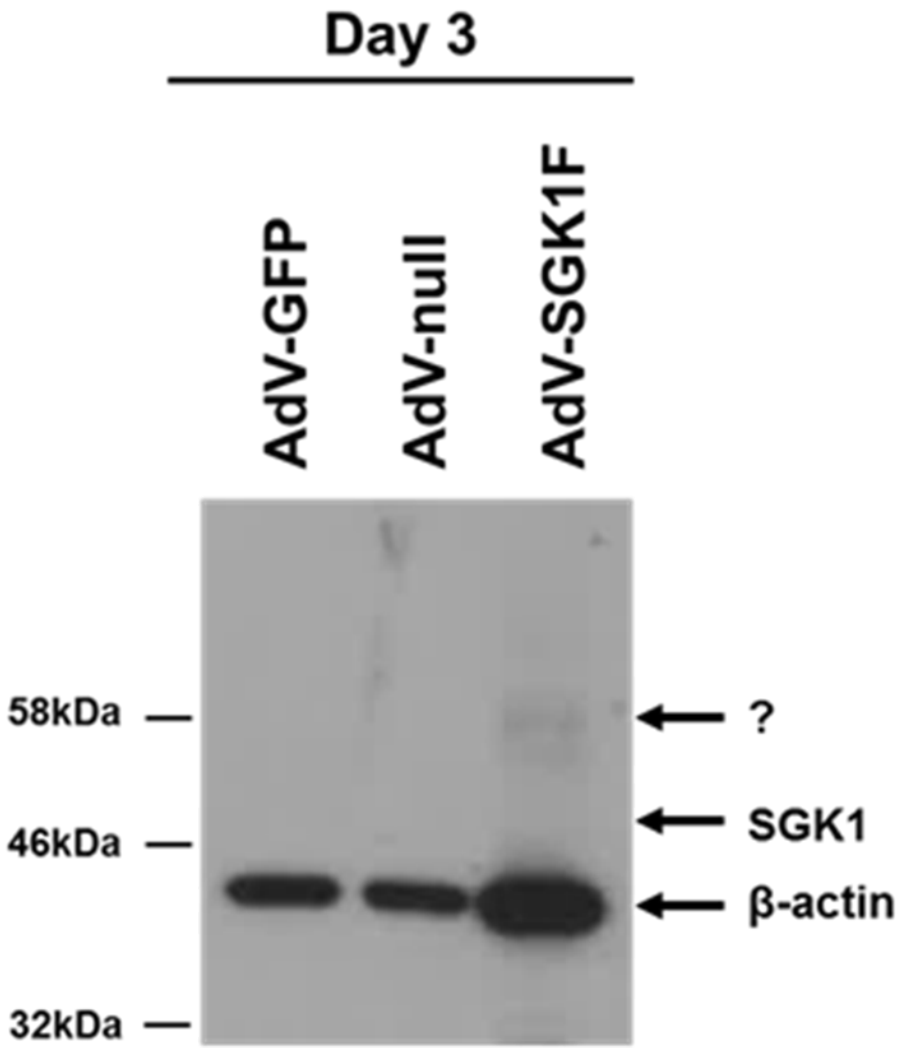

Figure 5.8 Early infection (at day 1) of iPSCs with AdV-SGK1F resulted in low levels of expression of SGK1F. Western blot analysed for the expression of flag tagged SGK1F followed by β-actin. Cells were repeatedly infected at day 0 at a MOI of 20.0 with the indicated AdV-SGK1F construct prior to harvest at day 3 and total cell protein analysis by Western blotting. Each lane contained a 20 μg protein/lane.β-actin was used as loading protein. Data typical of 3 separate experiments.

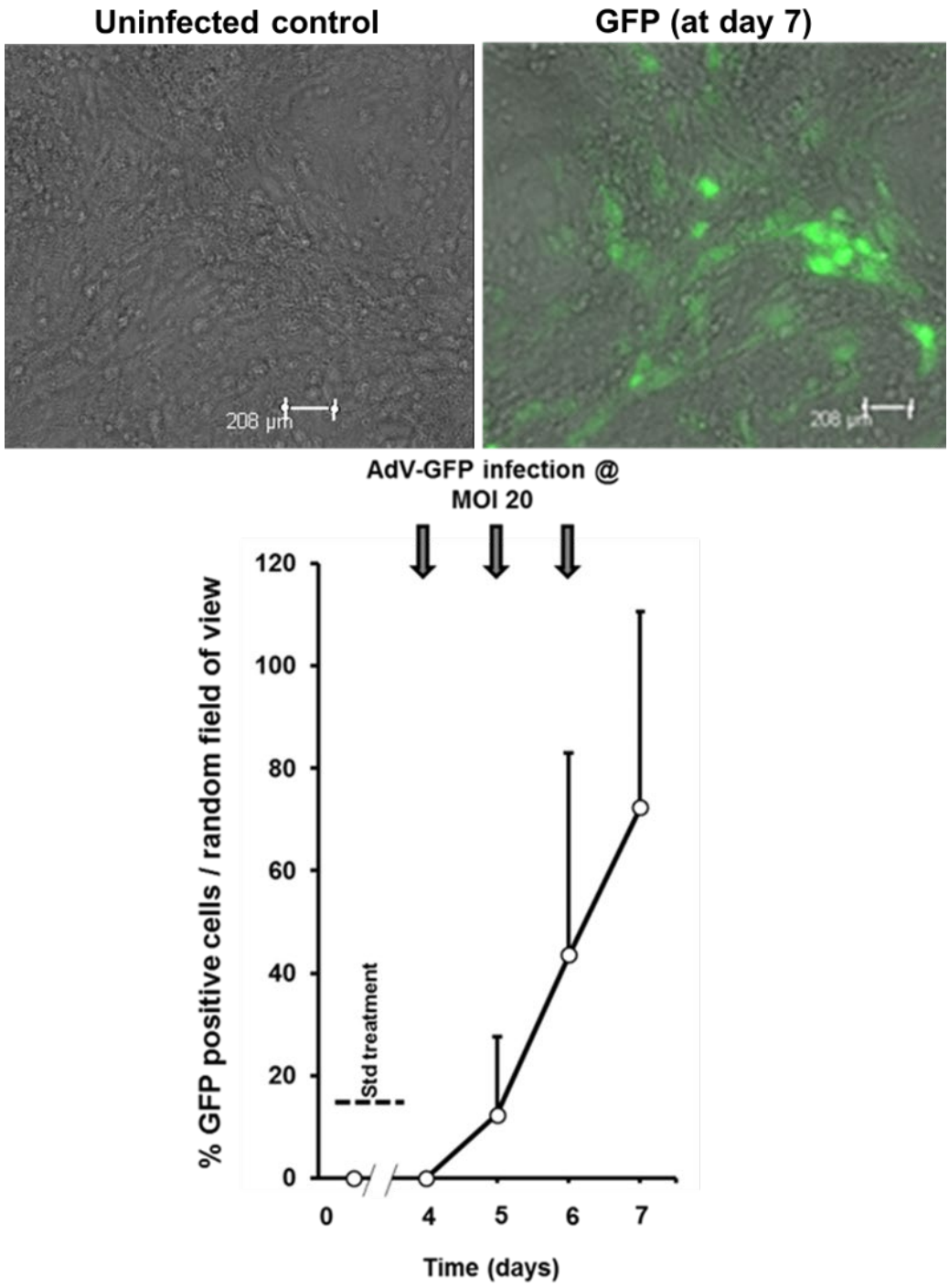

Figure 5.9 Infection of iPSCs at day 5 with AdV-GFP resulted in high infection rate. Effect of repeated infection of iPSCs after 5 days of differentiation with AdV-GFP on the percentage of cells expressing GFP at the indicated timepoints. iPSCs were infected at a MOI of 20 and the mean percentage and SD of cells expressing GFP determined by fluorescence microscopy from 3 randomly selected views (lower panel). Typical view shown in the upper panel. Data typical of 3 separate experiments.

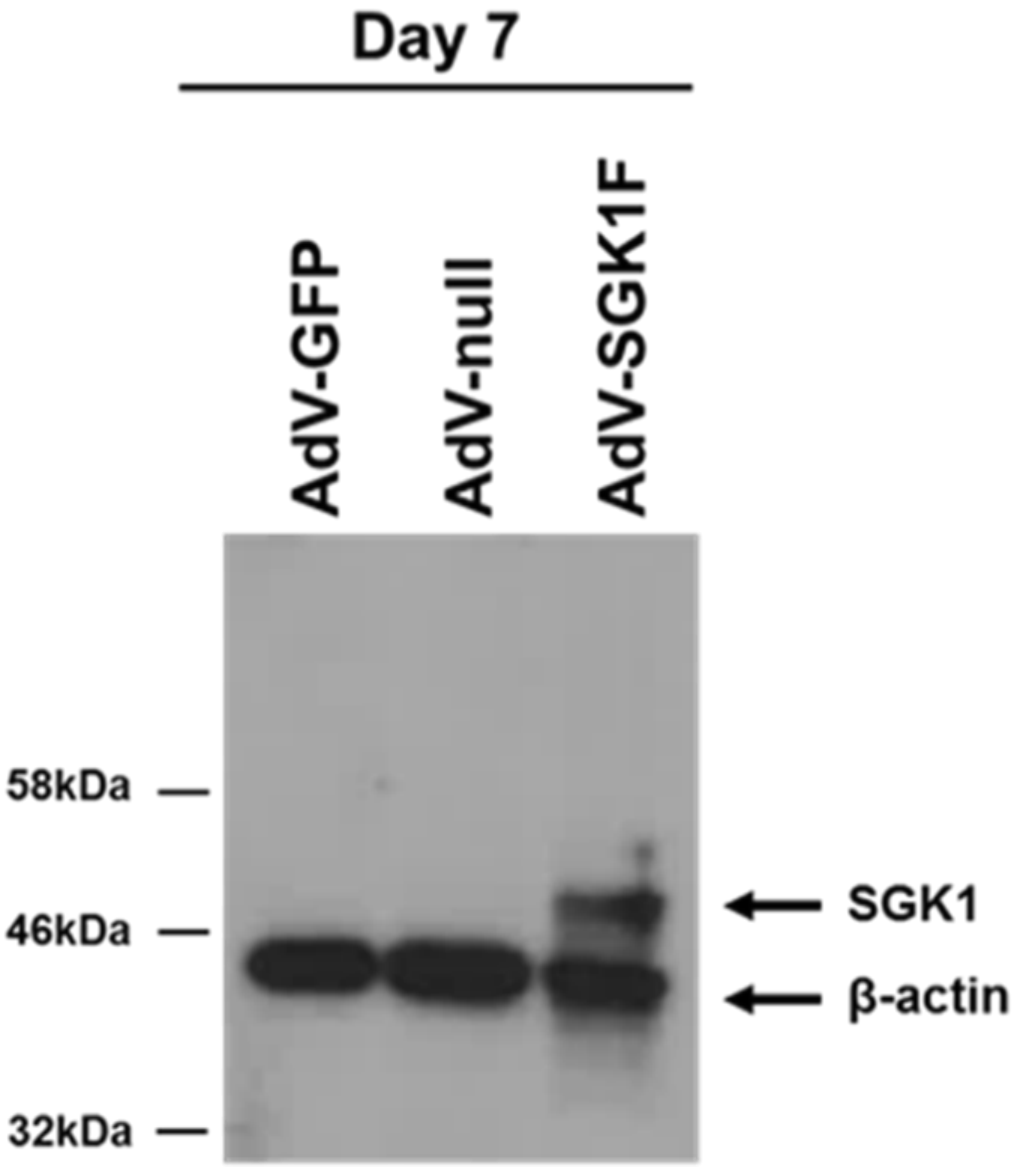

Figure 5.10 Infection of iPSCs at day 5 AdV-SGK1F resulted a robust SGK1F expression. Western blot analysed for the expression of flag tagged SGK1F followed by β-actin. Cells were repeatedly infected at day 4 at a MOI of 20.0 with the indicated AdV construct prior to harvest at day 7 and total cell protein analysis by Western blotting. Infection with AdV-SGK1F during this period (day5 to day 7)gave rise to the robust expression of a protein in the range of the

predicted 48.9 kDa size for the tagged SGK1F protein. Each lane contained a 20 µg protein/lane. β-actin was used as loading protein Data typical of 3 separate experiments.

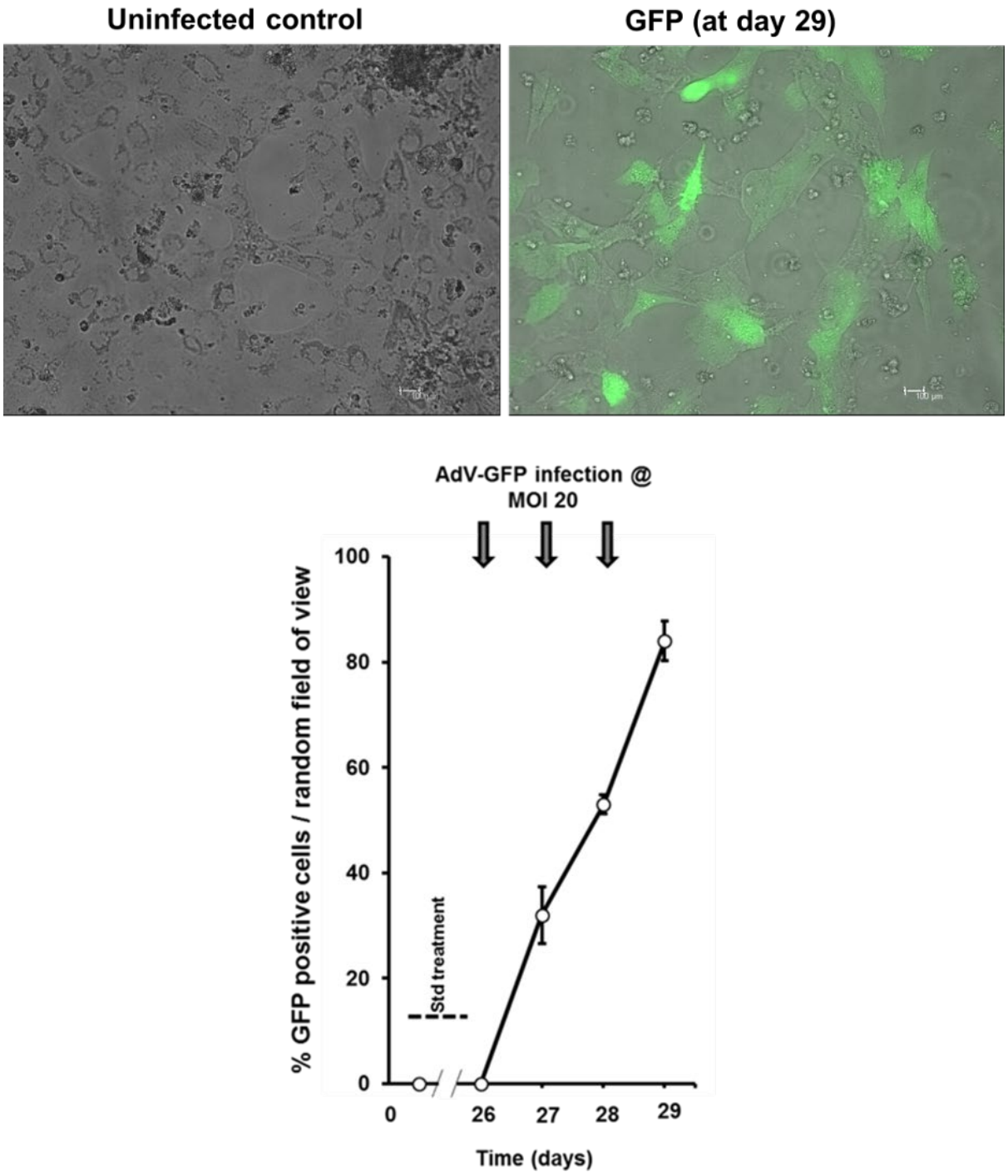

Figure 5.11 Infection of iPSCs at day 26 with AdV-GFP resulted in a high infection rate. Effect of repeated infection of iPSCs after 26 days of differentiation with AdV-GFP on the percentage of cells expressing GFP at the indicated timepoints. iPSC-derived hepatocytes were infected at a MOI of 20 and the mean percentage and SD of cells expressing GFP determined

by fluorescence microscopy from 3 randomly selected views (lower panel). Typical views shown in the upper panel. Data typical of 3 separate experiments.

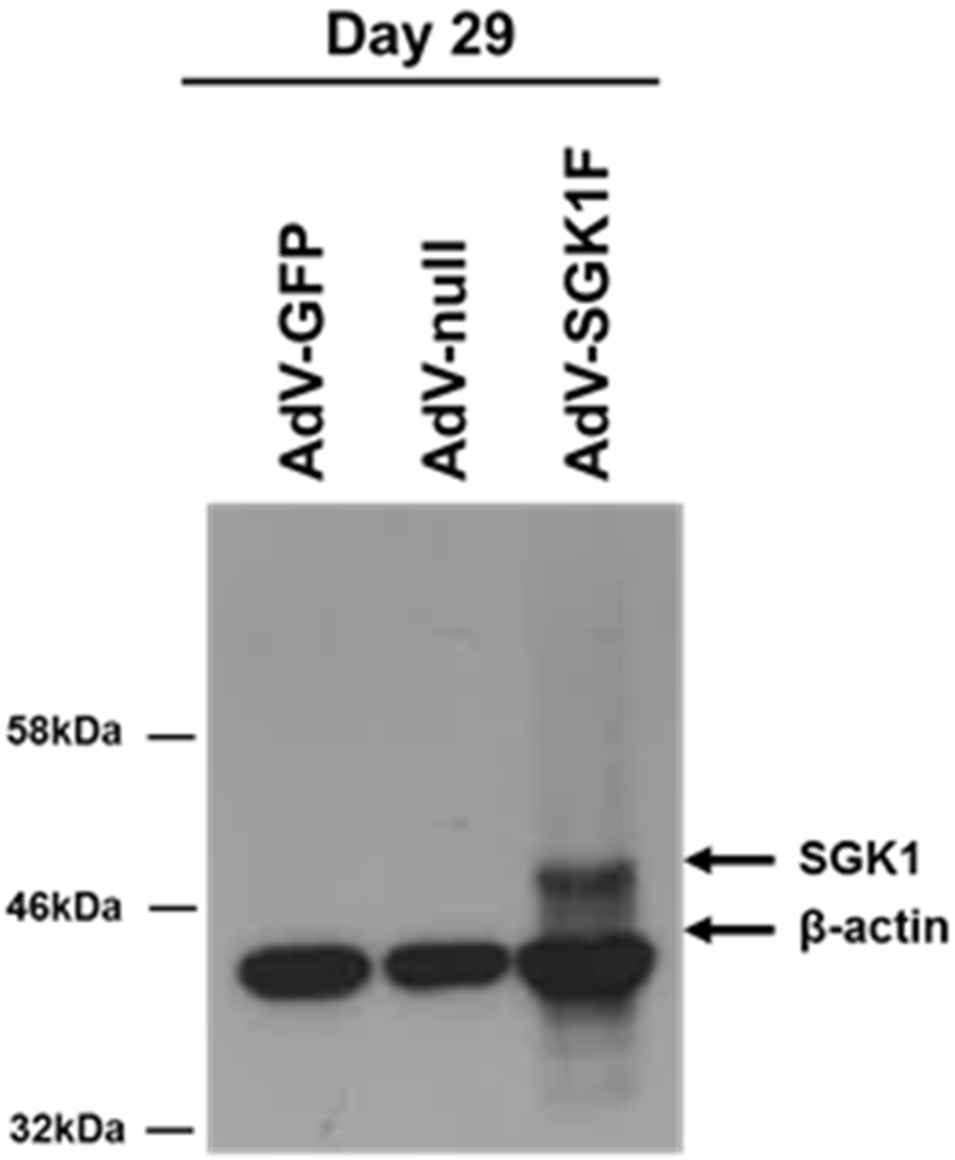

Figure 5.12 Infection of iPSCs at day 26 with AdV-SGK1F resulted in a robust SGK1F expression. Western blot analysed for the expression of flag tagged SGK1F followed by β-actin. Cells were repeatedly infected at day 26 at a MOI of 20.0 with the indicated AdV construct prior to harvest at day 29 and total cell protein analysis by Western blotting. Each lane contained a 20 μg protein/lane. β-actin was used as loading protein. Data typical of 3 separate experiments.

5.4 d SGK1 activity in hepatocyte-like-cells

To examine SGK1 activity in hepatocyte-like-cells, the SGK1F was expressed in hepatocyte-like-cells. Cells infected with AdV-SGK1F at an MOI 20 with AdV-SGK1F and AdV-GFP form day16 for 3days. Cell lysates and RNA were made from time 0, 24h, 48h, and 72h. RT-PCR was performed for SGK1 transcripts (A, B, C, D, F). As shown in Figure 5.13 SGK 1c expression was detected in cells infected with AdV-SGK1F for 24 h and SGK1F expressed by cells infected with AdV-SGK1F. Furthermore, a 500ng/ml concentration of protein was prepared from the cells lysate. After incubating the sample with 100 μM ATP and 1mg/ml AKT substrate, SGK1 activity versus the times cultured with MO 20 of AdV-SGK1F was measured using the ADP-Glo Kinase Assay that measures ADP formed from the kinase reaction; ADP is converted into ATP, which is converted into light by Ultra-Glo Luciferase. The luminescent signal is significantly different from the time zero infected cells, as can be seen from Figure 5.14. However, increased SGK1 activity was observed in AdV-GFP infected cells too.

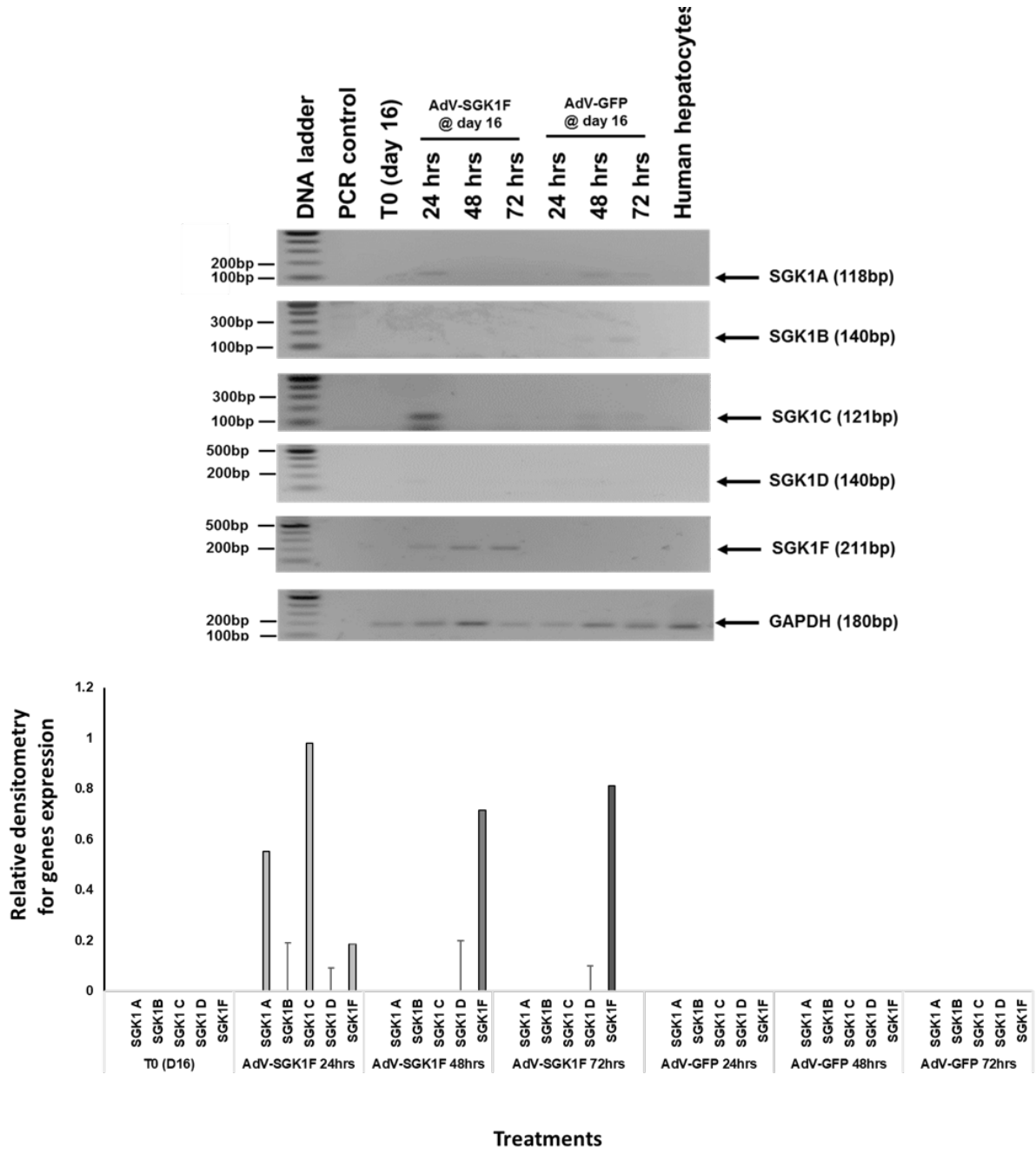

Figure 5.13 Expression of different SGK isoforms after repeated infection with AdV-SGK1F and AdV-GFP and its effect on SGK activity. Transcript expression: iPSCs were infected repeatedly at a MOI of 20.0 with AdV-SGK1F and AdV-GFP at day 16 of differentiation for 72 hours. RNA were isolated after 24 h, 48 h and 72 h and RT-PCR was performed to detect the indicated SGK1 isoforms. GAPDH was used as loading control. Agarose gel image (upper panel) was quantified using ImageJ software, GAPDH normailsed (lower panel). Data are similar for 3 separate experiments.

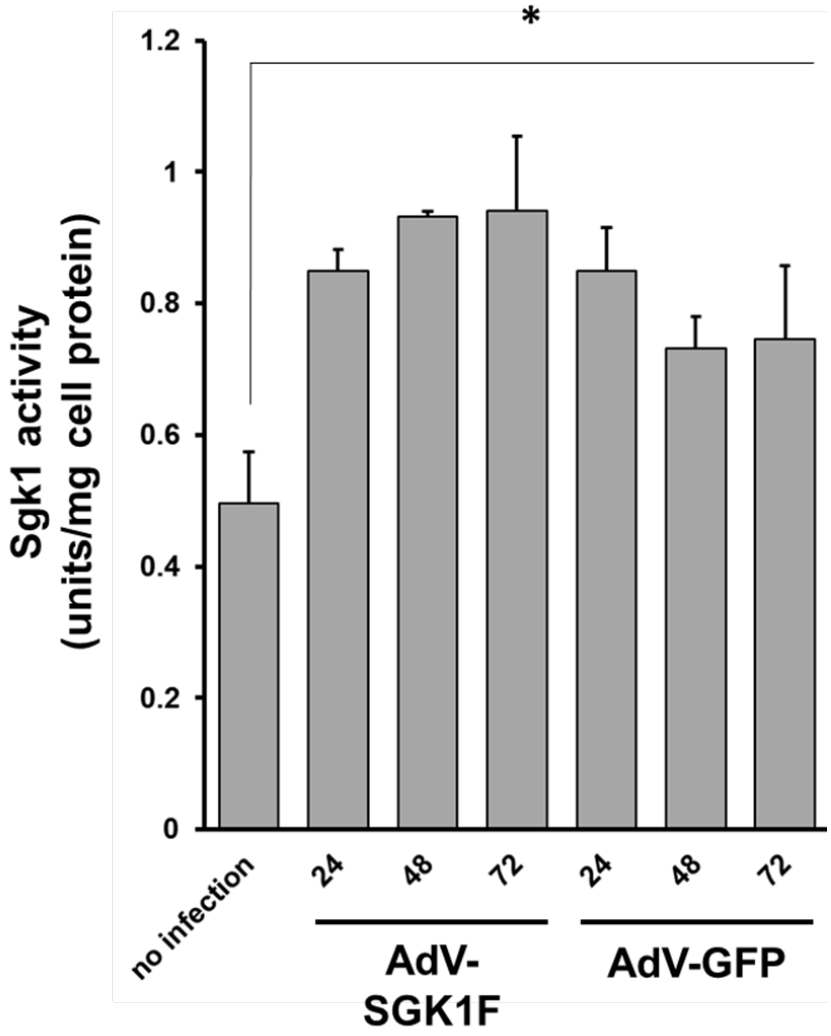

Figure 5.14 Repeated infection with AdV-SGK1F and AdV-GFP and its effect on SGK activity. SGK1 kinase activity: iPSCs were infected repeatedly at a MOI of 20.0 with AdV-SGK1F and AdV-GFP at day 16 of differentiation for 72 hours. Cells lysates was prepared from cells cultures after 24 hours, 48 hours and 72 hours and SGK1 kinase activity determined in cell extracts, as outlined in the methods section. Data are similar for 3 separate experiments. Significantly different results (*= $P < 0.05$) determined using the one way Anova test followed by the post-hoc test.

5.5 Expression of SGK1F promotes a hepatoblast state in stem cells directed to differentiate into hepatocytes

To test whether SGK1F over-expression at different differentiation stages has an effect on the maturity of iPSCs directed to hepatocyte-like cells. The hepatocyte differentiation protocol described previously was employed and the differentiating iPSCs were infected with AdV-SGK1F and AdV-null (at an MOI of 20) from day 1 when the cells are at a pluripotent/early transition to an endoderm stage of development, at day 5 when the cells are transiting between endodermal/anterior definitive endoderm stages of development and at day 26 when the cells are at the post-hepatoblast/foetal hepatocyte (hepatocyte-like) stage of development (Figure 5.15.A). RNA was isolated from AdV-SGK1F and AdV-null infected cells for qRT-PCR analysis, in addition to freshly isolated human liver which was used as a control. The RNA concentrations were quantified by Nanodrop spectrophotometer. Additionally, cDNA synthesised from 5 ng of total RNA was mixed with TaqMan Universal PCR Master Mix (Applied Biosystems) and a gene specific primer and probe mixture (predeveloped TaqMan Gene Expression Assays, Applied Biosystems) in a final volume of 20 µl was used. The probe sets used were designed to specifically amplify regions of the cDNAs for OCT4, SOX2, FOXA2, HEX, SOX17, HNF4α AFP, CYP3A7, Albumin, CPS1, CYP1A2 and CYP3A4). All samples were run in triplicate. The mRNA concentrations of specific genes were expressed in arbitrary units and normalised to the mean of 18s ribosomal RNA concentrations to correct the differences in cDNA loading.

The extent of the differentiation of AdV-SGK1F infected cells was compared to AdV-null infected cells. Figure 5.15B indicates that the SGK1F expression resulted in no significant changes in any transcript level (when compared to the AdV-null control) after 3 days of infection at the early stage of differentiation (day 1). These data suggest that early expression of SGK1F in iPSCs directed to differentiate into endoderm does not promote progression to endodermal cells, either because of low rates of infection (resulting in low levels of expression as demonstrated in Figure 5.8 in Section 5.3) or because any expressed protein is rapidly degraded.

The relative expression of hepatoblasts markers (AFP and CYP3A7) and mature hepatocyte markers (CPS1, ALB, CYPA1A2 and CYP3A4) after 7 day is shown in Figure 5.15 C which illustrates that SGK1F expression significantly increased hepatoblast transcript. This result suggests that the expression of SGK1F in iPSCs-derived endoderm directed to differentiate into anterior definitive endoderm and hepatoblasts results in promotion to an hepatoblast phenotype.

The relative expression of hepatoblast markers (AFP, CYP3A7) and mature hepatocyte (CPSI, albumin, CYP1A2 and CYP3A4) at day 29 showed in Figure 5.15D. This figure indicates SGK1F expression significantly increased the hepatoblast transcripts AFP and CYP3A7. In addition, there was a significant decrease in the mature transcript albumin and a tendency – though not significantly – for a reduction in CPSI transcripts. In contrast, the adult mature hepatocyte transcripts such as *CYP1A2* and *CYP3A4* were not reliably detectable in iPSC-derived hepatocyte-like cells (Figure 5.15D). Notably, SGK1F expression did not promote a more mature phenotype in hepatoblasts directed to differentiate towards a mature hepatocyte phenotype.

These data suggest that expression of SGK1F in iPSCs differentiating toward hepatocyte-like cells promotes a reversal to an hepatoblast phenotype.

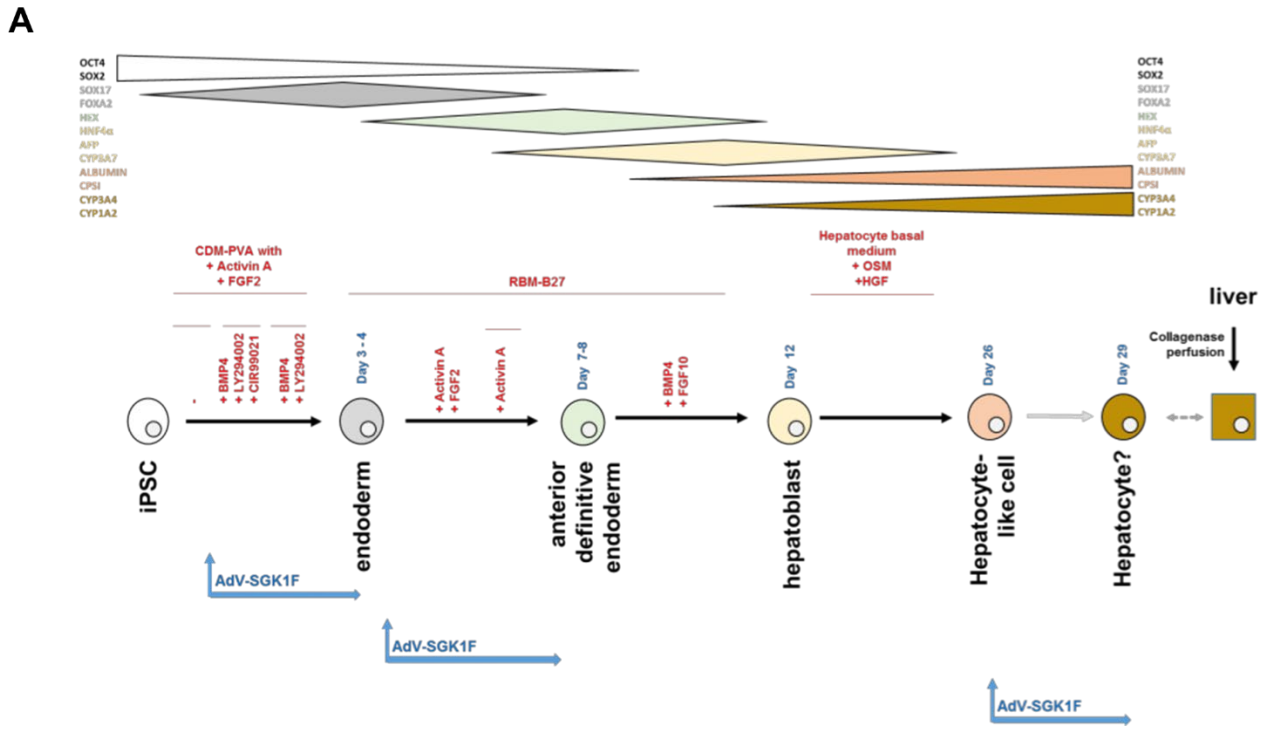

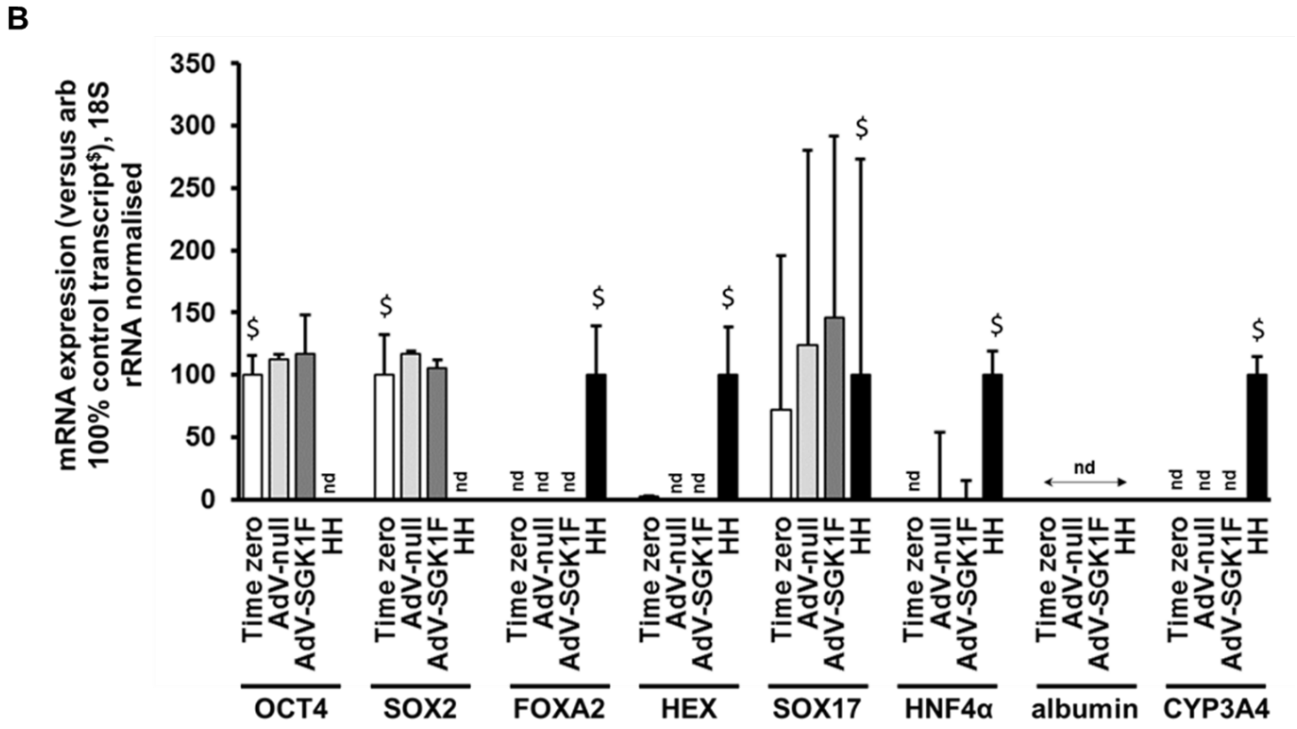
B
mRNA expression (versus arb 100% control transcript$), 18S rRNA normalised
350
300
250
200
150
100
50
0
$
nd
Time zero
AdV-null
AdV-SGK1F
HH
OCT4
SOX2
FOXA2
HEX
SOX17
HNF4α
albumin
CYP3A4

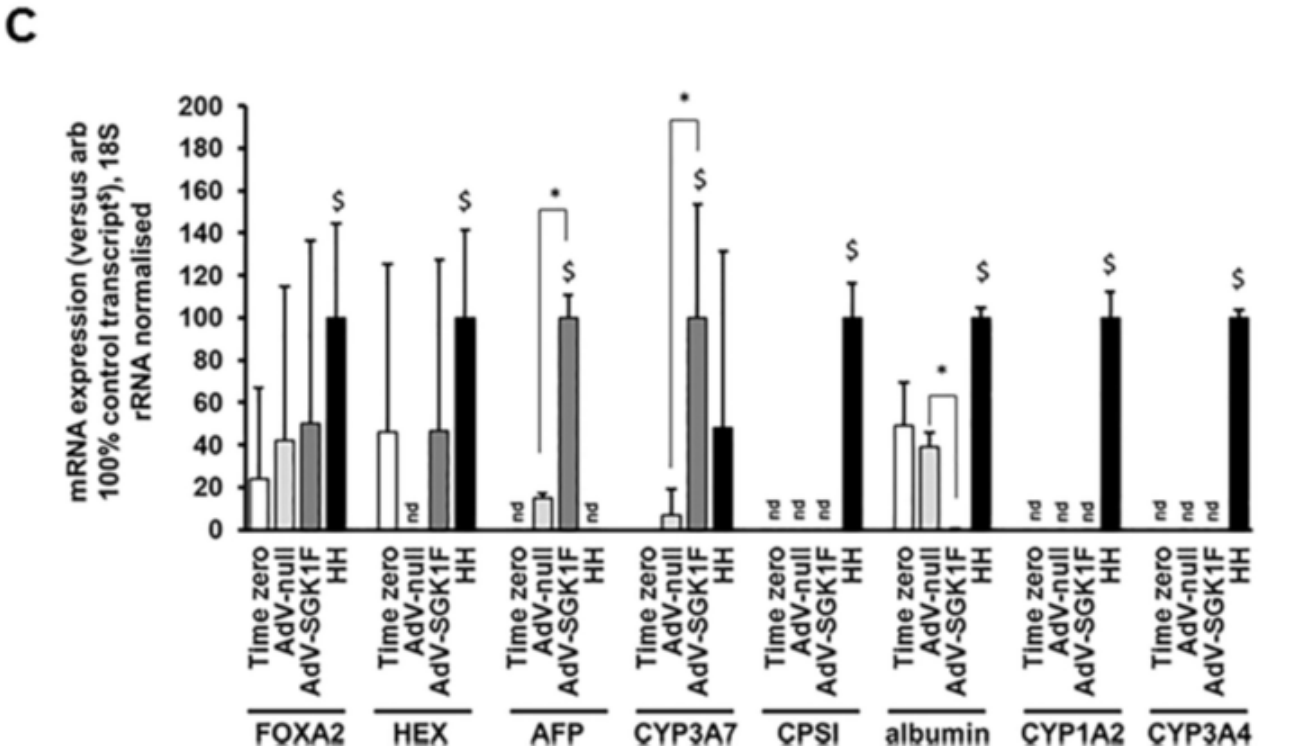
C
mRNA expression (versus arb 100% control transcript$), 18S rRNA normalised
200
180
160
140
120
100
80
60
40
20
0
*
$
nd
Time zero
AdV-null
AdV-SGK1F
HH
FOXA2
HEX
AFP
CYP3A7
CPSI
albumin
CYP1A2
CYP3A4

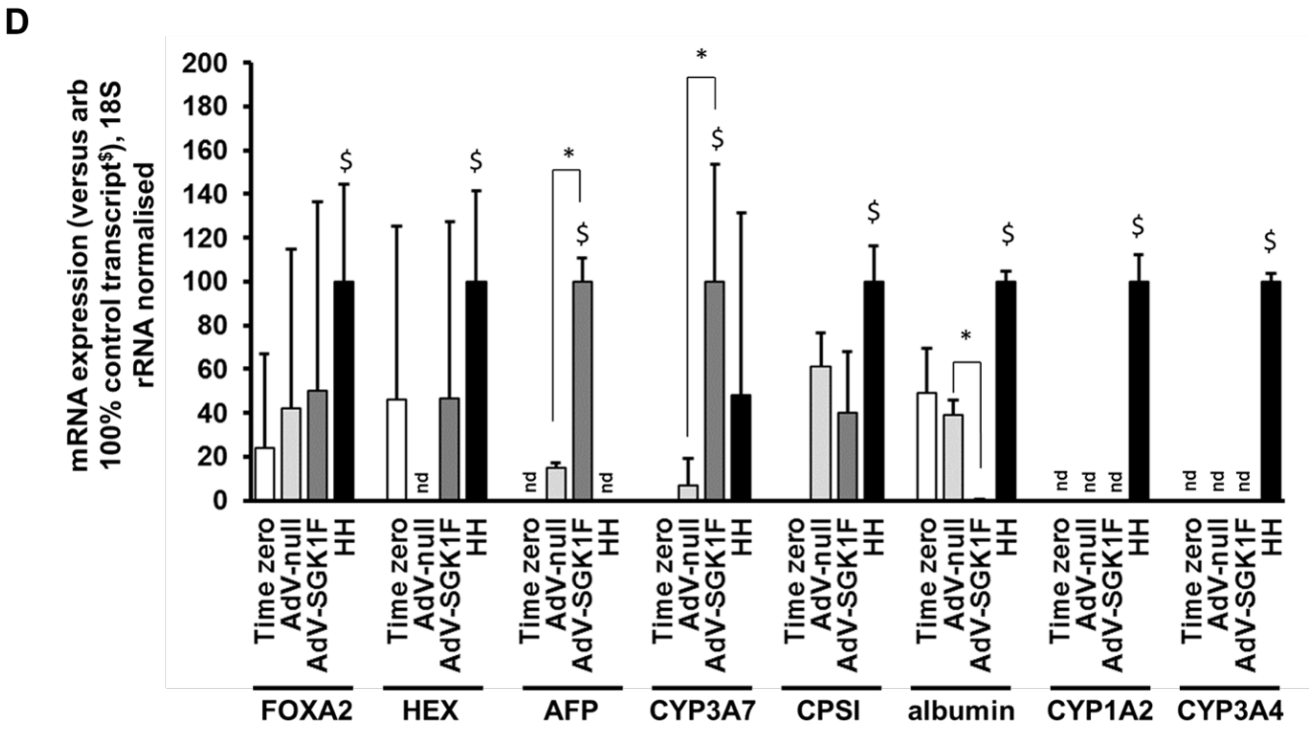

Figure 5.15 Adenoviral-mediated expression of SGK1F promotes an hepatoblast state in stem cells directed to differentiate into hepatocytes. **A**: schematic diagram depicting the protocol (Hannan et al., 2013) employed to direct iPSCs toward hepatocyte-like cells and the AdV-SGK1F infection stages. **B**: Early expression of SGK1F in iPSCs directed to differentiate into endoderm has no effect on progression to endodermal cells. Transcript expression. iPSCs after 1 day of differentiation were infected with the indicated AdV before total RNA was isolated at day 3 and transcript expression determined by qRT-PCR, as outlined in the methods section. Data are typical of 3 separate experiments. **C**: Expression of SGK1F in iPSCs-derived endoderm directed to differentiate into hepatoblasts promotes a hepatoblast phenotype. Transcript expression. iPSCs after 5 days of differentiation were infected with the indicated AdV before total RNA was isolated at day 8 and transcript expression determined by qRT-PCR as outlined in the methods section. Data are typical of 3 separate experiments. **D**: Expression of SGK1F in iPSC-derived hepatocytes results in promotion back to a hepatoblast phenotype. Transcript expression. iPSC-derived hepatocytes after 26 days of differentiation were infected with the indicated AdV before total RNA was isolated at day 29 and transcript expression determined by qRT-PCR, as outlined in the methods section. Data are typical of 3 separate experiments. Statistically significant differences were determined by the Student's 2-tailed t-test.

5.6 Adult human hepatocytes efficiently infected with AdV-GFP and AdV-hSGK1F

Human hepatocytes (HH) were isolated from a 60 year old male donor by collagenase perfusion (performed at the Freeman Hospital by colleagues in the Wright lab) and collagen coated 6 well plates of HH were obtained in order to examine the efficiency of HH infection with the adenovirus, HH infected repeatedly from day one of isolation with AdV-GFP at MOI 20 HH cells were found amenable to adenoviral infection based on infection with AdV-GFP, an approximate MOI of 20 resulted in high infection rates > 80 % by day 3 (Figure 5.16). Moreover, after 5 days of infection with AdV-SGK1F MOI 20, high level expression of the 48.9 kDa tagged SGK1F protein detected by Western blotting in AdV-SGK1F infected cells only in comparison to AdV-null and time zero cells (Figure 5.17).

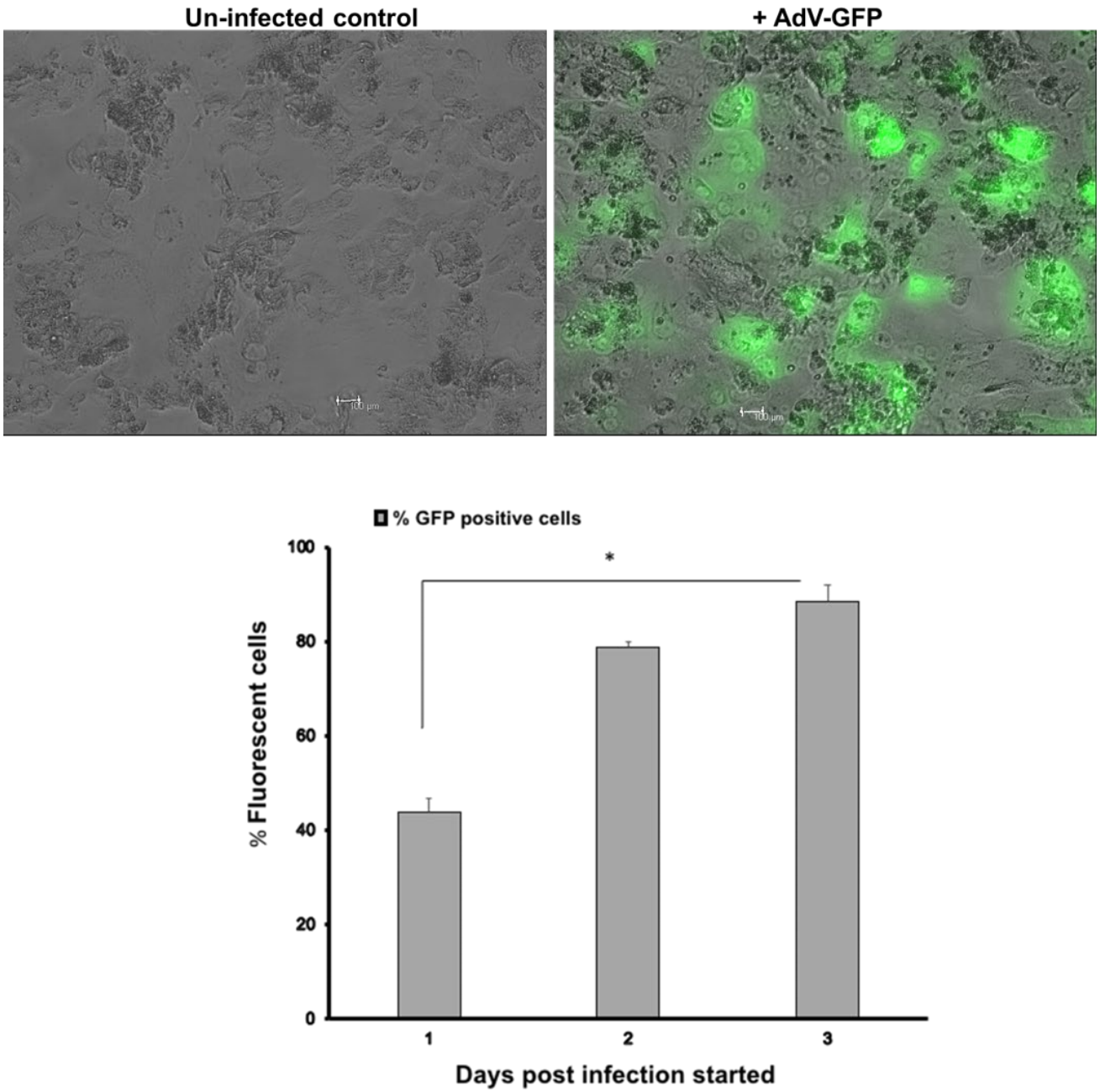

Figure 5.16 Adult human hepatocytes efficiently infected with AdV-GFP. Effect of repeated infection of adult human hepatocytes (HH) with AdV-GFP on the expression of GFP. HH were infected at a MOI of 20.0 on day 1 of isolation and the mean percentage and SD of cells expressing GFP determined by fluorescence microscopy from 3 randomly selected views up to 3 days later (lower panel). Typical views shown in the upper panel. Significantly different results (*= $P< 0.05$) determined using the one way Anova test followed by the post-hoc test. Data typical of 3 separate experiments (n=1).

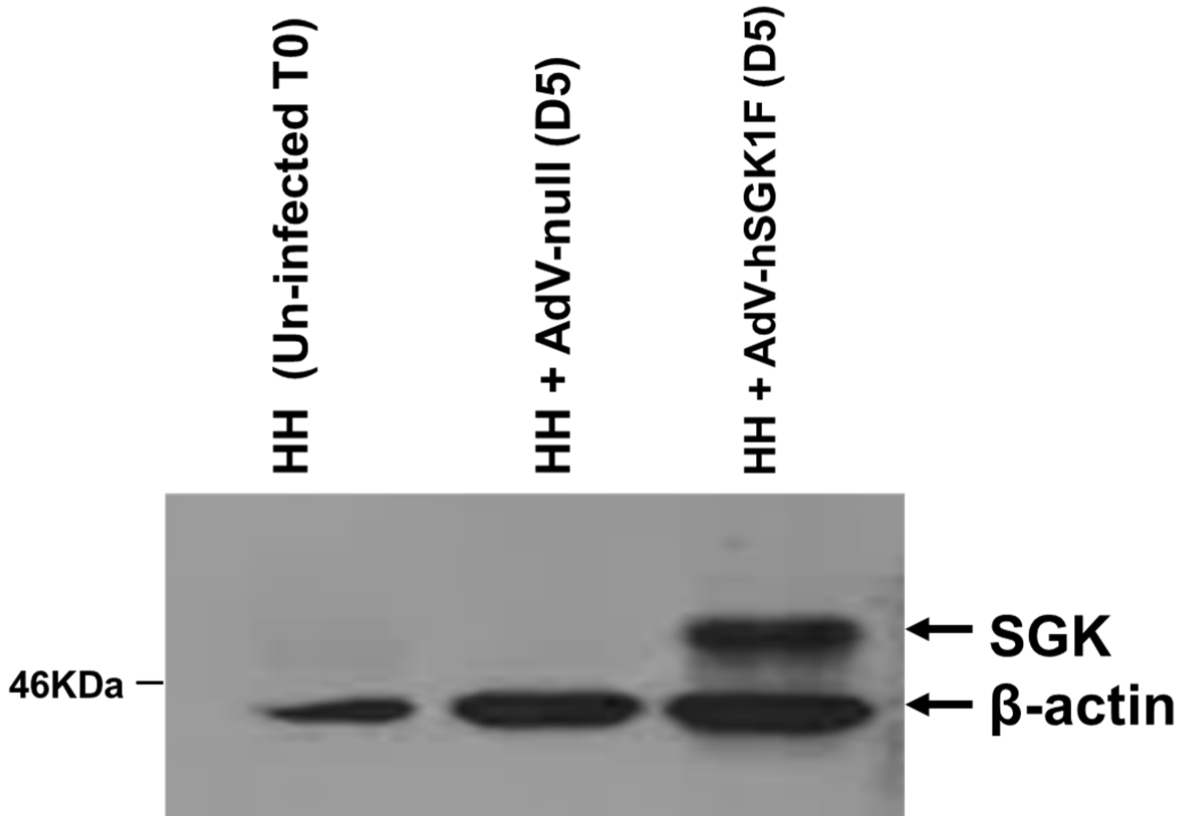

Figure 5.17 Adult human hepatocytes efficiently infected with AdV-SGK1F. Western blot analysed for the expression of flag tagged SGK1F followed by β-actin. Cells were repeatedly infected at day 1 at a MOI of 20.0 with the indicated AdV construct prior to harvest at day 5 and total cell protein analysis by Western blotting. Each lane contained a 20 μg protein/lane. Data typical of 3 separate experiments (n=1).

5.7 Expression of SGK1F did not promote mature adult hepatocyte reversal into a hepatoblast phenotype.

In order to investigate the effect of adenovirus mediated SGK1F gene expression on HH de-differentiation, cells were infected with AdV-SGK1F at a MOI 20 and AdV-null at a MOI 20. After 5 days, RNA was isolated from AdV-SGK1F and AdV-null infected cells in addition to freshly isolated HH (day 1) for qRT-PCR analysis. The RNA concentrations were quantified by Nanodrop spectrophotometer. cDNA synthesised from 5 ng of total RNA was mixed with TaqMan Universal PCR Master Mix (Applied Biosystems) and a gene specific primer and probe mixture (predeveloped TaqMan Gene Expression Assays, Applied Biosystems) in a final volume of 20 μl used. The probe sets used were designed to specifically amplify regions of the

cDNAs for *FOXA2*, *HEX*, *AFP*, *CYP3A7*, *CPS1*, *ALBUMIN*, *CYP1A2* and *CYP3A4*. All samples were run in triplicate (technical replicates). The mRNA concentrations of specific genes were expressed in arbitrary units and normalised to the mean 18s ribosomal RNA concentrations to correct for differences in cDNA loading. qRT-PCR results shown in Figure 5.18.A, B and C, indicate that SGK1F expression resulted in no significant changes in any transcript level (when compared to AdV-null control). These data suggest that the expression of SGK1F in HH did not promote the dedifferentiation of mature human hepatocytes into an hepatoblast phenotype.

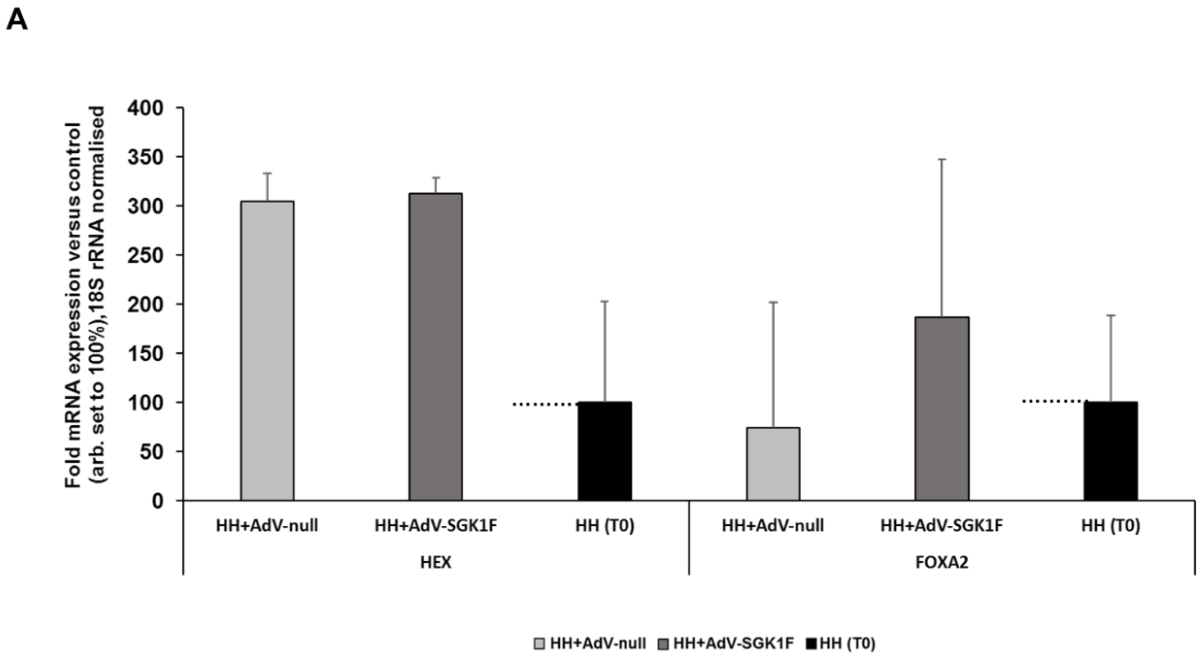

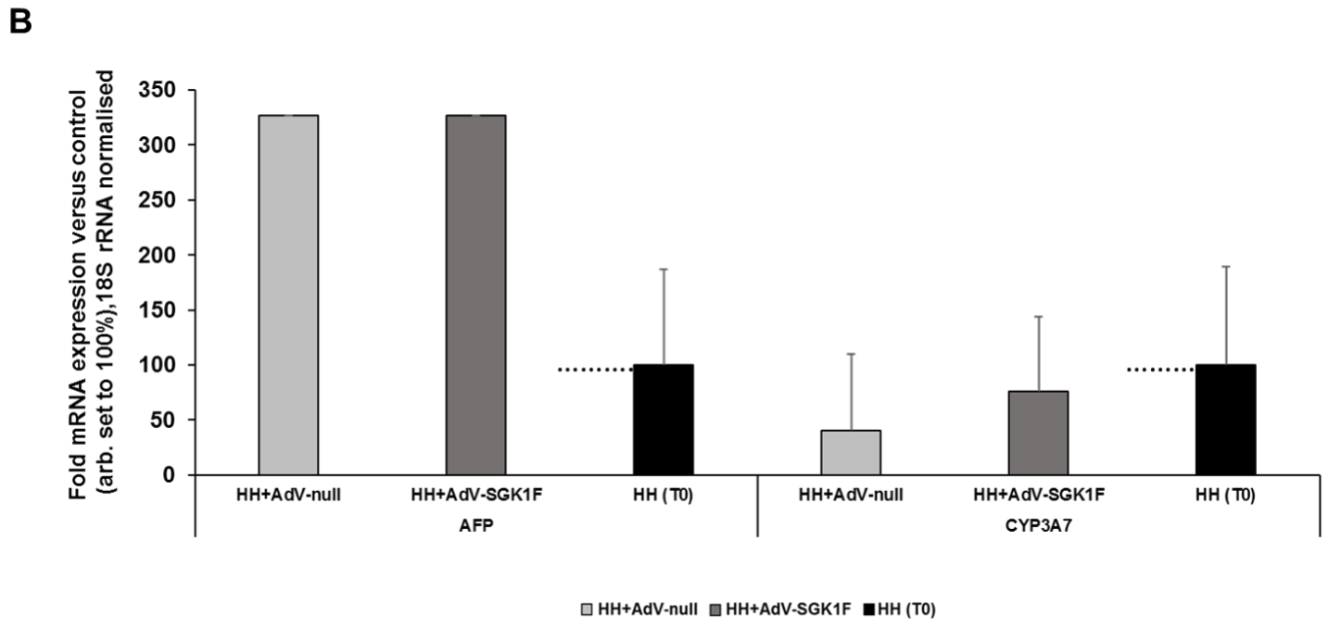

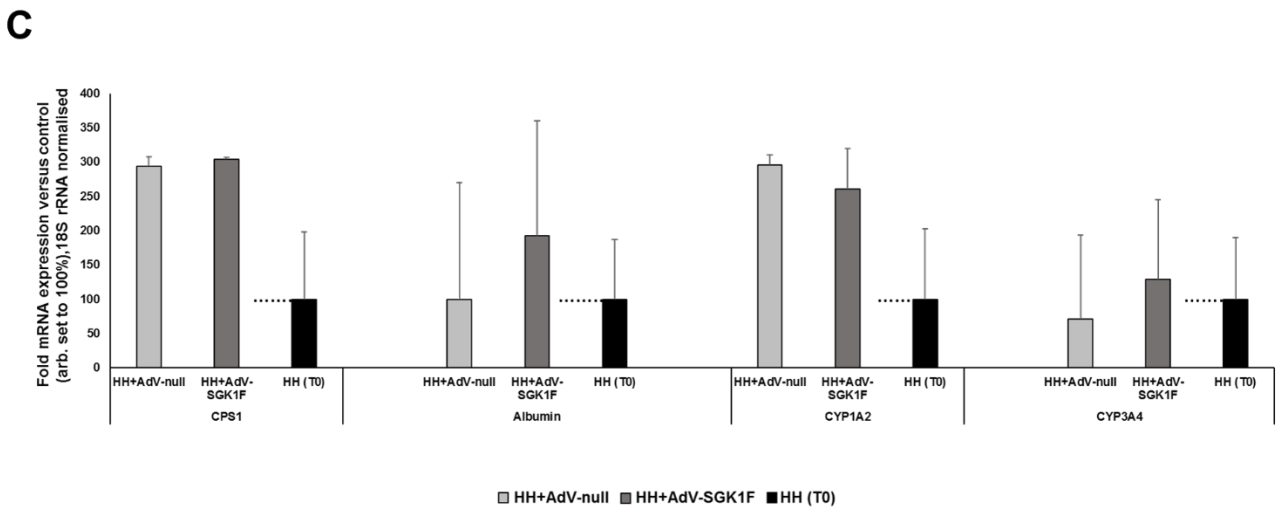

Figure 5.18 Adenoviral mediated expression of SGK1F did not result in a significant effect on HH transcripts levels. **A**: Expression of SGK1F did not promote significant changes in HEX and FOXA2 expression levels in adult hepatocyte. HH after 1 day of isolation were infected at a MOI of 20.0 with the indicated AdV before total RNA isolated at day 5 and transcript expression determined by qRT-PCR, as outlined in the methods section. Data are typical of 3 separate experiments. **B**: expression of SGK1F did not promote significant changes in AFP and CYP3A7 expression levels in adult hepatocyte. HH after 1 day of isolation were infected at a MOI of 20.0 with the indicated AdV before total RNA was isolated at day 5 and transcript expression determined by qRT-PCR, as outlined in the methods section. Data are typical of 3 separate experiments. **C**: expression of SGK1F did not promote significant changes in the expression levels of mature liver marker genes in adult hepatocyte. HH after 1 day of isolation were infected at a MOI of 20 with the indicated AdV before total RNA isolated at day 5 and transcript expression determined by qRT-PCR, as outlined in the methods section. The mRNA concentrations of specific genes were expressed in arbitrary units and normalised to the mean 18s ribosomal RNA concentrations Dotted lines indicate the level of time zero control sample (HH) used for results normalization. Data presented using the ΔΔCt methodology are typical of 3 separate experiments (technical replicates).

5.8 Addition of 1μM Dexamethasone to the initial protocol enhanced hepatic phenotype in iPSC-derived hepatocytes

To determine whether glucocorticoid affects the maturation of iPSCs into hepatocytes, AD3 cells where differentiated using the standard protocol with the addition of 1μM DEX at day 12. AD3 cells were differentiated over 26 days using three different protocols: the previously used standard protocol (a combination 30ng/ml OSM and 50ng/ml HGF), the amended protocols (a combination of 1μMDEX, 50ng/ml HGF and 30ng/ml OSM) and only 1μM DEX. Additionally, mRNA was isolated from cells treated with different treatments at day 26 in addition to AD3 cells at days 1, 5, 12 and 16 of the differentiation into hepatocyte-like-cells employing the standard protocol. RNA was purified and RT-PCR was performed. The results show a change

in the cell morphology, passing from colonies of small round cells with a high nuclear to cytoplasm ratio into individual large cells with a low nuclear to cytoplasm ratio with a more polygonal shape in day 26 (Figure 5.19 upper panel). RT-PCR results demonstrate that AD3 cells differentiated with the amended protocol used a combination of 1μMDEX, 50ng/ml HGF and 30ng/ml OSM show a robust expression of the mature liver marker gene, albumin. However, albumin transcript is also expressed at day 26 by cells subjected to the standard protocol (without DEX) but the expression seems low in comparison to cells treated with a combination of 1μMDEX, 50ng/ml HGF and 30ng/ml OSM. Moreover, CYP2E1 transcript expression were detected only in cells subjected to differentiation by the protocol which used a combination of 1μMDEX, 50ng/ml HGF and 30ng/ml OSM. The hepatocyte-like cells compared with human adult liver cells. Although RT-PCR is a semi-quantitative technique, this result suggests hepatocyte-like cells maturation is enhanced by the addition of 1μM DEX (Figure 5.19 lower panel). A weakness in this experiment is that ethanol vehicle control was not used (due to limitation in cells amount) to exclude the effect of the ethanol.

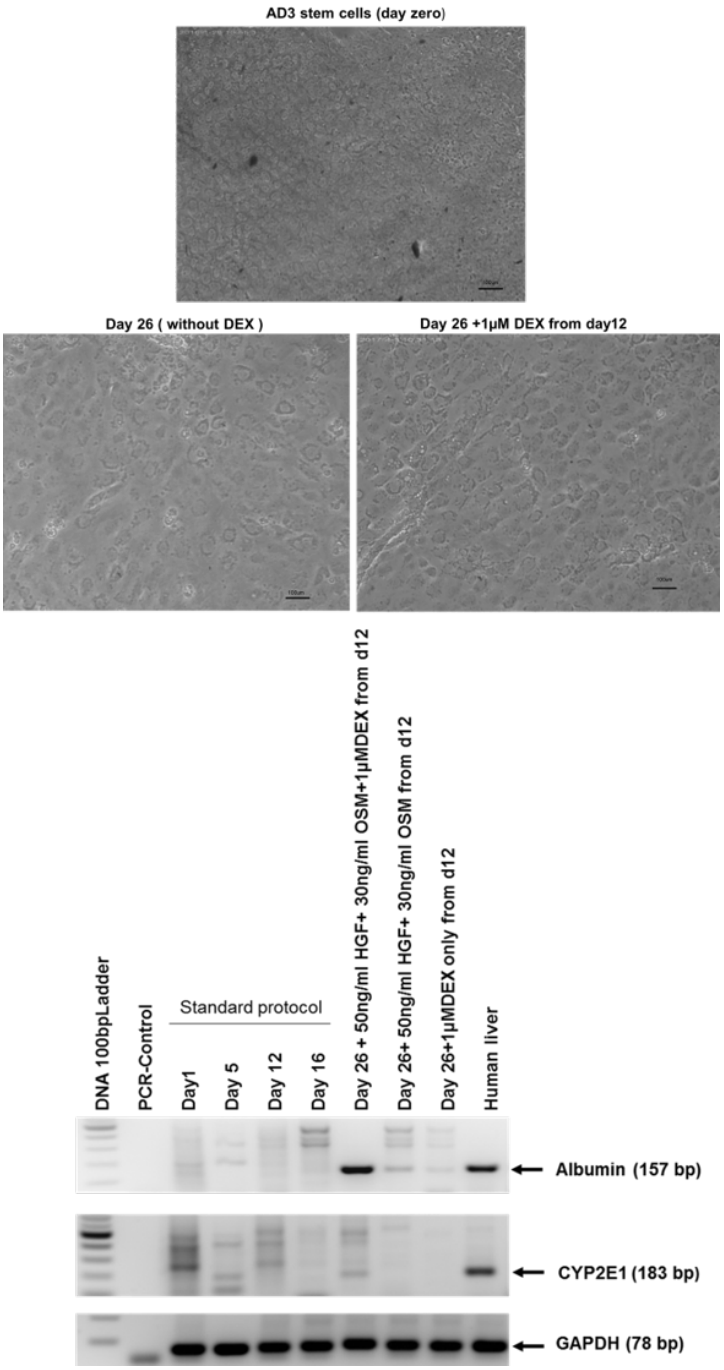

Figure 5.19 Addition of 1μM DEX to the initial protocol used enhanced hepatic phenotype in iPSCs derived hepatocyte-like cells. Upper panel: optical morphology of AD3 cells at day zero round cells with a high nuclear to cytoplasm ratio grow in colonies. Day 26 without DEX and day 26 with DEX from day 12; individual large cells with a low nuclear to cytoplasm ratio with a more polygonal shape. Lower panel: RT-PCR for Albumin, CYP2E1 and the house keeping gene (GAPDH). mRNA isolated at day 26 from AD3 cells differentiated with different combinations of 1μMDEX, 50ng/ml HGF and 30ng/ml OSM from day 12. Data are typical in at least 3 separate experiments.

5.9 Effect of SGK1F expression and/or dexamethasone treatment on the differentiation of human iPSCs into hepatocyte-like cells

iPSCs (AD3 cells) were differentiated to 26 days by the modified protocol using a combination of 1μMDEX, 50ng/ml HGF and 30ng/ml OSM from day 12 in addition to infection at a MOI of 20 for three days with AdV-SGK1F at day 5 (endoderm stage) and day 16 (early hepatocyte stage) and AdV-null at day 16. RT-PCR was performed for the housekeeping gene (*GAPDH*), *SGK1F*, *OCT4*, *Nanog*, *CK19*, *SOX17*, *C/EBPα*, *C/EBP β*, *HNF4α*, *AFP*, *CYP3A7*, *Albumin*, *CPS1*, *CYP3A4*, *CYP2C19* and *CYP1A2*. All these approaches were compared to time zero cells (day 1) and human hepatocytes. The semi quantitative RT-PCR results Figure 5.20 demonstrate clear expression of *SGK1F* by AdV-*SGK1F* infected cells. However, the level is higher via day 16 infected cells than those in day five, which suggests more mature cells are less resistant to adenoviral infection than those in the early differentiation stage which is consistent with the previous finding in Section 5.3. The results in Figure 5.20 also show pluripotency marker genes transcripts (OCT4 and Nanog) and the endodermal marker gene SOX17 were only detected in day 1 cells and completely absent in day 26 cells. A weak expression of epithelial marker gene CK19 was shown by hepatocyte-like cells. Conversely, liver transcription factors genes *C/EBPα*, *C/EBPβ* and *HNF4α* were expressed by hepatocyte-like cells. Hepatoblast marker genes transcripts (*AFP* and *CYP3A7*) were readily expressed in all hepatocyte-like cells. Interestingly, liver mature transcripts *albumin*, *CYP3A4* and *CYP2C19* was expressed by cells treated with DEX and without SGK1F expression at a level similar to that in human hepatocytes. In contrast, AdV-*SGK1F* infected cells showed low expression levels of *CYP3A4* and albumin, which is lower in AdV-*SGK1F* infected cells at day 16 where there was more expression of AdV-SGK1F. This suggests that SGK1F did not promote a more mature phenotype in hepatocyte-like cells and conversely, the cells maturation appears to have decreased or reversed into an hepatoblast phenotype.

.

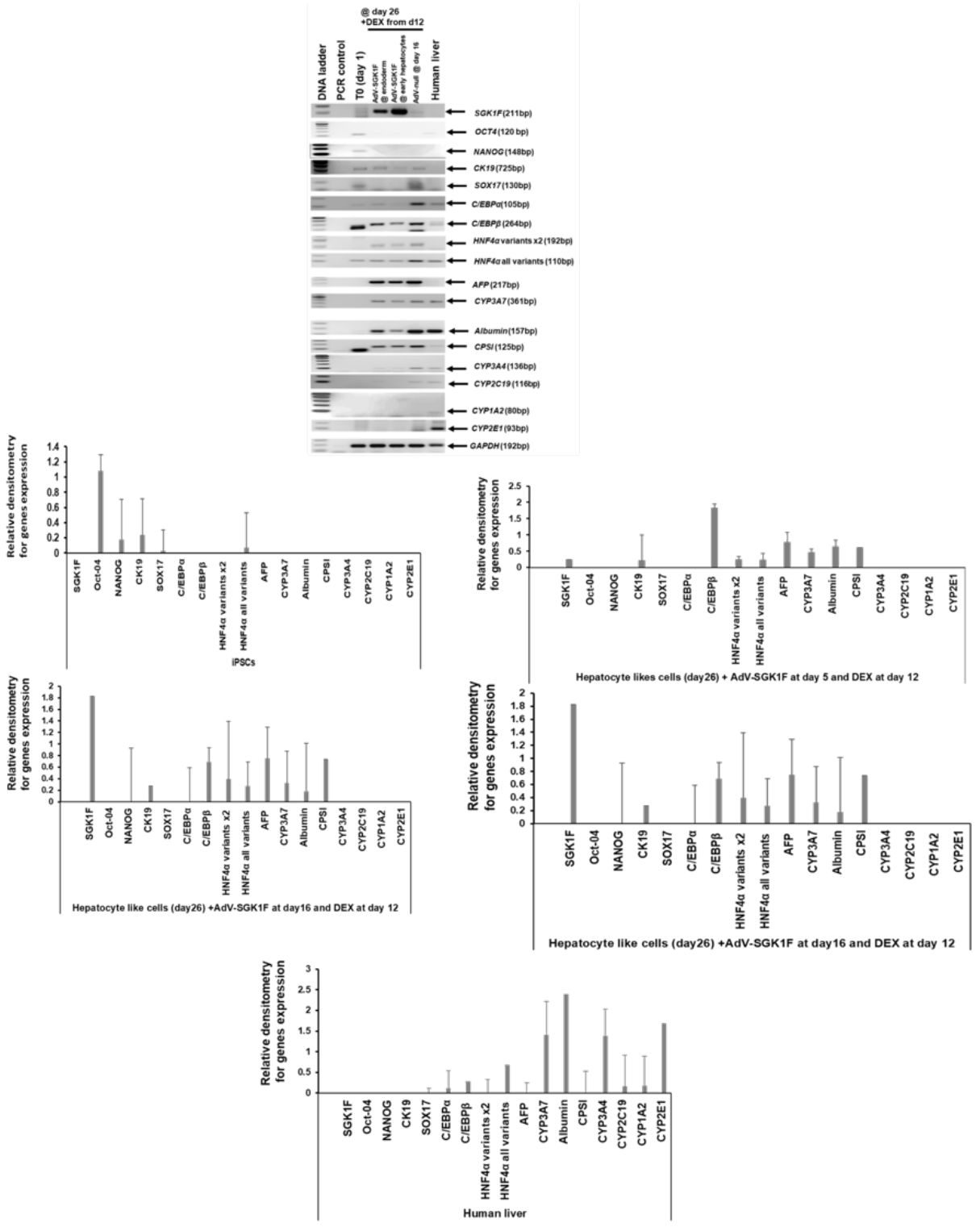

Figure 5.20 Effect of SGK1F expression and/or DEX treatment on the differentiation of human iPSCs derived hepatocyte-like cells. AD3 cells were differentiated to 26 days by being treated with1μM DEX from day 12 in addition to infection with MOI 20 AdV-SGK1F at day 5 (endoderm stage) for three days and day 16 (early hepatocyte stage) for three days. RT-PCR was carried out for the indicated transcripts. A house keeping gene, GAPDH, was used as a control. Densitometry analysis was performed using the ImageJ software and data for relative intensity was plotted as columns in graphs. Data are similar in at least three separate experiments.

A further experiment was performed to assess the effect of DEX treatment on the differentiation of human iPSCs into hepatocyte-like cells. AD3 cells were differentiated into hepatocyte-like cells (day 26) with the addition of 1μMDEX from day 12 and without DEX (standard protocol), as shown in the schematic diagram in Figure 5.21, upper panel. RNA was purified and quantified for qRT-PCR. The probe sets used were designed to specifically amplify regions of the cDNAs for *HNF4α, AFP*, *CYP3A7*, *Albumin*, *CPS1*, *CYP1A2*, *CYP2E1* and *CYP3A4*. Hepatocyte-like cells were compared to freshly isolated human hepatocytes. The results revealed a significant difference in *AFP* levels; DEX treated cells exhibited a lower level of immature liver marker transcript (*AFP*). In contrast, the *CYP3A7* transcript expression level is significantly high in the DEX treated cell suggesting the effect of DEX on *CYP3A7* induction. In addition, the expression levels of mature liver marker transcripts CPSI and albumin (however it is not significant) is higher in DEX treated cells in comparison to cells subjected to standard differentiation protocol. Surprisingly, the *CYP3A4* transcript expression level is markedly induced by DEX treatment when compared to the expression level in cells treated without DEX. The very high expression level of *CYP3A4* transcript confirms the effect of DEX on the maturation of cells besides its impact on cytochrome p450 enzyme induction (Figure 5.21 lower panel).

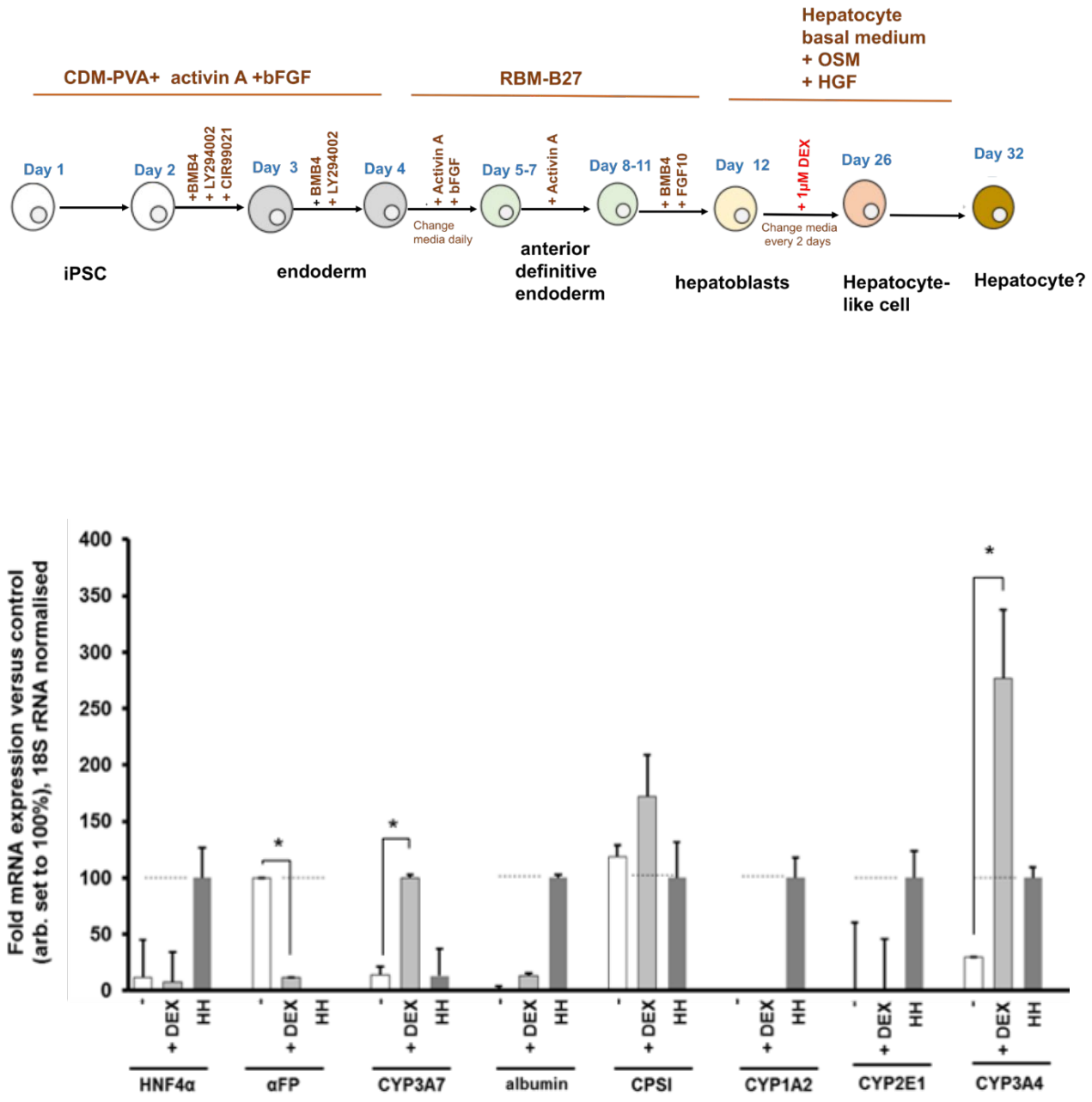

Figure 5.21 Effect of SGK1F expression and DEX treatment on the differentiation of human iPSCs into hepatocyte-like cells. AD3 cells were differentiated into hepatocyte-like cells (day26) with 1μMDEX from day 12 and without DEX, as demonstrated in the schematic flow chart in the upper panel. Q-RT-PCR was performed using TaqMan Gene Expression Assays for liver genes HNF4α, AFP, CYP3A7, Albumin, CPS1, CYP1A2, CYP2E1 and CYP3A4 (lower panel). *Significantly different (P<0.05) versus without DEX treated cells using Student's t-test (two tailed). All results typical of at least three separate experiments.

iPSCs derived hepatocyte-like cells at day 16 of differentiation were found amenable to adenoviral infection based on infection with adenovirus encoding green fluorescent protein

(AdV-GFP) with an approximate MOI of 20 which resulted in an infection rate of approximately 80% after 3 days (Figure 5.22).

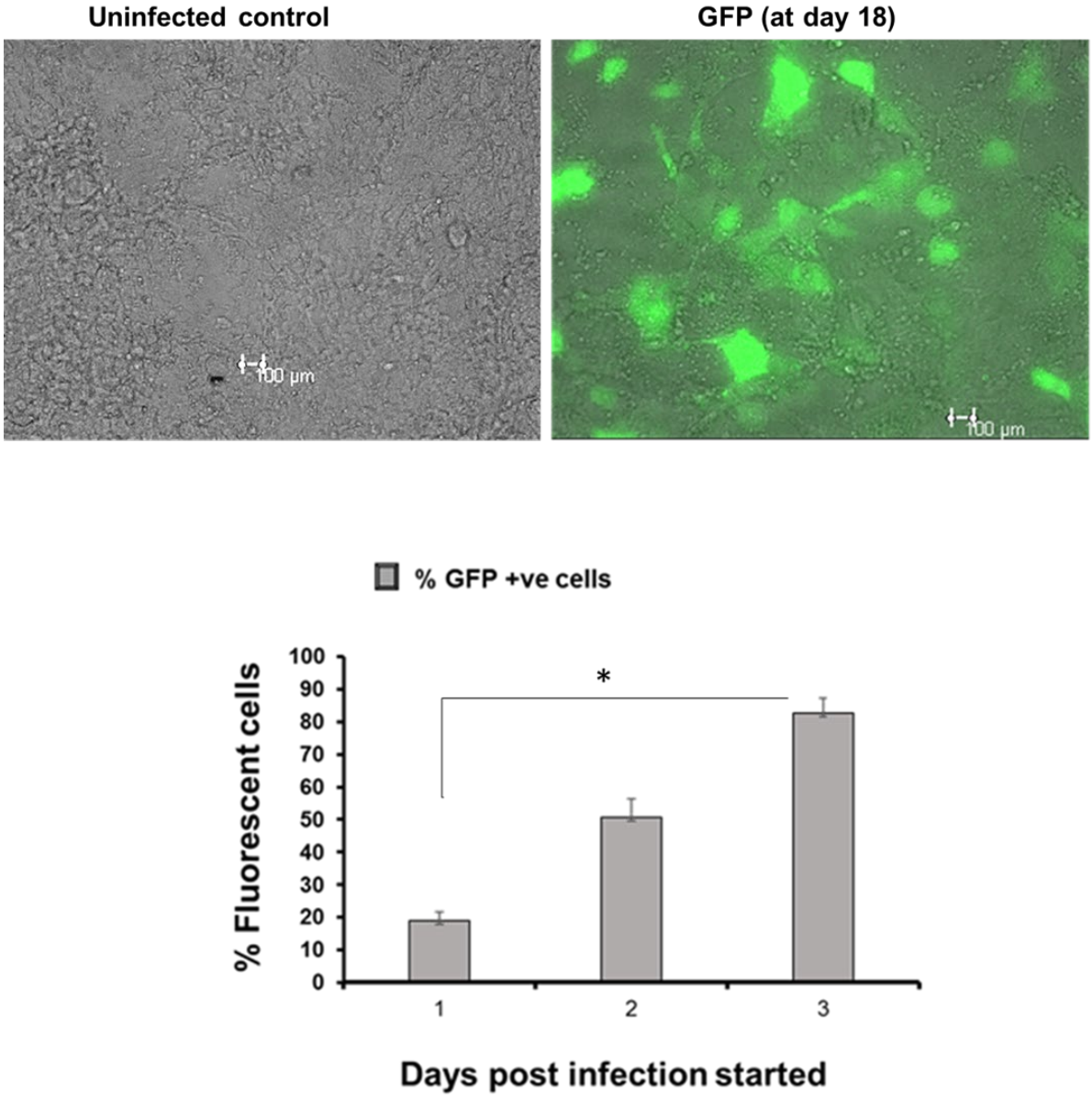

Figure 5.22 iPSCs derived hepatocyte-like cells (at early hepatocyte stage) are efficiently infected with AdV-GFP. iPSCs subjected to standard differentiation protocol and the derived hepatocyte-like cells at the early hepatocyte-like stage (day 16) were infected repeatedly with approximately MOI 20 of AdV-GFP, the mean percentage and SD of cells expressing GFP determined by fluorescence microscopy from 3 randomly selected views up to 3 days later (lower planel). In the upper panel typical views shown for uninfected control cells (left) and AdV-GFP infected cells day 18 (right). Data typical of 3 separate experiments. *Significantly different (P<0.05) was determined by using the one way Anova test followed by the post hoc test.

To examine the effect of SGK1F overexpression at day 16 (without the addition of DEX) on cells directed to hepatocyte-like-cells. iPSCs (AD3 cells) were subjected to the standard differentiation protocol and infected with AdV-SGK1F and AdV-null (at an MOI of 20) at day 16 for three days (Figure 5.23, upper panel). RNA was isolated from hepatocyte-like cells at day 26 and purified for qRT-PCR using predeveloped TaqMan Gene Expression Assays for *HNF4α*, *AFP*, *CYP3A7*, *Albumin*, *CPS1*, *CYP1A2*, *CYP2E1* and *CYP3A4*. RNA from freshly isolated human hepatocyte was used as a control (case 1). As shown in Figure 5.23.lower panel, there is no significant change in the mature liver markers transcripts level; however, there is a significant difference in the expression of hepatoblast markers *AFP*, *CYP3A7* in AdV-*SGK1F* infected cells in comparison to AdV-null infected cells. This is consistent with previous findings that suggest SGK1F reverse hepatocyte-like cells into an hepatoblast phenotype rather than promoting their maturation.

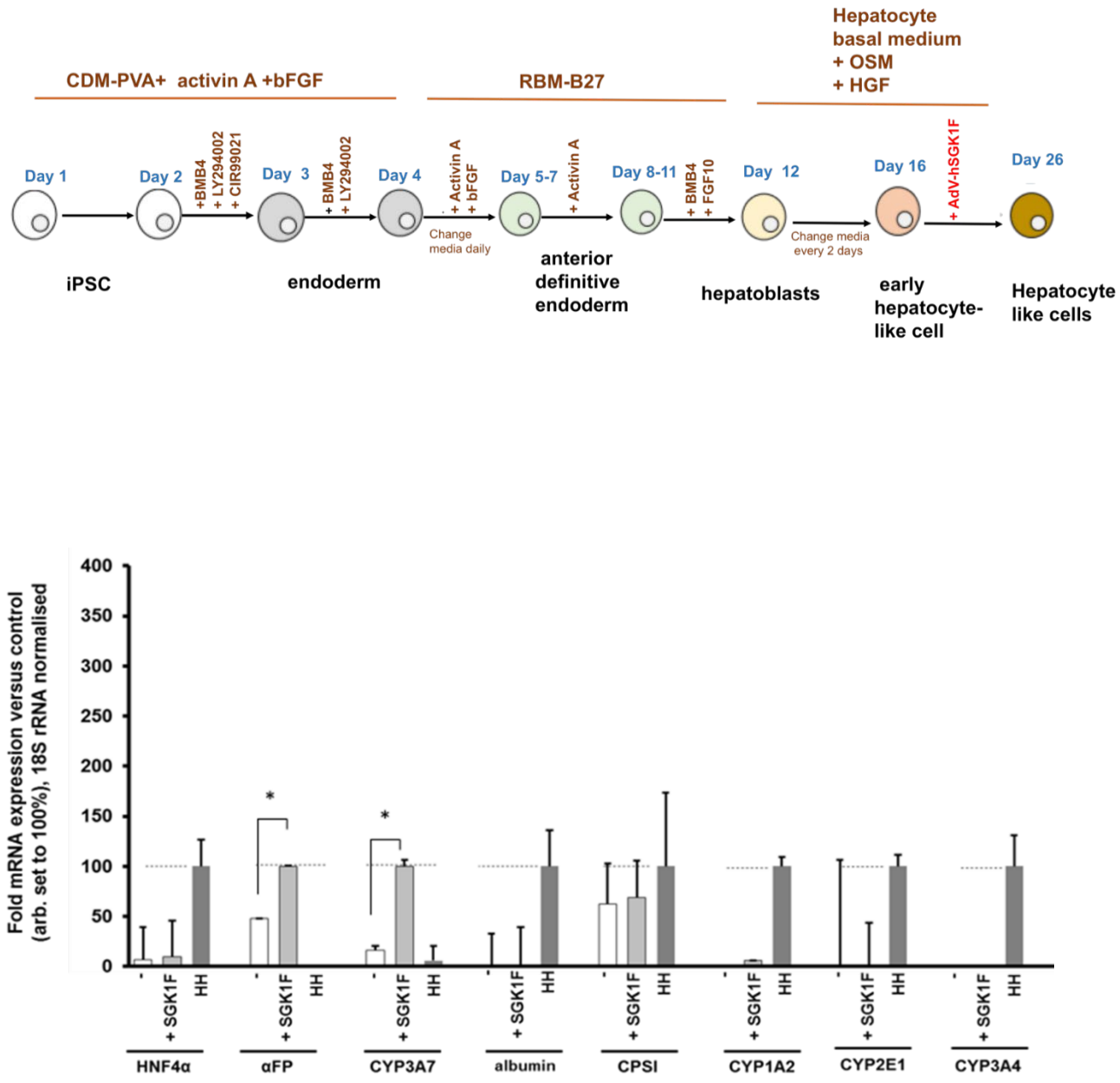

Figure 5.23 qRT-PCR for the effect of SGK1F expression on the differentiation of human iPSCs into hepatocytes-like cells at the early hepatocyte stage (day 16). RNA isolated from Ad3 cells were subjected to the standard protocol differentiation and cells infected with MOI 20 of AdV-SGK1F at day 16 for three days outlined in the schematic flow chart (upper panel) and RNA were isolated at day 26 of differentiation. QRT-PCR using TaqMan Gene Expression Assays was performed for the transcripts HNF4a, AFP, CYP3A7, Albumin, CPS1, CYP1A2, CYP2E1 and CYP3A4. Data are the mean and standard deviation of three replicates from the same experiment. Significantly different (P<0.05) versus AdV-null infected cells using Student's *t*-test (two tailed). All results typical of at least three separate experiments.

5.10 Chapter discussion

Although the differentiation of human embryonic stem cells and induced pluripotent stem cells into hepatocyte-like cells has been reported [346], additional development of this technology could lead to the scalable production of functional hepatocyte-like cells to be used for drug screening and to provide an alternative source of hepatocytes for liver transplantation.

SGK1 is transcriptionally upregulated by glucocorticoids and mineralocorticoids, and furthermore, it primarily regulates epithelial Na+ channel (ENaC) and sodium re-absorption by the kidney [233]. Cell line-based data associating SGK1 activation to particular developmental or differentiation pathways are somewhat limited. Wu et al. (2013) and Heitkamp et al. (2014) reported that SGK1 plays roles in cells differentiation [254,255], however, there is no apparent phenotype – developmental or otherwise - in Sgk1-/- mice (although there is impaired renal Na+ retention if mice are exposed to salt depletion [252,347]. Given that selected isoforms of Sgk1 have been shown to substitute for glucocorticoid and be critical for promoting differentiation to B-13/H cells (Wallace et al., 2011), we hypothesized that expression of the human SGK1F isoform will promote and maintain a hepatocyte phenotype in human stem cells directed to differentiate into hepatocyte-like cells.

In this chapter, a protocol comprising four stages to mimic the embryonic development of the liver [52], was used to convert iPSCs (AD3) into hepatocyte-like cells. After 26 days, the differentiated cells revealed hepatocyte-like phenotype judged by the disappearance of pluripotency and endodermal markers and expression mature hepatic markers transcript (Albumin); however, the cells still - at least in part- remained in an immature phenotype as confirmed by expression of foetal liver markers transcripts (AFP and CYP3A7). AdV-hSGK1 overexpression were used to study the effect of SGK1 on iPSC stem cells (AD3) differentiation and maturation for the first time. Adenovirus was used as a vector to introduce SGK1F into the cells. Adenovirus vector has attracted attention for its ability to safely and efficiently mediate gene targeting in a variety of cell types [348] [327]. Infecting differentiating iPSCs (from day 1) when the cells are at a pluripotent/early transition to an endoderm stage of development resulted in a low infection rate and low levels of the expression of a protein immunoreactive to the mouse anti-SGK1 antibody. In contrast, infecting cells at day 4-5 when the cells are transiting between endodermal/anterior definitive endoderm stages of development and at day 26 when the cells are at a post-hepatoblast/foetal hepatocyte (hepatocyte-like) stage of development resulted in a high rate of infection and robust expression of tagged SGK1F protein. Additionally, SGK1 enzyme activity showed significant differences with non-infected cells; however, the enzyme

activity was also significantly different in AdV-GFP infected cells as well, when compared to non-infected cells. An explanation for this could be for the reason that this assay is not certain to detect the ADP resulting only from SGK1 phosphorylation of AKT substrate. Possibly other enzymes catalysed the decomposition of ATP into ADP and a free phosphate ion. Likewise, the stress applied to the cells by adenoviral infection alone appears to induce SGK1 transcription, as the oxidative stress has been shown to induce SGK1 gene transcription [349] and this could mean using adenovirus for therapeutic purposes as gene delivery tool is unsafe. Besides, SGK1 mRNA has a short half-life, disappearing within 20 min of transcription [246]. All previous data confirm the functionality of the adenoviral-derived SGK1F protein in iPSCs directed to hepatocyte-like-cells.

In a study conducted by Wallace and Wright (unpublished data), the cells generated from ES differentiation into hepatocyte-like cells did not exhibit any detectable maturation phenotype after the plasmid-driven human SGK1 expression. However, it was not considered test since the transfection rates were extremely low. The data in this chapter obtained by Q-RT-PCR using TaqMan Gene Expression Assays suggest that progression to endoderm was not affected by expression of SGK1F soon after stimulation to differentiate from stem cells into endoderm, although this may be related to low levels of the infection of cells at this stage of development. However, expression of SGK1F in iPSCs-derived endoderm directed to differentiate into hepatoblasts resulted in the promotion to an hepatoblast phenotype. Despite this maturing effect on endoderm, late expression of SGK1F in iPSCs-derived hepatocytes resulted in an enhanced hepatoblast phenotype. On this basis, therefore, SGK1F expression does not act to promote an increase in the maturation of stem cell-derived terminally differentiating hepatocytes. Instead, SGK1F expression promoted the formation of hepatoblasts from both endoderm and hepatocytes. Accordingly, these data disregard the role of SGK1F in the differentiation of AD3 cells into mature hepatocytes but opens the question as to whether SGK1F expression promotes primary hepatocyte dedifferentiation into foetal hepatic phenotype *in vitro*? Preliminary results obtained from adenoviral mediated overexpression of SGK1F in adult hepatocytes soon after isolation for five days did not detect any significant changes in liver marker transcript levels when compared to AdV-null infected cells.

As SGK1 is a glucocorticoid-induced gene, the effect of glucocorticoid exposure (1µMDEX) at the hepatoblast stage of differentiation, (day12) was also examined. Schoneveld et al. (2004), used dexamethasone as a mature hepatic inducer. Clotman et al. (2005), used oncostatin or follistatin and HGF mixed along with dexamethasone to induce the maturation stage [350]. The use of follistatin or oncostatin is used to favour hepatocyte over cholangiocyte differentiation,

whereas HGF is used universally to mimic the hepatic environment [350]. Recently, Arnaud Carpentier et al. (2016), noticed that AFP positive hPSCs- derived hepatocyte-like cells could mature into positive albumin cells after dexamethasone treatment [351]. RT-PCR results demonstrate that AD3 cells differentiation with a combination of 1μMDEX, 50ng/ml HGF and 30ng/ml OSM at day 12 (hepatoblasts stage) resulted in mature liver marker genes albumin at a level similar to that expressed in human hepatocyte.

The effect of a combination of dexamethasone and SGK1F expression was examined. The semi-quantitative RT-PCR results demonstrated that the level of expression of SGK1F by AdV-SGK1F infected cells was higher by day 16 infected cells than those in day five. This observation suggested the less mature cells are more resistant to adenoviral infection. It was noticed that the expression of foetal markers - AFP and CYP3A7 - was extreme in all cells, including those infected with AdV-SGK1F at day five, day 16, as well as AdV-null infected cells. Notably, albumin was expressed by cells treated with DEX and AdV-null at a level similar to that in human hepatocytes. Conversely, albumin expression is less in cells treated with a combination of both DEX and AdV-SGK1F at day 16, which highly express hSGK1F. These findings suggest that the maturity is reduced in cells treated with SGK1F overexpression.

Q-RT-PCR was used to compare the effect of DEX (as mature hepatic inducer) to the standard protocol. After 26 days, in DEX-treated cells, CPS1 was high (although it is not a significant difference) and CYP3A4 were significantly induced by DEX treatment when compared to primary hepatocytes. The very high expression of CYP3A4 confirms the effect of DEX on the maturation of cells besides its impact on cytochrome p450 enzyme induction. The effect of SGK1F overexpression at day 16 without DEX via the standard protocol was also compared. Q-RT-PCR results exhibited that SGK1F overexpression did not enhance hepatocyte-like maturation, though there was a significant difference in the expression of AFP, CYP3A7 in AdV-SGK1F infected cells in comparison to AdV-null infected cells. This was consistent with previous findings that SGK1F overexpression results in hepatocyte dedifferentiation.

Taken together, the effect of expressing SGK1F in human iPSC-derived cells contrasts with its effects when expressed in B-13 cells. However, these effects on stem cells suggest that the role of Sgk1 in B-13 cell differentiation to B-13/H cells is likely associated with the induction of a (transient) hepatoblast-like phenotype. Previous investigations in B-13 cells suggest that Sgk1 cross-talks with the WNT signalling pathway through phosphorylation of β-catenin and thereby to reduced Tcf/Lef transcriptional activity [218] . However, it was also noted that these effects were transient and that WNT signalling activity (and Wnt3a expression, likely acting in an

autocrine fashion in B-13 cells) returned to near B-13 levels in B-13/H cells. However, the effect of dexamethasone (which SGK1 induces) is confirmed as an hepatic maturation inducer. The data in this chapter support a significant role for SGK1 that extends beyond what has continuously been considered SGK1's primary function (the control of ion transport across membranes). Understanding the mechanism underlying the involvement of SGK1 in promoting the hepatoblast differentiation and reversal of hepatocyte-like cells into the hepatoblasts stage in stem cells directed to differentiate into hepatocyte-like cells could help to improve stem cells differentiation to hepatoblast and to improve primary hepatocyte *in vitro* culturing.

Chapter 6. **General Discussion**

A common difficulty experienced with stem cell-derived differentiated cells *in vitro* is their maturation into completely differentiated phenotypes that quantitatively exhibit the function of cells *in vivo* or straight after isolation from tissues [352,353,354]. The primary functional cell of the liver – hepatocytes – is a paradigm of this setback [355]. Hepatocytes *in vivo* are extremely metabolically active and play a diverse range of functions (many of which are specific to this cell type). Stem cell-derived hepatocyte-like cells may resist functioning as hepatocytes *in vitro* for several reasons. These include sub-optimal differentiation protocols; a sub-optimal *in vitro* environment (e.g. extracellular matrix, appropriate cell-cell contacts, cell density) and abnormal levels of regulating factors (e.g. hormones controlling gene expression). Together they stimulate a de-differentiation process, a response also faced when hepatocytes are isolated from undamaged organs and placed under the same environments *in vitro* [355]. These problems have resulted in comprehensive attempts to modify the *in vitro* environment in order to generate and/or preserve hepatic functionality (e.g. co-culture systems [345], 3D culture systems [345] and flow cultures [293] etc).

Liver disease models and stem cell-derived hepatocyte-like-cellsimplantation experiments suggest that stem/progenitor cell-derived cells maintain the capacity to function sufficiently as hepatocytes (when in the appropriate *in vivo* environment) [356,357,358]. Thus, the degree to which stem cell-derived hepatocytes will find widespread exploitation for *in vitro* studies (e.g. drug metabolism and toxicity studies), will rely on how complicated and expensive it will be to copy the *in vivo* environment in culture systems.

An alternative method for generating more mature phenotypes *in vitro* is via forced over-expression of suitable transcription factors. The AR42J-B13 (B-13) cell provides reliability for this condition, given that B-13 cells are capable of differentiating into a mature hepatocyte phenotype (B-13/H cells) without a complex cultural environment.

In response to glucocorticoids, B-13 cell replication ceases, changes occur morphologically and several of the genes specific to hepatocytes are expressed at levels quantitatively comparable to normal rat hepatocytes [198,200,218,323]. The mechanism controlling this differentiation includes an activation of the glucocorticoid receptor; critical epigenetic alterations; induction of serine/threonine protein kinase 1 (Sgk1); Sgk1-dependent repression of constitutive WNT cell signalling activity and expression of a host of transcription factors that drive the hepatic phenotype [218,226,326]. This response takes place on simple plastic substrata [although it may also

occur in 3D and is enhanced by extracellular matrix [359] and in comparison to normal hepatocytes is not reversed by de-differentiation, at least for several weeks [218].

The rat Sgk1 gene is at present known to encode three validated mRNA transcripts and possibly one further transcript [NCBI database, see also Table 3.3]. All four transcripts encode an identical core amino acid sequence and differ only in their N terminal amino acid sequences. It is not known whether the Sgk1 isoforms have other functions; however, only the rat Sgk1c transcript appears to be irreversibly induced in B-13 cells after exposure to glucocorticoid [326]. This finding proposes that endogenous Sgk1c may be accountable for its differentiating effects in B-13 cells. This is supported by the high expression of the murine orthologue of Sgk1c in pancreatic tissue from transgenic mice with high levels of circulating endogenous glucocorticoids (these mice experience the transdifferentiation of the pancreatic exocrine tissue into hepatocyte-like cells), whereas wild type mice expressed neither liver markers nor Sgk1c mRNA [231].

Selected isoforms of Sgk1 (including SGK1F) have been shown to substitute for glucocorticoid and be critical for promoting differentiation to B-13/H cells [226]. Similarly, high levels of SGK1F mRNA transcripts were detected in the pancreas from a patient treated for many decades with systemic glucocorticoid experienced a degree of hepatic differentiation [227]. These data have driven the focus on SGK1F. Accordingly, this thesis hypothesises that the expression of the human SGK1F isoform will promote and maintain a hepatocyte phenotype in human stem cells directed to differentiate into hepatocyte-like cells. Additionally, cDNA for SGK1F transcript was cloned into a replication-deficient adenoviral genome to introduce the genetic material (SGK1F) into B-13 cells and iPSCs (AD3 cells) directed to differentiate to hepatocyte-like cells.

The data in this thesis demonstrate that glucocorticoid receptor antagonist (Ru486) prevented DEX-dependent trans-differentiation of B-13 cells into B1-13/H cells. This data support that the effect of DEX on transdifferentiation are mediated through the GR [226]. Moreover, the data demonstrate that B-13 cells treated with 10nM DEX treatment resulted in a significant decrease in WNT signalling. Moreover, in addition to the DEX effect on WNT signalling repression, it has also resulted in β-catenin phosphorylation which is consistent with findings of Wallace et al [231]. Antagonising progesterone receptor with RU486 have the same effect as DEX on WNT signalling. However, both RU486 and DEX repressed WNT signalling, and only DEX converted B-13 cells into B-13/H cells. This effect is probably because exposing B-13 cells to glucocorticoid leads to a Gr-dependent pulse in DNA methylation and possibly other epigenetic

changes, such as histone modifications that results in the constitutive expression of Sgk1c and the irreversible reprogramming of B-13 cells into B-13/H cells [326].

The data in this thesis reveals that B13 cells are readily infected with adenovirus. However, marked toxicity was observed with high MOIs. Therefore, the repeated infection strategy was employed in B-13 cells to maximise infection and SGK1F expression and minimise cell death. The data also demonstrates that adenoviral-mediated SGK1F expression in B-13 cells induces their differentiation into B-13/H cells, similar to their response to exposure to glucocorticoid also suggesting that Sgk1 activity is crucial in B13 conversion into B-13/H. Accordingly, SGK1F is implicated in the transdifferentiation of B-13 cells into B-13/H hepatocyte-like cells. Furthermore, the role of Sgk1 kinase activity in B-13 cells and WNT signalling was further tested by examining the effect of AdV-hSGK1F overexpression on WNT signalling transcriptional activity. Data in this thesis demonstrated a regulatory role for Sgk1 (SGK1F) in WNT signalling changes and suggested that SGK1F overexpression is upstream of β-catenin phosphorylation changes. The likelihood is therefore that the conversion of B-13 cells into B-13/H cells in response to glucocorticoid is associated with Sgk1 induction and WNT signalling changes. Taken together, these data therefore support the proposed glucocorticoid-dependent mechanism for converting B-13 cells into B-13/H cells, as schematically outlined in Figure 8, involving glucocorticoid receptor activation, Sgk1 induction, phosphorylation of β-catenin and suppression of endogenously high WNT signalling activity in B-13 cells.

The data in this thesis obtained by investigating (for the first time) the effect of adenoviral-mediated expression of SGK1F on iPSCs (AD3 cells) directed to differentiate into hepatocyte-like cells, propose that the expression of SGK1F did not influence differentiation to endoderm immediately after induction of stem cells differentiation into the endodermal stage. Even though this might be due to low levels of cells infection at this stage of development. Limited trial and error led us to the conclusion that MOI of 20 gave the best infection rates whilst limiting significant losses in cell viability. We were limited to the range of pilot studies we could perform because there were limitations to the number of iPSCs that could be generated each time and accordingly, limitations on examining the many potential variables impacting on optimal infection and gene expression. Conversely, expression of SGK1F in iPSCs-derived endoderm directed to differentiate into hepatoblasts phenotype resulted in promotion to an hepatoblast phenotype. Regardless of this maturing impact in endoderm, late expression of SGK1F in iPSCs-derived hepatocytes resulted in the boosted hepatoblast phenotype. According to this, SGK1F expression does not act to promote an increase in the maturation of stem cell-derived terminally differentiating hepatocytes. Instead, SGK1F expression promoted the

formation of hepatoblasts from both endoderm and hepatocytes. Therefore, these effects in stem cells suggest that the role of Sgk1 in B-13 cell differentiation to B-13/H cells is likely associated with the induction of a (transient) hepatoblast-like phenotype. The exact timepoints not analysed throughout in chapter 5 because of limitations in the number of iPSCs that can be matured. In addition, sometimes the RNA concentration selected was too low or lack purity, which required some flexibility around the day of culture used for some analyses.

In conclusion, the effect of expressing SGK1F in human iPSC-derived cells appears contrasting to its effects when expressed in B-13 cells; however, these effects in stem cells suggest that the role of Sgk1 in B-13 cell differentiation to B-13/H cells is likely associated with the induction of a (transient) hepatoblast-like phenotype. Preceding investigations in B-13 cells indicate that Sgk1 cross-talks with the WNT signalling pathway via phosphorylation of β-catenin to reduce Tcf/Lef transcriptional activity [218]. Though it was also observed that these effects were transient and that WNT signalling activity (and Wnt3a expression, possibly acting in an autocrine fashion in B-13 cells) returned to near B-13 levels in B-13/H cells. Besides, glucocorticoid exposure in B-13 cells initiates an epigenetic change(s) that accounts for the inability of B-13/H cells to revert to B-13 cells (and which may also be critical for their near quantitative functional trans-differentiation into hepatocytes)[326] (Figure 6.1). However, adding dexamethasone at the hepatoblast stage somewhat enhanced the stem cells maturity which is judged by the expression of higher expression level albumin in comparison to the no DEX treated cells. Future work could be directed to identifying what factors induce SGK1C and to identifying the precise epigenetic changes controlling Sgk1c expression in B-13 cells. Ideally, one would sequence the entire genome, however, this is impractical and remains costly at present. Additional work could examine why specific isoforms (sgk1c and SGK1F) interact with β-catenin, lead to β-catenin phosphorylation and result in a suppression of WNT signalling Although, there is no significant amino acid sequence similarity between SGK1F and SGK1C N- terminal sequences, peptides of these proteins sequences could be constructed and transfected to B-13 cells to examine their effect on beta-catenin phosphorylation using an immunoprecipitation technique. Moreover, SGK1F overexpression could be used to enhance B-13 transdifferentiation into B-13/H cells and to promote the hepatoblasts stage to improve the stem cells differentiation (to hepatoblasts) prior to conversion into hepatocyte-like cells.

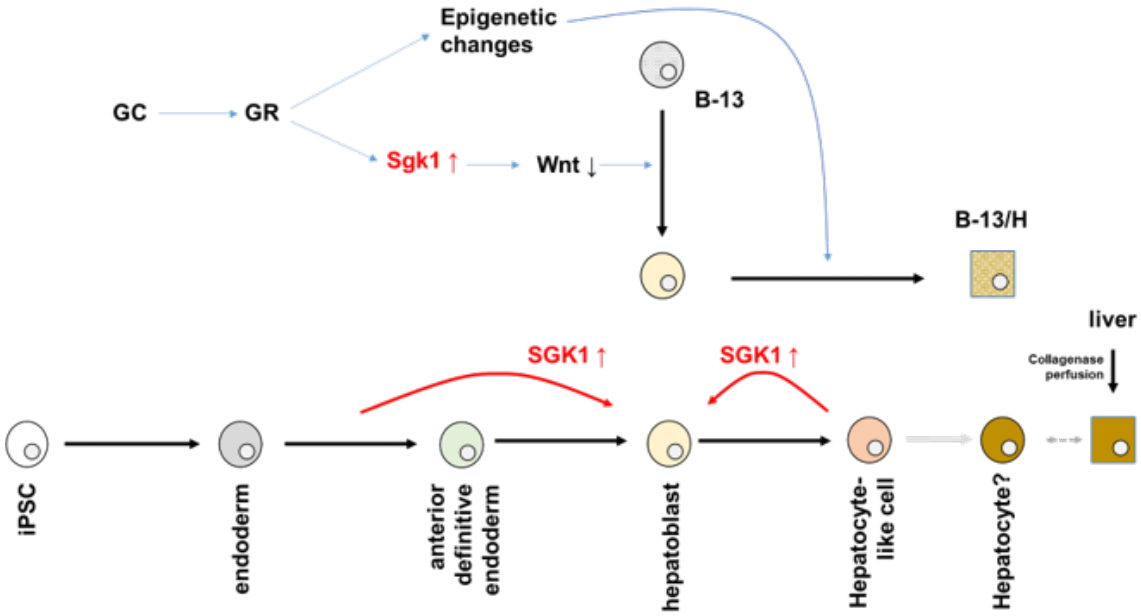

Figure 6.1: Proposed role of Sgk1 in B-13 differentiation and effects of SGK1F on human iPSC differentiation.

Appendix A. List of DNA oligonucleotide sequences employed in RT-PCR

Oligo ID	Primer sequence (5'-3')		Comments
primers for examining hiPSC to hepatocyte differentiation			
hOCT4	US	GTGGAGGAAGCTGACAACAA	Will hybridise to human OCT4 cDNA sequence [NM_002701.6] and amplify a fragment of 120 bp.[360]
	DS	ATTCTCCAGGTTGCCTCTCA	
hSOX2	**US**	TTCATCGACGAGGCTAAGCG	Will hybridise to human SOX2 cDNA sequence [NM_003106] and amplify a fragment of 255bp.
	DS	CATCATGCTGTAGCTGCCGT	
Nanog	**US**	AATGGTGTGACGCAGGGATG	Will hybridise to human Nanog homeobox (NANOG), transcript variant 2, cDNA sequence NM_001297698.1 and amplify a fragment of 148 bp.
	DS	TGCACCAGGTCTGAGTGTTC	

Oligo ID	Primer sequence (5'-3')		Comments
hSOX17	**US**	CAAGGGCGAGTCCCGTATC	Will hybridise to human SOX17 cDNA sequence [NM_022454] and amplify a fragment of 132bp.
	DS	CACGACTTGCCCAGCATCTTG	
hFOXA2	**US**	ACTGTTTCCTGAAGGTGCCC	Will hybridise to human FOXA2 cDNA sequence transcript variant 1[NM_021784] and transcript variant 2 [NM_153675] to amplify a fragment of 224bp.
	DS	CTCCCCGAGTTGAGCCTGTG	
hHHEX	**US**	CCCTGGGCAAACCTCTACTC	Will hybridise to human HHEX cDNA sequence [NM_002729] and amplify a fragment of 227bp.
	DS	TCTCCTCCATTTAGCGCGTC	
hHNF4A	**US**	GGACATGGCCGACTACAGTG	Will amplify sequence of 198 bp of human hepatocyte nuclear factor 4 alpha (HNF4A), transcript variant 2 (NM_000457.4)
	DS	CTCGAGGCACCGTAGTGTTT	

Oligo ID	Primer sequence (5'-3')		Comments
hHNF4A	**US**	TCCCCATCAGAAGGCACCAACCT	Will amplify sequence of 110 bp of human hepatocyte nuclear factor 4 alpha (HNF4A), NM_000457.4
	DS	CAGCTCGAGGCACCGTAGTG	
hCEBPα	**US**	CCAGTGACAATGACCGCCT	Will amplify sequence of 105 bp of human CCAAT enhancer binding protein beta (CEBPA), transcript variant 1(NM_004364.4)
	DS	CCTTGACCAAGGAGCTCTC	
hCEBPB	**US**	CCAGCCACCAGCCCCCTCACTAATA	Will amplify sequence of 264 bp of human CCAAT enhancer binding protein beta (CEBPB), transcript variant 1, mRNA NM_005194.3
	DS	CCAAGCAGTCCGCCTCGTAGT	
hAFP	**US**	TGCAGCCAAAGTGAAGAGGGAAGA	Will amplify sequence of 217bp [361]
	DS	CATAGCGAGCAGCCCAAAGAAGAA	

Oligo ID	Primer sequence (5'-3')		Comments
hCYP3A7	**US**	TTCACAAACCGGAGGCCTTT	Will hybridise to human CYP3A7 cDNA sequence [NM_000765] and amplify a fragment of 361bp.
	DS	GAGAGAACGAATGGATCTAATGGA	
hCK19	**US**	CAGCTTCTGAGACCAGGGTT	Will hybridise to human CK19 cDNA sequence [NM_002276.4] and amplify a fragment of 725 bp
	DS	GCCCCTCAGCGTACTGATTT	
hCPSI	**US**	CTGGAGAGGTGGCTTGCTTT	Will hybridise to human Cps1 cDNA sequence (NM_001122633.2) and amplify a fragment of 125 bp
	DS	TCTTGGCCGGAATGATTGCT	
hAlbumin	**US**	CTTGAATGTGCTGATGACAGG	Will amplify sequence of 157bp [362].
	DS	GCAAGTCAGCAGGCATCTCAT	
hCYP3A4	**US**	CTTCATCCAATGGACTGCATAAAT	Will amplify sequence of 87bp [363].
	DS	TCCCAAGTATAACACTCTACACAGACAA	

Oligo ID	Primer sequence (5'-3')		Comments
hCYP3A4	**US**	TGTCCTACCATAAGGGCTTTTGTAT	Will amplify sequence of 136 bp Human cytochrome P450 family 3 subfamily A member 4 (CYP3A4), transcript variant 2,(NM_001202855.2)
	DS	TTCACTAGCACTGTTTTGATCATGTC	
hCYP2E1	**US**	TCCTTCACCCGGTTGGCCCA	Will amplify sequence of 93 bp cytochrome P450 family 2 subfamily E member 1 (CYP2E1), (NM_000773.4)
	DS	CACCGCCTTGTAGCCGTGCA	
hCYP2E1	**US**	ACGGTATCACCGTGACTGTGG	Will hybridise to human CYP2E1 cDNA sequence (NM_000773.4) and amplify a fragment of 183 bp
	DS	GCATCTCTTGCCTATCCTTGA	
hCYP1A2	**US**	TCTTTGGAGCAGGATTTGAC	Will amplify sequence of 80 bp cytochrome P450 family 1 subfamily A member 2 (CYP1A2), NM_000761.5
	DS	CTGTATCTCAGGCTTGGTCAC	

Oligo ID	Primer sequence (5'-3')		Comments
hCYP2C19	**US**	TCTGTCCCGCCCTTCTATCA	Will amplify sequence of 116 bp of cytochrome P450 family 2 subfamily C member 19 (CYP2C19) NM_000769.4
	DS	AGATAGTGAAATTTGGACCAGAGGA	
Primers for B-13 and B-13/H cells			
r-Pgr	**US**	GGACTCTCCACACATCTGGC	Will amplify rat Rattus norvegicus progesterone receptor (Pgr) (NM_022847.1) cDNA sequence of 141 bp
	DS	CCAGGGAGATCGGTATTGGC	
r-PXR	**US**	GCTCCTGCTGGACCCGTTGA	Will amplify Rattus norvegicus nuclear receptor subfamily 1, group I, member 2 (Nr1i2 (NM_052980.2)115) cDNA sequence of 115bp
	DS	GCCAGGGCGATCTGGGGAGAA	
rCpsI	**US**	TGTGAAGGTCTTGGGAACATCGGT	Will hybridise to rat CpsI cDNA (NM_017072.1) sequence of 173bp at 59° C to produce a single amplimer [326].
	DS	CGCATTCCAACAGGTCGCCG	
rcyp2e1	**US**	ACCCCATGAAGCAACCAGAG	Will hybridise to rat cyp2e1 cDNA sequence [NM_031543.] and amplify a fragment of 86 bp.
	DS	AGAGGGAGTCCAGAGTTGGAA	

Oligo ID	Primer sequence (5'-3')		Comments
rmcyp2e1	**US**	TCGACTACAATGACAAGAAGTGT	Will amplify a rat CYP2E (NM_031543) cDNA sequence of 525bp [197]
	DS	CAAGATTGATGAATCTCTGGATCTC	
rAlbumin	**US**	TGGTCGCAGCTGTCCGTCAGA	Will hybridise to rat albumin cDNA (NM_134326.2) sequence of 192bp **at 61°C** to produce a single amplimer[326].
	DS	CGCATTCCAACAGGTCGCCG	
SGK1			
hSGK1a (w/t)	**US**	CGAGCCGGTCTTTC CGAGCCGGTCTTTGAGCGCTAAC	Will amplify 118bp of human SGK1 variant 1 mRNA (NM_005627.3). Also referred to as SGK1A and wild type sequence [364]
	DS	GAATTGCCACCATGCCCCTCATCC	
hSGK1b	US	AAAAGGCGTTTTCGGAAGCGACCC	Will amplify 140bp of human SGK1 variant 4 mRNA (NM_001143678.1). Also referred to as SGK1B [364]
	DS	CAGACGAGAGCGACCGGCGAG	

Oligo ID	Primer sequence (5'-3')		Comments
hSGK1c	US	GAACAGGGATAGCCGTCTCTGGC	Will amplify 121bp of human SGK1 variant 3 mRNA(NM_001143677.1). Also referred to as SGK1C [364]
	DS	TTCTGGAGGCTGGAGGTAGAGCC	
hSGK1d	US	CCCTCTGCCTTTCTGGCGCTGTTC	Will amplify 140bp of human SGK1 variant 2 (NM_001143676.1). Also referred to as SGK1D [364]
	DS	CTGGAGGCGGCTTGAGAGAGGAG	
hSGK1f	**US**	TCTCCTCCTTCATCCACAGCTTTCA	Will amplify 211bp of human SGK1F mRNA (FM205710.1)[364]
	DS	TGGACGACGGGCCAAGGTTG	
rSGK1a	**US**	CTGCTCGAAGTACCCTCACC	Will amplify rat (NM_019232) Sgk1acDNA sequence of 128 bp[226]
	DS	GCATGCATAGGAGTTGTTGG	

Oligo ID	Primer sequence (5'-3')		Comments
rSGK1b	**US**	GCCACAAAAAGCGAGTG	Will amplify rat Sgk1b cDNA sequence of 131 bp [226]
	DS	GCATGCATAGGAGTTGTTGG	
rSgk1c	**US**	AAGTAACCCCAGCCTTCACC	Will amplify rat Sgk1c - also referred to as variant 2 (NM_001193569.1) cDNA sequence of 143bp [226]
	DS	GCATGCATAGGAGTTGTTGG	
rsgk1 like loc	**US**	TGCCATCTGACAATGGGGAC	LOC102551865 serine /threonine-protein kinase Sgk1-like Will amplify rat Sgk1 like loc cDNA sequence of 379 bp
	DS	GTTCTGCGGTGTGCCTTTTC	
rsgk1 x2	**US**	CCCACTGGAACCTACACAATCA	Will amplify rat Sgk1 X2 (XM_006227723.1) cDNA sequence of 226 bp
	DS	GTAAGCATCACCGCAACAGG	

Oligo ID	Primer sequence (5'-3')		Comments
Housekeeping genes			
rmhGAPDH	**US**	GACATCAAGAAGGTGGTGAAG	Will hybridise to human GAPDH cDNA sequence [NM_001256799, NM_001289745, NM_001289746, NM_001357943 and NM_002046] and amplify fragments all of 180bp.
	DS	TTGTCATACCAGGAAATGAGCT	
rmhGAPDH	**US**	TGACATCAAGAAGGTGGTGAAG	Will amplify rat (NM_017008), human (NM_002046) or mouse (NM_008084) glyceraldehyde 3 phosphate dehydrogenase cDNA sequence of 243bp [226]
	DS	TCTTACTCCTTGGAGGCCATGT	
GAPDH	**US**	GAAGGTGAAGGTCGGAGTCAAC	Will amplify fragments 78 bp of human GAPDH cDNA[363]
	DS	CAGAGTTAAAAGCAGCCCTGGT	

All primer sets listed were run for 35 cycles at an annealing temperature of 55°C

Appendix B. Rat and human Sgk1 proteins sequences (raw sequence data)

Rat Sgk1 protein sequences

>NP_001180497.1 serine/threonine-protein kinase Sgk1 isoform 1 [Rattus norvegicus]
MGEMQGALARARLESLLRPRHKKRVEAQKRSESVLLSGLAFMKQRRMGLNDFIQKLANNSYACKHPEVQSYLKIS
QPQEPELMNANPSPPPSPSQQINLGPSSNPHAKPSDFHFLKVIGKGSFGKVLLARHKAEEAFYAVKVLQKKAILK
KKEEKHIMSERNVLLKNVKHPFLVGLHFSFQTADKLYFVLDYINGGELFYHLQRERCFLEPRARFYAAEIASALG
YLHSLNIVYRDLKPENILLDSQGHIVLTDFGLCKENIEHNGTTSTFCGTPEYLAPEVLHKQPYDRTVDWWCLGAV
LYEMLYGLPPFYSRNTAEMYDNILNKPLQLKPNITNSARHLLEGLLQKDRTKRLGAKDDFMEIKSHIFFSLINWD
DLINKKITPPFNPNVSGPSDLRHFDPEFTEEPVPSSIGRSPDSILVTASVKEAAEAFLGFSYAPPMDSFL

>NP_001180498.1 serine/threonine-protein kinase Sgk1 isoform 2 [Rattus norvegicus]
MREEALRSPWKAFMKQRRMGLNDFIQKLANNSYACKHPEVQSYLKISQPQEPELMNANPSPPPSPSQQINLGPSS
NPHAKPSDFHFLKVIGKGSFGKVLLARHKAEEAFYAVKVLQKKAILKKKEEKHIMSERNVLLKNVKHPFLVGLHF
SFQTADKLYFVLDYINGGELFYHLQRERCFLEPRARFYAAEIASALGYLHSLNIVYRDLKPENILLDSQGHIVLT
DFGLCKENIEHNGTTSTFCGTPEYLAPEVLHKQPYDRTVDWWCLGAVLYEMLYGLPPFYSRNTAEMYDNILNKPL
QLKPNITNSARHLLEGLLQKDRTKRLGAKDDFMEIKSHIFFSLINWDDLINKKITPPFNPNVSGPSDLRHFDPEF
TEEPVPSSIGRSPDSILVTASVKEAAEAFLGFSYAPPMDSFL

>NP_062105.2 serine/threonine-protein kinase Sgk1 isoform 3 [Rattus norvegicus]
MTVKTEAARSTLTYSRMRGMVAILIAFMKQRRMGLNDFIQKLANNSYACKHPEVQSYLKISQPQEPELMNANPSP
PPSPSQQINLGPSSNPHAKPSDFHFLKVIGKGSFGKVLLARHKAEEAFYAVKVLQKKAILKKKEEKHIMSERNVL
LKNVKHPFLVGLHFSFQTADKLYFVLDYINGGELFYHLQRERCFLEPRARFYAAEIASALGYLHSLNIVYRDLKP
ENILLDSQGHIVLTDFGLCKENIEHNGTTSTFCGTPEYLAPEVLHKQPYDRTVDWWCLGAVLYEMLYGLPPFYSR
NTAEMYDNILNKPLQLKPNITNSARHLLEGLLQKDRTKRLGAKDDFMEIKSHIFFSLINWDDLINKKITPPFNPN
VSGPSDLRHFDPEFTEEPVPSSIGRSPDSILVTASVKEAAEAFLGFSYAPPMDSFL

>XP_006227785.1 PREDICTED: serine/threonine-protein kinase Sgk1 isoform X1 [Rattus norvegicus]
MVNKDMNGFPVKKCSAFQFFKKRVRRWIKSPMVSVDKHQSPNLKYTGPAGVHLPPGEPDFEPALCQSCLGDHTFQ
RGMLSPEESRSWEIQPGGEVKEPCNHANILTKPDPRTFWTSDDPAFMKQRRMGLNDFIQKLANNSYACKHPEVQS
YLKISQPQEPELMNANPSPPPSPSQQINLGPSSNPHAKPSDFHFLKVIGKGSFGKVLLARHKAEEAFYAVKVLQK
KAILKKKEEKHIMSERNVLLKNVKHPFLVGLHFSFQTADKLYFVLDYINGGELFYHLQRERCFLEPRARFYAAEI
ASALGYLHSLNIVYRDLKPENILLDSQGHIVLTDFGLCKENIEHNGTTSTFCGTPEYLAPEVLHKQPYDRTVDWW
CLGAVLYEMLYGLPPFYSRNTAEMYDNILNKPLQLKPNITNSARHLLEGLLQKDRTKRLGAKDDFMEIKSHIFFS
LINWDDLINKKITPPFNPNVSGPSDLRHFDPEFTEEPVPSSIGRSPDSILVTASVKEAAEAFLGFSYAPPMDSFL

CLUSTAL O(1.2.4) multiple sequence alignment of rat Sgk1 protein sequences

```
4       MVNKDMNGFPVKKCSAFQFFKKRVRRWIKSPMVSVDKHQSPNLKYTGPAGVHLPPGEPDF          60
3       ------------------------------------------------------------          0
1       ------------------------------------------------------------          0
2       ------------------------------------------------------------          0


4       EPALCQSCLGDHTFQRGMLSPEESRSWEIQPGGEVKEPCNHANILTKPDPRTFWTSDDPA          120
3       ----------------------------M-----TVKTEAARSTLTYS-RMRGMVAILIA          26
1       --------MGEM---QGALARAR---LES-----LLRPRHKKRVEAQK-RSESVLLSGLA          40
2       ---------------------------------------------M-REEALRSPWKA           12
                                                                  *

4       FMKQRRMGLNDFIQKLANNSYACKHPEVQSYLKISQPQEPELMNANPSPPPSPSQQINLG          180
3       FMKQRRMGLNDFIQKLANNSYACKHPEVQSYLKISQPQEPELMNANPSPPPSPSQQINLG          86
1       FMKQRRMGLNDFIQKLANNSYACKHPEVQSYLKISQPQEPELMNANPSPPPSPSQQINLG          100
2       FMKQRRMGLNDFIQKLANNSYACKHPEVQSYLKISQPQEPELMNANPSPPPSPSQQINLG          72
        ************************************************************


4       PSSNPHAKPSDFHFLKVIGKGSFGKVLLARHKAEEAFYAVKVLQKKAILKKKEEKHIMSE          240
3       PSSNPHAKPSDFHFLKVIGKGSFGKVLLARHKAEEAFYAVKVLQKKAILKKKEEKHIMSE          146
1       PSSNPHAKPSDFHFLKVIGKGSFGKVLLARHKAEEAFYAVKVLQKKAILKKKEEKHIMSE          160
2       PSSNPHAKPSDFHFLKVIGKGSFGKVLLARHKAEEAFYAVKVLQKKAILKKKEEKHIMSE          132
        ************************************************************


4       RNVLLKNVKHPFLVGLHFSFQTADKLYFVLDYINGGELFYHLQRERCFLEPRARFYAAEI          300
3       RNVLLKNVKHPFLVGLHFSFQTADKLYFVLDYINGGELFYHLQRERCFLEPRARFYAAEI          206
1       RNVLLKNVKHPFLVGLHFSFQTADKLYFVLDYINGGELFYHLQRERCFLEPRARFYAAEI          220
2       RNVLLKNVKHPFLVGLHFSFQTADKLYFVLDYINGGELFYHLQRERCFLEPRARFYAAEI          192
        ************************************************************


4       ASALGYLHSLNIVYRDLKPENILLDSQGHIVLTDFGLCKENIEHNGTTSTFCGTPEYLAP          360
3       ASALGYLHSLNIVYRDLKPENILLDSQGHIVLTDFGLCKENIEHNGTTSTFCGTPEYLAP          266
1       ASALGYLHSLNIVYRDLKPENILLDSQGHIVLTDFGLCKENIEHNGTTSTFCGTPEYLAP          280
2       ASALGYLHSLNIVYRDLKPENILLDSQGHIVLTDFGLCKENIEHNGTTSTFCGTPEYLAP          252
        ************************************************************


4       EVLHKQPYDRTVDWWCLGAVLYEMLYGLPPFYSRNTAEMYDNILNKPLQLKPNITNSARH          420
3       EVLHKQPYDRTVDWWCLGAVLYEMLYGLPPFYSRNTAEMYDNILNKPLQLKPNITNSARH          326
1       EVLHKQPYDRTVDWWCLGAVLYEMLYGLPPFYSRNTAEMYDNILNKPLQLKPNITNSARH          340
2       EVLHKQPYDRTVDWWCLGAVLYEMLYGLPPFYSRNTAEMYDNILNKPLQLKPNITNSARH          312
        ************************************************************


4       LLEGLLQKDRTKRLGAKDDFMEIKSHIFFSLINWDDLINKKITPPFNPNVSGPSDLRHFD          480
3       LLEGLLQKDRTKRLGAKDDFMEIKSHIFFSLINWDDLINKKITPPFNPNVSGPSDLRHFD          386
1       LLEGLLQKDRTKRLGAKDDFMEIKSHIFFSLINWDDLINKKITPPFNPNVSGPSDLRHFD          400
2       LLEGLLQKDRTKRLGAKDDFMEIKSHIFFSLINWDDLINKKITPPFNPNVSGPSDLRHFD          372
        ************************************************************


4       PEFTEEPVPSSIGRSPDSILVTASVKEAAEAFLGFSYAPPMDSFL     525
3       PEFTEEPVPSSIGRSPDSILVTASVKEAAEAFLGFSYAPPMDSFL     431
1       PEFTEEPVPSSIGRSPDSILVTASVKEAAEAFLGFSYAPPMDSFL     445
2       PEFTEEPVPSSIGRSPDSILVTASVKEAAEAFLGFSYAPPMDSFL     417
        *******************************************
```

Human SGK1 protein sequences

Note: Transcripts from isoform 1 and isoform 5 generate the same N terminus but differ in that isoform 5 lacks an internal 44 residues present in all other proteins.

>NP_005618.2 serine/threonine-protein kinase Sgk1 isoform 1 [Homo sapiens]
MTVKTEAAKGTLTYSRMRGMVAILIAFMKQRRMGLNDFIQKIANNSYACKHPEVQSILKISQPQEPELMNANPSP
PPSPSQQINLGPSSNPHAKPSDFHFLKVIGKGSFGKVLLARHKAEEVFYAVKVLQKKAILKKKEEKHIMSERNVL
LKNVKHPFLVGLHFSFQTADKLYFVLDYINGGELFYHLQRERCFLEPRARFYAAEIASALGYLHSLNIVYRDLKP
ENILLDSQGHIVLTDFGLCKENIEHNSTTSTFCGTPEYLAPEVLHKQPYDRTVDWWCLGAVLYEMLYGLPPFYSR
NTAEMYDNILNKPLQLKPNITNSARHLLEGLLQKDRTKRLGAKDDFMEIKSHVFFSLINWDDLINKKITPPFNPN
VSGPNDLRHFDPEFTEEPVPNSIGKSPDSVLVTASVKEAAEAFLGFSYAPPTDSFL

>NP_001137148.1 serine/threonine-protein kinase Sgk1 isoform 2 [Homo sapiens]
MVNKDMNGFPVKKCSAFQFFKKRVRRWIKSPMVSVDKHQSPSLKYTGSSMVHIPPGEPDFESSLCQTCLGEHAFQ
RGVLPQENESCSWETQSGCEVREPCNHANILTKPDPRTFWTNDDPAFMKQRRMGLNDFIQKIANNSYACKHPEVQ
SILKISQPQEPELMNANPSPPPSPSQQINLGPSSNPHAKPSDFHFLKVIGKGSFGKVLLARHKAEEVFYAVKVLQ
KKAILKKKEEKHIMSERNVLLKNVKHPFLVGLHFSFQTADKLYFVLDYINGGELFYHLQRERCFLEPRARFYAAE
IASALGYLHSLNIVYRDLKPENILLDSQGHIVLTDFGLCKENIEHNSTTSTFCGTPEYLAPEVLHKQPYDRTVDW
WCLGAVLYEMLYGLPPFYSRNTAEMYDNILNKPLQLKPNITNSARHLLEGLLQKDRTKRLGAKDDFMEIKSHVFF
SLINWDDLINKKITPPFNPNVSGPNDLRHFDPEFTEEPVPNSIGKSPDSVLVTASVKEAAEAFLGFSYAPPTDSF
L

>NP_001137149.1 serine/threonine-protein kinase Sgk1 isoform 3 [Homo sapiens]
MSSQSSSLSEACSREAYSSHNWALPPASRSNPQPAYPWATRRMKEEAIKPPLKAFMKQRRMGLNDFIQKIANNSY
ACKHPEVQSILKISQPQEPELMNANPSPPPSPSQQINLGPSSNPHAKPSDFHFLKVIGKGSFGKVLLARHKAEEV
FYAVKVLQKKAILKKKEEKHIMSERNVLLKNVKHPFLVGLHFSFQTADKLYFVLDYINGGELFYHLQRERCFLEP
RARFYAAEIASALGYLHSLNIVYRDLKPENILLDSQGHIVLTDFGLCKENIEHNSTTSTFCGTPEYLAPEVLHKQ
PYDRTVDWWCLGAVLYEMLYGLPPFYSRNTAEMYDNILNKPLQLKPNITNSARHLLEGLLQKDRTKRLGAKDDFM
EIKSHVFFSLINWDDLINKKITPPFNPNVSGPNDLRHFDPEFTEEPVPNSIGKSPDSVLVTASVKEAAEAFLGFS
YAPPTDSFL

>NP_001137150.1 serine/threonine-protein kinase Sgk1 isoform 4 [Homo sapiens]
MGEMQGALARARLESLLRPRHKKRAEAQKRSESFLLSGLAFMKQRRMGLNDFIQKIANNSYACKHPEVQSILKIS
QPQEPELMNANPSPPPSPSQQINLGPSSNPHAKPSDFHFLKVIGKGSFGKVLLARHKAEEVFYAVKVLQKKAILK
KKEEKHIMSERNVLLKNVKHPFLVGLHFSFQTADKLYFVLDYINGGELFYHLQRERCFLEPRARFYAAEIASALG
YLHSLNIVYRDLKPENILLDSQGHIVLTDFGLCKENIEHNSTTSTFCGTPEYLAPEVLHKQPYDRTVDWWCLGAV
LYEMLYGLPPFYSRNTAEMYDNILNKPLQLKPNITNSARHLLEGLLQKDRTKRLGAKDDFMEIKSHVFFSLINWD
DLINKKITPPFNPNVSGPNDLRHFDPEFTEEPVPNSIGKSPDSVLVTASVKEAAEAFLGFSYAPPTDSFL

>NP_001278924.1 serine/threonine-protein kinase Sgk1 isoform 5 [Homo sapiens]
MTVKTEAAKGTLTYSRMRGMVAILIAFMKQRRMGLNDFIQKIANNSYACKHPEVQSILKISQPQEPELMNANPSP
PPSPSQQINLGPSSNPHAKPSDFHFLKVIGKGSFGKVLLARHKAEEVFYAVKVLQKKAILKKKELFYHLQRERCF
LEPRARFYAAEIASALGYLHSLNIVYRDLKPENILLDSQGHIVLTDFGLCKENIEHNSTTSTFCGTPEYLAPEVL
HKQPYDRTVDWWCLGAVLYEMLYGLPPFYSRNTAEMYDNILNKPLQLKPNITNSARHLLEGLLQKDRTKRLGAKD
DFMEIKSHVFFSLINWDDLINKKITPPFNPNVSGPNDLRHFDPEFTEEPVPNSIGKSPDSVLVTASVKEAAEAFL
GFSYAPPTDSFL

CLUSTAL O(1.2.4) multiple sequence alignment of human SGK1 protein sequences

```
2       MVNKDMNGFPVKKCSAFQFFKKRVRRWIKSPMVSVDKHQSPSLKYTGSSMVHIPPGEPDF 60
4       ------------------------------------------------------MGEM 4
3       ------------------------------------------------------MSSQ 4
1       ------------------------------------------------------------ 0
5       ------------------------------------------------------------ 0


2       ESSLCQTCLGEHAFQRGVLPQENESCSWETQSGCEVREPCNHANILTKPDPRTF------ 114
4       QGALA----------------------RARL---ESLLR---PRHK-------KRAEAQK 29
3       SSSLSE------------------ACSREAYSSHNWALP---PASRSNPQPAYPWATRRM 43
1       -----------------------------------MT----VKTEAAKGTLT----YS 15
5       -----------------------------------MT----VKTEAAKGTLT----YS 15


2       ----WTNDDPAFMKQRRMGLNDFIQKIANNSYACKHPEVQSILKISQPQEPELMNANPSP 170
4       RSESFLLSGLAFMKQRRMGLNDFIQKIANNSYACKHPEVQSILKISQPQEPELMNANPSP 89
3       KEEAIKPPLKAFMKQRRMGLNDFIQKIANNSYACKHPEVQSILKISQPQEPELMNANPSP 103
1       RMRGMVAILIAFMKQRRMGLNDFIQKIANNSYACKHPEVQSILKISQPQEPELMNANPSP 75
5       RMRGMVAILIAFMKQRRMGLNDFIQKIANNSYACKHPEVQSILKISQPQEPELMNANPSP 75
                 ************************************************


2       PPSPSQQINLGPSSNPHAKPSDFHFLKVIGKGSFGKVLLARHKAEEVFYAVKVLQKKAIL 230
4       PPSPSQQINLGPSSNPHAKPSDFHFLKVIGKGSFGKVLLARHKAEEVFYAVKVLQKKAIL 149
3       PPSPSQQINLGPSSNPHAKPSDFHFLKVIGKGSFGKVLLARHKAEEVFYAVKVLQKKAIL 163
1       PPSPSQQINLGPSSNPHAKPSDFHFLKVIGKGSFGKVLLARHKAEEVFYAVKVLQKKAIL 135
5       PPSPSQQINLGPSSNPHAKPSDFHFLKVIGKGSFGKVLLARHKAEEVFYAVKVLQKKAIL 135
        ************************************************************


2       KKKEEKHIMSERNVLLKNVKHPFLVGLHFSFQTADKLYFVLDYINGGELFYHLQRERCFL 290
4       KKKEEKHIMSERNVLLKNVKHPFLVGLHFSFQTADKLYFVLDYINGGELFYHLQRERCFL 209
3       KKKEEKHIMSERNVLLKNVKHPFLVGLHFSFQTADKLYFVLDYINGGELFYHLQRERCFL 223
1       KKKEEKHIMSERNVLLKNVKHPFLVGLHFSFQTADKLYFVLDYINGGELFYHLQRERCFL 195
5       KKK-------------------------------------------ELFYHLQRERCFL 151
        ***                                               *************


2       EPRARFYAAEIASALGYLHSLNIVYRDLKPENILLDSQGHIVLTDFGLCKENIEHNSTTS 350
4       EPRARFYAAEIASALGYLHSLNIVYRDLKPENILLDSQGHIVLTDFGLCKENIEHNSTTS 269
3       EPRARFYAAEIASALGYLHSLNIVYRDLKPENILLDSQGHIVLTDFGLCKENIEHNSTTS 283
1       EPRARFYAAEIASALGYLHSLNIVYRDLKPENILLDSQGHIVLTDFGLCKENIEHNSTTS 255
5       EPRARFYAAEIASALGYLHSLNIVYRDLKPENILLDSQGHIVLTDFGLCKENIEHNSTTS 211
        ************************************************************


2       TFCGTPEYLAPEVLHKQPYDRTVDWWCLGAVLYEMLYGLPPFYSRNTAEMYDNILNKPLQ 410
4       TFCGTPEYLAPEVLHKQPYDRTVDWWCLGAVLYEMLYGLPPFYSRNTAEMYDNILNKPLQ 329
3       TFCGTPEYLAPEVLHKQPYDRTVDWWCLGAVLYEMLYGLPPFYSRNTAEMYDNILNKPLQ 343
1       TFCGTPEYLAPEVLHKQPYDRTVDWWCLGAVLYEMLYGLPPFYSRNTAEMYDNILNKPLQ 315
5       TFCGTPEYLAPEVLHKQPYDRTVDWWCLGAVLYEMLYGLPPFYSRNTAEMYDNILNKPLQ 271
        ************************************************************


2       LKPNITNSARHLLEGLLQKDRTKRLGAKDDFMEIKSHVFFSLINWDDLINKKITPPFNPN 470
4       LKPNITNSARHLLEGLLQKDRTKRLGAKDDFMEIKSHVFFSLINWDDLINKKITPPFNPN 389
3       LKPNITNSARHLLEGLLQKDRTKRLGAKDDFMEIKSHVFFSLINWDDLINKKITPPFNPN 403
1       LKPNITNSARHLLEGLLQKDRTKRLGAKDDFMEIKSHVFFSLINWDDLINKKITPPFNPN 375
5       LKPNITNSARHLLEGLLQKDRTKRLGAKDDFMEIKSHVFFSLINWDDLINKKITPPFNPN 331
        ************************************************************


2       VSGPNDLRHFDPEFTEEPVPNSIGKSPDSVLVTASVKEAAEAFLGFSYAPPTDSFL     526
4       VSGPNDLRHFDPEFTEEPVPNSIGKSPDSVLVTASVKEAAEAFLGFSYAPPTDSFL     445
3       VSGPNDLRHFDPEFTEEPVPNSIGKSPDSVLVTASVKEAAEAFLGFSYAPPTDSFL     459
1       VSGPNDLRHFDPEFTEEPVPNSIGKSPDSVLVTASVKEAAEAFLGFSYAPPTDSFL     431
5       VSGPNDLRHFDPEFTEEPVPNSIGKSPDSVLVTASVKEAAEAFLGFSYAPPTDSFL     387
        ************************************************************
```

SGK1F forms

>CAR58098.1 serum/glucocorticoid regulated kinase 1 variant F [Homo sapiens]
MKPSKRFFISPPSSTAFMKQRRMGLNDFIQKIANNSYACKHPEVQSILKISQPQEPELMNANPSPPPSPSQQINL
GPSSNPHAKPSDFHFLKVIGKGSFGKVLLARHKAEEVFYAVKVLQKKAILKKKEEKHIMSERNVLLKNVKHPFLV
GLHFSFQTADKLYFVLDYINGGELFYHLQRERCFLEPRARFYAAEIASALGYLHSLNIVYRDLKPENILLDSQGH
IVLTDFGLCKENIEHNSTTSTFCGTPEYLAPEVLHKQPYDRTVDWWCLGAVLYEMLYGLPPFYSRNTAEMYDNIL
NKPLQLKPNITNSARHLLEGLLQKDRTKRLGAKDDFMEIKSHVFFSLINWDDLINKKITPPFNPNVSGPNDLRHF
DPEFTEEPVPNSIGKSPDSVLVTASVKEAAEAFLGFSYAPPTDSFL

>AdV-encoded_SGK1F
MDYKDDDDKKPSKRFFISPPSSTAFMKQRRMGLNDFIQKIANNSYACKHPEVQSILKISQPQEPELMNANPSPPP
SPSQQINLGPSSNPHAKPSDFHFLKVIGKGSFGKVLLARHKAEEVFYAVKVLQKKAILKKKEEKHIMSERNVLLK
NVKHPFLVGLHFSFQTADKLYFVLDYINGGELFYHLQRERCFLEPRARFYAAEIASALGYLHSLNIVYRDLKPEN
ILLDSQGHIVLTDFGLCKENIEHNSTTSTFCGTPEYLAPEVLHKQPYDRTVDWWCLGAVLYEMLYGLPPFYSRNT
AEMYDNILNKPLQLKPNITNSARHLLEGLLQKDRTKRLGAKDDFMEIKSHVFFSLINWDDLINKKITPPFNPNVS
GPNDLRHFDPEFTEEPVPNSIGKSPDSVLVTASVKEAAEAFLGFSYAPPTDSFL

CLUSTAL O(1.2.4) multiple sequence alignment of SGK1F (F) with human SGK1 isoform 1 (1)

```
F       ----------MKPSKRFFISPPSSTAFMKQRRMGLNDFIQKIANNSYACKHPEVQSILKI 50
1       MTVKTEAAKGTLTYSRMRGMVAILIAFMKQRRMGLNDFIQKIANNSYACKHPEVQSILKI 60
                     .*:        **********************************

F       SQPQEPELMNANPSPPPSPSQQINLGPSSNPHAKPSDFHFLKVIGKGSFGKVLLARHKAE 110
1       SQPQEPELMNANPSPPPSPSQQINLGPSSNPHAKPSDFHFLKVIGKGSFGKVLLARHKAE 120
        ************************************************************

F       EVFYAVKVLQKKAILKKKEEKHIMSERNVLLKNVKHPFLVGLHFSFQTADKLYFVLDYIN 170
1       EVFYAVKVLQKKAILKKKEEKHIMSERNVLLKNVKHPFLVGLHFSFQTADKLYFVLDYIN 180
        ************************************************************

F       GGELFYHLQRERCFLEPRARFYAAEIASALGYLHSLNIVYRDLKPENILLDSQGHIVLTD 230
1       GGELFYHLQRERCFLEPRARFYAAEIASALGYLHSLNIVYRDLKPENILLDSQGHIVLTD 240
        ************************************************************

F       FGLCKENIEHNSTTSTFCGTPEYLAPEVLHKQPYDRTVDWWCLGAVLYEMLYGLPPFYSR 290
1       FGLCKENIEHNSTTSTFCGTPEYLAPEVLHKQPYDRTVDWWCLGAVLYEMLYGLPPFYSR 300
        ************************************************************

F       NTAEMYDNILNKPLQLKPNITNSARHLLEGLLQKDRTKRLGAKDDFMEIKSHVFFSLINW 350
1       NTAEMYDNILNKPLQLKPNITNSARHLLEGLLQKDRTKRLGAKDDFMEIKSHVFFSLINW 360
        ************************************************************

F       DDLINKKITPPFNPNVSGPNDLRHFDPEFTEEPVPNSIGKSPDSVLVTASVKEAAEAFLG 410
1       DDLINKKITPPFNPNVSGPNDLRHFDPEFTEEPVPNSIGKSPDSVLVTASVKEAAEAFLG 420
        ************************************************************

F       FSYAPPTDSFL       421
1       FSYAPPTDSFL       431
        ***********
```

Appendix C. Publications

Toxicology Research

REVIEW

View Article Online
View Journal | View Issue

Cite this: *Toxicol. Res.*, 2015, 4, 203

An expandable donor-free supply of functional hepatocytes for toxicology

Philip M. E. Probert, Stephanie K. Meyer, Fouzeyyah Alsaeedi, Andrew A. Axon,† Emma A. Fairhall, Karen Wallace, Michelle Charles, Fiona Oakley, Paul A. Jowsey, Peter G. Blain and Matthew C. Wright*

The B-13 cell is a readily expandable rat pancreatic acinar-like cell that differentiates on simple plastic culture substrata into replicatively-senescent hepatocyte-like (B-13/H) cells in response to glucocorticoid exposure. B-13/H cells express a variety of liver-enriched and liver-specific genes, many at levels similar to hepatocytes *in vivo*. Furthermore, the B-13/H phenotype is maintained for at least several weeks *in vitro*, in contrast to normal hepatocytes which rapidly de-differentiate under the same simple – or even under more complex – culture conditions. The origin of the B-13 cell line and the current state of knowledge regarding differentiation to B-13/H cells are presented, followed by a review of recent advances in the use of B-13/H cells in a variety of toxicity endpoints. B-13 cells therefore offer Toxicologists a cost-effective and easy to use system to study a range of toxicologically-related questions. Dissecting the mechanism(s) regulating the formation of B-13/H cell may also increase the likelihood of engineering a human equivalent, providing Toxicologists with an expandable donor-free supply of functional rat and human hepatocytes, invaluable additions to the tool kit of *in vitro* toxicity tests.

Received 24th November 2014,
Accepted 27th January 2015
DOI: 10.1039/c4tx00214h
www.rsc.org/toxicology

Origin of the B-13 cell line

The AR42J-B13 (henceforth referred to as the B-13) cell line was sub-cloned from the rat adenocarcinoma AR42J cell line in the late 1970s. The AR42J cell line is an exocrine pancreatic adenocarcinoma cell line still used to the present day in basic exocrine pancreas research.[1–6] The AR42J cell line was derived from studies in which inbred Wistar/Lewis rats were treated with azaserine (*O*-diazoacetyl-L-serine).[7] Azaserine is a naturally occurring antibiotic first isolated from *Streptomyces fragilis*[8] that causes cytotoxicity in cells through at least 2 mechanisms:- inhibition of *N*-formylglycineamidine ribotide synthetase (PFAS, phosphoribosylformylglycinamidine

Institute Cellular Medicine, Level 4 Leech Building; Newcastle University, Framlington Place, Newcastle Upon Tyne, UK. E-mail: M.C.Wright@ncl.ac.uk
† Present address: Chemicals Regulation Directorate, Health and Safety Executive, 3 Peasholme Green, York, UK.

Pictured (left to right), Dr Hannah Walden, Dr Jess Dyson, Ally Leitch, Steph Meyer, Prof. Matt Wright, Dr Emma Fairhall, Dr Philip Probert and Prof. Peter Blain

The current members of the Toxicology group [liver theme] (pictured) lead by Prof. Matthew Wright at Newcastle University have spent several years working on in vitro alternatives for studying the response of the liver to acute and chronic injuries, including the B-13 cell line reviewed herein. The group are currently using this model as well as a variety of other cell types (hepatocytes, stellate cells, biliary epithelial cells, Kupffer cells) isolated from resected human liver in studies examining the potential link between environmental chemical exposures and primary biliary cirrhosis (currently funded by NIHR and Newcastle University).

PLOS ONE

RESEARCH ARTICLE

Expression of serine/threonine protein kinase SGK1F promotes an hepatoblast state in stem cells directed to differentiate into hepatocytes

Fouzeyyah Alsaeedi[1,2], Rachel Wilson[3], Charlotte Candlish[3], Ibrahim Ibrahim[1,4], Alistair C. Leitch[1], Tarek M. Abdelghany[1,5], Colin Wilson[4], Lyle Armstrong[3], Matthew C. Wright[1]*

1 Institute of Cellular Medicine, Newcastle University, Newcastle Upon Tyne, United Kingdom, 2 Faculty of Medical Sciences, Taif University, Taif, KSA, 3 Institute Human Genetics, Newcastle University, Newcastle Upon Tyne, United Kingdom, 4 Freeman Hospital, Newcastle Upon Tyne, United Kingdom, 5 Department of Pharmacology and Toxicology, Faculty of Pharmacy, Cairo University, Cairo, Egypt

* M.C.Wright@ncl.ac.uk

OPEN ACCESS

Citation: Alsaeedi F, Wilson R, Candlish C, Ibrahim I, Leitch AC, Abdelghany TM, et al. (2019) Expression of serine/threonine protein kinase SGK1F promotes an hepatoblast state in stem cells directed to differentiate into hepatocytes. PLoS ONE 14(6): e0218135. https://doi.org/10.1371/journal.pone.0218135

Editor: Yun-Wen Zheng, University of Tsukuba, JAPAN

Received: March 7, 2019

Accepted: May 25, 2019

Published: June 26, 2019

Data Availability Statement: All relevant data are within the manuscript, Supporting Information files and hosted at the following: PLOS2019 data file: https://data.ncl.ac.uk/s/151ae1af76a0929ba92a PLOS2019 Fig2apt2: https://data.ncl.ac.uk/s/2c05e0b75d62bfe02d52 PLOS2019 Fig2Apt1: https://data.ncl.ac.uk/s/6f94fb7815a7a62abbef PLOS2019 Fig2Apt4 sgk1 gPdx1 r V3: https://data.ncl.ac.uk/s/1933f57bdfd10940fb20 PLOS2019 Fig2Apt3 sgk1 ghnfa redv5.cz: https://data.ncl.ac.uk/s/8e9e912f1c6e3c431c2f

Abstract

The rat pancreatic AR42J-B13 (B-13) cell line differentiates into non-replicative hepatocyte-like (B-13/H) cells in response to glucocorticoid. Since this response is dependent on an induction of serine/threonine protein kinase 1 (SGK1), this may suggest that a general pivotal role for SGK1 in hepatocyte maturation. To test this hypothesis, the effects of expressing adenoviral-encoded flag tagged human SGK1F (AdV-SGK1F) was examined at 3 stages of human induced pluripotent stem cell (iPSC) differentiation to hepatocytes. B-13 cells infected with AdV-SGK1F in the absence of glucocorticoid resulted in expression of flag tagged SGK1F protein; increases in β-catenin phosphorylation; decreases in Tcf/Lef transcriptional activity; expression of hepatocyte marker genes and conversion of B-13 cells to a cell phenotype near-similar to B-13/H cells. Given this demonstration of functionality, iPSCs directed to differentiate towards hepatocyte-like cells using a standard protocol of chemical inhibitors and mixtures of growth factors were additionally infected with AdV-SGK1F, either at an early time point during differentiation to endoderm; during endoderm differentiation to anterior definitive endoderm and hepatoblasts and once converted to hepatocyte-like cells. SGK1F expression had no effect on differentiation to endoderm, likely due to low levels of expression. However, expression of SGK1F in both iPSCs-derived endoderm and hepatocyte-like cells both resulted in promotion of cells to an hepatoblast phenotype. These data demonstrate that SGK1 expression promotes an hepatoblast phenotype rather than maturation of human iPSC towards a mature hepatocyte phenotype and suggest a transient role for Sgk1 in promoting an hepatoblast state in B-13 trans-differentiation to B-13/H cells.

References

1. Evans, M.J. and Kaufman, M.H. (1981) 'Establishment in culture of pluripotential cells from mouse embryos', *Nature*, 292(5819), 154-6.
2. Thomson, J.A., Itskovitz-Eldor, J., Shapiro, S.S., Waknitz, M.A., Swiergiel, J.J., Marshall, V.S. and Jones, J.M. (1998) 'Embryonic stem cell lines derived from human blastocysts', *Science*, 282(5391), 1145-7.
3. Mitalipov, S. and Wolf, D. (2009) 'Totipotency, Pluripotency and Nuclear Reprogramming', *Adv Biochem Eng Biotechnol*, 114, 185-99.
4. Ulloa-Montoya, F., Verfaillie, C.M. and Hu, W.S. (2005) 'Culture systems for pluripotent stem cells', *J Biosci Bioeng*, 100(1), 12-27.
5. Pelton, T.A., Bettess, M.D., Lake, J., Rathjen, J. and Rathjen, P.D. (1998) 'Developmental complexity of early mammalian pluripotent cell populations in vivo and in vitro', *Reprod Fertil Dev*, 10(7-8), 535-49.
6. Karanes, C., Nelson, G.O., Chitphakdithai, P., Agura, E., Ballen, K.K., Bolan, C.D., Porter, D.L., Uberti, J.P., King, R.J. and Confer, D.L. (2008) 'Twenty years of unrelated donor hematopoietic cell transplantation for adult recipients facilitated by the National Marrow Donor Program', *Biol Blood Marrow Transplant*, 14(9 Suppl), 8-15.
7. Tuch, B.E. (2006) 'Stem cells--a clinical update', *Aust Fam Physician*, 35(9), 719-21.
8. Robinton, D.A. and Daley, G.Q. (2012) 'The promise of induced pluripotent stem cells in research and therapy', *Nature*, 481(7381), 295-305.
9. . Available at: https://vignette.wikia.nocookie.net/mmg-233-2014-genetics-genomics/images/f/f6/3D-Medical-Illustration-Pluripotent-Stem-Cells.jpg/revision/latest?cb=20141013062832 (Accessed: 21/02/2019).
10. Murry, C.E. and Keller, G. (2008) 'Differentiation of embryonic stem cells to clinically relevant populations: lessons from embryonic development', *Cell*, 132(4), 661-80.
11. Tam, P.P. and Behringer, R.R. (1997) 'Mouse gastrulation: the formation of a mammalian body plan', *Mech Dev*, 68(1-2), 3-25.
12. Hart, A.H., Hartley, L., Sourris, K., Stadler, E.S., Li, R., Stanley, E.G., Tam, P.P., Elefanty, A.G. and Robb, L. (2002) 'Mixl1 is required for axial mesendoderm morphogenesis and patterning in the murine embryo', *Development*, 129(15), 3597-608.
13. Kispert, A. and Herrmann, B.G. (1994) 'Immunohistochemical analysis of the Brachyury protein in wild-type and mutant mouse embryos', *Dev Biol*, 161(1), 179-93.
14. Kinder, S.J., Tsang, T.E., Wakamiya, M., Sasaki, H., Behringer, R.R., Nagy, A. and Tam, P.P. (2001) 'The organizer of the mouse gastrula is composed of a dynamic population of progenitor cells for the axial mesoderm', *Development*, 128(18), 3623-34.
15. Dush, M.K. and Martin, G.R. (1992) 'Analysis of mouse Evx genes: Evx-1 displays graded expression in the primitive streak', *Dev Biol*, 151(1), 273-87.
16. Forlani, S., Lawson, K.A. and Deschamps, J. (2003) 'Acquisition of Hox codes during gastrulation and axial elongation in the mouse embryo', *Development*, 130(16), 3807-19.
17. Kinder, S.J., Tsang, T.E., Quinlan, G.A., Hadjantonakis, A.K., Nagy, A. and Tam, P.P. (1999) 'The orderly allocation of mesodermal cells to the extraembryonic structures and the anteroposterior axis during gastrulation of the mouse embryo', *Development*, 126(21), 4691-701.
18. Yamaguchi, T.P. (2001) 'Heads or tails: Wnts and anterior-posterior patterning', *Curr Biol*, 11(17), R713-24.
19. Hogan, B.L. (1996) 'Bone morphogenetic proteins in development', *Curr Opin Genet Dev*, 6(4), 432-8.

20. Conlon, F.L., Lyons, K.M., Takaesu, N., Barth, K.S., Kispert, A., Herrmann, B. and Robertson, E.J. (1994) 'A primary requirement for nodal in the formation and maintenance of the primitive streak in the mouse', *Development*, 120(7), 1919-28.
21. Schier, A.F. and Shen, M.M. (2000) 'Nodal signalling in vertebrate development', *Nature*, 403(6768), 385-9.
22. Gadue, P., Huber, T.L., Nostro, M.C., Kattman, S. and Keller, G.M. (2005) 'Germ layer induction from embryonic stem cells', *Exp Hematol*, 33(9), 955-64.
23. Keirstead, H.S. (2001) 'Stem cell transplantation into the central nervous system and the control of differentiation', *Journal of neuroscience research*, 63(3), 233-236.
24. Wagers, A.J. and Weissman, I.L. (2004) 'Plasticity of adult stem cells', *Cell*, 116(5), 639-48.
25. Leblond, C.P. (1964) 'CLASSIFICATION OF CELL POPULATIONS ON THE BASIS OF THEIR PROLIFERATIVE BEHAVIOR', *Natl Cancer Inst Monogr*, 14, 119-50.
26. health, N.i.o. (2018) *Stem Cell Basics IV*. Available at: https://stemcells.nih.gov/info/basics/4.htm (Accessed: 25sep).
27. Muller-Sieburg, C.E., Cho, R.H., Thoman, M., Adkins, B. and Sieburg, H.B. (2002) 'Deterministic regulation of hematopoietic stem cell self-renewal and differentiation', *Blood*, 100(4), 1302-9.
28. Lewis, P.D. (1968) 'Mitotic activity in the primate subependymal layer and the genesis of gliomas', *Nature*, 217(5132), 974-5.
29. Bryder, D., Rossi, D.J. and Weissman, I.L. (2006) 'Hematopoietic stem cells: the paradigmatic tissue-specific stem cell', *Am J Pathol*, 169(2), 338-46.
30. Shi, S., Bartold, P.M., Miura, M., Seo, B.M., Robey, P.G. and Gronthos, S. (2005) 'The efficacy of mesenchymal stem cells to regenerate and repair dental structures', *Orthod Craniofac Res*, 8(3), 191-9.
31. Petersen, B.E., Goff, J.P., Greenberger, J.S. and Michalopoulos, G.K. (1998) 'Hepatic oval cells express the hematopoietic stem cell marker Thy-1 in the rat', *Hepatology*, 27(2), 433-45.
32. Liu, S., Dontu, G. and Wicha, M.S. (2005) 'Mammary stem cells, self-renewal pathways, and carcinogenesis', *Breast Cancer Res*, 7(3), 86-95.
33. Pan, G., Mu, Y., Hou, L. and Liu, J. (2019) *Annales d'endocrinologie*. Elsevier.
34. National Institutes of Health, U.S.D.o.H.a.H.S. (2016) *NIH Stem Cell Information* Available at: https://stemcells.nih.gov/info/basics/4.htm (Accessed: 17/04/2019).
35. Goldthwaite Jr, C.A. (2007) 'Mending a broken heart: Stem cells and cardiac repair', *NIH report*.
36. Jensen, J.N., Cameron, E., Garay, M.V., Starkey, T.W., Gianani, R. and Jensen, J. (2005) 'Recapitulation of elements of embryonic development in adult mouse pancreatic regeneration', *Gastroenterology*, 128(3), 728-41.
37. Krause, D.S., Theise, N.D., Collector, M.I., Henegariu, O., Hwang, S., Gardner, R., Neutzel, S. and Sharkis, S.J. (2001) 'Multi-organ, multi-lineage engraftment by a single bone marrow-derived stem cell', *Cell*, 105(3), 369-77.
38. Germain, L., Noel, M., Gourdeau, H. and Marceau, N. (1988) 'Promotion of growth and differentiation of rat ductular oval cells in primary culture', *Cancer Res*, 48(2), 368-78.
39. Sirica, A.E., Mathis, G.A., Sano, N. and Elmore, L.W. (1990) 'Isolation, culture, and transplantation of intrahepatic biliary epithelial cells and oval cells', *Pathobiology*, 58(1), 44-64.
40. Dabeva, M.D. and Shafritz, D.A. (1993) 'Activation, proliferation, and differentiation of progenitor cells into hepatocytes in the D-galactosamine model of liver regeneration', *Am J Pathol*, 143(6), 1606-20.
41. Lazaro, C.A., Rhim, J.A., Yamada, Y. and Fausto, N. (1998) 'Generation of hepatocytes from oval cell precursors in culture', *Cancer Res*, 58(23), 5514-22.

42. Lagasse, E., Connors, H., Al-Dhalimy, M., Reitsma, M., Dohse, M., Osborne, L., Wang, X., Finegold, M., Weissman, I.L. and Grompe, M. (2000) 'Purified hematopoietic stem cells can differentiate into hepatocytes in vivo', *Nat Med*, 6(11), 1229-34.
43. Smith, A.G., Heath, J.K., Donaldson, D.D., Wong, G.G., Moreau, J., Stahl, M. and Rogers, D. (1988) 'Inhibition of pluripotential embryonic stem cell differentiation by purified polypeptides', *Nature*, 336(6200), 688-90.
44. Wilmut, I., Schnieke, A.E., McWhir, J., Kind, A.J. and Campbell, K.H. (1997) 'Viable offspring derived from fetal and adult mammalian cells', *Nature*, 385(6619), 810-3.
45. Tada, M., Takahama, Y., Abe, K., Nakatsuji, N. and Tada, T. (2001) 'Nuclear reprogramming of somatic cells by in vitro hybridization with ES cells', *Curr Biol*, 11(19), 1553-8.
46. Takahashi, K. and Yamanaka, S. (2006) 'Induction of pluripotent stem cells from mouse embryonic and adult fibroblast cultures by defined factors', *Cell*, 126(4), 663-76.
47. Takahashi, K., Tanabe, K., Ohnuki, M., Narita, M., Ichisaka, T., Tomoda, K. and Yamanaka, S. (2007) 'Induction of pluripotent stem cells from adult human fibroblasts by defined factors', *Cell*, 131(5), 861-72.
48. Yu, J., Vodyanik, M.A., Smuga-Otto, K., Antosiewicz-Bourget, J., Frane, J.L., Tian, S., Nie, J., Jonsdottir, G.A., Ruotti, V., Stewart, R., Slukvin, II and Thomson, J.A. (2007) 'Induced pluripotent stem cell lines derived from human somatic cells', *Science*, 318(5858), 1917-20.
49. Lowry, W.E., Richter, L., Yachechko, R., Pyle, A.D., Tchieu, J., Sridharan, R., Clark, A.T. and Plath, K. (2008) 'Generation of human induced pluripotent stem cells from dermal fibroblasts', *Proc Natl Acad Sci U S A*, 105(8), 2883-8.
50. Vierbuchen, T., Ostermeier, A., Pang, Z.P., Kokubu, Y., Sudhof, T.C. and Wernig, M. (2010) 'Direct conversion of fibroblasts to functional neurons by defined factors', *Nature*, 463(7284), 1035-41.
51. Huang, P., He, Z., Ji, S., Sun, H., Xiang, D., Liu, C., Hu, Y., Wang, X. and Hui, L. (2011) 'Induction of functional hepatocyte-like cells from mouse fibroblasts by defined factors', *Nature*, 475(7356), 386-9.
52. Hannan, N.R.F., Segeritz, C.P., Touboul, T. and Vallier, L. (2013b) 'Production of hepatocyte-like cells from human pluripotent stem cells', *Nature Protocols*, 8(2), 430-437.
53. Ieda, M., Fu, J.D., Delgado-Olguin, P., Vedantham, V., Hayashi, Y., Bruneau, B.G. and Srivastava, D. (2010) 'Direct reprogramming of fibroblasts into functional cardiomyocytes by defined factors', *Cell*, 142(3), 375-86.
54. Szabo, E., Rampalli, S., Risueno, R.M., Schnerch, A., Mitchell, R., Fiebig-Comyn, A., Levadoux-Martin, M. and Bhatia, M. (2010) 'Direct conversion of human fibroblasts to multilineage blood progenitors', *Nature*, 468(7323), 521-6.
55. Chun, Y.S., Chaudhari, P. and Jang, Y.Y. (2010) 'Applications of patient-specific induced pluripotent stem cells; focused on disease modeling, drug screening and therapeutic potentials for liver disease', *Int J Biol Sci*, 6(7), 796-805.
56. Sommer, C.A., Stadtfeld, M., Murphy, G.J., Hochedlinger, K., Kotton, D.N. and Mostoslavsky, G. (2009) 'Induced pluripotent stem cell generation using a single lentiviral stem cell cassette', *Stem Cells*, 27(3), 543-549.
57. Yang, Y., Goldstein, B.G., Chao, H.H. and Katz, J.P. (2005) 'KLF4 and KLF5 regulate proliferation, apoptosis and invasion in esophageal cancer cells', *Cancer Biol Ther*, 4(11), 1216-21.
58. Ruggero, D. (2009) 'The role of Myc-induced protein synthesis in cancer', *Cancer Res*, 69(23), 8839-43.
59. Wernig, M., Zhao, J.P., Pruszak, J., Hedlund, E., Fu, D., Soldner, F., Broccoli, V., Constantine-Paton, M., Isacson, O. and Jaenisch, R. (2008) 'Neurons derived from reprogrammed fibroblasts functionally integrate into the fetal brain and improve

symptoms of rats with Parkinson's disease', *Proc Natl Acad Sci U S A*, 105(15), 5856-61.

60. Ranzani, M., Annunziato, S., Adams, D.J. and Montini, E. (2013) 'Cancer gene discovery: exploiting insertional mutagenesis', *Mol Cancer Res*, 11(10), 1141-58.
61. Nalla, A.K., Williams, T.F., Collins, C.P., Rae, D.T. and Trobridge, G.D. (2016) 'Lentiviral vector-mediated insertional mutagenesis screen identifies genes that influence androgen independent prostate cancer progression and predict clinical outcome', *Mol Carcinog*, 55(11), 1761-1771.
62. Huangfu, D., Osafune, K., Maehr, R., Guo, W., Eijkelenboom, A., Chen, S., Muhlestein, W. and Melton, D.A. (2008) 'Induction of pluripotent stem cells from primary human fibroblasts with only Oct4 and Sox2', *Nat Biotechnol*, 26(11), 1269-75.
63. Okita, K., Matsumura, Y., Sato, Y., Okada, A., Morizane, A., Okamoto, S., Hong, H., Nakagawa, M., Tanabe, K., Tezuka, K., Shibata, T., Kunisada, T., Takahashi, M., Takahashi, J., Saji, H. and Yamanaka, S. (2011a) 'A more efficient method to generate integration-free human iPS cells', *Nat Methods*, 8(5), 409-12.
64. Stadtfeld, M., Nagaya, M., Utikal, J., Weir, G. and Hochedlinger, K. (2008) 'Induced pluripotent stem cells generated without viral integration', *Science*, 322(5903), 945-9.
65. Fusaki, N., Ban, H., Nishiyama, A., Saeki, K. and Hasegawa, M. (2009) 'Efficient induction of transgene-free human pluripotent stem cells using a vector based on Sendai virus, an RNA virus that does not integrate into the host genome', *Proc Jpn Acad Ser B Phys Biol Sci*, 85(8), 348-62.
66. Warren, L., Manos, P.D., Ahfeldt, T., Loh, Y.H., Li, H., Lau, F., Ebina, W., Mandal, P.K., Smith, Z.D., Meissner, A., Daley, G.Q., Brack, A.S., Collins, J.J., Cowan, C., Schlaeger, T.M. and Rossi, D.J. (2010) 'Highly efficient reprogramming to pluripotency and directed differentiation of human cells with synthetic modified mRNA', *Cell Stem Cell*, 7(5), 618-30.
67. Anokye-Danso, F., Trivedi, C.M., Juhr, D., Gupta, M., Cui, Z., Tian, Y., Zhang, Y., Yang, W., Gruber, P.J., Epstein, J.A. and Morrisey, E.E. (2011) 'Highly efficient miRNA-mediated reprogramming of mouse and human somatic cells to pluripotency', *Cell Stem Cell*, 8(4), 376-88.
68. Maury, Y., Gauthier, M., Peschanski, M. and Martinat, C. (2012) 'Human pluripotent stem cells for disease modelling and drug screening', *Bioessays*, 34(1), 61-71.
69. Dimos, J.T., Rodolfa, K.T., Niakan, K.K., Weisenthal, L.M., Mitsumoto, H., Chung, W., Croft, G.F., Saphier, G., Leibel, R., Goland, R., Wichterle, H., Henderson, C.E. and Eggan, K. (2008) 'Induced pluripotent stem cells generated from patients with ALS can be differentiated into motor neurons', *Science*, 321(5893), 1218-21.
70. Ebert, A.D., Yu, J., Rose, F.F., Jr., Mattis, V.B., Lorson, C.L., Thomson, J.A. and Svendsen, C.N. (2009) 'Induced pluripotent stem cells from a spinal muscular atrophy patient', *Nature*, 457(7227), 277-80.
71. Ohuchi, K., Funato, M., Kato, Z., Seki, J., Kawase, C., Tamai, Y., Ono, Y., Nagahara, Y., Noda, Y., Kameyama, T., Ando, S., Tsuruma, K., Shimazawa, M., Hara, H. and Kaneko, H. (2016) 'Established Stem Cell Model of Spinal Muscular Atrophy Is Applicable in the Evaluation of the Efficacy of Thyrotropin-Releasing Hormone Analog', *Stem Cells Transl Med*, 5(2), 152-63.
72. Lee, G., Papapetrou, E.P., Kim, H., Chambers, S.M., Tomishima, M.J., Fasano, C.A., Ganat, Y.M., Menon, J., Shimizu, F., Viale, A., Tabar, V., Sadelain, M. and Studer, L. (2009) 'Modeling Pathogenesis and Treatment of Familial Dysautonomia using Patient Specific iPSCs', *Nature*, 461(7262), 402-406.
73. Stadtfeld, M. and Hochedlinger, K. (2010) 'Induced pluripotency: history, mechanisms, and applications', *Genes Dev*, 24(20), 2239-63.

74. de Lazaro, I., Yilmazer, A. and Kostarelos, K. (2014) 'Induced pluripotent stem (iPS) cells: a new source for cell-based therapeutics?', *Journal of Controlled Release*, 185, 37-44.
75. Modric, J. *Liver*. Available at: https://www.ehealthstar.com/anatomy/liver (Accessed: 22/02/2019).
76. Katz, N., Teutsch, H.F., Jungermann, K. and Sasse, D. (1977) 'Heterogeneous reciprocal localization of fructose-1,6-bisphosphatase and of glucokinase in microdissected periportal and perivenous rat liver tissue', *FEBS Lett*, 83(2), 272-6.
77. Rappaport, A.M., Borowy, Z.J., Lougheed, W.M. and Lotto, W.N. (1954) 'Subdivision of hexagonal liver lobules into a structural and functional unit; role in hepatic physiology and pathology', *Anat Rec*, 119(1), 11-33.
78. Blouin, A., Bolender, R.P. and Weibel, E.R. (1977) 'Distribution of organelles and membranes between hepatocytes and nonhepatocytes in the rat liver parenchyma. A stereological study', *J Cell Biol*, 72(2), 441-55.
79. Braet, F. and Wisse, E. (2002) 'Structural and functional aspects of liver sinusoidal endothelial cell fenestrae: a review', *Comp Hepatol*, 1(1), 1.
80. Godoy, P., Hewitt, N.J., Albrecht, U., Andersen, M.E., Ansari, N., Bhattacharya, S., Bode, J.G., Bolleyn, J., Borner, C., Bottger, J., Braeuning, A., Budinsky, R.A., Burkhardt, B., Cameron, N.R., Camussi, G., Cho, C.S., Choi, Y.J., Craig Rowlands, J., Dahmen, U., Damm, G., Dirsch, O., Donato, M.T., Dong, J., Dooley, S., Drasdo, D., Eakins, R., Ferreira, K.S., Fonsato, V., Fraczek, J., Gebhardt, R., Gibson, A., Glanemann, M., Goldring, C.E., Gomez-Lechon, M.J., Groothuis, G.M., Gustavsson, L., Guyot, C., Hallifax, D., Hammad, S., Hayward, A., Haussinger, D., Hellerbrand, C., Hewitt, P., Hoehme, S., Holzhutter, H.G., Houston, J.B., Hrach, J., Ito, K., Jaeschke, H., Keitel, V., Kelm, J.M., Kevin Park, B., Kordes, C., Kullak-Ublick, G.A., LeCluyse, E.L., Lu, P., Luebke-Wheeler, J., Lutz, A., Maltman, D.J., Matz-Soja, M., McMullen, P., Merfort, I., Messner, S., Meyer, C., Mwinyi, J., Naisbitt, D.J., Nussler, A.K., Olinga, P., Pampaloni, F., Pi, J., Pluta, L., Przyborski, S.A., Ramachandran, A., Rogiers, V., Rowe, C., Schelcher, C., Schmich, K., Schwarz, M., Singh, B., Stelzer, E.H., Stieger, B., Stober, R., Sugiyama, Y., Tetta, C., Thasler, W.E., Vanhaecke, T., Vinken, M., Weiss, T.S., Widera, A., Woods, C.G., Xu, J.J., Yarborough, K.M. and Hengstler, J.G. (2013) 'Recent advances in 2D and 3D in vitro systems using primary hepatocytes, alternative hepatocyte sources and non-parenchymal liver cells and their use in investigating mechanisms of hepatotoxicity, cell signaling and ADME', *Arch Toxicol*, 87(8), 1315-530.
81. Komal Arora, M.D. (2012) *Liver and intrahepatic bile ducts - nontumor General Normal histology* Available at: http://www.pathologyoutlines.com/topic/livernormalhistology.html (Accessed: 26/02/2019).
82. Jungermann, K. and Katz, N. (1989) 'Functional specialization of different hepatocyte populations', *Physiol Rev*, 69(3), 708-64.
83. Jungermann, K. and Kietzmann, T. (2000) 'Oxygen: modulator of metabolic zonation and disease of the liver', *Hepatology*, 31(2), 255-60.
84. Jungermann, K. (1988) *Seminars in liver disease*. © 1988 by Thieme Medical Publishers, Inc.
85. Torre, C., Perret, C. and Colnot, S. (2010) 'Molecular determinants of liver zonation', *Prog Mol Biol Transl Sci*, 97, 127-50.
86. Wallace, K., Burt, A.D. and Wright, M.C. (2008) 'Liver fibrosis', *Biochemical Journal*, 411(1), 1-18.
87. Benhamouche, S., Decaens, T., Godard, C., Chambrey, R., Rickman, D.S., Moinard, C., Vasseur-Cognet, M., Kuo, C.J., Kahn, A. and Perret, C. (2006) 'Apc tumor suppressor gene is the "zonation-keeper" of mouse liver', *Dev Cell*, 10(6), 759-770.

88. Wang, B., Zhao, L., Fish, M., Logan, C.Y. and Nusse, R. (2015) 'Self-renewing diploid Axin2(+) cells fuel homeostatic renewal of the liver', *Nature*, 524(7564), 180-5.
89. Burke, Z.D., Reed, K.R., Phesse, T.J., Sansom, O.J., Clarke, A.R. and Tosh, D. (2009) 'Liver zonation occurs through a beta-catenin-dependent, c-Myc-independent mechanism', *Gastroenterology*, 136(7), 2316-2324.e1-3.
90. McEnerney, L., Duncan, K., Bang, B.-R., Elmasry, S., Li, M., Miki, T., Ramakrishnan, S.K., Shah, Y.M. and Saito, T. (2017) 'Dual modulation of human hepatic zonation via canonical and non-canonical Wnt pathways', *Exp Mol Med*, 49(12), e413.
91. Colnot, S. and Perret, C. (2011) 'Liver Zonation', in Monga, S.P.S. (ed.) *Molecular Pathology of Liver Diseases*. Boston, MA: Springer US, 7-16.
92. Chiang, J. (2014) 'Liver Physiology: Metabolism and Detoxification'.
93. Russell, D.W. (2009) 'Fifty years of advances in bile acid synthesis and metabolism', *J Lipid Res*, 50 Suppl, S120-5.
94. Chiang, J.Y.L. and Ferrell, J.M. (2018) 'Bile Acid Metabolism in Liver Pathobiology', *Gene Expr*, 18(2), 71-87.
95. Schlichting, I., Berendzen, J., Chu, K., Stock, A.M., Maves, S.A., Benson, D.E., Sweet, R.M., Ringe, D., Petsko, G.A. and Sligar, S.G. (2000) 'The catalytic pathway of cytochrome p450cam at atomic resolution', *Science*, 287(5458), 1615-22.
96. Anzenbacher, P. and Anzenbacherova, E. (2001) 'Cytochromes P450 and metabolism of xenobiotics', *Cell Mol Life Sci*, 58(5-6), 737-47.
97. Guengerich, F.P. (2008) 'Cytochrome P450 and Chemical Toxicology', *Chem Res Toxicol*, 21(1), 70-83.
98. Chiang, J. (2014) 'Liver Physiology: MetaboLism and Detoxification', in, 1770-1782.
99. Siegel, G.J. (1999) *Basic neurochemistry: molecular, cellular and medical aspects*.
100. Krishna, M. (2013) 'Microscopic anatomy of the liver', *Clinical Liver Disease*, 2(S1), S4-S7.
101. Gissen, P. and Arias, I.M. (2015) 'Structural and functional hepatocyte polarity and liver disease', *J Hepatol*, 63(4), 1023-37.
102. Glaser, S.S., Gaudio, E., Miller, T., Alvaro, D. and Alpini, G. (2009) 'Cholangiocyte proliferation and liver fibrosis', *Expert Rev Mol Med*, 11, e7.
103. Park, S.M. (2012) 'The crucial role of cholangiocytes in cholangiopathies', *Gut Liver*, 6(3), 295-304.
104. Senoo, H. (2004) 'Structure and function of hepatic stellate cells', *Med Electron Microsc*, 37(1), 3-15.
105. Sleyster, E.C. and Knook, D.L. (1982) 'Relation between localization and function of rat liver Kupffer cells', *Lab Invest*, 47(5), 484-90.
106. Ramachandran, P. and Iredale, J.P. (2012) 'Macrophages: central regulators of hepatic fibrogenesis and fibrosis resolution', *J Hepatol*, 56(6), 1417-9.
107. Ju, C., Reilly, T.P., Bourdi, M., Radonovich, M.F., Brady, J.N., George, J.W. and Pohl, L.R. (2002) 'Protective role of Kupffer cells in acetaminophen-induced hepatic injury in mice', *Chem Res Toxicol*, 15(12), 1504-13.
108. Roberts, R.A., Ganey, P.E., Ju, C., Kamendulis, L.M., Rusyn, I. and Klaunig, J.E. (2007) 'Role of the Kupffer cell in mediating hepatic toxicity and carcinogenesis', *Toxicol Sci*, 96(1), 2-15.
109. Fraser, R., Dobbs, B.R. and Rogers, G.W. (1995) 'Lipoproteins and the liver sieve: the role of the fenestrated sinusoidal endothelium in lipoprotein metabolism, atherosclerosis, and cirrhosis', *Hepatology*, 21(3), 863-74.
110. Wisse, E., De Zanger, R.B., Charels, K., Van Der Smissen, P. and McCuskey, R.S. (1985) 'The liver sieve: considerations concerning the structure and function of endothelial fenestrae, the sinusoidal wall and the space of Disse', *Hepatology*, 5(4), 683-92.

111. Sorensen, K.K., McCourt, P., Berg, T., Crossley, C., Le Couteur, D., Wake, K. and Smedsrod, B. (2012) 'The scavenger endothelial cell: a new player in homeostasis and immunity', *Am J Physiol Regul Integr Comp Physiol*, 303(12), R1217-30.
112. Rossant, J. (2004) 'Lineage development and polar asymmetries in the peri-implantation mouse blastocyst', *Semin Cell Dev Biol*, 15(5), 573-81.
113. Lowe, L.A., Yamada, S. and Kuehn, M.R. (2001) 'Genetic dissection of nodal function in patterning the mouse embryo', *Development*, 128(10), 1831-43.
114. Zaret, K.S. (2002) 'Regulatory phases of early liver development: paradigms of organogenesis', *Nat Rev Genet*, 3(7), 499-512.
115. Tam, P.P., Kanai-Azuma, M. and Kanai, Y. (2003) 'Early endoderm development in vertebrates: lineage differentiation and morphogenetic function', *Curr Opin Genet Dev*, 13(4), 393-400.
116. Vincent, S.D., Dunn, N.R., Hayashi, S., Norris, D.P. and Robertson, E.J. (2003) 'Cell fate decisions within the mouse organizer are governed by graded Nodal signals', *Genes Dev*, 17(13), 1646-62.
117. Zorn, A.M. and Wells, J.M. (2007) 'Molecular basis of vertebrate endoderm development', *Int Rev Cytol*, 259, 49-111.
118. Dufort, D., Schwartz, L., Harpal, K. and Rossant, J. (1998) 'The transcription factor HNF3beta is required in visceral endoderm for normal primitive streak morphogenesis', *Development*, 125(16), 3015-25.
119. Moore-Scott, B.A., Opoka, R., Lin, S.C., Kordich, J.J. and Wells, J.M. (2007) 'Identification of molecular markers that are expressed in discrete anterior-posterior domains of the endoderm from the gastrula stage to mid-gestation', *Dev Dyn*, 236(7), 1997-2003.
120. Wells, J.M. and Melton, D.A. (2000) 'Early mouse endoderm is patterned by soluble factors from adjacent germ layers', *Development*, 127(8), 1563-72.
121. Chalmers, A.D. and Slack, J.M. (2000) 'The Xenopus tadpole gut: fate maps and morphogenetic movements', *Development*, 127(2), 381-92.
122. Tremblay, K.D. and Zaret, K.S. (2005) 'Distinct populations of endoderm cells converge to generate the embryonic liver bud and ventral foregut tissues', *Dev Biol*, 280(1), 87-99.
123. Dessimoz, J., Opoka, R., Kordich, J.J., Grapin-Botton, A. and Wells, J.M. (2006) 'FGF signaling is necessary for establishing gut tube domains along the anterior-posterior axis in vivo', *Mech Dev*, 123(1), 42-55.
124. McLin, V.A., Rankin, S.A. and Zorn, A.M. (2007) 'Repression of Wnt/beta-catenin signaling in the anterior endoderm is essential for liver and pancreas development', *Development*, 134(12), 2207-17.
125. Poulain, M. and Ober, E.A. (2011) 'Interplay between Wnt2 and Wnt2bb controls multiple steps of early foregut-derived organ development', *Development*, 138(16), 3557-3568.
126. Zorn, A. (2008) 'Liver development. StemBook', in *Cambridge: The Stem Cell Research Community*.
127. Okada, T. (1954) 'Experimental studies on the differentiation of the endodermal organs in Amphibia. I. Significance of the mesenchymatous tissue to the differentiation of the presumptive endo-derm', *Mem Coll Sci Univ Kyoto Ser B*, 21, 1-6.
128. Fukuda-Taira, S. (1981) 'Hepatic induction in the avian embryo: specificity of reactive endoderm and inductive mesoderm', *J Embryol Exp Morphol*, 63, 111-25.
129. Bossard, P. and Zaret, K.S. (1998) 'GATA transcription factors as potentiators of gut endoderm differentiation', *Development*, 125(24), 4909-17.
130. Cirillo, L.A., Lin, F.R., Cuesta, I., Friedman, D., Jarnik, M. and Zaret, K.S. (2002) 'Opening of compacted chromatin by early developmental transcription factors HNF3 (FoxA) and GATA-4', *Mol Cell*, 9(2), 279-89.

131. Bossard, P. and Zaret, K.S. (2000) 'Repressive and restrictive mesodermal interactions with gut endoderm: possible relation to Meckel's Diverticulum', *Development*, 127(22), 4915-23.
132. Shifley, E.T., Kenny, A.P., Rankin, S.A. and Zorn, A.M. (2012) 'Prolonged FGF signaling is necessary for lung and liver induction in Xenopus', *BMC Dev Biol*, 12, 27.
133. Rossi, J.M., Dunn, N.R., Hogan, B.L. and Zaret, K.S. (2001) 'Distinct mesodermal signals, including BMPs from the septum transversum mesenchyme, are required in combination for hepatogenesis from the endoderm', *Genes Dev*, 15(15), 1998-2009.
134. Calmont, A., Wandzioch, E., Tremblay, K.D., Minowada, G., Kaestner, K.H., Martin, G.R. and Zaret, K.S. (2006) 'An FGF response pathway that mediates hepatic gene induction in embryonic endoderm cells', *Dev Cell*, 11(3), 339-48.
135. Zorn, A.M. and Wells, J.M. (2009) 'Vertebrate endoderm development and organ formation', *Annu Rev Cell Dev Biol*, 25, 221-51.
136. Asrani, S.K., Devarbhavi, H., Eaton, J. and Kamath, P.S. (2019) 'Burden of liver diseases in the world', *J Hepatol*, 70(1), 151-171.
137. Anthony, P.P., Ishak, K.G., Nayak, N.C., Poulsen, H.E., Scheuer, P.J. and Sobin, L.H. (1977) 'The morphology of cirrhosis: definition, nomenclature, and classification', *Bull World Health Organ*, 55(4), 521-40.
138. Bilzer, M., Roggel, F. and Gerbes, A.L. (2006) 'Role of Kupffer cells in host defense and liver disease', *Liver Int*, 26(10), 1175-86.
139. Canbay, A., Feldstein, A.E., Higuchi, H., Werneburg, N., Grambihler, A., Bronk, S.F. and Gores, G.J. (2003) 'Kupffer cell engulfment of apoptotic bodies stimulates death ligand and cytokine expression', *Hepatology*, 38(5), 1188-98.
140. Iredale, J.P., Benyon, R.C., Pickering, J., McCullen, M., Northrop, M., Pawley, S., Hovell, C. and Arthur, M.J. (1998) 'Mechanisms of spontaneous resolution of rat liver fibrosis. Hepatic stellate cell apoptosis and reduced hepatic expression of metalloproteinase inhibitors', *J Clin Invest*, 102(3), 538-49.
141. Xiao, J.C., Ruck, P., Adam, A., Wang, T.X. and Kaiserling, E. (2003) 'Small epithelial cells in human liver cirrhosis exhibit features of hepatic stem-like cells: immunohistochemical, electron microscopic and immunoelectron microscopic findings', *Histopathology*, 42(2), 141-9.
142. Santoni-Rugiu, E., Jelnes, P., Thorgeirsson, S.S. and Bisgaard, H.C. (2005) 'Progenitor cells in liver regeneration: molecular responses controlling their activation and expansion', *Apmis*, 113(11-12), 876-902.
143. Falkowski, O., An, H.J., Ianus, I.A., Chiriboga, L., Yee, H., West, A.B. and Theise, N.D. (2003) 'Regeneration of hepatocyte 'buds' in cirrhosis from intrabiliary stem cells', *J Hepatol*, 39(3), 357-64.
144. Kamiya, A., Kakinuma, S., Yamazaki, Y. and Nakauchi, H. (2009) 'Enrichment and clonal culture of progenitor cells during mouse postnatal liver development in mice', *Gastroenterology*, 137(3), 1114-26, 1126.e1-14.
145. Lee, J.S., Heo, J., Libbrecht, L., Chu, I.S., Kaposi-Novak, P., Calvisi, D.F., Mikaelyan, A., Roberts, L.R., Demetris, A.J., Sun, Z., Nevens, F., Roskams, T. and Thorgeirsson, S.S. (2006) 'A novel prognostic subtype of human hepatocellular carcinoma derived from hepatic progenitor cells', *Nat Med*, 12(4), 410-6.
146. Fausto, N. (2004) 'Liver regeneration and repair: hepatocytes, progenitor cells, and stem cells', *Hepatology*, 39(6), 1477-87.
147. Farber, E. (1956) 'Similarities in the sequence of early histological changes induced in the liver of the rat by ethionine, 2-acetylamino-fluorene, and 3'-methyl-4-dimethylaminoazobenzene', *Cancer Res*, 16(2), 142-8.
148. Petersen, B.E., Bowen, W.C., Patrene, K.D., Mars, W.M., Sullivan, A.K., Murase, N., Boggs, S.S., Greenberger, J.S. and Goff, J.P. (1999) 'Bone marrow as a potential source of hepatic oval cells', *Science*, 284(5417), 1168-70.

149. Kordes, C., Sawitza, I., Gotze, S., Herebian, D. and Haussinger, D. (2014) 'Hepatic stellate cells contribute to progenitor cells and liver regeneration', *J Clin Invest*, 124(12), 5503-15.
150. Tarlow, B.D., Pelz, C., Naugler, W.E., Wakefield, L., Wilson, E.M., Finegold, M.J. and Grompe, M. (2014) 'Bipotential adult liver progenitors are derived from chronically injured mature hepatocytes', *Cell Stem Cell*, 15(5), 605-18.
151. Spee, B., Carpino, G., Schotanus, B.A., Katoonizadeh, A., Vander Borght, S., Gaudio, E. and Roskams, T. (2010) 'Characterisation of the liver progenitor cell niche in liver diseases: potential involvement of Wnt and Notch signalling', *Gut*, 59(2), 247-57.
152. Boulter, L., Govaere, O., Bird, T.G., Radulescu, S., Ramachandran, P., Pellicoro, A., Ridgway, R.A., Seo, S.S., Spee, B., Van Rooijen, N., Sansom, O.J., Iredale, J.P., Lowell, S., Roskams, T. and Forbes, S.J. (2012) 'Macrophage-derived Wnt opposes Notch signaling to specify hepatic progenitor cell fate in chronic liver disease', *Nat Med*, 18(4), 572-9.
153. Scadden, D.T. (2006) 'The stem-cell niche as an entity of action', *Nature*, 441(7097), 1075-9.
154. Miyajima, A., Tanaka, M. and Itoh, T. (2014) 'Stem/progenitor cells in liver development, homeostasis, regeneration, and reprogramming', *Cell Stem Cell*, 14(5), 561-74.
155. Ionescu-Tirgoviste, C., Gagniuc, P.A., Gubceac, E., Mardare, L., Popescu, I., Dima, S. and Militaru, M. (2015) 'A 3D map of the islet routes throughout the healthy human pancreas', *Sci Rep*, 5, 14634.
156. Young, B., Lowe, J., Stevens, A. and Heath, J. (2006) 'Wheater's Functional Histology, 5 th Edn. Churchill Livingstone', in Elsevier, Glasgow UK.
157. Van Nest, G.A., MacDonald, R.J., Raman, R.K. and Rutter, W.J. (1980) 'Proteins synthesized and secreted during rat pancreatic development', *J Cell Biol*, 86(3), 784-94.
158. Slack, J.M. (1995) 'Developmental biology of the pancreas', *Development*, 121(6), 1569-80.
159. Triplitt, C.L. (2012) 'Examining the mechanisms of glucose regulation', *Am J Manag Care*, 18(1 Suppl), S4-10.
160. Dimitriadis, G., Mitrou, P., Lambadiari, V., Maratou, E. and Raptis, S.A. (2011) 'Insulin effects in muscle and adipose tissue', *Diabetes Res Clin Pract*, 93 Suppl 1, S52-9.
161. *Human Anatomy & Physiology of Pancreas* (2013). Available at: http://www.pharmatips.in/Articles/Human-Anatomy/Human-Anatomy-Physiology-Of-Pancreas.aspx (Accessed: 16/04/2019).
162. Bort, R., Signore, M., Tremblay, K., Martinez Barbera, J.P. and Zaret, K.S. (2006) 'Hex homeobox gene controls the transition of the endoderm to a pseudostratified, cell emergent epithelium for liver bud development', *Dev Biol*, 290(1), 44-56.
163. Bort, R., Martinez-Barbera, J.P., Beddington, R.S. and Zaret, K.S. (2004) 'Hex homeobox gene-dependent tissue positioning is required for organogenesis of the ventral pancreas', *Development*, 131(4), 797-806.
164. Hebrok, M., Kim, S.K. and Melton, D.A. (1998) 'Notochord repression of endodermal Sonic hedgehog permits pancreas development', *Genes Dev*, 12(11), 1705-13.
165. Slack, J.M. and Tosh, D. (2001) 'Transdifferentiation and metaplasia--switching cell types', *Curr Opin Genet Dev*, 11(5), 581-6.
166. Tosh, D. and Slack, J.M. (2002) 'How cells change their phenotype', *Nat Rev Mol Cell Biol*, 3(3), 187-94.
167. Slack, J.M. (2009) 'Metaplasia and somatic cell reprogramming', *J Pathol*, 217(2), 161-8.
168. Slack, J.M. (1986) 'Epithelial metaplasia and the second anatomy', *Lancet*, 2(8501), 268-71.

169. Matsukura, N., Suzuki, K., Kawachi, T., Aoyagi, M., Sugimura, T., Kitaoka, H., Numajiri, H., Shirota, A., Itabashi, M. and Hirota, T. (1980) 'Distribution of marker enzymes and mucin in intestinal metaplasia in human stomach and relation to complete and incomplete types of intestinal metaplasia to minute gastric carcinomas', *J Natl Cancer Inst*, 65(2), 231-40.
170. Eguchi, G. and Kodama, R. (1993) 'Transdifferentiation', *Curr Opin Cell Biol*, 5(6), 1023-8.
171. Selman, K. and Kafatos, F.C. (1974) 'Transdifferentiation in the labial gland of silk moths: is DNA required for cellular metamorphosis?', *Cell Differ*, 3(2), 81-94.
172. Scarpelli, D.G. and Rao, M.S. (1981) 'Differentiation of regenerating pancreatic cells into hepatocyte-like cells', *Proc Natl Acad Sci U S A*, 78(4), 2577-81.
173. Rao, M.S., Reddy, M.K., Reddy, J.K. and Scarpelli, D.G. (1982) 'Response of chemically induced hepatocytelike cells in hamster pancreas to methyl clofenapate, a peroxisome proliferator', *J Cell Biol*, 95(1), 50-6.
174. Reddy, J.K., Rao, M.S., Qureshi, S.A., Reddy, M.K., Scarpelli, D.G. and Lalwani, N.D. (1984) 'Induction and origin of hepatocytes in rat pancreas', *J Cell Biol*, 98(6), 2082-90.
175. Rao, M.S., Subbarao, V. and Reddy, J.K. (1986b) 'Induction of hepatocytes in the pancreas of copper-depleted rats following copper repletion', *Cell Differ*, 18(2), 109-17.
176. Dabeva, M.D., Hwang, S.G., Vasa, S.R., Hurston, E., Novikoff, P.M., Hixson, D.C., Gupta, S. and Shafritz, D.A. (1997) 'Differentiation of pancreatic epithelial progenitor cells into hepatocytes following transplantation into rat liver', *Proc Natl Acad Sci U S A*, 94(14), 7356-61.
177. Rao, M.S., Dwivedi, R.S., Subbarao, V., Usman, M.I., Scarpelli, D.G., Nemali, M.R., Yeldandi, A., Thangada, S., Kumar, S. and Reddy, J.K. (1988a) 'Almost total conversion of pancreas to liver in the adult rat: a reliable model to study transdifferentiation', *Biochem Biophys Res Commun*, 156(1), 131-6.
178. Dabeva, M.D., Hurston, E. and Shafritz, D.A. (1995) 'Transcription factor and liver-specific mRNA expression in facultative epithelial progenitor cells of liver and pancreas', *Am J Pathol*, 147(6), 1633-48.
179. Rao, M.S., Yukawa, M., Omori, M., Thorgeirsson, S.S. and Reddy, J.K. (1996) 'Expression of transcription factors and stem cell factor precedes hepatocyte differentiation in rat pancreas', *Gene Expr*, 6(1), 15-22.
180. Cereghini, S. (1996) 'Liver-enriched transcription factors and hepatocyte differentiation', *Faseb j*, 10(2), 267-82.
181. Chia-Ning, S., Seckl, J.R., Slack, J.M. and David, T. (2003) 'Glucocorticoids suppress β-cell development and induce hepatic metaplasia in embryonic pancreas', *Biochemical Journal*, 375(1), 41-50.
182. Krakowski, M.L., Kritzik, M.R., Jones, E.M., Krahl, T., Lee, J., Arnush, M., Gu, D. and Sarvetnick, N. (1999) 'Pancreatic expression of keratinocyte growth factor leads to differentiation of islet hepatocytes and proliferation of duct cells', *Am J Pathol*, 154(3), 683-91.
183. Wells, J.M. and Melton, D.A. (1999) 'Vertebrate endoderm development', *Annu Rev Cell Dev Biol*, 15, 393-410.
184. Rao, M.S., Bendayan, M., Kimbrough, R.D. and Reddy, J.K. (1986a) 'Characterization of pancreatic-type tissue in the liver of rat induced by polychlorinated biphenyls', *J Histochem Cytochem*, 34(2), 197-201.
185. Lee, B.C., Hendricks, J.D. and Bailey, G.S. (1989) 'Metaplastic pancreatic cells in liver tumors induced by diethylnitrosamine', *Exp Mol Pathol*, 50(1), 104-13.
186. Paner, G.P., Thompson, K.S. and Reyes, C.V. (2000) 'Hepatoid carcinoma of the pancreas', *Cancer*, 88(7), 1582-9.
187. Ferber, S., Halkin, A., Cohen, H., Ber, I., Einav, Y., Goldberg, I., Barshack, I., Seijffers, R., Kopolovic, J., Kaiser, N. and Karasik, A. (2000) 'Pancreatic and duodenal homeobox

gene 1 induces expression of insulin genes in liver and ameliorates streptozotocin-induced hyperglycemia', *Nat Med*, 6(5), 568-72.

188. Shternhall-Ron, K., Quintana, F.J., Perl, S., Meivar-Levy, I., Barshack, I., Cohen, I.R. and Ferber, S. (2007) 'Ectopic PDX-1 expression in liver ameliorates type 1 diabetes', *J Autoimmun*, 28(2-3), 134-42.
189. Longnecker, D.S., Lilja, H.S., French, J., Kuhlmann, E. and Noll, W. (1979) 'Transplantation of azaserine-induced carcinomas of pancreas in rats', *Cancer letters*, 7(4), 197-202.
190. Ehrlich, J., Anderson, L.E., Coffey, G.L., Hillegas, A.B., Knudsen, M.P., Koepsell, H.J., Kohberger, D.L. and Oyaas, J.E. (1954) 'Antibiotic studies of azaserine', *Nature*, 173(4393), 72.
191. Loser, C., Stuber, E. and Folsch, U.R. (1995) 'Dissimilar effect of the carcinogenic agent azaserine on pancreatic and hepatic polyamine metabolism in rats', *Pancreas*, 10(1), 44-52.
192. Chu, J., Ji, H., Lu, M., Li, Z., Qiao, X., Sun, B., Zhang, W. and Xue, D. (2013) 'Proteomic analysis of apoptotic and oncotic pancreatic acinar AR42J cells treated with caerulein', *Mol Cell Biochem*, 382(1-2), 1-17.
193. Jessop, N. (1980) 'Characteristics of two rat pancreatic exocrine cell lines derived from transplantable tumors', *In vitro*, 16, 212-216.
194. Mashima, H., Ohnishi, H., Wakabayashi, K., Mine, T., Miyagawa, J.-i., Hanafusa, T., Seno, M., Yamada, H. and Kojima, I. (1996 a) 'Betacellulin and activin A coordinately convert amylase-secreting pancreatic AR42J cells into insulin-secreting cells', *J Clin Invest*, 97(7), 1647-1654.
195. Mashima, H., Shibata, H., Mine, T. and Kojima, I. (1996 b) 'Formation of insulin-producing cells from pancreatic acinar AR42J cells by hepatocyte growth factor', *Endocrinology*, 137(9), 3969-3976.
196. Shen, C.-N., Slack, J.M. and Tosh, D. (2000) 'Molecular basis of transdifferentiation of pancreas to liver', *Nat Cell Biol*, 2(12), 879.
197. Wallace, K., Marek, C.J., Currie, R.A. and Wright, M.C. (2009) 'Exocrine pancreas trans-differentiation to hepatocytes-A physiological response to elevated glucocorticoid in vivo', *Journal of Steroid Biochemistry and Molecular Biology*, 116(1-2), 76-85.
198. Marek, C.J., Cameron, G.A., Elrick, L.J., Hawksworth, G.M. and Wright, M.C. (2003) 'Generation of hepatocytes expressing functional cytochromes P450 from a pancreatic progenitor cell line in vitro', *Biochemical Journal*, 370, 763-769.
199. Burke, Z.D., Shen, C.N., Ralphs, K.L. and Tosh, D. (2006) 'Characterization of liver function in transdifferentiated hepatocytes', *Journal of cellular physiology*, 206(1), 147-159.
200. Probert, P.M., Meyer, S.K., Alsaeedi, F., Axon, A.A., Fairhall, E.A., Wallace, K., Charles, M., Oakley, F., Jowsey, P.A. and Blain, P.G. (2015) 'An expandable donor-free supply of functional hepatocytes for Toxicology', *Toxicology Research*, 4(2), 203-222.
201. Al-Adsani, A., Burke, Z.D., Eberhard, D., Lawrence, K.L., Shen, C.-N., Rustgi, A.K., Sakaue, H., Farrant, J.M. and Tosh, D. (2010) 'Dexamethasone treatment induces the reprogramming of pancreatic acinar cells to hepatocytes and ductal cells', *PLoS One*, 5(10), e13650.
202. Xie, G. and Diehl, A.M. (2013) 'Evidence for and against epithelial-to-mesenchymal transition in the liver', *American Journal of Physiology-Gastrointestinal and Liver Physiology*, 305(12), G881-G890.
203. Shen, C.-N., Horb, M.E., Slack, J.M. and Tosh, D. (2003) 'Transdifferentiation of pancreas to liver', *Mech Dev*, 120(1), 107-116.

204. Wallace, K., Marek, C.J., Hoppler, S. and Wright, M.C. (2010) 'Glucocorticoid-dependent transdifferentiation of pancreatic progenitor cells into hepatocytes is dependent on transient suppression of WNT signalling', *J Cell Sci*, 123(12), 2102-2109.
205. Cadigan, K.M. and Nusse, R. (1997) 'Wnt signaling: a common theme in animal development', *Genes Dev*, 11(24), 3286-305.
206. Nusse, R. and Varmus, H.E. (1992) 'Wnt genes', *Cell*, 69(7), 1073-87.
207. Tolwinski, N.S., Wehrli, M., Rives, A., Erdeniz, N., DiNardo, S. and Wieschaus, E. (2003) 'Wg/Wnt signal can be transmitted through arrow/LRP5,6 and Axin independently of Zw3/Gsk3beta activity', *Dev Cell*, 4(3), 407-18.
208. Pinson, K.I., Brennan, J., Monkley, S., Avery, B.J. and Skarnes, W.C. (2000) 'An LDL-receptor-related protein mediates Wnt signalling in mice', *Nature*, 407(6803), 535-8.
209. Logan, C.Y. and Nusse, R. (2004) 'The Wnt signaling pathway in development and disease', *Annu Rev Cell Dev Biol*, 20, 781-810.
210. Pai, S.G., Carneiro, B.A., Mota, J.M., Costa, R., Leite, C.A., Barroso-Sousa, R., Kaplan, J.B., Chae, Y.K. and Giles, F.J. (2017) 'Wnt/beta-catenin pathway: modulating anticancer immune response', *J Hematol Oncol*, 10(1), 101.
211. Yanagawa, S., Matsuda, Y., Lee, J.S., Matsubayashi, H., Sese, S., Kadowaki, T. and Ishimoto, A. (2002) 'Casein kinase I phosphorylates the Armadillo protein and induces its degradation in Drosophila', *Embo j*, 21(7), 1733-42.
212. Lustig, B. and Behrens, J. (2003) 'The Wnt signaling pathway and its role in tumor development', *J Cancer Res Clin Oncol*, 129(4), 199-221.
213. Moon, R.T. (2005) 'Wnt/beta-catenin pathway', *Sci STKE*, 2005(271), cm1.
214. van Amerongen, R. and Nusse, R. (2009) 'Towards an integrated view of Wnt signaling in development', *Development*, 136(19), 3205-14.
215. Zeng, G., Awan, F., Otruba, W., Muller, P., Apte, U., Tan, X., Gandhi, C., Demetris, A.J. and Monga, S.P. (2007) 'Wnt'er in liver: expression of Wnt and frizzled genes in mouse', *Hepatology*, 45(1), 195-204.
216. Burke, Z.D. and Tosh, D. (2006) 'The Wnt/beta-catenin pathway: master regulator of liver zonation?', *Bioessays*, 28(11), 1072-7.
217. Wallace, K., Marek, C.J., Currie, R.A. and Wright, M.C. (2009) 'Exocrine pancreas trans-differentiation to hepatocytes--a physiological response to elevated glucocorticoid in vivo', *J Steroid Biochem Mol Biol*, 116(1-2), 76-85.
218. Wallace, K., Marek, C.J., Hoppler, S. and Wright, M.C. (2010 b) 'Glucocorticoid-dependent transdifferentiation of pancreatic progenitor cells into hepatocytes is dependent on transient suppression of WNT signalling', *J Cell Sci*, 123(Pt 12), 2103-10.
219. Barnes, P.J. (2014) 'Glucocorticoids', *Chem Immunol Allergy*, 100, 311-6.
220. Silverman, M.N. and Sternberg, E.M. (2012) 'Glucocorticoid regulation of inflammation and its functional correlates: from HPA axis to glucocorticoid receptor dysfunction', *Ann N Y Acad Sci*, 1261, 55-63.
221. Flammer, J.R. and Rogatsky, I. (2011) 'Minireview: Glucocorticoids in autoimmunity: unexpected targets and mechanisms', *Mol Endocrinol*, 25(7), 1075-86.
222. Seckl, J.R. and Holmes, M.C. (2007) 'Mechanisms of disease: glucocorticoids, their placental metabolism and fetal 'programming' of adult pathophysiology', *Nat Clin Pract Endocrinol Metab*, 3(6), 479-88.
223. Reynolds, R.M. (2013) 'Glucocorticoid excess and the developmental origins of disease: two decades of testing the hypothesis--2012 Curt Richter Award Winner', *Psychoneuroendocrinology*, 38(1), 1-11.
224. Grier, D.G. and Halliday, H.L. (2004) 'Effects of glucocorticoids on fetal and neonatal lung development', *Treat Respir Med*, 3(5), 295-306.
225. Munck, A., Guyre, P.M. and Holbrook, N.J. (1984) 'Physiological functions of glucocorticoids in stress and their relation to pharmacological actions', *Endocr Rev*, 5(1), 25-44.

226. Wallace, K., Long, Q.A., Fairhall, E.A., Charlton, K.A. and Wright, M.C. (2011) 'Serine/threonine protein kinase SGK1 in glucocorticoid-dependent transdifferentiation of pancreatic acinar cells to hepatocytes', *J Cell Sci*, 124(3), 405-413.
227. Fairhall, E.A., Wallace, K., White, S.A., Huang, G.C., Shaw, J.A., Wright, S.C., Charlton, K.A., Burt, A.D. and Wright, M.C. (2013) 'Adult human exocrine pancreas differentiation to hepatocytes - potential source of a human hepatocyte progenitor for use in toxicology research', *Toxicology Research*, 2(1), 80-87.
228. Seckl, J.R. and Walker, B.R. (2001) 'Minireview: 11β-hydroxysteroid dehydrogenase type 1—a tissue-specific amplifier of glucocorticoid action', *Endocrinology*, 142(4), 1371-1376.
229. Sumitran-Holgersson, S., Nowak, G., Thowfeequ, S., Begum, S., Joshi, M., Jaksch, M., Kjaeldgaard, A., Jorns, C., Ericzon, B.-G. and Tosh, D. (2009) 'Generation of hepatocyte-like cells from in vitro transdifferentiated human fetal pancreas', *Cell Transplant*, 18(2), 183-193.
230. Lonser, R.R., Nieman, L. and Oldfield, E.H. (2017) 'Cushing's disease: pathobiology, diagnosis, and management', *J Neurosurg*, 126(2), 404-417.
231. Wallace, K., Flecknell, P.A., Burt, A.D. and Wright, M.C. (2010 c) 'Disrupted Pancreatic Exocrine Differentiation and Malabsorption in Response to Chronic Elevated Systemic Glucocorticoid', *American Journal of Pathology*, 177(3), 1225-1232.
232. Pearce, L.R., Komander, D. and Alessi, D.R. (2010) 'The nuts and bolts of AGC protein kinases', *Nat Rev Mol Cell Biol*, 11(1), 9-22.
233. Lang, F. and Shumilina, E. (2013) 'Regulation of ion channels by the serum-and glucocorticoid-inducible kinase SGK1', *The FASEB Journal*, 27(1), 3-12.
234. Waerntges, S., Klingel, K., Weigert, C., Fillon, S., Buck, M., Schleicher, E., Rodemann, H.P., Knabbe, C., Kandolf, R. and Lang, F. (2002) 'Excessive transcription of the human serum and glucocorticoid dependent kinase hSGK1 in lung fibrosis', *Cell Physiol Biochem*, 12(2-3), 135-42.
235. Rauz, S., Walker, E.A., Hughes, S.V., Coca-Prados, M., Hewison, M., Murray, P.I. and Stewart, P.M. (2003) 'Serum- and glucocorticoid-regulated kinase isoform-1 and epithelial sodium channel subunits in human ocular ciliary epithelium', *Invest Ophthalmol Vis Sci*, 44(4), 1643-51.
236. Fillon, S., Klingel, K., Warntges, S., Sauter, M., Gabrysch, S., Pestel, S., Tanneur, V., Waldegger, S., Zipfel, A., Viebahn, R., Haussinger, D., Broer, S., Kandolf, R. and Lang, F. (2002) 'Expression of the serine/threonine kinase hSGK1 in chronic viral hepatitis', *Cell Physiol Biochem*, 12(1), 47-54.
237. Alliston, T.N., Gonzalez-Robayna, I.J., Buse, P., Firestone, G.L. and Richards, J.S. (2000) 'Expression and localization of serum/glucocorticoid-induced kinase in the rat ovary: relation to follicular growth and differentiation', *Endocrinology*, 141(1), 385-95.
238. Klingel, K., Warntges, S., Bock, J., Wagner, C.A., Sauter, M., Waldegger, S., Kandolf, R. and Lang, F. (2000) 'Expression of cell volume-regulated kinase h-sgk in pancreatic tissue', *Am J Physiol Gastrointest Liver Physiol*, 279(5), G998-g1002.
239. Friedrich, B., Warntges, S., Klingel, K., Sauter, M., Kandolf, R., Risler, T., Muller, G.A., Witzgall, R., Kriz, W., Grone, H.J. and Lang, F. (2002) 'Up-regulation of the human serum and glucocorticoid-dependent kinase 1 in glomerulonephritis', *Kidney Blood Press Res*, 25(5), 303-7.
240. Brickley, D.R., Mikosz, C.A., Hagan, C.R. and Conzen, S.D. (2002) 'Ubiquitin modification of serum and glucocorticoid-induced protein kinase-1 (SGK-1)', *J Biol Chem*, 277(45), 43064-70.
241. Loffing, J., Flores, S.Y. and Staub, O. (2006) 'Sgk kinases and their role in epithelial transport', *Annu Rev Physiol*, 68, 461-90.
242. Boyd, C. and Naray-Fejes-Toth, A. (2005) 'Gene regulation of ENaC subunits by serum- and glucocorticoid-inducible kinase-1', *Am J Physiol Renal Physiol*, 288(3), F505-12.

243. Diakov, A. and Korbmacher, C. (2004) 'A novel pathway of epithelial sodium channel activation involves a serum- and glucocorticoid-inducible kinase consensus motif in the C terminus of the channel's alpha-subunit', *J Biol Chem*, 279(37), 38134-42.
244. Seckl, J.R. and Walker, B.R. (2001) 'Minireview: 11beta-hydroxysteroid dehydrogenase type 1- a tissue-specific amplifier of glucocorticoid action', *Endocrinology*, 142(4), 1371-6.
245. Chen, S.Y., Bhargava, A., Mastroberardino, L., Meijer, O.C., Wang, J., Buse, P., Firestone, G.L., Verrey, F. and Pearce, D. (1999) 'Epithelial sodium channel regulated by aldosterone-induced protein sgk', *Proc Natl Acad Sci U S A*, 96(5), 2514-9.
246. Waldegger, S., Barth, P., Raber, G. and Lang, F. (1997) 'Cloning and characterization of a putative human serine/threonine protein kinase transcriptionally modified during anisotonic and isotonic alterations of cell volume', *Proceedings of the National Academy of Sciences*, 94(9), 4440-4445.
247. Waldegger, S., Klingel, K., Barth, P., Sauter, M., Rfer, M.L., Kandolf, R. and Lang, F. (1999) 'h-sgk serine-threonine protein kinase gene as transcriptional target of transforming growth factor beta in human intestine', *Gastroenterology*, 116(5), 1081-8.
248. Akutsu, N., Lin, R., Bastien, Y., Bestawros, A., Enepekides, D.J., Black, M.J. and White, J.H. (2001) 'Regulation of gene Expression by 1alpha,25-dihydroxyvitamin D3 and Its analog EB1089 under growth-inhibitory conditions in squamous carcinoma Cells', *Mol Endocrinol*, 15(7), 1127-39.
249. Khan, Z.A., Barbin, Y.P., Farhangkhoee, H., Beier, N., Scholz, W. and Chakrabarti, S. (2005) 'Glucose-induced serum- and glucocorticoid-regulated kinase activation in oncofetal fibronectin expression', *Biochem Biophys Res Commun*, 329(1), 275-80.
250. Mizuno, H. and Nishida, E. (2001) 'The ERK MAP kinase pathway mediates induction of SGK (serum- and glucocorticoid-inducible kinase) by growth factors', *Genes Cells*, 6(3), 261-8.
251. You, H., Jang, Y., You-Ten, A.I., Okada, H., Liepa, J., Wakeham, A., Zaugg, K. and Mak, T.W. (2004) 'p53-dependent inhibition of FKHRL1 in response to DNA damage through protein kinase SGK1', *Proc Natl Acad Sci U S A*, 101(39), 14057-62.
252. Wulff, P., Vallon, V., Huang, D.Y., Volkl, H., Yu, F., Richter, K., Jansen, M., Schlunz, M., Klingel, K., Loffing, J., Kauselmann, G., Bosl, M.R., Lang, F. and Kuhl, D. (2002) 'Impaired renal Na(+) retention in the sgk1-knockout mouse', *J Clin Invest*, 110(9), 1263-8.
253. Sobiesiak, M., Shumilina, E., Lam, R.S., Wolbing, F., Matzner, N., Kaesler, S., Zemtsova, I.M., Lupescu, A., Zahir, N., Kuhl, D., Schaller, M., Biedermann, T. and Lang, F. (2009) 'Impaired mast cell activation in gene-targeted mice lacking the serum- and glucocorticoid-inducible kinase SGK1', *J Immunol*, 183(7), 4395-402.
254. Wu, C., Yosef, N., Thalhamer, T., Zhu, C., Xiao, S., Kishi, Y., Regev, A. and Kuchroo, V.K. (2013) 'Induction of pathogenic TH17 cells by inducible salt-sensing kinase SGK1', *Nature*, 496(7446), 513-7.
255. Heikamp, E.B., Patel, C.H., Collins, S., Waickman, A., Oh, M.H., Sun, I.H., Illei, P., Sharma, A., Naray-Fejes-Toth, A., Fejes-Toth, G., Misra-Sen, J., Horton, M.R. and Powell, J.D. (2014) 'The AGC kinase SGK1 regulates TH1 and TH2 differentiation downstream of the mTORC2 complex', *Nat Immunol*, 15(5), 457-64.
256. Wallace, K., Long, Q., Fairhall, E.A., Charlton, K.A. and Wright, M.C. (2011) 'Serine/threonine protein kinase SGK1 in glucocorticoid-dependent transdifferentiation of pancreatic acinar cells to hepatocytes', *J Cell Sci*, 124(Pt 3), 405-13.
257. Fairhall, E.A., Charles, M.A., Probert, P.M., Wallace, K., Gibb, J., Ravindan, C., Soloman, M. and Wright, M.C. (2016) 'Pancreatic B-13 Cell Trans-Differentiation to Hepatocytes Is Dependent on Epigenetic-Regulated Changes in Gene Expression', *PLoS One*, 11(3), e0150959.

258. Puppi, J. and Dhawan, A. (2009) 'Human hepatocyte transplantation overview', *Methods Mol Biol*, 481, 1-16.
259. Strain, A.J. (1994) 'Isolated hepatocytes: use in experimental and clinical hepatology', *Gut*, 35(4), 433-6.
260. Terry, C., Hughes, R.D., Mitry, R.R., Lehec, S.C. and Dhawan, A. (2007) 'Cryopreservation-induced nonattachment of human hepatocytes: role of adhesion molecules', *Cell Transplant*, 16(6), 639-47.
261. Padgham, C.R., Boyle, C.C., Wang, X.J., Raleigh, S.M., Wright, M.C. and Paine, A.J. (1993) 'Alteration of transcription factor mRNAs during the isolation and culture of rat hepatocytes suggests the activation of a proliferative mode underlies their de-differentiation', *Biochem Biophys Res Commun*, 197(2), 599-605.
262. Rodriguez-Ariza, A. and Paine, A.J. (1999) 'Rapid induction of NF-kappaB binding during liver cell isolation and culture: inhibition by L-NAME indicates a role for nitric oxide synthase', *Biochem Biophys Res Commun*, 257(1), 145-8.
263. Heslop, J.A., Rowe, C., Walsh, J., Sison-Young, R., Jenkins, R., Kamalian, L., Kia, R., Hay, D., Jones, R.P., Malik, H.Z., Fenwick, S., Chadwick, A.E., Mills, J., Kitteringham, N.R., Goldring, C.E. and Kevin Park, B. (2017) 'Mechanistic evaluation of primary human hepatocyte culture using global proteomic analysis reveals a selective dedifferentiation profile', *Arch Toxicol*, 91(1), 439-452.
264. Schmelzer, E., Zhang, L., Bruce, A., Wauthier, E., Ludlow, J., Yao, H.L., Moss, N., Melhem, A., McClelland, R., Turner, W., Kulik, M., Sherwood, S., Tallheden, T., Cheng, N., Furth, M.E. and Reid, L.M. (2007) 'Human hepatic stem cells from fetal and postnatal donors', *J Exp Med*, 204(8), 1973-87.
265. Aurich, H., Sgodda, M., Kaltwasser, P., Vetter, M., Weise, A., Liehr, T., Brulport, M., Hengstler, J.G., Dollinger, M.M., Fleig, W.E. and Christ, B. (2009) 'Hepatocyte differentiation of mesenchymal stem cells from human adipose tissue in vitro promotes hepatic integration in vivo', *Gut*, 58(4), 570-81.
266. Palakkan, A.A., Nanda, J. and Ross, J.A. (2017) 'Pluripotent stem cells to hepatocytes, the journey so far', *Biomed Rep*, 6(4), 367-373.
267. Si-Tayeb, K., Noto, F.K., Nagaoka, M., Li, J., Battle, M.A., Duris, C., North, P.E., Dalton, S. and Duncan, S.A. (2010) 'Highly efficient generation of human hepatocyte-like cells from induced pluripotent stem cells', *Hepatology*, 51(1), 297-305.
268. Yiangou, L., Ross, A.D.B., Goh, K.J. and Vallier, L. (2018) 'Human Pluripotent Stem Cell-Derived Endoderm for Modeling Development and Clinical Applications', *Cell Stem Cell*, 22(4), 485-499.
269. Touboul, T., Hannan, N.R., Corbineau, S., Martinez, A., Martinet, C., Branchereau, S., Mainot, S., Strick-Marchand, H., Pedersen, R. and Di Santo, J. (2010) 'Generation of functional hepatocytes from human embryonic stem cells under chemically defined conditions that recapitulate liver development', *Hepatology*, 51(5), 1754-1765.
270. Yamanaka, Y. and Ralston, A. (2010) 'Early embryonic cell fate decisions in the mouse', *Adv Exp Med Biol*, 695, 1-13.
271. Vallier, L., Touboul, T., Chng, Z., Brimpari, M., Hannan, N., Millan, E., Smithers, L.E., Trotter, M., Rugg-Gunn, P., Weber, A. and Pedersen, R.A. (2009) 'Early cell fate decisions of human embryonic stem cells and mouse epiblast stem cells are controlled by the same signalling pathways', *PLoS One*, 4(6), e6082.
272. Teo, A.K., Ali, Y., Wong, K.Y., Chipperfield, H., Sadasivam, A., Poobalan, Y., Tan, E.K., Wang, S.T., Abraham, S., Tsuneyoshi, N., Stanton, L.W. and Dunn, N.R. (2012) 'Activin and BMP4 synergistically promote formation of definitive endoderm in human embryonic stem cells', *Stem Cells*, 30(4), 631-42.
273. McLean, A.B., D'Amour, K.A., Jones, K.L., Krishnamoorthy, M., Kulik, M.J., Reynolds, D.M., Sheppard, A.M., Liu, H., Xu, Y., Baetge, E.E. and Dalton, S. (2007) 'Activin a efficiently specifies definitive endoderm from human embryonic stem cells

only when phosphatidylinositol 3-kinase signaling is suppressed', *Stem Cells*, 25(1), 29-38.

274. Sakaki-Yumoto, M., Liu, J., Ramalho-Santos, M., Yoshida, N. and Derynck, R. (2013) 'Smad2 is essential for maintenance of the human and mouse primed pluripotent stem cell state', *J Biol Chem*, 288(25), 18546-60.
275. Loh, K.M., Ang, L.T., Zhang, J., Kumar, V., Ang, J., Auyeong, J.Q., Lee, K.L., Choo, S.H., Lim, C.Y., Nichane, M., Tan, J., Noghabi, M.S., Azzola, L., Ng, E.S., Durruthy-Durruthy, J., Sebastiano, V., Poellinger, L., Elefanty, A.G., Stanley, E.G., Chen, Q., Prabhakar, S., Weissman, I.L. and Lim, B. (2014) 'Efficient endoderm induction from human pluripotent stem cells by logically directing signals controlling lineage bifurcations', *Cell Stem Cell*, 14(2), 237-52.
276. Tam, P.P. and Loebel, D.A. (2007) 'Gene function in mouse embryogenesis: get set for gastrulation', *Nat Rev Genet*, 8(5), 368-81.
277. Toivonen, S., Lundin, K., Balboa, D., Ustinov, J., Tamminen, K., Palgi, J., Trokovic, R., Tuuri, T. and Otonkoski, T. (2013) 'Activin A and Wnt-dependent specification of human definitive endoderm cells', *Exp Cell Res*, 319(17), 2535-44.
278. Touboul, T., Chen, S., To, C.C., Mora-Castilla, S., Sabatini, K., Tukey, R.H. and Laurent, L.C. (2016) 'Stage-specific regulation of the WNT/beta-catenin pathway enhances differentiation of hESCs into hepatocytes', *J Hepatol*, 64(6), 1315-26.
279. Hengstler, J.G., Brulport, M., Schormann, W., Bauer, A., Hermes, M., Nussler, A.K., Fandrich, F., Ruhnke, M., Ungefroren, H., Griffin, L., Bockamp, E., Oesch, F. and von Mach, M.A. (2005) 'Generation of human hepatocytes by stem cell technology: definition of the hepatocyte', *Expert Opin Drug Metab Toxicol*, 1(1), 61-74.
280. Hannan, N.R., Fordham, R.P., Syed, Y.A., Moignard, V., Berry, A., Bautista, R., Hanley, N.A., Jensen, K.B. and Vallier, L. (2013a) 'Generation of multipotent foregut stem cells from human pluripotent stem cells', *Stem Cell Reports*, 1(4), 293-306.
281. Pagliuca, F.W., Millman, J.R., Gurtler, M., Segel, M., Van Dervort, A., Ryu, J.H., Peterson, Q.P., Greiner, D. and Melton, D.A. (2014) 'Generation of functional human pancreatic beta cells in vitro', *Cell*, 159(2), 428-39.
282. Cai, J., Zhao, Y., Liu, Y., Ye, F., Song, Z., Qin, H., Meng, S., Chen, Y., Zhou, R., Song, X., Guo, Y., Ding, M. and Deng, H. (2007) 'Directed differentiation of human embryonic stem cells into functional hepatic cells', *Hepatology*, 45(5), 1229-39.
283. Brolen, G., Sivertsson, L., Bjorquist, P., Eriksson, G., Ek, M., Semb, H., Johansson, I., Andersson, T.B., Ingelman-Sundberg, M. and Heins, N. (2010) 'Hepatocyte-like cells derived from human embryonic stem cells specifically via definitive endoderm and a progenitor stage', *J Biotechnol*, 145(3), 284-94.
284. Ameri, J., Stahlberg, A., Pedersen, J., Johansson, J.K., Johannesson, M.M., Artner, I. and Semb, H. (2010) 'FGF2 specifies hESC-derived definitive endoderm into foregut/midgut cell lineages in a concentration-dependent manner', *Stem Cells*, 28(1), 45-56.
285. Hannoun, Z., Steichen, C., Dianat, N., Weber, A. and Dubart-Kupperschmitt, A. (2016) 'The potential of induced pluripotent stem cell derived hepatocytes', *J Hepatol*, 65(1), 182-199.
286. Agarwal, S., Holton, K.L. and Lanza, R. (2008) 'Efficient differentiation of functional hepatocytes from human embryonic stem cells', *Stem Cells*, 26(5), 1117-27.
287. Heslop, J.A. and Duncan, S.A. (2018) 'The use of human pluripotent stem cells for modelling liver development and disease', *Hepatology*.
288. Yu, Y., Liu, H., Ikeda, Y., Amiot, B.P., Rinaldo, P., Duncan, S.A. and Nyberg, S.L. (2012) 'Hepatocyte-like cells differentiated from human induced pluripotent stem cells: relevance to cellular therapies', *Stem Cell Res*, 9(3), 196-207.
289. Baxter, M., Withey, S., Harrison, S., Segeritz, C.P., Zhang, F., Atkinson-Dell, R., Rowe, C., Gerrard, D.T., Sison-Young, R., Jenkins, R., Henry, J., Berry, A.A., Mohamet, L.,

Best, M., Fenwick, S.W., Malik, H., Kitteringham, N.R., Goldring, C.E., Piper Hanley, K., Vallier, L. and Hanley, N.A. (2015) 'Phenotypic and functional analyses show stem cell-derived hepatocyte-like cells better mimic fetal rather than adult hepatocytes', *J Hepatol*, 62(3), 581-9.

290. Kia, R., Sison, R.L., Heslop, J., Kitteringham, N.R., Hanley, N., Mills, J.S., Park, B.K. and Goldring, C.E. (2013) 'Stem cell-derived hepatocytes as a predictive model for drug-induced liver injury: are we there yet?', *Br J Clin Pharmacol*, 75(4), 885-96.
291. Pettinato, G., Ramanathan, R., Fisher, R.A., Mangino, M.J., Zhang, N. and Wen, X. (2016) 'Scalable differentiation of human iPSCs in a multicellular spheroid-based 3D culture into hepatocyte-like cells through direct Wnt/β-catenin pathway inhibition', *Sci Rep*, 6, 32888.
292. Yamashita, T., Takayama, K., Sakurai, F. and Mizuguchi, H. (2018) 'Billion-scale production of hepatocyte-like cells from human induced pluripotent stem cells', *Biochem Biophys Res Commun*, 496(4), 1269-1275.
293. Dash, A., Simmers, M.B., Deering, T.G., Berry, D.J., Feaver, R.E., Hastings, N.E., Pruett, T.L., LeCluyse, E.L., Blackman, B.R. and Wamhoff, B.R. (2013) 'Hemodynamic flow improves rat hepatocyte morphology, function, and metabolic activity in vitro', *American Journal of Physiology-Cell Physiology*, 304(11), C1053-C1063.
294. Takayama, K., Inamura, M., Kawabata, K., Tashiro, K., Katayama, K., Sakurai, F., Hayakawa, T., Furue, M.K. and Mizuguchi, H. (2011) 'Efficient and directive generation of two distinct endoderm lineages from human ESCs and iPSCs by differentiation stage-specific SOX17 transduction', *PLoS One*, 6(7), e21780.
295. Inamura, M., Kawabata, K., Takayama, K., Tashiro, K., Sakurai, F., Katayama, K., Toyoda, M., Akutsu, H., Miyagawa, Y., Okita, H., Kiyokawa, N., Umezawa, A., Hayakawa, T., Furue, M.K. and Mizuguchi, H. (2011) 'Efficient generation of hepatoblasts from human ES cells and iPS cells by transient overexpression of homeobox gene HEX', *Mol Ther*, 19(2), 400-7.
296. Takayama, K., Inamura, M., Kawabata, K., Katayama, K., Higuchi, M., Tashiro, K., Nonaka, A., Sakurai, F., Hayakawa, T., Furue, M.K. and Mizuguchi, H. (2012) 'Efficient generation of functional hepatocytes from human embryonic stem cells and induced pluripotent stem cells by HNF4alpha transduction', *Mol Ther*, 20(1), 127-37.
297. Breyer, B., Jiang, W., Cheng, H., Zhou, L., Paul, R., Feng, T. and He, T.C. (2001) 'Adenoviral vector-mediated gene transfer for human gene therapy', *Curr Gene Ther*, 1(2), 149-62.
298. 'Assessment of adenoviral vector safety and toxicity: report of the National Institutes of Health Recombinant DNA Advisory Committee', (2002) *Hum Gene Ther*, 13(1), 3-13.
299. Rowe, W.P., Huebner, R.J., Gilmore, L.K., Parrott, R.H. and Ward, T.G. (1953) 'Isolation of a cytopathogenic agent from human adenoids undergoing spontaneous degeneration in tissue culture', *Proceedings of the Society for Experimental Biology and Medicine*, 84(3), 570-573.
300. Ginsberg, H.S. (2013) *The adenoviruses*. Springer Science & Business Media.
301. Wold, W.S. and Toth, K. (2013) 'Adenovirus vectors for gene therapy, vaccination and cancer gene therapy', *Curr Gene Ther*, 13(6), 421-33.
302. Tomko, R.P., Xu, R. and Philipson, L. (1997) 'HCAR and MCAR: the human and mouse cellular receptors for subgroup C adenoviruses and group B coxsackieviruses', *Proc Natl Acad Sci U S A*, 94(7), 3352-6.
303. Wickham, T.J., Mathias, P., Cheresh, D.A. and Nemerow, G.R. (1993) 'Integrins αvβ3 and αvβ5 promote adenovirus internalization but not virus attachment', *Cell*, 73(2), 309-319.
304. Greber, U.F., Willetts, M., Webster, P. and Helenius, A. (1993) 'Stepwise dismantling of adenovirus 2 during entry into cells', *Cell*, 75(3), 477-86.

305. Gao, G.P., Yang, Y. and Wilson, J.M. (1996) 'Biology of adenovirus vectors with E1 and E4 deletions for liver-directed gene therapy', *J Virol*, 70(12), 8934-43.
306. Colosimo, A., Goncz, K.K., Holmes, A.R., Kunzelmann, K., Novelli, G., Malone, R.W., Bennett, M.J. and Gruenert, D.C. (2000) 'Transfer and expression of foreign genes in mammalian cells', *Biotechniques*, 29(2), 314-8, 320-2, 324 passim.
307. Volpers, C. and Kochanek, S. (2004) 'Adenoviral vectors for gene transfer and therapy', *J Gene Med*, 6 Suppl 1, S164-71.
308. abm *Cell Culture - Adenovirus Techniques*. Available at: https://www.abmgood.com/marketing/knowledge_base/cell_culture_adenovirus_techniques.php#advantdiadvant (Accessed: 17/04/2019).
309. Graham, F.L., Smiley, J., Russell, W.C. and Nairn, R. (1977) 'Characteristics of a human cell line transformed by DNA from human adenovirus type 5', *J Gen Virol*, 36(1), 59-74.
310. Engelhardt, J.F., Ye, X., Doranz, B. and Wilson, J.M. (1994) 'Ablation of E2A in recombinant adenoviruses improves transgene persistence and decreases inflammatory response in mouse liver', *Proc Natl Acad Sci U S A*, 91(13), 6196-200.
311. Armentano, D., Sookdeo, C.C., Hehir, K.M., Gregory, R.J., St George, J.A., Prince, G.A., Wadsworth, S.C. and Smith, A.E. (1995) 'Characterization of an adenovirus gene transfer vector containing an E4 deletion', *Hum Gene Ther*, 6(10), 1343-53.
312. Knowles, B.B. and Aden, D.P. (1983) 'Human hepatoma derived cell line, process for preparation thereof, and uses therefor'. Google Patents.
313. Neganova, I., Zhang, X., Atkinson, S. and Lako, M. (2009) 'Expression and functional analysis of G1 to S regulatory components reveals an important role for CDK2 in cell cycle regulation in human embryonic stem cells', *Oncogene*, 28(1), 20.
314. Neganova, I., Shmeleva, E., Munkley, J., Chichagova, V., Anyfantis, G., Anderson, R., Passos, J., Elliott, D.J., Armstrong, L. and Lako, M. (2016) 'JNK/SAPK signaling is essential for efficient reprogramming of human fibroblasts to induced pluripotent stem cells', *Stem Cells*, 34(5), 1198-1212.
315. Diaz, D., Fabre, I., Daujat, M., Saint Aubert, B., Bories, P., Michel, H. and Maurel, P. (1990) 'Omeprazole is an aryl hydrocarbon-like inducer of human hepatic cytochrome P450', *Gastroenterology*, 99(3), 737-47.
316. Vogelstein, B. and Gillespie, D. (1979) 'Preparative and analytical purification of DNA from agarose', *Proceedings of the National Academy of Sciences*, 76(2), 615-619.
317. Addgene *M50 Super 8x TOPFlash*. Available at: http://n2t.net/addgene:12456
318. addgene *M51 Super 8x FOPFlash (TOPFlash mutant)*. Available at: http://www.addgene.org/12457/ (Accessed: 17/04/2019).
319. Medhurst, A.D., Harrison, D.C., Read, S.J., Campbell, C.A., Robbins, M.J. and Pangalos, M.N. (2000) 'The use of TaqMan RT-PCR assays for semiquantitative analysis of gene expression in CNS tissues and disease models', *Journal of neuroscience methods*, 98(1), 9-20.
320. Lowry, O.H., Rosebrough, N.J., Farr, A.L. and Randall, R.J. (1951) 'Protein measurement with the Folin phenol reagent', *Journal of biological chemistry*, 193, 265-275.
321. Laemmli, U.K. (1970) 'Cleavage of structural proteins during the assembly of the head of bacteriophage T4', *Nature*, 227(5259), 680.
322. Promega *Kinase Enzyme System Protocol*. Available at: https://www.promega.com/-/media/files/resources/protocols/technical-bulletins/kinase-enzyme-system-protocol.pdf (Accessed: 6/03/2019).
323. Shen, C.N., Slack, J.M. and Tosh, D. (2000) 'Molecular basis of transdifferentiation of pancreas to liver', *Nat Cell Biol*, 2(12), 879-87.

324. Dingemanse, M.A., de Boer, P.A., Moorman, A.F., Charles, R. and Lamers, W.H. (1994) 'The expression of liver-specific genes within rat embryonic hepatocytes is a discontinuous process', *Differentiation*, 56(3), 153-162.
325. Kamiya, A., Kinoshita, T., Ito, Y., Matsui, T., Morikawa, Y., Senba, E., Nakashima, K., Taga, T., Yoshida, K., Kishimoto, T. and Miyajima, A. (1999) 'Fetal liver development requires a paracrine action of oncostatin M through the gp130 signal transducer', *Embo Journal*, 18(8), 2127-2136.
326. Fairhall, E.A., Charles, M.A., Probert, P.M.E., Wallace, K., Gibb, J., Ravindan, C., Soloman, M. and Wright, M.C. (2016) 'Pancreatic B-13 Cell Trans-Differentiation to Hepatocytes Is Dependent on Epigenetic-Regulated Changes in Gene Expression', *PLoS One*, 11(3).
327. Russell, D.W. and Hirata, R.K. (1998) 'Human gene targeting by viral vectors', *Nature genetics*, 18(4), 325.
328. Monga, S.P., Monga, H.K., Tan, X., Mule, K., Pediaditakis, P. and Michalopoulos, G.K. (2003) 'Beta-catenin antisense studies in embryonic liver cultures: role in proliferation, apoptosis, and lineage specification', *Gastroenterology*, 124(1), 202-16.
329. Micsenyi, A., Tan, X., Sneddon, T., Luo, J.H., Michalopoulos, G.K. and Monga, S.P. (2004) 'Beta-catenin is temporally regulated during normal liver development', *Gastroenterology*, 126(4), 1134-46.
330. Tan, X., Behari, J., Cieply, B., Michalopoulos, G.K. and Monga, S.P. (2006) 'Conditional deletion of beta-catenin reveals its role in liver growth and regeneration', *Gastroenterology*, 131(5), 1561-72.
331. Thompson, M.D. and Monga, S.P. (2007) 'WNT/beta-catenin signaling in liver health and disease', *Hepatology*, 45(5), 1298-305.
332. Benhamouche, S., Decaens, T., Godard, C., Chambrey, R., Rickman, D.S., Moinard, C., Vasseur-Cognet, M., Kuo, C.J., Kahn, A., Perret, C. and Colnot, S. (2006) 'Apc tumor suppressor gene is the "zonation-keeper" of mouse liver', *Dev Cell*, 10(6), 759-70.
333. Spangler, P.R. and Delidow, B.C. (1998) 'Co-regulation of pituitary tumor cell adhesion and prolactin gene expression by glucocorticoid', *J Cell Physiol*, 174(1), 115-24.
334. Naito, M., Omoteyama, K., Mikami, Y., Takahashi, T. and Takagi, M. (2012) 'Inhibition of Wnt/beta-catenin signaling by dexamethasone promotes adipocyte differentiation in mesenchymal progenitor cells, ROB-C26', *Histochemistry and Cell Biology*, 138(6), 833-845.
335. Smith, E., Coetzee, G.A. and Frenkel, B. (2002) 'Glucocorticoids inhibit cell cycle progression in differentiating osteoblasts via glycogen synthase kinase-3 beta', *Journal of biological chemistry*, 277(20), 18191-18197.
336. Iansante, V., Mitry, R.R., Filippi, C., Fitzpatrick, E. and Dhawan, A. (2018) 'Human hepatocyte transplantation for liver disease: current status and future perspectives', *Pediatr Res*, 83(1-2), 232-240.
337. Guillouzo, A. (1998) 'Liver cell models in in vitro toxicology', *Environ Health Perspect*, 106 Suppl 2, 511-32.
338. Brandon, E.F., Raap, C.D., Meijerman, I., Beijnen, J.H. and Schellens, J.H. (2003) 'An update on in vitro test methods in human hepatic drug biotransformation research: pros and cons', *Toxicol Appl Pharmacol*, 189(3), 233-46.
339. Gebhardt, R., Hengstler, J.G., Muller, D., Glockner, R., Buenning, P., Laube, B., Schmelzer, E., Ullrich, M., Utesch, D., Hewitt, N., Ringel, M., Hilz, B.R., Bader, A., Langsch, A., Koose, T., Burger, H.J., Maas, J. and Oesch, F. (2003) 'New hepatocyte in vitro systems for drug metabolism: metabolic capacity and recommendations for application in basic research and drug development, standard operation procedures', *Drug Metab Rev*, 35(2-3), 145-213.

340. Miranda, J.P., Leite, S.B., Muller-Vieira, U., Rodrigues, A., Carrondo, M.J. and Alves, P.M. (2009) 'Towards an extended functional hepatocyte in vitro culture', *Tissue Eng Part C Methods*, 15(2), 157-67.
341. Cheng, N., Wauthier, E. and Reid, L.M. (2008) 'Mature human hepatocytes from ex vivo differentiation of alginate-encapsulated hepatoblasts', *Tissue Eng Part A*, 14(1), 1-7.
342. Fox, I.J. and Strom, S.C. (2008) 'To be or not to be: generation of hepatocytes from cells outside the liver', *Gastroenterology*, 134(3), 878-81.
343. Wong, N., Lai, P., Pang, E., Leung, T.W., Lau, J.W. and Johnson, P.J. (2000) 'A comprehensive karyotypic study on human hepatocellular carcinoma by spectral karyotyping', *Hepatology*, 32(5), 1060-8.
344. Lake, B.G. (2009) 'Species differences in the hepatic effects of inducers of CYP2B and CYP4A subfamily forms: relationship to rodent liver tumour formation', *Xenobiotica*, 39(8), 582-96.
345. Pan, X.P., Wang, Y.N., Yu, X.P., Zhu, C.X., Li, J.Z., Du, W.B., Zhang, Y.M., Cao, H.C., Zhang, Y.H., Zhu, D.H., Yeoh, G.C. and Li, L.J. (2016) 'Efficient generation of functional hepatocyte-like cells from mouse liver progenitor cells via indirect co-culture with immortalized human hepatic stellate cells', *Hepatobiliary Pancreat Dis Int*, 15(2), 173-9.
346. Heslop, J.A. and Duncan, S.A. (2019) 'The Use of Human Pluripotent Stem Cells for Modeling Liver Development and Disease', *Hepatology*, 69(3), 1306-1316.
347. Fejes-Tóth, G., Frindt, G., Náray-Fejes-Tóth, A. and Palmer, L.G. (2008) 'Epithelial Na+ channel activation and processing in mice lacking SGK1', *American Journal of Physiology-Renal Physiology*, 294(6), F1298-F1305.
348. Mitsui, K., Suzuki, K., Aizawa, E., Kawase, E., Suemori, H., Nakatsuji, N. and Mitani, K. (2009) 'Gene targeting in human pluripotent stem cells with adeno-associated virus vectors', *Biochem Biophys Res Commun*, 388(4), 711-717.
349. Leong, M.L., Maiyar, A.C., Kim, B., O'Keeffe, B.A. and Firestone, G.L. (2003) 'Expression of the serum- and glucocorticoid-inducible protein kinase, Sgk, is a cell survival response to multiple types of environmental stress stimuli in mammary epithelial cells', *J Biol Chem*, 278(8), 5871-82.
350. Clotman, F., Jacquemin, P., Plumb-Rudewiez, N., Pierreux, C.E., Van der Smissen, P., Dietz, H.C., Courtoy, P.J., Rousseau, G.G. and Lemaigre, F.P. (2005) 'Control of liver cell fate decision by a gradient of TGF beta signaling modulated by Onecut transcription factors', *Genes Dev*, 19(16), 1849-54.
351. Carpentier, A., Nimgaonkar, I., Chu, V., Xia, Y.C., Hu, Z.Y. and Liang, T.J. (2016) 'Hepatic differentiation of human pluripotent stem cells in miniaturized format suitable for high-throughput screen', *Stem Cell Res*, 16(3), 640-650.
352. Chen, C., Soto-Gutierrez, A., Baptista, P.M. and Spee, B. (2018) 'Biotechnology Challenges to In Vitro Maturation of Hepatic Stem Cells', *Gastroenterology*, 154(5), 1258-1272.
353. Godoy, P., Schmidt-Heck, W., Hellwig, B., Nell, P., Feuerborn, D., Rahnenfuhrer, J., Kattler, K., Walter, J., Bluthgen, N. and Hengstler, J.G. (2018) 'Assessment of stem cell differentiation based on genome-wide expression profiles', *Philos Trans R Soc Lond B Biol Sci*, 373(1750).
354. Williams, D.P. (2018) 'Application of hepatocyte-like cells to enhance hepatic safety risk assessment in drug discovery', *Philos Trans R Soc Lond B Biol Sci*, 373(1750).
355. Wallace, K., Fairhall, E.A., Charlton, K.A. and Wright, M.C. (2010 a) 'AR42J-B-13 cell: An expandable progenitor to generate an unlimited supply of functional hepatocytes', *Toxicology*, 278(3), 277-287.

356. Wang, X., Foster, M., Al-Dhalimy, M., Lagasse, E., Finegold, M. and Grompe, M. (2003) 'The origin and liver repopulating capacity of murine oval cells', *Proc Natl Acad Sci U S A*, 100 Suppl 1, 11881-8.
357. Zhu, S., Rezvani, M., Harbell, J., Mattis, A.N., Wolfe, A.R., Benet, L.Z., Willenbring, H. and Ding, S. (2014) 'Mouse liver repopulation with hepatocytes generated from human fibroblasts', *Nature*, 508(7494), 93-7.
358. Nagamoto, Y., Takayama, K., Tashiro, K., Tateno, C., Sakurai, F., Tachibana, M., Kawabata, K., Ikeda, K., Tanaka, Y. and Mizuguchi, H. (2015) 'Efficient Engraftment of Human Induced Pluripotent Stem Cell-Derived Hepatocyte-Like Cells in uPA/SCID Mice by Overexpression of FNK, a Bcl-xL Mutant Gene', *Cell Transplant*, 24(6), 1127-38.
359. Richter, M., Fairhall, E.A., Hoffmann, S.A., Trobs, S., Knospel, F., Probert, P.M.E., Oakley, F., Stroux, A., Wright, M.C. and Zeilinger, K. (2016) 'Pancreatic progenitor-derived hepatocytes are viable and functional in a 3D high density bioreactor culture system', *Toxicol Res (Camb)*, 5(1), 278-290.
360. Meyer, J.S., Shearer, R.L., Capowski, E.E., Wright, L.S., Wallace, K.A., McMillan, E.L., Zhang, S.-C. and Gamm, D.M. (2009) 'Modeling early retinal development with human embryonic and induced pluripotent stem cells', *Proceedings of the National Academy of Sciences*, 106(39), 16698-16703.
361. Kamiyama, T., Takahashi, M., Nakagawa, T., Nakanishi, K., Kamachi, H., Suzuki, T., Shimamura, T., Taniguchi, M., Ozaki, M. and Matsushita, M. (2006) 'AFP mRNA detected in bone marrow by real-time quantitative RT-PCR analysis predicts survival and recurrence after curative hepatectomy for hepatocellular carcinoma', *Annals of surgery*, 244(3), 451.
362. Sirico, M.L., Guida, B., Procino, A., Pota, A., Sodo, M., Grandaliano, G., Simone, S., Pertosa, G., Riccio, E. and Memoli, B. (2012) 'Human mature adipocytes express albumin and this expression is not regulated by inflammation', *Mediators of inflammation*, 2012.
363. Bowen, W.P., Carey, J.E., Miah, A., McMurray, H.F., Munday, P.W., James, R.S., Coleman, R.A. and Brown, A.M. (2000) 'Measurement of cytochrome P450 gene induction in human hepatocytes using quantitative real-time reverse transcriptase-polymerase chain reaction', *Drug Metabolism and Disposition*, 28(7), 781-788.
364. Fairhall, E.A., Wallace, K., White, S.A., Huang, G.C., Shaw, J.A., Wright, S.C., Charlton, K.A., Burt, A.D. and Wright, M.C. (2013) 'Adult human exocrine pancreas differentiation to hepatocytes–potential source of a human hepatocyte progenitor for use in toxicology research', *Toxicology Research*, 2(1), 80-87.